Herbal extracts and their active compounds as modulators of the inflammatory signaling pathways of Toll-like receptor 2 and 4

Dissertation

zur Erlangung des Grades eines ’Doctor rerum naturalium (Dr. rer. nat.)’ der Fachbereiche:

08 – Physik, Mathematik und Informatik,
09 – Chemie, Pharmazie und Geowissenschaften,
10 – Biologie,
Universitätsmedizin
der Johannes Gutenberg-Universität
Max Planck Graduate Center

Anne Katharina Schink

Mainz, Mai 2018

1. Berichterstatter:
2. Berichterstatter:

Tag der mündlichen Prüfung:

Declaration

I hereby declare that I wrote the dissertation submitted without any unauthorized external assistance and used only sources acknowledged in the work. All textual passages which are appropriated verbatim or paraphrased from published and unpublished texts as well as all information obtained from oral sources are duly indicated and listed in accordance with bibliographical rules. In carrying out this research, I complied with the rules of standard scientific practice as formulated in the statutes of Johannes Gutenberg-University Mainz to insure standard scientific practice.

Mainz, 29 May 2018

Abstract

Acute and especially chronic inflammation significantly contribute to the progression of many severe diseases, e.g. intestinal and extraintestinal inflammation, autoimmune diseases, chronic obstructive pulmonary disease (COPD), allergic asthma and many more. Toll-like receptors (TLRs) are part of the innate immune system and play a key role in inflammatory processes. Particularly the TLR4 pathway, whose myeloid differentiation primary response 88 (MyD88)-dependent signaling cascade is, among others, shared with TLR2, comprises important target molecules to mitigate immune reactions. To date, no effective orally active TLR4 antagonists are available for clinical application. Herbal extracts and their active compounds with potent TLR4 antagonistic activities would be of very high interest as opportunity for oral treatment of different inflammatory diseases.

The extensive screening of 99 herbal extracts revealed a great potential still hidden in this field of research. Among others, anti-inflammatory herbal extracts with formerly not described influences on multiple TLR signaling pathways were found, e.g. *Castanea sativa* leaves and *Alchemilla vulgaris* plant. In addition, anti-inflammatory extracts were identified, where previously only single constituents in the extracts were observed to mitigate effects on stimulated TLR2 or TLR4 signaling pathways, but not the whole complex mixtures themselves, such as *Arctostaphylos uva-ursi* leaves, *Cinchona pubescens* bark and *Humulus lupulus* cones, with arbutin, cinchonine and xanthohumol, respectively. Furthermore, several extracts, especially *Rheum palmatum* root and *Arctostaphylos uva-ursi* leaves, were shown to polarize pro-inflammatory M1 macrophages to anti-inflammatory M2 macrophages.

One of the most promising extracts, *Cinnamomum verum* (cinnamon) bark extract was fractionated and the comprised (active) compounds were identified. *Cinnamomum verum* extract and its active compounds *trans*-cinnamaldehyde and *p*-cymene were shown to mitigate stimulated TLR2 and TLR4 signaling pathways. In addition, formerly unknown synergistic effects between active compounds and other compounds, which do not show anti-inflammatory activities by themselves, were revealed. *Cinnamomum verum* extract, *trans*-cinnamaldehyde and *p*-cymene were generally shown to influence early TLR2 and TLR4 signaling pathway molecules *in vitro*, without toxic effects. Therefore, the results may contribute to the development of new oral treatment strategies for different inflammatory diseases.

Zusammenfassung

Akute und insbesondere chronische Entzündungen tragen wesentlich zum Fortschreiten von vielen schweren Erkrankungen bei, z.B. bei intestinalen und extraintestinalen Entzündungen, Autoimmunerkrankungen, COPD, allergischem Asthma und vielen weiteren. Toll-like Rezeptoren des angeborenen Immunsystems spielen bei den Entzündungsprozessen eine wichtige Rolle. Insbesondere der TLR4 Signalweg, dessen MyD88-abhängige Signalkaskade u.a. mit TLR2 geteilt wird, enthält wichtige Zielmoleküle um die Immunreaktion zu verringern. Bislang ist noch kein oral wirksamer TLR4 Antagonist für die klinische Anwendung verfügbar. Pflanzenextrakte und ihre aktiven Substanzen mit starkem TLR4 antagonistischem Potential bergen interessante Möglichkeiten zur oralen Behandlung verschiedener Entzündungskrankheiten.

Ein umfangreiches Screening von 99 Pflanzenextrakten offenbarte ein großes Potential, welches in diesem Forschungsfeld noch verborgen liegt. Unter anderem wurden antientzündliche Pflanzenextrakte gefunden, deren Einflüsse auf verschiedene TLR Signalwege noch nicht dokumentiert wurden, z.B. die Blätter der Edelkastanie und der Spitzlappige Frauenmantel. Zudem wurden antientzündliche Extrakte identifiziert, bei denen bisher nur einzelne Bestandteile, jedoch nicht das komplexe Gemisch des Extraktes, eine abschwächende Wirkung auf stimulierte TLR2 und TLR4 Signalwege zeigten, z.B. Bärentraubenblätter, Chinarinde und Hopfenzapfen mit entsprechend Arbutin, Cinchonin und Xanthohumol. Ferner bewirkten verschiedene Extrakte, insbesondere Rhabarberwurzel und Bärentraubenblätter, eine Polarisierung von proinflammatorischen M1 Makrophagen zu antiinflammatorischen M2 Makrophagen.

Das Rindenextrakt des Ceylon-Zimtes, eines der vielversprechendsten Extrakte, wurde fraktioniert und die (aktiven) Inhaltsstoffe identifiziert. Zimt-Extrakt und seine aktiven Wirkstoffe *trans*-Zimtaldehyd und *p*-Cymol schwächten die Signale der stimulierten TLR2 und TLR4 Signalwege ab. Zudem konnten bisher unbekannte synergistische Effekte zwischen aktiven Zimt-Bestandteilen und Substanzen ohne eigene antientzündliche Wirkung beobachtet werden. Generell zeigten Zimt-Extrakt, *trans*-Zimtaldehyd und *p*-Cymol *in vitro* einen Einfluss auf frühe TLR2- und TLR4-Signalwegmoleküle, ohne das Auftreten von toxischen Effekten. Somit könnten diese Ergebnisse zur Entwicklung neuer oraler Behandlungsstrategien für verschiedene Entzündungskrankheiten beitragen.

Table of contents

1. Introduction and motivation 1
1.1. Herbal medicines 1
1.2. Anti-inflammatory activities of herbal extracts 2
1.3. Inflammatory diseases 13
1.4. TLR signaling pathways 14
1.5. Cinnamon 17
1.5.1. Cinnamon species 17
1.5.2. Compounds of cinnamon extract 18
1.5.3. Beneficial health effects 20
1.6. Aim of research 21
2. Equipment and materials 23
2.1. Equipment 23
2.2. Consumables 24
2.3. Chemicals and reagents 25
2.4. Extracts 27
2.5. Solutions and buffer 31
2.5.1. Cell culture medium 31
2.5.2. SDS-PAGE and Western Blot buffer 32
2.5.3. Antibody solutions 34
2.6. Cell lines 35
2.6.1. HeLa-TLR4 stable transfected reporter cell line 35
2.6.2. THP-1 cell line 36
2.6.3. HEK-TLR2 and HEK-TLR4 stable transfected reporter cell lines 36
2.6.4. HeLa-TLR4 stable transfected dual reporter cell line 37
2.7. Animals 37
3. Methods 37
3.1. Preparation of ethanolic extracts and compounds 37
3.2. Cell culture treatments 38
3.2.1. HeLa-TLR4 reporter cell line 38

3.2.2. THP-1 monocytes 39
3.2.3. THP-1 macrophages 40
3.2.4. HEK-TLR2 and HEK-TLR4 reporter cell lines 40
3.2.5. HeLa-TLR4 dual reporter cell line 41
3.3. Cell viability assays 42
3.3.1. MTT assay 42
3.3.2. WST-8 assay 42
3.3.3. Alamar Blue assay 43
3.4. TLR2 and TLR4 stimulation assays 44
3.4.1. LightSwitch Luciferase assay 44
3.4.2. ELISA 45
3.4.3. HEK-Blue Detection assay 46
3.5. LAL assay 46
3.6. TLR2 and TLR4 pathway analysis 47
3.6.1. Quantitative fluorescence microscopy 47
3.6.2. Sample preparation and SDS-PAGE 47
3.6.3. Western Blot analysis 48
3.7. Inflammatory mouse model 49
3.8. Analysis of cinnamon extract 50
3.8.1. Fractionation using HPLC-DAD 50
3.8.2. Identification of compounds using HRMS and GC-MS 50
3.9. Statistical analyses 52
4. Results and discussion 53
4.1. Identification of optimal experimental conditions 53
4.1.1. Optimizing LPS treatment for HeLa-TLR4 reporter cell line 53
4.1.2. Comparison of different cell viability assays 54
4.1.3. Investigation of nickel solutions as substitution for LPS 55
4.1.4. Optimizing LPS treatment for THP-1 monocytes 57
4.2. Screening of different extracts for their anti-inflammatory effects 58
4.2.1. Screening for TLR-dependent anti-inflammatory effects 58

4.2.2. Screening for exclusive TLR4 antagonistic effects 66
4.2.3. Inhibition of NF-κB p65 translocation 74
4.2.4. Repolarization of macrophages 76
4.3. Analysis of *C. verum* bark extract and its active compounds 78
4.3.1. Effects in inflammatory mouse model 80
4.3.2. Fractionation and identification of compounds 81
4.3.3. TLR-dependent anti-inflammatory effects 86
4.3.4. Influence on repolarization of macrophages 92
4.3.5. Influence on phosphorylation of TLR signaling pathway molecules 93
5. Conclusions 99
6. Lists 100
6.1. List of abbreviations 100
6.2. List of figures 104
6.3. List of tables 106
7. References 107
8. Acknowledgement IX
9. Appendix X

1. Introduction and motivation

1.1. Herbal medicines

Treatment of indispositions and diseases in ancient times heavily relied on herbal medications, leading to numerous plants used in the traditional medicine of different nations. In general, herbal extracts comprise a wide source of natural mixtures improving human health, with often secondary metabolites as active compounds (Wink, 2008). Two of the most prominent plants, which were originally used in traditional medicine and whose identification of the active compounds led to the discovery of powerful medications in modern medicine, are *Salix alba* (white willow) and *Cinchona pubescens* (cinchona).

White willow bark is used for more than 3500 years in traditional medicine as analgesic and antipyretic plant. After centuries of usage, especially for the treatment of unspecific pain, its active compound, the alcoholic β-glucoside salicin, was identified in 1828. In the following years, several salicin derivatives were developed, which finally led to the discovery of acetylsalicylic acid in 1897, commonly marketed as Aspirin. Elucidation of the mechanism of action as cyclooxygenase (COX) inhibitor followed in 1971. Despite some adverse reactions, especially gastrointestinal side effects, Aspirin is still one of the most widely used medicines in the world (Desborough and Keeling, 2017). Besides the usage for pain relief, low doses of Aspirin are e.g. used for primary and secondary prevention of cardiovascular diseases as well as for prevention of cerebrovascular disease (Sarma and Scott, 2016; Desborough and Keeling, 2017). In contrast to Aspirin and its active compound acetylsalicylic acid, salicin is metabolized into several salicylate derivatives during absorption, resulting in pharmaceutical activities based on various components. This leads to a different mode of action compared to Aspirin, with often less severe side effects (Vlachojannis et al., 2011). In numerous *in vitro* and *in vivo* studies, anti-inflammatory effects have been shown for white willow extract, e.g. downregulation of several pro-inflammatory cytokines like Tumor necrosis factor-α (TNF-α) and inhibition of nuclear factor-κB (NF-κB) translocation (Bonaterra et al., 2010; Shara and Stohs, 2015). Most of the anti-inflammatory effects have been credited to its main pharmacologically active ingredient, salicin (Bonaterra et al., 2010). However, salicin alone cannot satisfactorily explain the anti-inflammatory effects, so other compounds within white willow bark, especially polyphenols such as flavonoids and proanthocyanidins, have been supposed to contribute to its overall activity and thereby broaden the mechanisms of action (Nahrstedt et al., 2007; Bonaterra et al., 2010; Vlachojannis et al., 2011).

Another prominent example is cinchona bark, which is used since ancient times to treat shivering and fever. Later, these were identified to be symptoms of malaria caused by a blood-borne parasitic protozoan of the genus *Plasmodium*. In 1920, quinine was identified to be the compound within cinchona bark responsible for its potent antipyretic activity. This

discovery led to its chemically synthetization as well as to the development of further quinine derivatives (An et al., 2017). Treatment of malaria with quinine was the first successful use of a chemical compound to treat an infectious disease (Achan et al., 2011). Most common side effects, when applying therapeutic doses of quinine, are tinnitus, vertigo, headache, dysphoria, nausea and vomiting, which are combined as cinchonism. Quinine treatment does not prevent malaria infection itself, but suppresses the infection within the human blood. Therefore, occasional symptomatic episodes of malaria may occur in the affected patients (Shanks, 2016). The complex mechanisms of its antimalarial effects are not yet entirely understood. Although, quinine resistance is observed in Africa and South East Asia, even around 400 years after the first documentation of quinine effectiveness, it still remains an important antimalarial drug, especially for the treatment of severe malaria or as second line treatment in uncomplicated malaria (Achan et al., 2011; Okombo et al., 2011; An et al., 2017).

Besides these two prominent examples, where traditionally used plants resulted in the discovery of still commonly used powerful medications, various other herbal extracts have been reported to possess beneficial health effects. Since herbal extracts are highly complex mixtures, their beneficial effects are often based on several compounds as well as on their synergistic effects (Wink, 2008). Therefore, investigation of efficacy and elucidation of the mechanism(s) of action are often rather complicated. Especially interesting for our research is the focus on herbal extracts containing anti-inflammatory properties.

1.2. Anti-inflammatory activities of herbal extracts

Herbal extracts and their active compounds have been used since ancient times, but their potential to modulate inflammatory pathways has only been discovered during the last decades (Chahal et al., 2013). Select plants, their (hypothesized) active compounds, influences on inflammatory markers as well as their reported beneficial impact on human health are exemplarily presented in **Table 1**.

Table 1: Overview of plants and their active compounds comprising beneficial effects
The effects of cinnamon and its active compounds are described more detailed in **chapter 1.5**.

Latin name	Common English name	Common German name	Family	(Hypothesized) active compound	Compound classification	Influence on (inflammatory) marker	Beneficial human health effect	Reference
Achillea millefolium	Common yarrow	Gemeine Schafgarbe	*Asteraceae*	Kaempferol, luteolin, apigenin	Flavonoids	↓ ALT, ↓ AST, ↑ GSH, ↓ MPO, ↑ SOD	Ameliorating several neuro-degenerative disorders	Potrich et al., 2010; Yaeesh et al., 2006; Ayoobi et al., 2017
Aesculus hippocastanum	Horse-chestnut	Gewöhnliche Rosskastanie	*Sapindaceae*	Escin	Saponin	↓ IκBα, ↓ NF-κB, ↑ ROS	Prolongation of survival in thyroid cancer patients	Cheong et al., 2018
Alchemilla vulgaris	Common lady's mantle	Spitzlappiger Frauenmantel	*Rosaceae*				Weight loss (when combined with other plants)	Said et al., 2011
Allium sativum	Garlic	Knoblauch	*Amaryllidaceae*	Diallyl sulfide	Sulfide	↓ ALT, ↓ AST, ↓ COX-2, ↓ IL-1β, ↓ iNOS, ↑ insulin, ↓ NF-κB, ↓ TNF-α	Reduction of body fat mass and body weight	Eidi et al., 2006; Soleimani et al., 2016; Suman and Shukla, 2016
Aloe ferox	Aloe	Aloen	*Xanthorrhoeaceae*	Aloeresin I	Glucoside	↓ caspase-1, ↓ COX-1, ↓ ERK, ↓ IL-1β, ↓ IL-6, ↓ IL-8, ↓ JNK, ↓ NF-κB, ↓ NLRP3, ↓ p38, ↓ TNF-α	Wound healing	Speranza et al., 2005; Fawole et al., 2010; Budai et al., 2013; Radha and Laxmipriya, 2014
Alpinia officinarum	Galangal	Galgant	*Zingiberaceae*	Galangin	Flavonoid	↓ IL-6, ↑ IL-10, ↓ NO, ↓ ROS, ↓ TNF-α		Choi et al., 2017
Althaea officinalis	Common marshmallow	Eibisch	*Malvaceae*				Treatment of Old World cutaneous leishmaniasis; Cough reduction	Cravotto et al., 2010
Arctostaphylos uva-ursi	Bearberry	Bärentrauben	*Ericaceae*	Arbutin	Glucoside	↓ COX-2, ↓ IL-1β, ↓ iNOS, ↓ NF-κB, ↓ NO,		Lee and Kim, 2012

Latin name	Common English name	Common German name	Family	(Hypothesized) active compound	Compound classification	Influence on (inflammatory) marker	Beneficial human health effect	Reference
						↓ TNF-α		
Armoracia rusticana	Horseradish	Meerrettich	*Brassicaceae*			↓ c-Jun, ↓ COX-2, ↓ ERK1/2, ↓ IL-6, ↓ NO, ↓ PGE_2, ↓ TNF-α		Marzocco et al., 2015; Herz et al., 2017
Arnica montana	Arnica	Arnika	*Asteraceae*	Helenalin	Sesquiterpene	↓ IL-1β, ↓ IL-6, ↓ IL-12, ↓ NF-κB, ↓ NO, ↓ TNF-α	Beneficial effects in osteoarthritis	Lass et al., 2008; Chahal et al., 2013; Dragos et al., 2017
Artemisia absinthium	Wormwood	Wermutkraut	*Asteraceae*		Flavonoids	↓ COX-2, ↓ iNOS, ↓ NF-κB, ↓ NO, ↓ PGE_2, ↓ TNF-α	Beneficial in Crohn's disease	Lee et al., 2004; Omer et al., 2007; Krebs et al., 2010
Avena sativa	Oat	Saat-Hafer	*Poaceae*	β-Glucan	Glucan	↓ COX-2, ↓ NO, ↑ TGFβ1, ↓ TNF-α	Several beneficial effects, e.g. anti-diabetic, prevention of cardiovascular diseases, protection against breast cancer	Singh et al., 2013
Boswellia carterii	Frankincense	Afrikanischer Weihrauch	*Burseraceae*	Boswellic acid	Triterpene	↓ 5-LOX, ↓ AChE, ↑ GSH, ↓ MDA		Safayhi et al., 2000; Ebrahimpour et al., 2017
Boswellia serrata	Frankincense	Weihrauch	*Burseraceae*	Boswellic acid	Triterpene	↓ 5-LOX, ↓ IFNγ, ↓ IL-1β, ↓ IL-2, ↑ IL-4, ↓ IL-6, ↑ IL-10, ↓ IL-12, ↓ NO, ↓ TNF-α	Beneficial effects in osteoarthritis	Safayhi et al., 2000; Gayathri et al., 2007; Dragos et al., 2017
Calendula officinalis	Marigold	Ringelblume	*Asteraceae*		Several triterpenes and flavonoids	↓ COX-2, ↓ IL-1(β), ↓ TNF-α	Wound healing; Prevention of acute dermatitis	Ukiya et al., 2006; Cravotto et al., 2010; Kirichenko et al., 2016; Alexandre et al., 2017

Latin name	Common English name	Common German name	Family	(Hypothesized) active compound	Compound classification	Influence on (inflammatory) marker	Beneficial human health effect	Reference
Camellia sinensis (L.)	Green tea	Grüner Tee	*Theaceae*	EGCG	Flavonoid	↓ COX-2, ↓ IFNγ, ↓ NF-κB, ↑ ROS, ↓ TNF-α	Beneficial effects on metabolism, cardiovascular system, neuro-degenerative diseases and cancer	Cooper et al., 2005; Arab et al., 2009; Shirakami et al., 2016
Capsicum frutescens	Chili	Chili	*Solanaceae*	Capsaicin	Polyunsaturated alkamide	↓ AP-1, ↓ IκBα, ↓ NF-κB	Pain reduction	Han et al., 2001; Bortolotti and Porta, 2011; Gagnier et al., 2016
Carum carvi	Caraway	Echter Kümmel	*Apiaceae*			↓ cholesterol, ↓ triglycerides	Antiobesity effect	Lemhadri et al., 2006; Kazemipoor et al., 2013
Castanea sativa	Sweet chestnut	Edelkastanie	*Fagaceae*		Phenols	↓ NF-κB, ↓ RAGE, ↓ $O_2^{\cdot-}$, ↓ $^{\cdot}OH$		Calliste et al., 2005; Jovanović et al., 2017
Chelidonium majus	Celandine	Schöllkraut	*Papaveraceae*	Berberine, norchelidonine, chelidonine, 8-hydroxydihydro-sanguinarine	Alkaloids	↓ COX-2, ↓ iNOS, ↓ NO, ↓ PGE_2	Anticancer drug (Ukrain) based on plant extract	Kuo et al., 2004; Ernst and Schmidt, 2005; Park et al., 2011
Chlorella pyrenoidosa	Chlorella	Chlorella	*Chlorellaceae*	Rhamnose, glucose, galactose, mannose, xylose	Mono-saccharides	↑ IL-1β	Beneficial in pregnant and breastfeeding women	Nakano et al., 2007; Nakano et al., 2010; Chahal et al., 2013
Cinchona pubescens	Cinchona	Chinarinde	*Rubiaceae*	Quinine	Quinoline	↓ NF-κB	Malaria treatment	An et al., 2017
Cinnamomum verum	Cinnamon	Zimt	*Lauraceae*	Cinnamaldehyde	Flavonoid	↓ COX-2, ↓ IκB, ↓ IL-1β, ↓ iNOS, ↓ MyD88, ↓ NF-κB, ↓ ROS, ↓ TNF-α	Anti-hyperlipidaemic and blood pressure lowering, stimulation of glycogen	Khan et al., 2003; Kim et al., 2007; Chao et al., 2008; Kanuri et al., 2009; Gunawardena et al., 2015; Hariri and Ghiasvand,

Latin name	Common English name	Common German name	Family	(Hypothesized) active compound	Compound classification	Influence on (inflammatory) marker	Beneficial human health effect	Reference
							synthesis and insulin secretion	2016; Ranasinghe et al., 2017
Coriandrum sativum	Coriander	Echter Koriander	*Apiaceae*			↓ COX-2, ↓ IL-1β, ↓ iNOS, ↓ NO, ↓ PGE_2	Reduction of UV-induced erythema	Reuter et al., 2008; Wu et al., 2010
Crataegus species	Hawthorn	Weißdorn	*Rosaceae*	Vitexin	Flavonoid	↓ IL-1(β), ↑ IL-10, ↓ NO, ↓ p-ERK1/2, ↓ PGE_2, ↓ p-JNK, ↓ p-p38, ↓ TNF-α	Beneficial in adjunctive treatment for chronic heart failure; Hypotensive and hypolipidemic effects	Pittler et al., 2003; Walker et al., 2006; Dalli et al., 2011; Kirichenko et al., 2016; Rosa et al., 2016
Curcuma longa	Turmeric	Kurkuma	*Zingiberaceae*	Curcumin	Catechol	↓ AP-1, ↓ COX-2, ↓ IFNγ, ↓ IL-1, ↓ IL-6, ↓ IL-8, ↓ IL-12, ↓ iNOS, ↓ JNK, ↓ NF-κB, ↓ RANKL, ↓ TNF-α	Suppression of IBD symptoms; Beneficial effects in osteoarthritis	Joe et al., 2004; Goel et al., 2008; Pari et al., 2008; Baliga et al., 2012; Dragos et al., 2017
Cynara scolymus	Artichoke	Artischocken	*Asteraceae*			↓ CRP, ↓ Fg, ↓ MDA	Decreased cholesterol level	Bundy et al., 2008; Ben Salem et al., 2017
Daucus carota subsp. *sativus*	Carrot	Karotte	*Apiaceae*	*trans*-Asarone 2,4,5-Trimethoxybenz-aldehyde	Anisole Benzaldehyde	↓ COX-2		Momin et al., 2003
Digitalis purpurea	Common foxglove	Roter Fingerhut	*Plantaginaceae*	Digoxin	Cardiac glycoside		Treatment of cardiac disorders	Hauptman and Kelly, 1999
Dioscorea villosa	Yam	Yams	*Dioscoreaceae*	Diosgenin	Cholestane	↓ p-AKT, ↓ p-ERK, ↓ p-JNK, ↓ p-p38, ↓ ROS, ↓ TNF-α		Choi et al., 2010
Echinacea	Purple	Purpur-	*Asteraceae*		Alkamides	↓ COX-1,		Senchina et al., 2006; Woelkart

Latin name	Common English name	Common German name	Family	(Hypothesized) active compound	Compound classification	Influence on (inflammatory) marker	Beneficial human health effect	Reference
purpurea	coneflower	Sonnenhut				↓ COX-2, ↓ IL-1β, ↓ IL-6, ↓ IL-8, ↓ NO, ↓ TNF-α		and Bauer, 2007; Sharma et al., 2009
Elettaria cardamomum	Cardamom	Kardamom	*Zingiberaceae*	Cardamonin	Flavonoid	↓ COX-2, ↓ IL-1β, ↓ IL-6, ↓ iNOS, ↓ NF-κB, ↓ NO, ↓ PGE_2, ↓ TNF-α		Prasad and Aggarwal, 2014
Equisetum arvense	Field horsetail	Acker-Schachtelhalm	*Equisetaceae*	Kynurenic acid	Quinoline	↓ IFNγ, ↓ TNF-α	Beneficial effects in rheumatoid arthritis	Gründemann et al., 2014; Dragos et al., 2017
Erythraea centaurium	Common centaury	Echtes Tausendgülden-kraut	*Gentianaceae*			↓ ALT, ↓ AST, ↓ LDH		Mroueh et al., 2004
Euphrasia officinalis	Eyebright	Gemeiner Augentrost	*Orobanchaceae*			↓ IL-1β, ↓ IL-6, ↓ TNF-α		Paduch et al., 2014
Filipendula ulmaria	Meadowsweet	Mädesüß	*Rosaceae*	Quercetin	Flavonoid	↓ COX-1, ↓ COX-2, ↓ IL-1β, ↓ IL-6, ↓ TNF-α		Drummond et al., 2013; Katanić et al., 2016
Foeniculum vulgare	Fennel	Fenchel	*Apiaceae*	Limonene *trans*-Anethole	Cyclohexene Anisole	↓ IL-6, ↓ LDH, ↓ NO, ↓ p-ERK, ↓ TNF-α		Lee et al., 2015
Fucus vesiculosus	Bladderwrack	Blasentang	*Fucaceae*	Fucoidan	Polysaccharide	↓ COX-2, ↓ NO		Lim et al., 2015
Gentiana lutea	Gentian	Enzian	*Gentianaceae*	Gentiopicroside	Glucoside	↓ ERK 1/2, ↓ iNOS, ↓ MPO, ↓ NO		Nastasijević et al., 2012; Kesavan et al., 2013
Geranium robertianum	Herb robert	Ruprechtskraut	*Geraniaceae*			↓ NO		Catarino et al., 2017
Ginkgo biloba	Ginkgo	Ginkgo	*Ginkgoaceae*	Bilobalide	Ginkgolide	↓ ERK1/2	Enhancing neuro-psychological / memory processes	Mix and Crews, 2002; Dodge et al., 2008; Weinmann et al., 2010; Chahal et

Latin name	Common English name	Common German name	Family	(Hypothesized) active compound	Compound classification	Influence on (inflammatory) marker	Beneficial human health effect	Reference
								al., 2013
Glycyrrhiza glabra	Liquorice	Süßholz	*Fabaceae*	Isoliquiritigenin	Flavonoid	↓ COX-2, ↓ iNOS, ↓ IRF3, ↓ NF-κB	Decrease of mucositis and oral mucosal irritation	Park and Youn, 2010; Najafi et al., 2017
Hamamelis virginiana	Witch hazel	Hamamelis	*Hamamelidaceae*	Hamamelitannin	Benzoate	↓ TNF-α	Erythema suppression	Hughes-Formella et al., 1998; Habtemariam, 2002
Harpagophytum procumbens	Devil's claw	Afrikanische Teufelskralle	*Pedaliaceae*	Harpagoside, harpagide, procumbide	Iridoid glycosides	↓ c-FOS, ↓ COX-2, ↓ IL-1β, ↓ iNOS, ↓ NF-κB, ↓ TNF-α	Beneficial effects in osteoarthritis and low back pain	Gagnier et al., 2004; Rodriguez Villanueva et al., 2016; Dragos et al., 2017
Hedera helix	Common ivy	Efeu	*Araliaceae*	α-Hederin	Saponin	↓ IL-17		Ebrahimi et al., 2016
Hibiscus sabdariffa	Roselle	Roselle	*Malvaceae*		Polyphenols	↓ COX-2, ↓ ERK1/2, ↓ IFNγ, ↓ IL-6, ↑ IL-10, ↓ JNK, ↓ NF-κB, ↓ NO, ↓ p38, ↓ PGE_2, ↓ ROS, ↓ TNF-α		Da-Costa-Rocha et al., 2014; Herranz-López et al., 2017
Humulus lupulus	Hops	Hopfen	*Cannabaceae*	Xanthohumol	Flavonoid	↓ IL-1β, ↓ MCP-1, ↓ NF-κB, ↓ NO, ↓ TNF-α		Lupinacci et al., 2009; Lee et al., 2011
Hypericum perforatum	St John's wort	Echtes Johanniskraut	*Hypericaceae*	Pseudohypericin	Benz(a)-anthracene	↓ COX-2, ↓ IL-1, ↓ IL-6, ↓ NO, ↓ PGE_2, ↓ TNF-α	Treatment of depression	Schulz, 2006; Kasper et al., 2010; Huang et al., 2012; Kirichenko et al., 2016; Bonaterra et al., 2018
				Amentoflavone, quercetin	Flavonoids			
				Chlorogenic acid	Cyclohexane			
Ilex paraguariensis	Yerba mate	Mate-Strauch	*Aquifoliaceae*	Quercetin	Flavonoid	↓ COX-2, ↑ IκBα, ↓ iNOS, ↓ NF-κB, ↓ TNF-α		Arçari et al., 2011; Bracesco et al., 2011; Pimentel et al., 2013

Latin name	Common English name	Common German name	Family	(Hypothesized) active compound	Compound classification	Influence on (inflammatory) marker	Beneficial human health effect	Reference
Juniperus communis	Common juniper	Gemeiner Wacholder	*Cupressaceae*	Amentoflavone	Flavonoid	↓ ALT, ↓ ALP, ↓ AST, ↓ TNF-α		Bais et al., 2017
Marrubium vulgare	Common horehound	Andornkraut	*Lamiaceae*	Marrubiin	Diterpene	↓ COX-2		Sahpaz et al., 2002; Meyre-Silva et al., 2005
Matricaria chamomilla	Chamomile	Kamille	*Asteraceae*	Apigenin	Flavonoid	↓ IL-1β, ↓ IL-6, ↓ TNF-α		Drummond et al., 2013
Melilotus officinalis	Sweet clover	Steinkleekraut	*Fabaceae*	Caffeic acid	Cinnamate	↓ COX-2, ↓ IL-6, ↓ iNOS, ↓ NF-κB, ↓ NO, ↓ PGE_2, ↓ TNF-α		Bazazzadegan et al., 2017; Liu et al., 2018
Melissa officinalis	Lemon balm	Zitronenmelisse	*Lamiaceae*	Rosmarinic acid	Benzoate	↓ IL-1β, ↓ IL-6, ↓ IRAK1, ↓ MyD88, ↓ TLR4, ↓ TNF-α, ↓ TRAF6		Jiang et al., 2017b; Chizzola et al., 2018
Mentha piperita	Peppermint	Pfefferminze	*Lamiaceae*			↓ PGE_2, ↓ NO		Sun et al., 2014
Origanum majorana	Marjoram	Majoran	*Lamiaceae*	Rosmarinic acid	Benzoate	↓ IL-1β, ↓ IL-6, ↓ TNF-α		Villalva et al., 2018
Panax ginseng	Ginseng	Ginseng	*Araliaceae*	Ginsan	Polysaccharide Saponins	↓ COX-2, ↓ IFNγ, ↓ IL-1β, ↓ IL-6, ↓ IL-12, ↓ IL-18, ↓ iNOS, ↓ MyD88, ↓ TLR4, ↓ TNF-α	Beneficial effects in osteoarthritis; Improvement of glucose metabolism and modulating of immune response	Kang and Min, 2012; Chahal et al., 2013; Shergis et al., 2013; Dragos et al., 2017
Petroselinum crispum	Parsley	Petersilie	*Apiaceae*	Apigenin	Flavonoid	↓ NO	Increase in anti-oxidant enzymes	Nielsen et al., 1999; Farzaei et al., 2013
Pimpinella anisum	Anise	Anis	*Apiaceae*	Anethole	Anisole	↓ AP-1, ↑ IL-10, ↓ NF-κB, ↓ p38, ↓ TNF-α		Aprotosoaie et al., 2016
Plantago lanceolata	Ribwort	Spitzwegerich	*Plantaginaceae*	Acteoside	Phenol glycoside	(↓ COX-1), (↓ COX-2),		Murai et al., 1995; Vigo et al., 2005; Fakhrudin et al.,

Latin name	Common English name	Common German name	Family	(Hypothesized) active compound	Compound classification	Influence on (inflammatory) marker	Beneficial human health effect	Reference
						↓ IL-8, ↓ iNOS, ↓ MCP-1, ↓ NO		2017
Rheum palmatum	Rhubarb	Rhabarber	*Polygonaceae*	Rhein, emodin	Anthraquinones	↓ TNF-α		Chahal et al., 2013
Rosmarinus officinalis	Rosemary	Rosmarin	*Lamiaceae*	Rosmarinic acid	Benzoate	↓ IL-1β, ↓ IL-6, ↑ NF-κB, ↓ TNF-α		Rocha et al., 2015
Rubus fruticosus	Blackberry	Brombeere	*Rosaceae*	Cyanidin-3-O-glucoside	Anthocyanin	↓ iNOS, ↓ NF-κB, ↓ NO		Pergola et al., 2006; Zia-Ul-Haq et al., 2014
Salix alba	White willow	Silber-Weide	*Salicaceae*	Salicin	Glucoside	↓ COX-2, ↓ IL-6, ↓ NF-κB, ↓ TNF-α	Pain relief	Drummond et al., 2013; Shara and Stohs, 2015; Dragos et al., 2017
Salvia officinalis	Salvia	Salbei	*Lamiaceae*		Different flavonoids and terpenes	↓ MDA, ↓ NF-κB, ↓ NO, ↓ TNF-α		Ghorbani and Esmaeilizadeh, 2017; Kolac et al., 2017
Sambucus nigra (L.)	Elderflowers	Holunder	*Adoxaceae*		Anthocyanins	↓ IFNγ, ↓ IL-1, ↓ TNF-α		Badescu et al., 2015; Kirichenko et al., 2016
Schinus terebinthifolius	Brazilian pepper tree	Brasilianischer Pfefferbaum	*Anacardiaceae*			↓ CXCL1, ↓ IL-1β, ↓ IL-6, ↓ TNF-α	Reduction of gingival inflammation	Freires et al., 2013; Rosas et al., 2015
Spirulina	Spirulina	Spirulina	*Spirulinaceae*	Phycocyanin	Phycobiliprotein	↓ IL-6, ↑ Nrf2, ↓ TNF-α		Khafaga and El-Sayed, 2018; Kim et al., 2018
Symphytum officinale	Comfrey	Echter Beinwell	*Boraginaceae*	Rosmarinic acid Salvianolic acid	Benzoate Cinnamate	↓ IL-1β, ↓ IL-6, ↓ NF-κB, ↓ NO, ↓ TNF-α	Reduction of pain, inflammation and swelling	Koll et al., 2004; Giannetti et al., 2010; Staiger, 2013; Dragos et al., 2017; Trifan et al., 2018
Syzygium aromaticum	Clove	Nelken	*Myrtaceae*	Eugenol	Cinnamate	↓ COX-2, ↓ NF-κB	Local anti-inflammatory, antiseptic, and anesthetic effects on dental	Fujisawa and Murakami, 2016

Latin name	Common English name	Common German name	Family	(Hypothesized) active compound	Compound classification	Influence on (inflammatory) marker	Beneficial human health effect	Reference
							pulp	
Tanacetum parthenium	Feverfew	Mutterkraut	*Asteraceae*	Tanetin Parthenolide	Flavonoid Sesquiterpene	↓ 5-LOX, ↓ COX-2, ↓ IL-6, ↓ IL-8, ↓ iNOS, ↓ NF-κB, ↓ NO, ↓ TNF-α		Williams et al., 1995; Mazor et al., 2000; Aviram et al., 2012; Magni et al., 2012
Taraxacum officinale	Dandelion	Löwenzahn	*Asteraceae*	Taraxinic acid β-d-glucopyranosyl ester	Sesquiterpene	↑ Hmox1, ↓ iNOS, ↓ NF-κB, ↑ Nrf2		Liu et al., 2014; Esatbeyoglu et al., 2017
Thymus vulgaris	Common thyme	Thymian	*Lamiaceae*	Thymol	Monoterpene	↓ IL-1β, ↓ TNF-α		Amirghofran et al., 2011; Oliveira et al., 2017
Tropaeolum majus	Nasturtium	Kapuzinerkresse	*Tropaeolaceae*	Benzyl glucosinolate	Isothiocyanate	↓ COX-2, ↓ ERK1/2, ↓ JNK, ↓ PGE_2		Rodriguez Villanueva et al., 2016
Uncaria tomentosa	Cat's claw	Katzenkralle	*Rubiaceae*	Mitraphylline	Indole alkaloid	↓ c-Fos, ↓ c-Jun, ↓ IL-1α, ↓ IL-1β, ↓ IL-4, ↓ IL-17, ↓ Jun-B, ↓ Jun-D, ↓ TNF-α	Adjuvant treatment for reducing adverse chemotherapy effects	Sandoval et al., 2000; Allen-Hall et al., 2010; Rojas-Duran et al., 2012; Santos Araújo et al., 2012
Urtica dioica	Stinging nettle	Große Brennnessel	*Urticaceae*	Hydroxycinnamic acid, chlorogenic acid	Cinnamate	↓ 12-LOX, ↓ COX-1, ↓ COX-2, ↓ MCP-1, ↓ NO		Carvalho et al., 2017; Franciškovič et al., 2017
Usnea barbata	Barber’s itch	Bartflechte	*Parmeliaceae*	Usnic acid	Benzofuran	↓ PGE_2		Engel et al., 2007; Ranković et al., 2012
Vaccinium myrtillus	Bilberry	Heidelbeere	*Ericaceae*		Anthocyanins	↓ COX-2, ↓ IL-6, ↓ IL-12, ↓ iNOS	Modulation of different inflammatory processes	Sautebin et al., 2004; Karlsen et al., 2010; Kolehmainen et al., 2012
Valeriana officinalis (L.)	Common valerian	Echter Baldrian	*Caprifoliaceae*	Valerenic acid	Sesquiterpene	↓ MDA		Nam et al., 2013
Vanilla planifolia	Vanilla	Gewürzvanille	*Orchidaceae*	Vanillin	Benzaldehyde	↑ GSH, ↓ MDA, ↓ NF-κB, ↓ TNF-α		Elseweidy et al., 2017

Latin name	Common English name	Common German name	Family	(Hypothesized) active compound	Compound classification	Influence on (inflammatory) marker	Beneficial human health effect	Reference
Verbena officinalis	Common vervain	Echtes Eisenkraut	*Verbenaceae*					
Vigna radiata	Mung bean (dried)	Mungbohnen (getrocknet)	*Fabaceae*	Gallic acid Vitexin, isovitexin	Benzoate Flavonoids	↓ IL-1β, ↓ IL-6, ↓ IL-12β, ↓ iNOS, ↓ TNF-α		Tang et al., 2014
Vigna radiata	Mung bean (cooked in boiling water for 20 min)	Mungbohnen (gekocht)	*Fabaceae*	Gallic acid Vitexin, isovitexin	Benzoate Flavonoids	↓ IL-1β, ↓ IL-6, ↓ IL-12β, ↓ iNOS, ↓ TNF-α		Tang et al., 2014
Viscum album	European mistletoe	Weißbeerige Mistel	*Santalaceae*		Diarylheptanoids	↓ IL-6, ↓ IL-12, ↓ TNF-α	Beneficial impact on quality of life and reduction of side effects in cancer	Kienle and Kiene, 2010; Büssing et al., 2012; Nhiem et al., 2013
Zingiber officinale	Ginger	Ingwer	*Zingiberaceae*	6-Gingerol, 6-shogaol	Catechols	↓ AP-1, ↓ COX-1, ↓ COX-2, ↓ IL-1β, ↓ IL-12, ↓ IκBα, ↓ LOX, ↓ NF-κB, ↓ TNF-α	Antiemetic and inhibition of nausea and vomiting in pregnancy; Beneficial effects in osteoarthritis	Prasad and Aggarwal, 2014; Mohd Yusof, 2016; Dragos et al., 2017

↓: downregulation, ↑: upregulation, AChE: acetylcholinesterase, ALP: alkaline phosphatase, ALT: alanine transaminase, AP-1: activator protein 1, AST: aspartate transaminase, COX: cyclooxygenase, CRP: C-reactive protein, CXCL1: chemokine (C-X-C motif) ligand 1, EGCG: epigallocatechin-3-gallate, ERK: extracellular signal-regulated kinase, Fg: fibrinogen, GSH: glutathione, Hmox1: heme oxygenase (decycling) 1, IBD: inflammatory bowel disease, IFN: interferon, IL: interleukin, iNOS: inducible nitric oxide synthase, IRAK1: IL-1 receptor-associated kinase, IRF: interferon regulatory factor, IκBα: NF-κB inhibitor alpha, JNK: c-Jun N-terminal kinase, LDH: lactate dehydrogenase, LOX: lipoxygenase, MCP-1: monocyte chemoattractant protein-1, MDA: malondialdehyde, MPO: myeloperoxidase, MyD88: myeloid differentiation primary response 88, NF-κB: nuclear factor-κB, NLRP3: NOD-like receptor family pyrin domain-containing 3, NO: nitric oxide, Nrf2: nuclear factor erythroid 2-related factor 2, PGE_2: prostaglandin E_2, RAGE: receptor for advanced glycation end products, RANKL: receptor activator of nuclear factor kappa-B ligand, ROS: reactive oxygen species, SOD: superoxide dismutase, TLR4: Toll-like receptor 4, TGFβ1: transforming growth factor beta 1, TRAF6: TNF receptor-associated factor 6.

Since inflammatory processes are involved in many severe diseases, plant extracts or their active compounds attenuating the inflammatory processes might contribute to a substantial relief for the affected patients.

In recent years, also the interest in cyanobacteria and their usage as food additives (e.g. *Spirulina* and *Nostoc* spp.) increased (Ku et al., 2013). Hereby, especially cyanobacteria species with beneficial health effects e.g. anti-inflammatory properties might open up new promising treatment strategies.

1.3. Inflammatory diseases

Inflammation in general is a response of the innate and adaptive immune system to potential harmful stimuli (e.g. pathogens) or injuries, but can also affect adversely the own body, leading to autoimmune reactions. The different causes can lead to the production of chemoattractants and the release of pro-inflammatory cytokines. In combination with apoptotic and necrotic cells, they promote the recruitment of innate immune leukocytes, especially macrophages and neutrophils, to the affected side. Hereby, the classical activated type 1 (M1) macrophages release pro-inflammatory cytokines and contribute to the inflammatory process as well as to the suppression of tumor cells. In contrast, the alternatively activated type 2 (M2) macrophages release anti-inflammatory factors and are involved in tissue repair and angiogenesis (Fraternale et al., 2015; Smigiel and Parks, 2018). On the one hand, inflammatory processes have the important function to fight infections and repair dangerous effects, on the other hand, persistent reactions can result in chronic inflammation (Slavich and Irwin, 2014).

Acute and especially chronic inflammation play an important role in the progression of many severe diseases. In 2010, the estimated prevalence of chronic inflammatory diseases was 5-7% in the Western population (El-Gabalawy et al., 2010). Global diseases with emerging incidence are e.g. inflammation of the gastrointestinal tract such as inflammatory bowel disease (IBD), which includes both Crohn's disease and ulcerative colitis. The highest prevalence is reported in the westernized nations, e.g. 322 cases per 100.000 people for Crohn's disease in Germany. Especially areas with prior low incidence, like newly industrialized countries in Africa, Asia and South America, show an increasing IBD incidence since 1990 (Ng et al., 2018). Besides genetic predisposition and environmental exposure, also lifestyle exposure like risk or protective dietary factors have been shown to influence IBD development (Ponder and Long, 2013). Intestinal inflammation has been reported to be triggered, among others, by wheat amylase trypsin inhibitors (ATIs) after ingestion of wheat or wheat derived products. Particularly the ATI variants CM3 and 0.19 have been identified as potent stimulator of TLR4, resulting in the release of pro-inflammatory cytokines (Junker

et al., 2012; Schuppan et al., 2015; Zevallos et al., 2017; Schuppan and Gisbert-Schuppan, 2018). ATI-challenged mice have been reported to upregulate pro-inflammatory cytokine production and worsening ongoing intra- and extraintestinal inflammation (Junker et al., 2012; Zevallos et al., 2016; Bellinghausen et al., 2018; Zevallos et al., 2018).

Besides the gastrointestinal inflammatory diseases, also autoimmune diseases have been reported to be accompanied by inflammatory processes involving TLR4. In brain lesions and blood of patients with multiple sclerosis, expression of the multiple sclerosis associated retrovirus envelope protein (MSRV-Env) was observed. Its expression might play an important role in the associated chronic inflammation as well as in progression of demyelination of the central nervous system (CNS). Furthermore, MSRV-Env has been shown to be a highly potent TLR4 agonist, leading to a TLR4-dependent pro-inflammatory stimulation (Madeira et al., 2016). TLR4 signaling has also been demonstrated to be involved in chronic airway inflammation, like COPD. Hereby, a systemic defect in TLR4 signaling might contribute to the airway inflammation and the enlarged vulnerability to bacterial infections (Knobloch et al., 2016). As another example, in allergic asthma, a chronic inflammatory lung disease, a distinct TLR4 expression contributes to the inflammatory response to inhaled allergens (McAlees et al., 2015).

Plant extracts attenuating these inflammatory processes might help to improve the life quality of people affected by severe diseases accompanied by acute and/or chronic inflammation. Especially the involvement of TLR signaling pathways, as shown in the examples above, demonstrate important targets for potential new anti-inflammatory drugs developed from herbal extracts or their active compounds.

1.4. TLR signaling pathways

Inflammatory activities on the molecular level are associated with variations of a cyclic process. This process prominently involves the stimulation of TLRs e.g. via pathogen-associated molecular patterns (PAMPs), the production of reactive oxygen and nitrogen species (ROS/RNS), the secretion of pro-inflammatory cytokines and chemokines as well as the production of host-derived damage associated molecular patterns (DAMPs). These stimuli provoke further immune responses, including an adjuvant effect on adaptive (T cell mediated) immunity (Lucas and Maes, 2013; Walsh et al., 2013). Hereby, especially the activation of TLR4 and translocation of the transcription factor NF-κB into the cell nucleus play key roles in inflammation and diseases. Activation of TLR4 by PAMPs, e.g. lipopolysaccharides (LPS), requires the binding of LPS to lipid binding protein (LBP) and the presentation to TLR4 via cluster of differentiation 14 (CD14). In addition, myeloid

differentiation factor 2 (MD-2) is necessary for the binding of LPS to TLR4 (Yang et al., 2016). For complete activation, the TLR4/MD-2 complex has to translocate into lipid rafts, where clustering takes place. Lipid rafts are domains of the cell membrane characterized by a high content of cholesterol and glycosphingolipids (Pike, 2003; Szabo et al., 2007). After TLR4 stimulation, the inflammatory signal can be transmitted through two different signaling pathways: on the one side the canonical pathway of NF-κB p50/p65 activation or MyD88-dependent pathway (**Figure 1**, left) and on the other side the TIR-domain-containing adapter-inducing interferon-β (TRIF)/TRIF-related adaptor molecule (TRAM) pathway or MyD88-independent pathway (**Figure 1**, right). In contrast to TLR4, TLR2-induced NF-κB activation is only induced via the MyD88-dependent pathway (Takeuchi and Akira, 2001; Ghosh and Dass, 2016). In a simplified MyD88-dependent signaling pathway (**Figure 1**, left), MyD88 in complex with TIR domain containing adaptor protein (TIRAP) binds upon TLR4 activation to the interleukin 1 (IL-1) receptor-associated kinase (IRAK) complex consisting of IRAK4 and IRAK1/2. The IRAK complex then interacts with TNF receptor-associated factor 6 (TRAF6), forming a complex with transforming growth factor β activated kinase 1 (TAK1). After an activation of the NF-κB inhibitor (IκB) kinase (IKK) complex (IKKα/IKKβ/IKKγ) by TAK1, phosphorylation of the inhibitory protein IκBα on Ser-32 and Ser-36 leads to targeting for ubiquitination and degradation by proteasomes. Subsequently, NF-κB is activated and translocates into the cell nucleus (Tak and Firestein, 2001; Clark et al., 2013; Cullen et al., 2015; Yang et al., 2016). Furthermore, upon stimulation of TLR4, glucan phosphate (GP) can lead to a dissociation of TLR4 from MyD88. After binding to phosphatidylinositol 3-kinase (PI3K), the serine/threonine kinase AKT, also known as protein kinase B (PKB), is phosphorylated. Activated AKT phosphorylates itself numerous proteins controlling cell survival, proliferation and motility. In addition, AKT was shown to regulate the transcriptional activity of NF-κB by inducing phosphorylation and degradation of IκBα (Bai et al., 2009; Yang et al., 2016). TAK1 can furthermore activate the mitogen-activated protein kinase (MAPK) signaling pathways, including extracellular signal-regulated kinase (ERK), c-Jun N-terminal kinase (JNK) and p38, leading to an activation of the transcription factor activator protein 1 (AP-1) and its translocation into the cell nucleus. Together with NF-κB, AP-1 contributes to the expression of several pro-inflammatory cytokines, e.g. IL-1, IL-6, IL-8 and TNF-α (Zarubin and Han, 2005; Yang et al., 2016; Lee and Kim, 2017).

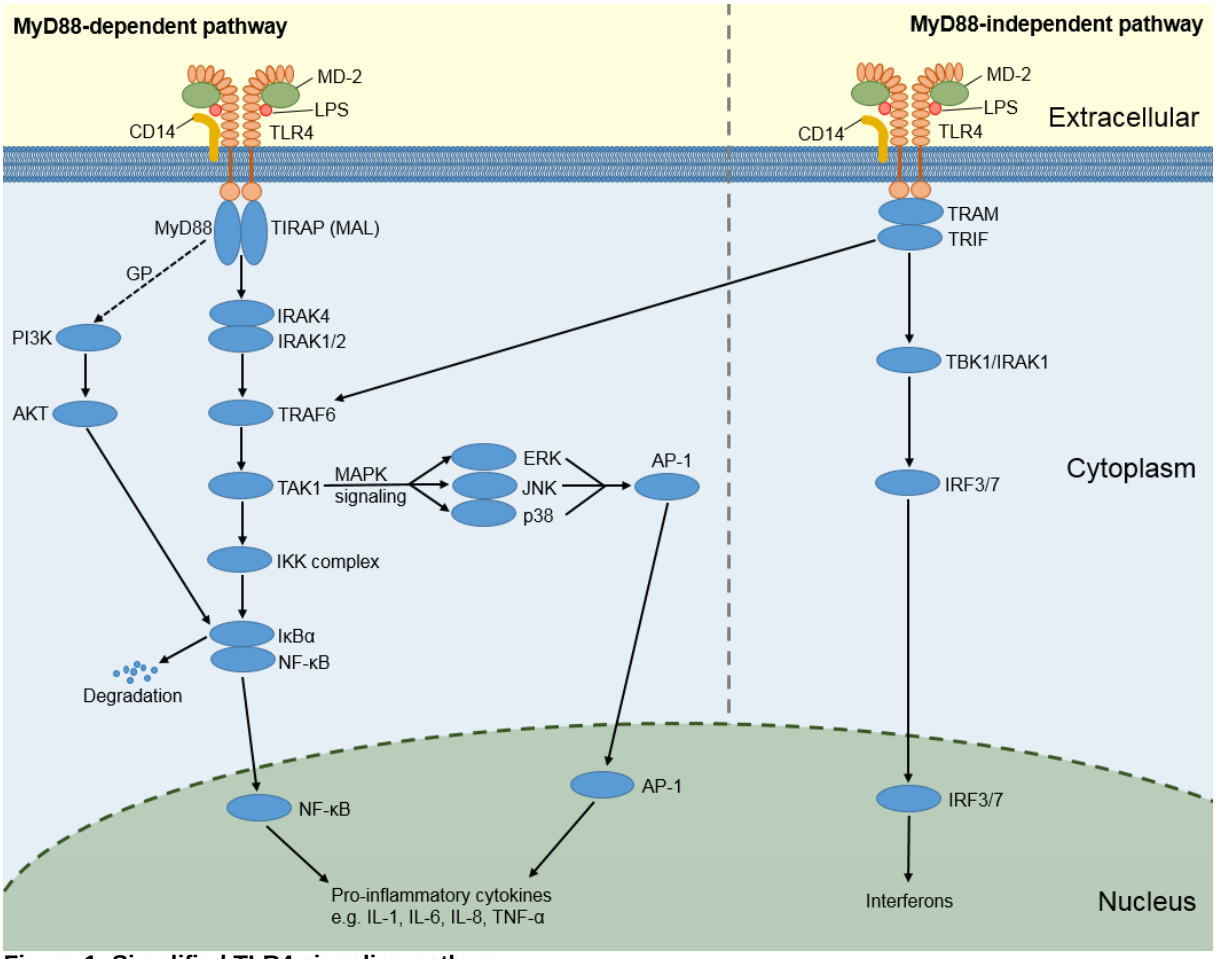

Figure 1: Simplified TLR4 signaling pathway
LPS is presented to TLR4 via CD14. MD-2 is required for binding of LPS to TLR4. After stimulation, the inflammatory signal can be transmitted through MyD88-dependent (left) or MyD88-independent pathway (right). In a simplified MyD88-dependent pathway, MyD88 in complex with TIRAP (MAL) binds to the IRAK complex consisting of IRAK4 and IRAK1/2, which interact with TRAF6. TRAF6 then forms a complex with TAK1. After activation of IKK complex by TAK1, IκBα is phosphorylated, which leads to its ubiquitination and degradation. Subsequently, NF-κB is activated and translocates into the cell nucleus. Furthermore, upon stimulation of TLR4, GP can lead to a dissociation of TLR4 from MyD88. After binding to PI3K, AKT is phosphorylated and phosphorylates itself IκBα. TAK1 can additionally activate MAPK signaling pathway including ERK, JNK and p38, leading to an activation of AP-1 and its translocation into the cell nucleus. NF-κB and AP-1 contribute to the expression of several pro-inflammatory cytokines, e.g. IL-1, IL-6, IL-8 and TNF-α. The simplified MyD88-independent pathway (right) is initiated by TRAM and TRIF. After activation, TBK1 and IRAK1 phosphorylate IRF3 and IRF7, respectively. Activated IRFs translocate into the cell nucleus and contribute to the expression of antiviral interferons. TRIF can also act on the MyD88-dependent pathway by recruiting TRAF6 and activation of TAK1. CD14: Cluster of differentiation 14, GP: glucan phosphate, IKK: IκB kinase, LPS: lipopolysaccharide, MAL: MyD88 adapter-like, MAPK: mitogen-activated protein kinase, MD-2: myeloid differentiation factor 2, PI3K: phosphatidylinositol 3-kinase, TAK1: transforming growth factor β-activated kinase 1, TBK1: TANK-binding kinase 1, TIRAP: TIR domain containing adaptor protein, TRAM: TRIF-related adaptor molecule, TRIF: TIR-domain-containing adapter-inducing interferon-β.

Although NF-κB and AP-1 are controlled by different mechanisms, they seem to be activated simultaneously via the same intracellular signaling cascades. Many genes, like the IL-8 promoter require the activation of both proteins, leading to the suggestion that these transcription factors work cooperatively and might even mutually influence their activities (Fujioka et al., 2004). Since several pro-inflammatory signaling pathways cumulate in the translocation of the transcription factor NF-κB p50/p65 from the cytoplasm into the cell nucleus, inhibition of NF-κB translocation is an important aim in the treatment of inflammation

(Takeuchi and Akira, 2001; Ghosh and Dass, 2016). NF-κB was also shown to strongly influence macrophage polarization (Fraternale et al., 2015). The simplified MyD88-independent signaling pathway (**Figure 1**, right) is initiated by TRAM and TRIF. After being recruited, TRIF interacts with TANK-binding kinase 1 (TBK1) to activate the transcription factor interferon regulatory factor 3 (IRF3). TRIF furthermore interacts with IRAK1 to phosphorylate the transcription factor IRF7. The activated IRFs translocate into the nucleus and contribute to the expression of antiviral interferons, such as interferon β (IFNβ). TRIF can also act on the MyD88-dependent pathway by recruiting TRAF6 and activation of TAK1 (Yang et al., 2016). Molecules within the TLR2/TLR4 signaling cascades, which were further investigated with this research, are e.g. IκBα and AKT, whose activations lead to translocation of NF-κB into the cell nucleus, as well as p38, which primarily induces AP-1 translocation into the cell nucleus (**chapter 4.2.3** and **chapter 4.3.5**).

The initial immune response is mitigated over time in healthy individuals by negative feedback loops, leading to a reduced pro-inflammatory cytokine production. In contrast, the appropriate control of TLRs and their signaling cascades might be missing in maladies associated with chronic inflammatory processes, leading to overreactions (Chahal et al., 2013). Therefore, antagonists for TLR signaling, particularly TLR4, might play an important role in counter-regulation. Some synthetic compounds, e.g. eritoran and TAK-242 (resatorvid) were shown to mitigate TLR4-dependent inflammatory signaling via the intravenous route and are explored for sepsis treatment (Yamada et al., 2005; Tidswell et al., 2010; Peri and Calabrese, 2014). In addition, natural compounds, e.g. epigallocatechin-3-gallate (EGCG) and 6-shogaol (**chapter 1.2**) are known to modestly inhibit TLR4 signaling, but also interfere with many other pathways (Youn et al., 2006a; Park et al., 2009; Peri and Calabrese, 2014). Nonetheless, to date, no effective orally active TLR4 antagonists are available for clinical application.

1.5. Cinnamon

One prominent plant extract comprising anti-inflammatory activities is cinnamon bark extract. Besides screening of several herbal extracts, a main focus of this work was set on cinnamon. Therefore, its species, reported (active) compounds and beneficial health effects will be discussed more detailed.

1.5.1. Cinnamon species

Cinnamon, the inner bark of a tropical evergreen tree, is one of the most important and oldest known spices used worldwide for flavouring as well as in traditional and modern

medicines. Cinnamon trees commonly grow at lower altitudes, but can also be observed in altitudes up to 500 m (Jayaprakasha and Rao, 2011). The genus *Cinnamomum (C.)*, which belongs to the *Lauraceae* family, comprises approximately 250 species with trees spread all over the world (Rao and Gan, 2014). Some of the important cinnamon species used in food industry and/or in traditional and modern medicine, are listed in **Table 2** (Jayaprakasha and Rao, 2011).

Table 2: Cinnamon species

Latin name	Common English name(s)	Originated in
C. cassia (botanical synonym: *C. aromaticum*)	Chinese cinnamon, Cassia	China
C. verum (botanical synonym: *C. zeylanicum*)	True cinnamon, Ceylon cinnamon	Sri Lanka, India
C. burmannii	Indonesian cassia, Indonesian cinnamon	Indonesia
C. loureirii	Vietnamese cassia, Saigon cinnamon	Vietnam
C. tamala	Indian cassia	India, Nepal
C. cordatum		Malaysia

C. verum is the preferred cinnamon species of the food industry, whereas both *C. cassia* and *C. verum* are used by pharmaceutical manufacturers interchangeably (Jayaprakasha and Rao, 2011). Due to its fragrance, which can be integrated into various foods, perfumes and medicinal products, cinnamon is largely used in aroma and essence industries (Rao and Gan, 2014). Furthermore, several beneficial health effects have been reported for cinnamon and/or its active compounds (**chapter 1.5.3**).

1.5.2. Compounds of cinnamon extract

Cinnamon as complex mixture consists of more than 80 compounds, which often strongly differ in the contained ratios. Besides the varying distribution of the compounds depending on different cultivation areas, cinnamon species and plant parts (e.g. leaf, bark, fruit and flower), compound identification is also highly influenced by the solvents and methods used for extraction. The major compounds generally identified in cinnamon are cinnamaldehyde in barks, eugenol in leaves, camphor in roots and *trans*-cinnamyl acetate in fruits and flowers (Jayaprakasha and Rao, 2011; Hariri and Ghiasvand, 2016). The spicy taste and fragrance of cinnamon has been mainly attributed to cinnamaldehyde (Hariri and Ghiasvand, 2016). One of the more critical compounds present in different species of cinnamon is coumarin, a secondary phytochemical, which has been reported to possess hepatotoxic and carcinogenic properties (Abraham et al., 2011; Fotland et al., 2012). Its content in *C. verum* powder is rather low (from below detection limit up to 297 mg/kg), whereas *C. cassia* contains substantially more coumarin (from 1740 mg/kg up to 7670 mg/kg) (Woehrlin et al., 2010).

The lowest dose documented to induce hepatoxicity was 25 mg coumarin/person per day (corresponding to 0.4 mg/kg bodyweight per day) for a few days. A tolerable daily intake (TDI) of 0.1 mg coumarin/kg bodyweight has been established by the European food safety authority (EFSA). Furthermore, a coumarin exposure three times higher than the TDI for one to two weeks was stated to be safe (Abraham et al., 2011; Fotland et al., 2012). Therefore, for the majority of the population, which are consuming low or moderate cinnamon amounts, no risk of hepatotoxicity due to coumarin content is expected (Abraham et al., 2010). Nevertheless, consumption of *C. verum* instead of *C. cassia* additionally decreases the risk for coumarin-induced hepatotoxicity. Since bark from *C. verum* has been investigated in this work, **Table 3** focuses on the main compounds reported to be present in this cinnamon species.

Table 3: Main compounds of *C. verum*

Plant part	Compound	Molecular formula	Molecular weight (g/mol)	Amount (%)	Reference
Bark	Cinnamaldehyde	C_9H_8O	132.162	60-83	Jayaprakasha and Rao, 2011; Gunawardena et al., 2015; Hariri and Ghiasvand, 2016
				33-39	Khuwijitjaru et al., 2012
	Camphor	$C_{10}H_{16}O$	152.237	15	Jayaprakasha and Rao, 2011
	o-Methoxycinnamaldehyde	$C_{10}H_{10}O_2$	162.188	13-23	Gunawardena et al., 2015
	trans-Cinnamyl acetate	$C_{11}H_{12}O_2$	176.215	5-10	Jayaprakasha and Rao, 2011
	Eugenol	$C_{10}H_{12}O_2$	164.204	5-10	Hariri and Ghiasvand, 2016
	Caryophyllene	$C_{15}H_{24}$	204.357	6	Jayaprakasha and Rao, 2011
	α-Terpineol	$C_{10}H_{18}O$	154.253	4	Jayaprakasha and Rao, 2011
	Coumarin	$C_9H_6O_2$	146.145	4	Khuwijitjaru et al., 2012
				3	Jayaprakasha and Rao, 2011
				<1	Woehrlin et al., 2010; Gunawardena et al., 2015
	Benzyl benzoate	$C_{14}H_{12}O_2$	212.248	1	Gunawardena et al., 2015
	Cinnamic acid	$C_9H_8O_2$	148.161	<1	Gunawardena et al., 2015
				<1	Khuwijitjaru et al., 2012
	Cinnamyl alcohol	$C_9H_{10}O$	134.178	<1	Gunawardena et al., 2015
				<1	Khuwijitjaru et al., 2012
Leaves	Eugenol	$C_{10}H_{12}O_2$	164.204	70-95	Jayaprakasha and Rao, 2011; Hariri and Ghiasvand, 2016
	p-Cymene	$C_{10}H_{14}$	134.222	21	Jayaprakasha and Rao, 2011
	Linalool	$C_{10}H_{18}O$	154.253	2-9	Jayaprakasha and Rao, 2011
	Caryophyllene	$C_{15}H_{24}$	204.357	2-6	Jayaprakasha and Rao, 2011
	Cinnamaldehyde	C_9H_8O	132.162	1-5	Hariri and Ghiasvand, 2016
	Piperitone	$C_{10}H_{16}O$	152.237	3	Jayaprakasha and Rao, 2011
	trans-Cinnamyl acetate	$C_{11}H_{12}O_2$	176.215	2	Jayaprakasha and Rao, 2011
	Benzyl benzoate	$C_{14}H_{12}O_2$	212.248	<1	Jayaprakasha and Rao, 2011
Flowers	*trans*-Cinnamyl acetate	$C_{11}H_{12}O_2$	176.215	42	Jayaprakasha et al., 2000
	α-Bergamotene	$C_{15}H_{24}$	204.357	8	Jayaprakasha et al., 2000
	Caryophyllene oxide	$C_{15}H_{24}O$	220.356	7	Jayaprakasha et al., 2000

Plant part	Compound	Molecular formula	Molecular weight (g/mol)	Amount (%)	Reference
Fruits	*trans*-Cinnamyl acetate	$C_{11}H_{12}O_2$	176.215	42-55	Jayaprakasha and Rao, 2011; Hariri and Ghiasvand, 2016
	Caryophyllene	$C_{15}H_{24}$	204.357	9-14	Hariri and Ghiasvand, 2016
Fruit stalks	*trans*-Cinnamyl acetate	$C_{11}H_{12}O_2$	176.215	37	Jayaprakasha et al., 2003
	Caryophyllene	$C_{15}H_{24}$	204.357	22	Jayaprakasha et al., 2003
Roots	Camphor	$C_{10}H_{16}O$	152.237	60	Hariri and Ghiasvand, 2016
Buds	α-Bergamotene	$C_{15}H_{24}$	204.357	27	Hariri and Ghiasvand, 2016
	α-Copaene	$C_{15}H_{24}$	204.357	23	Hariri and Ghiasvand, 2016

1.5.3. Beneficial health effects

The inner bark of cinnamon has been used in traditional medicine for centuries, e.g. for the treatment of common cold, prevention of nausea and vomiting as well as for the treatment of cardiovascular and chronic gastrointestinal disorders, or as general stimulant (Jayaprakasha and Rao, 2011; Hong et al., 2012). But also from current literature, several beneficial health effects have been revealed for cinnamon bark. Ethanolic *C. verum* bark extracts have been observed to mitigate the release of several pro-inflammatory markers, e.g. TNF-α in LPS-stimulated human peripheral blood mononuclear cells (PBMCs) (Gunawardena et al., 2014), nitric oxide (NO), TNF-α, IL-1β and IL-6 production in LPS-activated BV2 microglia cells, as well as to reduce NF-κB activation (Ho et al., 2013). Furthermore, the cinnamon extract obtained from Maros Arznei, which was also used for our studies, has been shown to possess anti-inflammatory effects in a mouse model of alcohol-induced fatty liver (Kanuri et al., 2009) and on colitis in IL-10 knockout mice (Hagenlocher et al., 2016; Hagenlocher et al., 2017). In addition, cinnamon extract has been demonstrated to possess anti-inflammatory effects in mouse models of multiple sclerosis (Mondal and Pahan, 2015), arthritis and diabetes (Sheng et al., 2008; Hariri and Ghiasvand, 2016). In a pilot study, cinnamon bark extract in combination with acerola fruit concentrate and Spanish needles leaf and stem dehydrated powder has been shown to be safe and to possess antiallergic properties in patients with seasonal allergic rhinitis (Corren et al., 2008). In a phase I clinical study with healthy adults, *C. verum* treatment for three months with monthly increasing doses from 85 mg per day to 500 mg per day has been demonstrated to induce neither toxic nor serious side effects. Furthermore, beneficial blood pressure lowering and antihyperlipidemic effects have been observed (Ranasinghe et al., 2017).

trans-Cinnamaldehyde, the major compound in *C. verum* bark (**chapter 1.5.2**) has been observed to possess diverse beneficial health effects, e.g. antiallergic (Hagenlocher et al., 2015), anti-neuroinflammatory (Ho et al., 2013), antifungal, anticancer, antidiabetic and anti-inflammatory effects (de Cássia da Silveira et al., 2014; Gunawardena et al., 2015; Zhu et al., 2017). The cinnamaldehyde-dependent inhibition of the production of pro-inflammatory

markers, e.g. IL-1β, TNF-α, ROS, inducible nitric oxide synthase (iNOS) and COX-2 has been demonstrated in several studies (Kim et al., 2007; Chao et al., 2008; Gunawardena et al., 2015). Despite some toxic effects at high cinnamaldehyde doses, this compound is considered as safe and well tolerated in animals and humans with 1.25 mg/kg as suggested acceptable daily intake (ADI) by EFSA and food and drug administration (FDA) (Zhu et al., 2017). One mechanism of the potent anti-inflammatory effects of cinnamaldehyde has been revealed to be the suppression of TLR4 receptor oligomerization (Youn et al., 2008). Furthermore, TLR4-independent beneficial effects have been described e.g. in diabetes via upregulation of peroxisome proliferator-activated receptor gamma (PPARγ) gene expression (Hosni et al., 2017). PPARγ activation can inhibit several major signaling pathways, such as the signaling pathways of the MAPKs ERK1/2 and p38 as well as NF-κB (Giaginis et al., 2009). In addition to the observed anti-inflammatory effects for cinnamaldehyde treatment, also further compounds of cinnamon extract have been observed to reduce inflammatory signals. Benzyl benzoate and *o*-methoxycinnamaldehyde have been reported to strongly decrease TNF-α production (Gunawardena et al., 2015). Furthermore, benzyl benzoate, *o*-methoxycinnamaldehyde, eugenol, cinnamyl alcohol and cinnamic acid have been shown to inhibit NO production (Ho et al., 2013; Gunawardena et al., 2015). Inhibition of TNF-α, IL-1β and IL-6 production in combination with an increase of the anti-inflammatory marker IL-10 has been reported for *p*-cymene treatment (Zhong et al., 2013).

1.6. Aim of research

Acute and chronic inflammation play an important role in many severe diseases, often with the involvement TLR signaling pathways. Particularly the signaling pathway of TLR4, whose MyD88-dependent signaling cascade is, among others, shared with TLR2, offer important targets to mitigate the inflammatory reactions. Various herbal extracts, each consisting of numerous compounds, are reported to improve human health, but the active compounds and underlying biochemical mechanisms are often not fully identified. Moreover, the biological activities may be positively or negatively modulated by combinations of several compounds within the extracts.

Therefore, the objective of this research was to identify herbal extracts and their active compounds attenuating the signaling pathways of inflammation, especially through TLR2 and TLR4. In different LPS-stimulated cell lines, 99 ethanolic extracts were screened for their anti-inflammatory activities. The most promising candidates were additionally tested for TLR4 specific antagonistic properties in cell culture-based assays. The second part focused on one of the most promising extracts. Compounds of the extract were identified and their anti-inflammatory potential as well as their synergistic effects were explored. Additionally, the

influences of the extract and its active compounds on TLR2 and TLR4 signaling pathway molecules were investigated.

2. Equipment and materials

2.1. Equipment

Equipment used in this work is listed in **Table 4**. Further equipment corresponds to general laboratory equipment.

Table 4: Used equipment

Name	Company
Analytical balance AET 200-4NM	Kern&Sohn, Balingen, Germany
Autoclave Systec 2540EL	Tuttnauer, Breda, The Netherlands
Autoclave VX-40	Systec, Linden, Germany
Automated Cell Counter TC20	Bio-Rad Laboratories, München, Germany
Cell culture CO_2 incubator Heracell 240i	Thermo Fisher Scientific, Darmstadt, Germany
Centrifuge Heraeus Megafuge 16R	Thermo Fisher Scientific, Darmstadt, Germany
ChemiDoc Touch Imaging System with ImageLab software	Bio-Rad Laboratories, München, Germany
Concentrator RVC 2-25 CDplus	Martin Christ Gefriertrocknungsanlagen, Osterode am Harz, Germany
Concentrator Six Port Mini-Vap	Sigma-Aldrich, Darmstadt, Germany
Dishwasher G 7883 CD	Miele, Gütersloh, Germany
Drying oven FED 53	Binder, Tuttlingen, Germany
Electrophoresis SDS-PAGE Mini-Protean Tetra Cell	Bio-Rad Laboratories, München, Germany
GC column DB-5MS+DG 30 m x 0.250 mm I.D., 0.25 µm film thickness	Agilent Technologies, Waldbronn, Germany
GC-MS Trace 1310 GC – TSQ 8000 Evo MS	Thermo Fisher Scientific, Darmstadt, Germany
GraphPad Prism version 5.01 for Windows	GraphPad Software, San Diego, CA, USA
HP 6890 gas chromatograph coupled to HP 5972 mass spectrometer with NIST 2005 mass spectral library	Hewlett-Packard, Bad Homburg, Germany
HPLC 1260 Infinity coupled to UHD Accurate Mass Quadrupole-time-of-flight (Q-TOF) LC/MS 6540	Agilent Technologies, Waldbronn, Germany
HPLC 1290 Infinity	Agilent Technologies, Waldbronn, Germany
HPLC column Zorbax Eclipse XDB-C18 2.1x150 mm, 3.5 µm + guard column	Agilent Technologies, Waldbronn, Germany
HPLC column Zorbax Eclipse XDB-C18 4.6x150 mm, 5 µm + guard column	Agilent Technologies, Waldbronn, Germany
Incubation shaker Innova 42 New Brunswick	Eppendorf, Hamburg, Germany
LightPad 930	Artograph, Delano, MN, USA
Microcentrifuge Micro Star 17	VWR, Darmstadt, Germany
Microscope Axio	Zeiss, Oberkochen, Germany
Microscope Eclipse TS100 with software NIS Elements Documentation	Nikon, Tokyo, Japan
Multi detection reader Synergy Neo with Gen5 software	BioTek, Bad Friedrichshall, Germany
Opera Phenix High-Content Screening system with Harmony software	PerkinElmer, Rodgau, Germany
Pipette boy Accu-jet pro	BRAND, Wertheim, Germany

Name	Company
Plate washer Hydro speed	Tecan, Männedorf, Switzerland
Shaker KS 130 basic	IKA, Wilmington, NC, USA
Shaker Rocker 3D basic	IKA, Wilmington, NC, USA
Sterile hood MSC-Advantage	Thermo Fisher Scientific, Darmstadt, Germany
Thermomixer C	Eppendorf, Hamburg, Germany
Thermomixer comfort	Eppendorf, Hamburg, Germany
Tube Roller SUN1400	Sunlab Instruments, Mannheim, Germany
Ultrasonic cleaner USC-T	VWR, Darmstadt, Germany
Vacuum bags Caso, 20x30cm	CASO Germany - Firma Braukmann, Arnsberg, Germany
Vacuum device V.200 Premium	Landig + Lava, Bad Saulgau, Germany
Water bath	Memmert, Schwabach, Germany
Water remote dispenser, Q-POD ultrapure	Merck, Darmstadt, Germany
Western blotting device Trans-Blot Cell	Bio-Rad Laboratories, München, Germany

2.2. Consumables

Consumables used in this work are listed in **Table 5**. Further consumables correspond to general laboratory equipment.

Table 5: Used consumables

Name	Company
12-well plate (glass bottom)	Cellvis, Mountain View, CA, USA
48-well microtiter plate cell culture (clear plate, clear F-bottom)	Eppendorf, Hamburg, Germany
96-well microtiter plate (clear plate, clear F-bottom), microloan, medium binding	Greiner Bio-One, Solingen, Germany
96-well microtiter plate (white plate, white F-bottom)	Greiner Bio-One, Solingen, Germany
96-well microtiter plate cell culture (black plate, clear F-bottom)	Greiner Bio-One, Solingen, Germany
96-well microtiter plate cell culture (clear plate, clear F-bottom)	Greiner Bio-One, Solingen, Germany
96-well microtiter plate cell culture (clear plate, clear V-bottom)	Greiner Bio-One, Solingen, Germany
Blotting paper	Carl Roth, Karlsruhe, Germany
Cell culture flasks Cellstar, diverse sizes	Becton Dickinson, Heidelberg, Germany
Collecting test tubes for HPLC, 12x48 mm	Agilent Technologies, Waldbronn, Germany
Counting slides, dual chamber for cell counter	Bio-Rad Laboratories, München, Germany
Cryotubes	Greiner Bio-One, Solingen, Germany
Filters, Rotilabo-folded (type 113P)	Carl Roth, Karlsruhe, Germany
Needle, agani, 25G x 1½ ‘‘	Terumo, Eschborn, Germany
Pipette tips, diverse sizes	Eppendorf, Hamburg, Germany
Pipette tips, diverse sizes	STARLAB, Hamburg, Germany
Plate sealer, Easyseal, transparent, 79x135 mm	Greiner Bio-One, Solingen, Germany
Polysine adhesion microscope slides	Thermo Fisher Scientific, Darmstadt, Germany

Name	Company
Reagent reservoirs, sterile	Carl Roth, Karlsruhe, Germany
Serological pipettes, diverse sizes	Greiner Bio-One, Solingen, Germany
Syringe, single-use, Omnifix-F	B. Braun Melsungen, Melsungen, Germany
Tubes, diverse sizes	Eppendorf, Hamburg, Germany
Tubes, diverse sizes	Corning, Amsterdam, The Netherlands
Vials, 2 ml amber with 9 mm screw caps	Agilent Technologies, Waldbronn, Germany
0.2 µm Nalgene Rapid-Flow sterile filtration product	Thermo Fisher Scientific, Darmstadt, Germany
Nitrocellulose membrane, 0.2 µm	Bio-Rad Laboratories, München, Germany
Centrifuge tube filters Spin-X, 0.22 µm cellulose/acetate membrane	Corning, Amsterdam, The Netherlands

2.3. Chemicals and reagents

Chemicals and reagents used in this work are listed in **Table 6**. Further chemicals and reagents correspond to general laboratory equipment.

Table 6: Used chemicals

Name	Company
2-Propanol	Sigma-Aldrich, Darmstadt, Germany
Acetone	Carl Roth, Karlsruhe, Germany
Acetonitrile	VWR, Darmstadt, Germany
Acetonitrile	Thermo Fisher Scientific, Darmstadt, Germany
Acrylamide (30% Acrylamide/Bis Solution)	Bio-Rad Laboratories, München, Germany
Acrylamide (30% Acrylamide/Bis Solution)	Sigma-Aldrich, Darmstadt, Germany
AKT (pan) (11E7) western blot primary antibody (rabbit)	Cell Signaling Technology, Leiden, The Netherlands
Alamar Blue Cell Viability Assay	Thermo Fisher Scientific, Darmstadt, Germany
Ancillary Reagent Kit 2	R&D Systems, Abingdon, United Kingdom
Anti-mouse IgG (H+L)-HRPO (goat)	Dianova, Hamburg, Germany
Anti-rabbit IgG (H+L) cross-adsorbed secondary antibody, Alexa Fluor 568 (goat)	Thermo Fisher Scientific, Darmstadt, Germany
Anti-rabbit IgG (H+L)-HRPO (goat)	Dianova, Hamburg, Germany
Anti-rat IgG (H+L)-HRPO (goat)	Dianova, Hamburg, Germany
APS	Sigma-Aldrich, Darmstadt, Germany
ATIs	Institute for Translational Immunology of University Medicine, Mainz, Germany
BCA Protein Assay Kit Pierce	Thermo Fisher Scientific, Darmstadt, Germany
Benzoic acid	Sigma-Aldrich, Darmstadt, Germany
Blasticidine S hydrochloride	Sigma-Aldrich, Darmstadt, Germany
Bromophenol blue	Carl Roth, Karlsruhe, Germany
BSA	Cell Signaling Technology, Leiden, The Netherlands
Chloroform	Carl Roth, Karlsruhe, Germany
Cinnamyl alcohol	Sigma-Aldrich, Darmstadt, Germany
Color Prestained Protein Standard, Broad Range	New England BioLabs, Frankfurt, Germany
Dichloromethane (GC Ultragrade)	Carl Roth, Karlsruhe, Germany

Name	Company
Dichloromethane for analysis	Merck, Darmstadt, Germany
DMEM, high glucose	Thermo Fisher Scientific, Darmstadt, Germany
DMSO	Sigma-Aldrich, Darmstadt, Germany
DPBS, calcium, magnesium	Thermo Fisher Scientific, Darmstadt, Germany
DPBS, no calcium, no magnesium	Thermo Fisher Scientific, Darmstadt, Germany
DTT	Sigma-Aldrich, Darmstadt, Germany
ECL Plus Western Blotting Substrate	Thermo Fisher Scientific, Darmstadt, Germany
ELISA Reagent B Set	BD Biosciences, Heidelberg, Germany
Ethanol, absolute	Carlo Erba, Val de Reuil, France
Ethanol, absolute	Merck, Darmstadt, Germany
Ethanol, absolute	Sigma-Aldrich, Darmstadt, Germany
Ethanol, absolute	VWR, Darmstadt, Germany
Ethanol, GC purity	Merck, Darmstadt, Germany
FCS	Biochrom, Berlin, Germany
Formaldehyde (Pierce 16%, methanol-free)	Thermo Fisher Scientific, Darmstadt, Germany
Geneticindisulfat (G418-Sulfat)	Carl Roth, Karlsruhe, Germany
Gluten-free diet (mouse)	Ssniff, Soest, Germany
Glycerol	Sigma-Aldrich, Darmstadt, Germany
Glycine	Sigma-Aldrich, Darmstadt, Germany
HEK-Blue Detection	InvivoGen, Toulouse, France
HEK-Blue Selection	InvivoGen, Toulouse, France
Helium (>99.9999%)	Messer Austria, Gumpoldskirchen, Austria
Human IL-10 ELISA	BD Biosciences, Heidelberg, Germany
Human IL-8 ELISA	BD Biosciences, Heidelberg, Germany
Human TNF ELISA	BD Biosciences, Heidelberg, Germany
Hydrochloric acid	Merck, Darmstadt, Germany
Hygromycin B gold (solution)	InvivoGen, Toulouse, France
IFNγ	Thermo Fisher Scientific, Darmstadt, Germany
Incidin Plus	VWR, Darmstadt, Germany
Isopropanol 70%	Carl Roth, Karlsruhe, Germany
IκBα western blot primary antibody (mouse)	Cell Signaling Technology, Leiden, The Netherlands
Ketamine	Siegfried Hameln, Hameln, Germany
LAL Chromogenic Endotoxin Quantitation Kit Pierce	Thermo Fisher Scientific, Darmstadt, Germany
LPS-EB (from *E. coli* OIII:B4)	InvivoGen, Toulouse, France
LPS-EB ultrapure (from *E. coli* OIII:B4)	InvivoGen, Toulouse, France
Luciferase Assay LightSwitch	Novus Biologicals, Littleton, CO, USA
Methanol	VWR, Darmstadt, Germany
Methanol (gradient grade for LC)	Merck, Darmstadt, Germany
Methanol (gradient grade)	Sigma-Aldrich, Darmstadt, Germany
Methyl salicylate	Sigma-Aldrich, Darmstadt, Germany
Milk powder, nonfat dry milk	Cell Signaling Technology, Leiden, The Netherlands
Mouse CXCL1/KC ELISA	R&D Systems, Abingdon, United Kingdom
Mouse IL-6 ELISA	eBiosciences, Thermo Fisher Scientific, Darmstadt, Germany
MTT assay	Sigma-Aldrich, Darmstadt, Germany

Name	Company
NaCl	Sigma-Aldrich, Darmstadt, Germany
NF-κB p65 (D14E12) primary antibody (rabbit)	Cell Signaling Technology, Leiden, The Netherlands
Nickel(II)-chloride hexahydrate	Carl Roth, Karlsruhe, Germany
Nickel(II)-sulfate hexahydrate	Carl Roth, Karlsruhe, Germany
Nitrogen gas	Westfalen, Münster, Germany
p38α (9F12) western blot primary antibody (mouse)	Santa Cruz Biotechnology, Heidelberg, Germany
P-AKT (Ser473) (D9E) western blot primary antibody (rabbit)	Cell Signaling Technology, Leiden, The Netherlands
Palmitic acid	Sigma-Aldrich, Darmstadt, Germany
Pam2CSK4	InvivoGen, Toulouse, France
p-Cymene	Sigma-Aldrich, Darmstadt, Germany
Penicillin/streptomycin (10,000 U/ml)	Thermo Fisher Scientific, Darmstadt, Germany
P-IκBα (Ser36) western blot primary antibody (rabbit)	Abcam, Cambridge, United Kingdom
PMA	Sigma-Aldrich, Darmstadt, Germany
Ponceau S solution	Sigma-Aldrich, Darmstadt, Germany
P-p38 (E-1) western blot primary antibody (mouse)	Santa Cruz Biotechnology, Heidelberg, Germany
Puromycin	Sigma-Aldrich, Darmstadt, Germany
Rompun	Bayer, Leverkusen, Germany
RPMI 1640 medium	Thermo Fisher Scientific, Darmstadt, Germany
SDS 20%	Carl Roth, Karlsruhe, Germany
SILMAS	Sigma-Aldrich, Darmstadt, Germany
Stearic acid	Sigma-Aldrich, Darmstadt, Germany
TEMED	Sigma-Aldrich, Darmstadt, Germany
trans-Cinnamaldehyde	Sigma-Aldrich, Darmstadt, Germany
trans-Cinnamic acid	Sigma-Aldrich, Darmstadt, Germany
Tris	Carl Roth, Karlsruhe, Germany
Trypsin-EDTA (0.25%), phenol red	Thermo Fisher Scientific, Darmstadt, Germany
Tubulin western blot primary antibody (rat)	Abcam, Cambridge, United Kingdom
Tween-20	Carl Roth, Karlsruhe, Germany
Vinculin western blot primary antibody (mouse)	Abcam, Cambridge, United Kingdom
Water with 0.1% formic acid	VWR, Darmstadt, Germany
Water with 0.1% formic acid	Sigma-Aldrich, Darmstadt, Germany
WST-8 assay	Sigma-Aldrich, Darmstadt, Germany
β-Mercaptoethanol	Sigma-Aldrich, Darmstadt, Germany

2.4. Extracts

Ethanolic extracts used for screening are listed in **Table 7**. Most of them were purchased from Maros Arznei. Further samples were obtained from different sources to freshly prepare the extracts (**chapter 3.1**).

Table 7: Ethanolic extracts tested for anti-inflammatory properties

Latin name	Common English name	Used part	Source
Achillea millefolium	Common yarrow	Whole plant	Maros Arznei, Fürth, Germany
Aconitum napellus	Monkshood	Whole plant	Maros Arznei, Fürth, Germany
Aesculus hippocastanum	Horse-chestnut	Fruit/berry/seed	Maros Arznei, Fürth, Germany
Alchemilla vulgaris	Common lady's mantle	Whole plant	Maros Arznei, Fürth, Germany
Allium sativum	Garlic	Root[2]	Farmer's market, Mainz, Germany
Allium ursinum	Wild garlic	Leaf[1]	Tee und Gewürze Lilianna Kamberg und Marianne Schmidt, Offenbach, Germany
Aloe ferox	Aloe	Whole plant	Maros Arznei, Fürth, Germany
Alpinia officinarum	Galangal	Root	Maros Arznei, Fürth, Germany
Althaea officinalis	Common marshmallow	Root	Maros Arznei, Fürth, Germany
Arctostaphylos uva-ursi	Bearberry	Leaf	Maros Arznei, Fürth, Germany
Armoracia rusticana	Horseradish	Root[2]	Farmer's market, Mainz, Germany
Arnica montana	Arnica	Whole plant	Maros Arznei, Fürth, Germany
Arnica montana	Arnica	Flower	Maros Arznei, Fürth, Germany
Artemisia absinthium	Wormwood	Whole plant	Maros Arznei, Fürth, Germany
Avena sativa	Oat	Whole plant	Maros Arznei, Fürth, Germany
Betula alba	Birch	Juice/resin	Maros Arznei, Fürth, Germany
Betula verrucosa	Weeping birch	Juice/resin	Maros Arznei, Fürth, Germany
Boswellia carterii	Frankincense	Whole plant[1]	Olibanum B.V., Kerkrade, Netherlands
Boswellia serrata	Frankincense	Juice/resin	Maros Arznei, Fürth, Germany
Calendula officinalis	Marigold	Flower	Maros Arznei, Fürth, Germany
Camellia sinensis (L.)	Green tea	Leaf[1]	Ostfriesische Tee Gesellschaft, Seevetal, Germany
Capsicum frutescens	Chili	Fruit/berry/seed[1]	Tee und Gewürze Lilianna Kamberg und Marianne Schmidt, Offenbach, Germany
Carum carvi	Caraway	Fruit/berry/seed	Maros Arznei, Fürth, Germany
Castanea sativa	Sweet chestnut	Leaf	Maros Arznei, Fürth, Germany
Chelidonium majus	Celandine	Root	Maros Arznei, Fürth, Germany
Chlorella pyrenoidosa	Chlorella	Whole green algae[1]	Naturya, Southstoke, United Kingdom
Cinchona pubescens	Cinchona	Bark	Maros Arznei, Fürth, Germany
Cinnamomum verum	Cinnamon	Bark	Maros Arznei, Fürth, Germany
Convallaria majalis	Lily of the valley	Whole plant	Maros Arznei, Fürth, Germany
Coriandrum sativum	Coriander	Fruit/berry/seed	Maros Arznei, Fürth, Germany
Crataegus species	Hawthorn	Fruit/berry/seed	Maros Arznei, Fürth, Germany
Curcuma longa	Turmeric	Root	Maros Arznei, Fürth, Germany
Cynara scolymus	Artichoke	Leaf	Maros Arznei, Fürth, Germany
Daucus carota subsp. *sativus*	Carrot	Root[2]	Aldi Süd, Mainz, Germany
Digitalis purpurea	Common foxglove	Leaf	Maros Arznei, Fürth, Germany
Dioscorea villosa	Yam	Root	Maros Arznei, Fürth, Germany
Echinacea purpurea	Purple coneflower	Whole plant	Maros Arznei, Fürth, Germany

Latin name	Common English name	Used part	Source
Elettaria cardamomum	Cardamom	Fruit/berry/seed[1]	Tee und Gewürze Lilianna Kamberg und Marianne Schmidt, Offenbach, Germany
Equisetum arvense	Field horsetail	Whole plant	Maros Arznei, Fürth, Germany
Erythraea centaurium	Common centaury	Whole plant	Maros Arznei, Fürth, Germany
Euphrasia officinalis	Eyebright	Whole plant	Maros Arznei, Fürth, Germany
Filipendula ulmaria	Meadowsweet	Flower	Maros Arznei, Fürth, Germany
Foeniculum vulgare	Fennel	Fruit/berry/seed	Maros Arznei, Fürth, Germany
Fucus vesiculosus	Bladderwrack	Whole plant	Maros Arznei, Fürth, Germany
Gentiana lutea	Gentian	Root	Maros Arznei, Fürth, Germany
Geranium robertianum	Herb robert	Whole plant	Maros Arznei, Fürth, Germany
Ginkgo biloba	Ginkgo	Leaf	Maros Arznei, Fürth, Germany
Glycyrrhiza glabra	Liquorice	Root	Maros Arznei, Fürth, Germany
Hamamelis virginiana	Witch hazel	Leaf	Maros Arznei, Fürth, Germany
Harpagophytum procumbens	Devil's claw	Root	Maros Arznei, Fürth, Germany
Hedera helix	Common ivy	Leaf	Maros Arznei, Fürth, Germany
Hibiscus sabdariffa	Roselle	Leaf	Maros Arznei, Fürth, Germany
Humulus lupulus	Hops	Flower	Maros Arznei, Fürth, Germany
Hypericum perforatum	St John's wort	Whole plant	Maros Arznei, Fürth, Germany
Ilex paraguariensis	Yerba mate	Leaf	Maros Arznei, Fürth, Germany
Juniperus communis	Common juniper	Fruit/berry/seed	Maros Arznei, Fürth, Germany
Lavandula angustifolia	Lavender	Flower	Maros Arznei, Fürth, Germany
Marrubium vulgare	Common horehound	Whole plant	Maros Arznei, Fürth, Germany
Matricaria chamomilla	Chamomile	Whole plant	Maros Arznei, Fürth, Germany
Melilotus officinalis	Sweet clover	Whole plant	Maros Arznei, Fürth, Germany
Melissa officinalis	Lemon balm	Leaf	Maros Arznei, Fürth, Germany
Mentha piperita	Peppermint	Whole plant	Maros Arznei, Fürth, Germany
Nicotiana tabacum	Tobacco	Leaf[1]	British American Tobacco Nederland B.V., Amstelveen, Netherlands
Origanum majorana	Marjoram	Whole plant	Maros Arznei, Fürth, Germany
Panax ginseng	Ginseng	Root	Maros Arznei, Fürth, Germany
Petroselinum crispum	Parsley	Whole plant	Maros Arznei, Fürth, Germany
Pimpinella anisum	Anise	Fruit/berry/seed	Maros Arznei, Fürth, Germany
Plantago lanceolata	Ribwort	Whole plant	Maros Arznei, Fürth, Germany
Primula officinalis	Common cowslip	Root	Maros Arznei, Fürth, Germany
Primula vulgaris	Common primrose	Root	Maros Arznei, Fürth, Germany
Pulmonaria officinalis	Common lungwort	Flower	Maros Arznei, Fürth, Germany
Quercus robur	English oak	Bark[1]	Holger Senger Naturrohstoffe und

Latin name	Common English name	Used part	Source
			Gartenbau, Dransfeld, Germany
Rheum palmatum	Rhubarb	Root	Maros Arznei, Fürth, Germany
Rosmarinus officinalis	Rosemary	Leaf	Maros Arznei, Fürth, Germany
Rubus fruticosus	Blackberry	Leaf	Maros Arznei, Fürth, Germany
Salix alba	White willow	Bark	Maros Arznei, Fürth, Germany
Salvia officinalis	Salvia	Leaf	Maros Arznei, Fürth, Germany
Sambucus nigra (L.)	Elderflowers	Flower[1]	Tee und Gewürze Lilianna Kamberg und Marianne Schmidt, Offenbach, Germany
Schinus terebinthifolius	Brazilian pepper tree	Fruit/berry/seed[1]	Tee und Gewürze Lilianna Kamberg und Marianne Schmidt, Offenbach, Germany
Scrophularia nodosa	Common figwort	Whole plant	Maros Arznei, Fürth, Germany
Spirulina	Spirulina	Whole cyanobacteria[1]	VegaVital UG, Berlin, Germany
Symphytum officinale	Comfrey	Root	Maros Arznei, Fürth, Germany
Syzygium aromaticum	Clove	Flower[1]	FUCHS Gewürze, Dissen, Germany
Tanacetum parthenium	Feverfew	Whole plant	Maros Arznei, Fürth, Germany
Taraxacum officinale	Dandelion	Whole plant	Maros Arznei, Fürth, Germany
Thymus vulgaris	Common thyme	Whole plant	Maros Arznei, Fürth, Germany
Tropaeolum majus	Nasturtium	Whole plant	Maros Arznei, Fürth, Germany
Uncaria tomentosa	Cat's claw	Whole plant[1]	Herbathek Naturheilmittel, Berlin, Germany
Urtica dioica	Stinging nettle	Root	Maros Arznei, Fürth, Germany
Usnea barbata	Barber’s itch	Whole plant	Maros Arznei, Fürth, Germany
Vaccinium myrtillus	Bilberry	Fruit/berry/seed	Maros Arznei, Fürth, Germany
Valeriana officinalis (L.)	Common valerian	Root	Maros Arznei, Fürth, Germany
Vanilla planifolia	Vanilla	Fruit/berry/seed	Maros Arznei, Fürth, Germany
Verbena officinalis	Common vervain	Whole plant	Maros Arznei, Fürth, Germany
Vigna radiata	Mung bean (dried)	Fruit/berry/seed[1]	Thai World Import Export, Bangkok, Thailand
Vigna radiata	Mung bean (cooked in boiling water for 20 min)	Fruit/berry/seed[2]	Thai World Import Export, Bangkok, Thailand
Viscum album	European mistletoe	Whole plant	Maros Arznei, Fürth, Germany
Xanthoria parietina	Common orange lichen	Whole lichen[1]	AG Weber, Max Planck Institute for Chemistry, Mainz, Germany
Zingiber officinale	Ginger	Root	Maros Arznei, Fürth, Germany

[1] 10 g dry sample used for extract preparation, [2] 10 g wet sample used for extract preparation

Tested cyanobacteria samples, which were solved in phosphate-buffered saline (PBS), are listed in **Table 8**. All samples were obtained from Culture Collection of Algae at Goettingen University, Germany.

Table 8: Cyanobacteria extracts tested for anti-inflammatory properties

Latin name	Strain
Anabaena ambigua	SAG 1403-7
Cylindrospermum siamensis	SAG 11.82
Lyngbya lagerheimii	SAG 24.99
Microcystis aeruginosa	SAG 1450-1
Nostoc sp.	SAG 70.79
Phormidium sp.	SAG 9.92
Planktothrix agardhii	SAG 3.82
Synechocystis sp.	SAG 37.92

Japanese knotweed (*Fallopia japonica* Houtt.) leaves and roots samples, each solved in 70% acetone, 70% acetonitrile or 70% ethanol, were obtained from Irena Vovk, National Institute of Chemistry, Ljubljana, Slovenia.

2.5. Solutions and buffer

2.5.1. Cell culture medium

Medium for HeLa-TLR4 transfected reporter cell line

Dulbecco's Modified Eagle Medium (DMEM), high glucose
10% fetal calf serum (FCS)
1% penicillin/streptomycin
1 µg/ml puromycin
5 µg/ml blasticidin
1 mg/ml geneticin (G418)

Medium for THP-1 cell line

Roswell Park Memorial Institute (RPMI) 1640 medium
10% FCS (heat-inactivated)
1% penicillin/streptomycin
0.05 mM ß-mercaptoethanol

Medium for HEK-TLR2 and HEK-TLR4 transfected reporter cell lines

DMEM, high glucose
10% FCS (heat-inactivated)
1% penicillin/streptomycin
1x HEK-Blue Selection

Medium for HeLa-TLR4 transfected dual reporter cell line

DMEM, high glucose
10% FCS (heat-inactivated)
1% penicillin/streptomycin
140 µg/ml hygromycin B gold

Freezing medium for HeLa-TLR4 transfected reporter cell lines

90% FCS (heat-inactivated)
10% dimethylsulfoxid (DMSO)

Freezing medium for THP-1 monocytes

RPMI 1640 medium
10% FCS (heat-inactivated)
0.05 mM ß-mercaptoethanol
5% DMSO

Freezing medium for HEK-TLR2 and HEK-TLR4 transfected reporter cell lines

DMEM, high glucose
20% FCS (heat-inactivated)
10% DMSO

HEK-Blue Detection medium

One pouch of HEK-Blue Detection powder was poured in a sterile bottle. The powder was solubilized with 50 ml of endotoxin-free water and homogenized by vortexing the solution. The HEK-Blue Detection solution was warmed for 40 min at 37°C and was afterwards filtered through a Nalgene Rapid-Flow sterile filter (0.2 µm membrane) in a sterile bottle. The HEK-Blue Detection medium was stored at 4°C and used within 2 weeks.

2.5.2. SDS-PAGE and Western Blot buffer

2x Laemmli sample buffer (without bromophenol blue)

10 ml 1 M Tris-hydrogen chloride (Tris-HCl), pH 6.8
20 ml sodium dodecyl sulfate (SDS) (10%)
20 ml glycerol
add high-purity water to 100 ml

2x Laemmli sample buffer (with bromophenol blue)

1 ml Tris-HCl, pH 6.7 (1M)

7 ml glycerol

6 ml SDS (10%)

200 µl bromophenol blue (0.5% stock solution) or 0.035 g bromophenol blue

before usage: add 100 mM dithiothreitol (DTT)

10% Resolving gel (spacer 1.5 mm)

7.7 ml high-purity water

6.7 ml acrylamide (29:1)

5.2 ml 1.5 M Tris, pH 8.8 (prepared with a ratio of 18 g Tris and 2.5 ml HCl)

200 µl SDS (10%)

200 µl ammonium persulfate (APS) (10%)

8 µl tetramethylethylenediamine (TEMED)

Stacking gel

8.2 ml high-purity water

2 ml acrylamide (29:1)

1.52 ml 1 M Tris, pH 6.8

120 µl SDS (10%)

120 µl APS (10%)

12 µl TEMED

10x Running buffer (10x TrisGlycine 10% SDS)

60 g Tris base

288 g glycine

20 g SDS

add high-purity water to 2000 ml

1x Running buffer

100 ml 10x Running buffer

900 ml high-purity water

10x Transfer buffer

144 g glycine

30.28 g Tris base

800 ml high-purity water

1x Transfer buffer

100 ml 10x Transfer Buffer

700 ml high-purity water

200 ml methanol

Note: Transfer buffer should be prepared ice-cold

10x Tris-buffered saline (TBS)

121.14 g Tris base (500 mM)

175.32 g sodium chloride (NaCl) (1.5 M)

With HCl (~ 50 ml concentrated HCl) to pH 7.5

1x TBS with Tween-20 (TBS-T)

100 ml 10x TBS

900 ml high-purity water

1 ml Tween-20

5% Fat-free milk powder solution

6 g fat-free milk powder in 120 ml TBS-T

2.5.3. Antibody solutions

Primary and secondary antibodies used for detection of NF-κB translocation (**chapter 3.6.1**) are listed in **Table 9**. Both antibodies were diluted in PBS containing 1% bovine serum albumin (BSA) and 0.3% Triton X-100.

Table 9: Antibodies for detection of NF-κB translocation

Antibody type	Target (Anti-)	Conjugate	Host species	Used dilution
Primary antibody	NF-κB p65	No conjugate	Rabbit	1:400
Secondary antibody	Rabbit-IgG	Alexa Fluor 568	Goat	1:400

Primary and secondary antibodies used for Western Blot analysis (**chapter 3.6.3**) are listed in **Table 10** and **Table 11**. All primary antibodies were diluted in 5% fat-free milk powder solution. Secondary antibodies were diluted in TBS-T.

Table 10: Primary antibodies for Western Blot analysis

Target (Anti-)	Host species	Used dilution
Vinculin	Mouse	1:2.500
Tubulin	Rat	1:10.000
AKT pan	Rabbit	1:500
P-AKT	Rabbit	1:1.000
IκBα	Mouse	1:1.000
P-IκBα	Rabbit	1:30.000
p38	Mouse	1:267
P-p38	Mouse	1:1.000

Table 11: Secondary antibodies for Western Blot analysis

Target (Anti-)	Conjugate	Host species	Used dilution
Mouse-IgG	HRP	Goat	1:10.000
Rabbit-IgG	HRP	Goat	1:10.000
Rat-IgG	HRP	Goat	1:10.000

2.6. Cell lines

Henrietta Lacks (HeLa)-TLR4 transfected reporter cells, the human monocytic cell line THP-1 as well as human embryonic kidney (HEK)-TLR2 and HEK-TLR4 transfected reporter cells were tested to analyze the influences of different extracts and compounds on TLR2 and TLR4 signaling pathways. All cell lines were cultured in 75 cm^2 cell culture flasks with 20 ml complete growth medium (**chapter 2.5.1**) at 37°C in atmospheric air containing 95% relative humidity and 5% CO_2. Cells were counted every three to four days with a Bio-Rad TC20 Automated Cell Counter to determine the amount of cells and the viability rate. For every new passage, $1x10^6$ – $1.5x10^6$ cells were seeded in a 75 cm^2 cell culture flask.

2.6.1. HeLa-TLR4 stable transfected reporter cell line

For determination of the anti-inflammatory potential of different ethanolic extracts, a HeLa-TLR4 transfected reporter cell line of the clone NBP2-26263 (Novusbio, Wiesbaden Nordenstadt, Germany) was used. The HeLa cell line was obtained from a human cervical adenocarcinoma and was stable transfected with a human TLR4/MD-2/CD14-complex. The reporter gene for Renilla luciferase expression is under transcriptional control of the IL-8 promoter. IL-8 is one of the most important pro-inflammatory cytokines, which is induced via TLR4 stimulation. Upon activation of the promoter, Renilla luciferase reporter luminescence signal can be measured using LightSwitch Luciferase assay system, which is based on oxidation of coelenterazine to coelenteramide (Novus Biologicals, 2018).

2.6.2. THP-1 cell line

THP-1 monocytes were used to verify the results received with the HeLa-TLR4 transfected reporter cell line and to test further extracts and compounds for their anti-inflammatory effects. The THP-1 cell line TIB-202 (ATCC; LGC Standards, Wesel, Germany) is a human monocytic cell line, which was obtained from the peripheral blood of a one year old boy who suffered from acute lymphoblastic leukemia (LGC Standards, 2016). This cell line naturally expresses the TLR4/MD-2/CD14-complex and is known to secrete cytokines, e.g. IL-8 after stimulation with LPS (Baqui et al., 1999; Zarember and Godowski, 2002; Chanput et al., 2010). After differentiation with phorbol 12-myristate 13-acetate (PMA) to M0 macrophages, cells can be polarized into M1 macrophages or M2 macrophages. Both types express markers similar to polarized macrophages obtained from freshly isolated monocytes. M1 macrophages produce pro-inflammatory cytokines like TNF-α, IL-1β, IL-6, IL-12 and chemokine (C-X-C motif) ligand 10 (CXCL10), whereas M2 macrophages are characterized by anti-inflammatory cytokine production like IL-10, chemokine (C-C motif) ligand 18 (CCL18) and CCL22 as well as the expression of several receptors, e.g. mannose receptor CD206 and scavenging receptor CD163 (Genin et al., 2015).

2.6.3. HEK-TLR2 and HEK-TLR4 stable transfected reporter cell lines

To analyze the potential of different extracts and compounds to specifically inhibit TLR2 or TLR4, a comparative assay with Pam2CSK4 (a TLR2 ligand)-stimulated HEK-TLR2 and LPS-EB ultrapure (a TLR4 ligand)-stimulated HEK-TLR4 transfected reporter cell lines (both InvivoGen, Toulouse, France) was performed. Differences in the inflammatory response should be attributed to direct receptor interference, since TLR2 and TLR4 share the MyD88-dependent intracellular signaling cascade. The HEK-TLR2 reporter cell line is a stable transfected HEK293 cell line, which expresses human TLR2 and CD14. The inducible reporter gene secreted embryonic alkaline phosphatase (SEAP) is under control of the IFNβ minimal promoter fused to five NF-κB and AP-1 binding sides. Stimulation of TLR2 activates NF-κB and AP-1, which induce the secretion of SEAP. This phosphatase can hydrolyze a specific substrate, producing a spectrophotometric measurable purple/blue colour. The HEK-TLR4 reporter cell line is a stable transfected HEK293 cell line, which expresses the human TLR4/MD-2/CD14-complex. The inducible reporter gene SEAP is under control of the IL-12 p40 minimal promoter fused to five NF-κB and AP-1 binding sides. Analog to the HEK-TLR2 reporter cell line, stimulation of TLR4 activates NF-κB and AP-1, which induces the production of SEAP and the hydrolysis of the specific substrate resulting in a purple/blue colour (InvivoGen, 2016).

2.6.4. HeLa-TLR4 stable transfected dual reporter cell line

To analyze the impact of different extracts on NF-κB translocation, a monoclonal HeLa-TLR4 transfected dual reporter cell line (provided by Kira Ziegler, Max Planck Institute for Chemistry, Mainz, Germany) was used. This is a reporter cell line based on the HeLa-TLR4 transfected reporter cell line described in **chapter 2.6.1**. In addition to the Renilla luciferase, a stable transfection with a constitutive active Firefly luciferase plasmid enables simultaneous measurement of TLR4 stimulation (Renilla luciferase activity) and viability of the cells (Firefly luciferase activity).

2.7. Animals

Four week old male C57BL/6 wild type mice were obtained from Harlan (An Venray, The Netherlands). Before starting the experiment, the animals were set for at least two weeks on a gluten-free diet with food and water at libitum. They were housed on a 12-hour dark and light cycle and were set without food overnight before starting the experiment. After the first dosage, they received gluten-free diet again. All animal experiments were conducted at the Institute of Translational Immunology (TIM) and were approved by the Animal Care and Use Committee of Rhineland Palatinate, Germany.

3. Methods

3.1. Preparation of ethanolic extracts and compounds

The majority of the ethanolic extracts were purchased from Maros Arznei, Fürth, Germany. All other samples listed in **Table 7** (**chapter 2.4**) were prepared with the following protocol: the sample was grinded with mortar and pestle until receiving a fine powder. If necessary, e.g. for liquid-rich samples like garlic, this process was performed under liquid nitrogen. Afterwards, 10 g powder was resuspended in 50 ml of 70% aqueous ethanol. The mixture was incubated for ten days at room temperature (RT) in the dark, being shaken once a day. After ten days, the extracts were filtered through Rotilabo-folded filters to remove unsolved residues. All extracts were stored at RT in the dark for further usage.

8 mg of compounds identified to be present in cinnamon extract (*p*-cymene, methyl salicylate, cinnamyl alcohol, *trans*-cinnamic acid, benzoic acid, *trans*-cinnamaldehyde, stearic acid and palmitic acid) were solved each in 2 ml 70% aqueous ethanol to receive stock solutions of 4 mg/ml. Until further usage, samples were stored at 4°C in the dark.

3.2. Cell culture treatments

Various extracts and compounds were tested regarding their influence to mitigate stimulated TLR2 and TLR4 signaling pathways in different cell lines.

3.2.1. HeLa-TLR4 reporter cell line

Thawing of the cells

Stocks of HeLa-TLR4 reporter cells were stored in a cryotube with 2 ml freezing medium at -80°C. For thawing of the cells, the cryotube was carefully held in a water bath (37°C) until the ice was melted. Afterwards, the cell suspension from the cryotube was pipetted in 20 ml medium (4°C) without antibiotics. The cells were centrifuged at 100 *g* for 5 min (4°C) and the supernatant was discarded. To reduce the DMSO-content in the medium of the cells, the cell pellet was resuspended in 10 ml 37°C-warm medium without antibiotics. The cells were transferred to a 25 cm^2 cell culture flask. After 24h in a cell culture incubator at 37°C, the medium was replaced by selective medium with antibiotics. Before using the cells for experiments, they were passaged at least three times.

Incubation with extracts and stimulation of receptor activity

In 96-well microtiter plates (black plate, clear F-bottom), $2x10^5$ cells/ml were seeded in 100 µl complete growth medium and were allowed to settle overnight. Meanwhile, extracts and vehicle control (70% ethanol) were diluted 1:10 and 1:100 in PBS. Next day, experiments were conducted with extract concentrations ranging from 0.01% to 3% in final cell culture medium or the same amount of vehicle. Cells were preincubated with extracts or vehicle for 2h at 37°C. If the pipetted volume exceeded 20 µl, the same volume of medium was removed from the cells before incubation with extracts or vehicle to ensure a correct final concentration. LPS-EB stock solution (5 µg/µl) was diluted with complete growth medium to a working solution of 50 ng/ml. 100 µl of the LPS-EB working solution (or the same amount of complete growth medium as control) were added to each well, resulting in a final LPS-EB concentration of 25 ng/ml. Incubation with LPS-EB for 8h at 37°C was performed to induce the TLR4 activity of the cells. As alternative to LPS-EB stimulation, $NiCl_2$ and $NiSO_4$ were tested. Therefore, stock concentrations of 1 M were prepared using each 23.77 g Nickel(II)-chloride hexahydrate or 26.29 g Nickel(II)-sulfate hexahydrate solved in 100 ml high-purity water. Incubations with different concentrations of $NiCl_2$ and $NiSO_4$ were performed analog to LPS-EB treatment. Afterwards, cell viability was measured (**chapter 3.3**) and TLR4 stimulation was determined using LightSwitch Luciferase assay (**chapter 3.4.1**).

3.2.2. THP-1 monocytes

Thawing of the cells

Stocks of THP-1 monocytes were stored in a cryotube with 2 ml freezing medium at -80°C. Thawing of the cells was performed as described in **chapter 3.2.1** for HeLa-TLR4 reporter cells.

Incubation with extracts/compounds and stimulation of receptor activity

In 96-well microtiter plates (clear plate, clear V-bottom), $4x10^5$ cells/ml were seeded in 100 µl complete growth medium and were allowed to settle for 1h. Meanwhile, extracts or compounds (stock concentration of compounds: 4 mg/ml in 70% ethanol) and vehicle control (in most cases 70% ethanol) were diluted 1:10 and 1:100 in PBS. After 1h, cells were preincubated with different concentrations of extracts, compounds or vehicle for 2h at 37°C. If the pipetted volume exceeded 20 µl, plates were centrifuged for 5 min at 100 *g* and the same volume of medium was removed from the cells before incubation with extracts, compounds or vehicle to ensure a correct final concentration. The LPS-EB stock solution (5 µg/µl) was diluted with complete growth medium to a working solution of 112.5 ng/ml. 80 µl of the LPS-EB working solution was added to each well (final LPS-EB concentration: 50 ng/ml). Wells, which were not incubated with LPS-EB, received 80 µl complete growth medium. Incubation with LPS-EB for 4h (or 1h for Western Blot analysis experiments) at 37°C was performed to induce TLR4 activity of the cells. Afterwards, Alamar Blue assay (**chapter 3.3.3**), enzyme-linked immunosorbent assay (ELISA) (**chapter 3.4.2**) and/or SDS-polyacrylamide gel electrophoresis (SDS-PAGE) followed by Western Blot analysis (**chapter 3.6.2** and **3.6.3**) were performed.

Incubation with HPLC fractions and stimulation of receptor activity

In 48-well microtiter plates (clear plate, clear F-bottom), 500 µl of isolated high-performance liquid chromatography (HPLC) fractions (**chapter 3.8.1**) were dried in two runs (each with 250 µl) using a RVC 2-25 CDplus concentrator with vacuum concentration. The samples were dried at 45°C with a vacuum of 35 mbar (duration of drying: up to 7h). Afterwards, the plates were disinfected with 70% ethanol and dried under the sterile hood for 1h. The plates were stored at 4°C in the dark overnight before conducting the cell culture experiments. In the plates with the dried HPLC samples, $4x10^5$ cells/ml were seeded in 150 µl complete growth medium, shaken for 10 min at 240 rpm and incubated for 2h at 37°C. The LPS-EB stock solution (5 µg/µl) was diluted with complete growth medium to a working solution of 125 ng/ml. 100 µl of the LPS-EB working solution was added to each well, leading to a final LPS-EB concentration of 50 ng/ml. Wells, which were not incubated with LPS-EB, received 100 µl complete growth medium. Incubation with LPS-EB for 4h at 37°C was performed to

induce TLR4 activity of the cells. Afterwards, Alamar Blue assay (**chapter 3.3.3**) and ELISA (**chapter 3.4.2**) were performed.

3.2.3. THP-1 macrophages

In 96-well microtiter plates (black plate, clear F-bottom), THP-1 monocytes with $1.5x10^5$ cells/ml were seeded in 200 µl complete growth medium containing 10 ng/ml PMA. The cells were allowed to rest for three days at 37°C to differentiate into M0 macrophages. Afterwards, THP-1 M0 macrophages were washed 1x with 200 µl PBS. 200 µl complete growth medium without PMA was added and cells were incubated overnight at 37°C. Polarization to M1 macrophages was performed using 20 ng/ml IFNγ for 24h (stock solution of IFNγ: 100 µg/ml in water with 0.1% FCS). Meanwhile, extracts or compounds (stock concentration of compounds: 4 mg/ml in 70% ethanol) and vehicle control (70% ethanol) were diluted 1:10 in PBS. Supernatant of the cells was removed and 100 µl complete growth medium was added. Subsequently, different concentrations of extracts, compounds or vehicle were added to the cells and they were incubated for 2h at 37°C. LPS-EB stock solution (5 µg/µl) was diluted with complete growth medium to a working solution of 100 ng/ml. 100 µl of the LPS-EB working solution was added to each well (final LPS-EB concentration: 50 ng/ml) for 4h. Wells, which were not incubated with LPS-EB, received 100 µl complete growth medium. Afterwards, Alamar Blue assay (**chapter 3.3.3**) and ELISAs (**chapter 3.4.2**) were performed.

3.2.4. HEK-TLR2 and HEK-TLR4 reporter cell lines

Preparation of cell culture stock

Upon arrival, HEK-TLR2 and HEK-TLR4 reporter cell lines were directly thawn to ensure a good cell viability and assay performance. All thawing steps were performed in complete growth medium without HEK-Blue Selection. After thawing the cells in a 37°C water bath, they were transferred into 15 ml growth medium. The cells were centrifuged for 5 min at 200 *g* and the supernatant was removed. The cell pellet was resuspended in 1 ml medium and transferred into a 25 cm^2 cell culture flask containing 5 ml growth medium. Cells were placed in a 37°C cell incubator. Growth medium was supplemented with 1x HEK-Blue Selection after passaging twice. Aliquots of HEK-TLR2 and HEK-TLR4 reporter cells were frozen to ensure a sufficient stock of cells for further analyses. Before freezing, cells were resuspended at a density of $1\text{-}2x10^6$ cells/ml in freezing medium freshly prepared with growth medium (4°C). Cryogenic vials were filled each with 2 ml cell suspension and were frozen at -80°C.

Thawing of the cells

Thawing of the cells was performed as described in **chapter 3.2.1** for HeLa-TLR4 reporter cells.

Incubation with extracts and stimulation of receptor activity

Extracts or compounds (stock concentration of compounds: 4 mg/ml in 70% ethanol) and vehicle control (70% ethanol) were diluted 1:10 and 1:100 in PBS. Different concentrations of extracts, compounds or vehicle were added in empty 96-well microtiter plates (clear plate, clear F-bottom). Directly afterwards, $2.8x10^5$ cells/ml were seeded in 180 µl complete growth medium and were incubated for 2h at 37°C. To determine the cell viability, HEK-TLR2 and HEK-TLR4 reporter cells were cultured in medium without HEK-Blue Selection. For HEK-TLR2 reporter cells, the specific agonist Pam2CSK4 (stock solution: 1 mg/ml) was diluted with complete growth medium to a working solution of 10 ng/ml. 20 µl of the Pam2CSK4 working solution was added to each well (final Pam2CSK4 concentration: 1 ng/ml). For HEK-TLR4 reporter cells, the specific agonist LPS-EB ultrapure (stock solution: 5 µg/µl) was diluted with complete growth medium to a working solution of 1 µg/ml. 20 µl of the LPS-EB ultrapure working solution was added to each well (final LPS-EB ultrapure concentration: 100 ng/ml). Wells, which were not incubated with Pam2CSK4 or LPS-EB ultrapure, received 20 µl complete growth medium. Cells were incubated with the specific agonists overnight at 37°C to induce TLR2 or TLR4 activity. Next day, Alamar Blue assay (**chapter 3.3.3**) and HEK-Blue Detection assay (**chapter 3.4.3**) were performed.

3.2.5. HeLa-TLR4 dual reporter cell line

Thawing of the cells

Stocks of HeLa-TLR4 dual reporter cells were stored in a cryotube with 2 ml freezing medium at -80°C. Thawing of the cells was performed as described in **chapter 3.2.1** for HeLa-TLR4 reporter cells.

Incubation with extracts and stimulation of receptor activity

For NF-κB p65 translocation assay, $2x10^5$ cells/ml were seeded in 1 ml complete growth medium in 12-well plates with glass bottom. Cells were incubated for 48h at 37°C. Medium was removed and the cells were preincubated with 0.6% extract in final cell culture medium or with the same amount of vehicle 70% ethanol for 2h at 37°C. LPS-EB stock solution (5 µg/µl) was diluted with complete growth medium to a working solution of 100 ng/ml. 1 ml of the LPS-EB working solution (or the same amount of complete growth medium as control) was added to each well, resulting in a final LPS-EB concentration of 50 ng/ml. Incubation with LPS-EB for 1h at 37°C was performed to induce TLR4 activity and subsequent NF-κB

translocation into the cell nucleus. Cells were washed 1x with PBS (containing calcium and magnesium) and afterwards fixated for 10 min at 37°C using 500 µl prewarmed 4% formaldehyde in PBS. After fixation, cells were washed 3x 5 min with PBS (without calcium and magnesium) and immunostaining against NF-κB and quantitative fluorescence microscopy were performed (**chapter 3.6.1**).

3.3. Cell viability assays

Cell viability was measured to largely exclude toxic effects affecting TLR2 and TLR4 stimulation. For HeLa-TLR4 reporter cells, three different cell viability assays (MTT assay, WST-8 assay and Alamar Blue assay) were compared. For all other cell lines, viability was determined using Alamar Blue assay.

3.3.1. MTT assay

Cell viability of treated HeLa-TLR4 reporter cells (**chapter 3.2.1**) was measured by MTT assay. For this assay, cells were incubated with 20 µl 3-(4,5-dimethylthiazol-2-yl)-2,5-diphenyltetrazolium bromide (MTT) Labeling Reagent (final concentration: 0.5 mg/ml) for 4h at 37°C. The MTT assay measures cell metabolic activity depending on the ability of mitochondrial dehydrogenases to reduce the tetrazolium dye MTT to the insoluble purple/blue formazan (Merck, 2018a). After incubation with MTT, cells were incubated overnight with 100 µl solubilization solution to lyse the cells and to dissolve the formazan crystals. Next day, absorption at 565 nm with a reference wavelength of 650 nm was measured using the microplate reader Synergy Neo. The amount of the produced colour is directly proportional to the number of viable cells. Due to the toxicity of the MTT reagents, no further tests were performed with cells used in the MTT assay.

3.3.2. WST-8 assay

Cell viability of treated HeLa-TLR4 reporter cells (**chapter 3.2.1**) was measured by WST-8 assay, also known as Cell Counting Kit-8 (CCK-8). Cells were incubated with 20 µl 2-(2-methoxy-4-nitrophenyl)-3-(4-nitrophenyl)-5-(2,4-disulfophenyl)-2H-tetrazolium, monosodium salt (WST-8) mixture (freshly thawn). WST-8 is reduced by the dehydrogenase activity of living cells to a yellow formazan-colourant. The formazan amount is directly proportional to the amount of living cells with higher detection sensitivity than the MTT assay described above (Merck, 2018b). The absorption in the WST-8 assay was measured using the microplate reader Synergy Neo at a wavelength of 450 nm. Due to the non-toxic effects of

the WST-8 reagents, further tests could be performed with the same cells afterwards. First, cells were washed with 200 µl PBS to remove the colourant. Afterwards, 50 µl PBS was added and the cells were frozen at -80°C before further analysis of the TLR4 activity with luciferase assay (**chapter 3.4.1**).

3.3.3. Alamar Blue assay

Viability of cells treated with extracts and specific agonists (**chapter 3.2**) was measured using Alamar Blue assay. Alamar Blue (resazurin) is the oxidized form of a redox-indicator, which is blue and non-fluorescent. If resazurin comes in contact with metabolic active cells and their reducing environment in the cytoplasm, mainly nicotinamide adenine dinucleotide (NADH) and nicotinamide adenine dinucleotide phosphate (NADPH), it is irreversibly reduced to resorufin, a pink dye which is highly red fluorescent. This change can be detected via fluorescent measurement (Thermo Fisher Scientific, 2016). Since some extracts showed strong autofluorescent signals and/or were darkly coloured, washing steps were performed, where possible, to reduce their influence. Before and after the washing steps, cells were examined under the microscope to document a potential loss of cells during washing. In particular, for HeLa-TLR4 reporter cells, the supernatant was removed and 200 µl PBS was added. After removal of the PBS, 100 µl complete growth medium and 10 µl Alamar Blue solution were added to each well and cells were incubated for 4h at 37°C in the dark. In contrast to the adherent HeLa-TLR4 reporter cells, THP-1 monocytes are suspension cells. During washing steps, cells were centrifuged for 5 min at 100 *g*. Afterwards, 150 µl of supernatant was collected for ELISA and each well of cells received 100 µl complete growth medium. After another centrifugation step for 5 min at 100 *g*, 100 µl of the supernatant was discarded to have a final volume of 100 µl per well. 10 µl Alamar Blue solution were added per well and incubated overnight at 37°C in the dark. HEK-TLR2 and HEK-TLR4 reporter cells are very sensitive to temperature changes. Therefore, no washing steps were performed before Alamar Blue assay. 20 µl Alamar Blue solution were directly added per well and incubated overnight at 37°C in the dark. Fluorescence intensity was measured for all cell lines using a Synergy Neo microplate reader with the settings listed in **Table 12**.

Table 12: Alamar Blue fluorescence measurement settings

Setting type	Adjustment
Shaking before measurement	5 sec orbital
Excitation wavelength	560 nm
Emission wavelength	590 nm
Gain	70
Delay after plate movement	350 msec
Measurements of data point	30
Well used for auto-adjust read height	TLR agonist control

After the Alamar Blue assay, HeLa-TLR4 reporter cells were washed with 200 µl PBS to remove the colourant. Finally, 50 µl PBS were added and the cells were frozen at -80°C for LightSwitch Luciferase measurements (**chapter 3.4.1**). All other cell lines were discarded after Alamar Blue measurement.

3.4. TLR2 and TLR4 stimulation assays

Different assays were performed to identify extracts and compounds mitigating TLR2 and TLR4 stimulation. For HeLa-TLR4 reporter cells, LightSwitch Luciferase assay was performed, THP-1 supernatant was tested in ELISAs and HEK-Blue Detection assay was conducted with HEK-TLR2 and HEK-TLR4 reporter cell lines.

3.4.1. LightSwitch Luciferase assay

For analysis of the TLR4 activity in HeLa-TLR4 reporter cells, treated cells (**chapter 3.2.1**), which were frozen at -80°C after cell viability measurement (**chapter 3.3.3**) were thawn for 1h at RT. The freezing of the cells at -80°C enables a high flexibility when to perform the experiment as well a better lysis of the cells, which is needed for the LightSwitch Luciferase assay. The Luciferase assay solution was thawn in a 37°C-warm water bath. Directly before usage, the reconstituted substrate was added in a 1:100 dilution. 50 µl assay-substrate-solution was directly added per cell culture well and mixed thoroughly with the sample. Afterwards, 50 µl of the mixture was added in a white 96-well microtiter plate. TLR4 activity was measured using luminescence with a Synergy Neo microplate reader and the settings listed in **Table 13**.

Table 13: LightSwitch Luciferase luminescence measurement settings

Setting type	Adjustment
Filter	LUM
Position	Top
Shaking before measurement	5 sec orbital
Well used for auto-adjust read height	LPS control
Delay after plate movement	350 msec
Duration per measurement	2 sec
Gain	195

3.4.2. ELISA

ELISAs were used to determine IL-8, TNF and IL-10 concentrations in supernatant of treated THP-1 monocytes and macrophages (**chapter 3.2.2** and **chapter 3.2.3**). In this indirect sandwich ELISA, capture antibodies specific for the desired antigen are coated on a microtiter plate. In a next step, the sample is added and the defined antigens bind to the coated antibodies. Detection antibodies are added to bind to the antigens and are themselves detected using horseradish peroxidase (HRP)-conjugated antibodies. Incubation of the HRP with tetramethylbenzidine (TMB) reagent leads to the development of a blue color. The reaction is stopped using a stop solution, which changes the color to yellow. The concentration of the analyzed antigen is proportional to the optical density, which can be measured spectrophotometrically (Growther, 2002). In the performed experiments, supernatant of treated THP-1 monocytes was collected after centrifugation of the cells for 5 min at 100 *g*. Supernatant of treated THP-1 macrophages was collected without prior centrifugation. All supernatants were stored at -20°C until usage. ELISAs were performed following manufacturer's protocol with washing buffer volume optimized to 20 ml 20x wash buffer diluted in 950 ml high-purity water. All washing steps were performed using a tecan plate washer for automated washing. In short, medium binding 96-well microtiter plates (clear plate, clear F-bottom) were coated with 100 µl capture antibody in coating buffer overnight at 4°C. Next day, plates were washed 3x with 300 µl washing buffer, followed by blocking for 1h at RT with 200 µl assay diluent. Afterwards, plates were washed 3x with 300 µl washing buffer. For IL-8 ELISA, supernatant was diluted 6-fold with assay diluent to ensure an IL-8 concentration within the detection range. For all other ELISAs, supernatant was diluted 1.1-fold. 100 µl diluted samples and standards were added in the 96-well microtiter plates for 2h at RT. Plates were washed 5x with 300 µl washing buffer, followed by incubation with 100 µl detection antibody and enzyme reagent for 1h. Afterwards, plates were washed 7x with 300 µl washing buffer. During each of the last seven washing steps, plates were soaked 30 sec in washing buffer. 100 µl substrate solution was added to each well and the plates were incubated for 30 min at RT in the dark. Finally, the reaction was stopped with

50 µl stop solution. Absorbance was measured using a Synergy Neo microplate reader and the instrument settings listed in **Table 14**.

Table 14: Human ELISA absorbance measurement settings

Setting type	Adjustment
Shaking before measurement	5 sec orbital
Wavelength	450 nm
Reference wavelength	570 nm
Delay after plate movement	350 msec

The average absorbance of the blanks was subtracted from all experimental wells. In addition, the values measured with the reference wavelength were subtracted from the corresponding values at 450 nm. The Gen5 software on SynergyNeo was used to determine a standard curve (4 parameter logarithmic) per plate with the pipetted standard values. IL-8, TNF and IL-10 concentrations were calculated according to standard curve and dilution factor.

3.4.3. HEK-Blue Detection assay

Production of inducible SEAP based on activation of NF-κB and AP-1 in treated HEK-TLR2 and HEK-TLR4 reporter cells (**chapter 3.2.4**) was determined using the HEK-Blue Detection assay. Treated cells, which were cultured in HEK-Blue Detection medium, were shaken 5 sec orbital. Afterwards, plates were measured in a Synergy Neo microplate reader at a wavelength of 640 nm with a delay after plate movement of 350 msec.

3.5. LAL assay

The endotoxin concentration in the extract with the highest inflammatory potential was determined to exclude an LPS contamination as possible influence on TLR activity. A *Limulus* Amebocyte Lysate (LAL) assay, where a chromogenic signal is generated in the presence of endotoxins, was performed according to manufacturer's protocol. In short, 25 µl standard (containing 0.1 endotoxin unit/ml (EU/ml) up to 1 EU/ml) or sample were pipetted in a 96-well microtiter plate (clear plate, clear F-bottom) and were incubated for 5 min at 37°C. Subsequently, 25 µl LAL reagent, which contains lysate prepared from the circulating amebocytes of the horseshoe crab *Limulus Polyphemus*, was added. The plate was shaken for 10 sec, followed by incubation at 37°C. After exactly 10 min, 50 µl chromogenic substrate solution was added to each well, mixed for 10 sec and incubated for 6 min at 37°C. Afterwards, 25 µl stop reagent (25% acetic acid) was added to stop the reaction. The plate

was mixed for 10 sec and samples were measured on a Synergy Neo microplate reader at a wavelength of 405 nm. Endotoxin concentration was calculated according to a linear standard curve.

3.6. TLR2 and TLR4 pathway analysis

Besides the measurement of different TLR2 and TLR4 stimulation assays, influence of extracts and compounds on NF-κB translocation was investigated using quantitative fluorescence microscopy. Furthermore, phosphorylation of different TLR2 and TLR4 pathway molecules was determined using SDS-PAGE followed by Western Blot analysis.

3.6.1. Quantitative fluorescence microscopy

NF-κB p65 translocation was determined using quantitative fluorescence microscopy. HeLa-TLR4 dual reporter cells treated with extracts or vehicle (**chapter 3.2.5**) were stained for NF-κB with the following protocol: fixed cells were permeabilized and blocked with 1 ml PBS (without calcium and magnesium) containing 5% BSA and 0.3% Triton X-100 for 1h at RT. Afterwards, cells were stained for the p65 subunit of NF-κB using a primary antibody (**Table 9** in **chapter 2.5.3**) at 4°C overnight. Cells were washed 3x 5 min with PBS, before incubation with Alexa Fluor 568-conjugated secondary antibody (**Table 9** in **chapter 2.5.3**) for 1h at RT in the dark. Subsequently, they were washed 3x 5 min with PBS, followed by counterstaining of the cell nuclei using 300 nM 4',6-diamidino-2-phenylindole (DAPI) for 3 min at RT. Cells were washed 3x 1 min with PBS on a shaker with 80 rpm. The stained cells were cleaned using absolute ethanol. 15 µl ProLong Gold antifade reagent was added as embedding medium overnight. Samples were sealed and stored at 4°C before image acquisition with an Opera Phenix High-Content Screening system. Laser lines at 405 nm excitation and 435-480 nm emission (DAPI) as well as 568 nm excitation and 570-630 nm emission (Alexa Fluor 568) were used for the detection. Image analysis was performed using the Harmony software. The mean ratio of nuclear to cytoplasm NF-κB fluorescence intensity was measured after applying nuclear masks for DAPI stained cell nuclei and surrounding ring-like masks containing the cytoplasm.

3.6.2. Sample preparation and SDS-PAGE

Treatment of LPS-stimulated THP-1 monocytes with cinnamon extract and its active compounds (**chapter 3.2.2**) was tested on the potential to influence the phosphorylation ratio of different TLR2 and TLR4 pathway proteins. Each six wells of a 96-well microtiter plate with

treated THP-1 monocytes were combined in 1.5 ml tubes to receive enough protein for SDS-PAGE followed by Western Blot analysis. The samples were centrifuged for 5 min at 300 *g* to separate the cells from cell culture medium. The pellet was resuspended in 500 µl PBS for washing. After another centrifugation for 5 min at 300 *g*, the supernatant was discarded and the pellet resuspended in 70 µl 2x Laemmli sample buffer (without bromophenol blue). The suspension was pipetted at least 10 times through a syringe with a 25G needle to lyse the cells. Afterwards, the samples were boiled for 10 min at 100°C and centrifuged for 10 min at 13.000 *g*. The supernatant, which contains the fractionated proteins, was collected into 1.5 ml tubes. The protein concentrations were measured using a bicinchoninic acid (BCA) assay according to manufacturer's protocol. In short, 10 µl standard (with a final BSA concentrations from 25 µg/ml up to 2 mg/ml) or sample were pipetted in a 96-well microtiter plate (clear plate, clear F-bottom). BCA reagents A and B were mixed in a ratio of 50:1. 200 µl of the mixture was directly added to each well. The plate was covered from light and thoroughly mixed on a shaker for 30 sec at 700 rpm. Afterwards, it was incubated for 30 min at 37°C in the dark. After cooling to RT, bubbles were removed and the plate was shaken 5 sec at low speed (double orbital) and was measured at a wavelength of 562 nm using a Synergy Neo microplate reader. The average absorbance of the blanks was subtracted from all experimental wells. The Gen5 software was used to determine a standard curve (linear regression) per plate with the pipetted standard values. Protein concentrations were calculated according to the standard curve. Using mean values, the volume containing 15 µg protein was calculated per sample for loading on the SDS-PAGE. Before loading, samples were diluted with 2x Laemmli sample buffer (with bromophenol blue) in a ratio of 2:1 and boiled at 95°C for 5 min in a thermocycler. Afterwards, they were spin down shortly. On a 10% SDS gel (**chapter 2.5.2**), 20 µl of protein marker solution (5 µl protein marker and 15 µl sample buffer) and 15 µg sample (approximately 20 µl per sample) were loaded. The separation according to the molecular weight was run in an Electrophoresis SDS-PAGE Mini-Protean Tetra Cell filled with running buffer for 10-15 min at 100 V followed by 100 min at 120 V.

3.6.3. Western Blot analysis

After SDS-PAGE, the proteins were transferred onto 0.2 µm nitrocellulose membranes through the blot apparatus Trans-Blot Cell. During the run, the blotting chamber was filled with transfer buffer and a cooling block. Gel and membrane were put in a sandwich consisting of sponge, filter paper, gel, membrane, a second filter paper and a second sponge. Everything was pre-wet with transfer buffer before preparing the sandwich. The transfer was run for 1h at 400 mA (using one gel) or for 1h at 600 mA (using two gels). After checking the successful transfer by colouring the proteins on the membrane with ponceau

red, the membrane was washed with TBS-T for de-coloring. Each membrane was blocked with 5% fat-free milk powder solution in TBS-T for 1h at RT on a shaker at 240 rpm. Select proteins were revealed with the appropriate primary antibodies (**Table 10** in **chapter 2.5.3**) overnight at 4°C while shaking at 170 rpm. After washing 3x 5 min with TBS-T while shaking, IgG HRP-conjugated secondary antibodies (**Table 11** in **chapter 2.5.3**) were applied for visualization of the select protein bands. The membranes were incubated for 2h at RT on a shaker at 240 rpm. Afterwards, membranes were washed 5x 5 min with TBS-T while shaking, followed by development of the protein bands using an enhanced chemiluminescence (ECL) system according to manufacturer's protocol. In short, ECL solutions were prewarmed to RT in the dark. 5 min before the end of the membrane washing steps, 3 ml ECL reagent A was mixed with 75 µl reagent B. Subsequently, membranes were incubated with the ECL mixture for 5 min in the dark. Chemiluminescence of the membranes was developed on a ChemiDoc Touch Imaging System. Marker bands were visualized in the same system using colorimetric measurements. Relative expression of proteins was calculated with ImageLab software and was normalized to the respective vinculin or tubulin loading control.

3.7. Inflammatory mouse model

The anti-inflammatory potential of cinnamon extract was tested on male C57BL/6 mice with five animals per treatment group. The mice were pretreated by oral gavage with 50 µl cinnamon extract diluted in 150 µl PBS. 70% ethanol diluted the same way served as vehicle control. 2h after treatment, all mice received 200 µl ATI with a concentration of 10 mg/ml to induce gastrointestinal inflammation. Animals were euthanized 4h after ATI treatment with 100-200 µl ketamine-rompun-mixture containing rompun, ketamine and PBS in a ratio of 2:8:1. Blood was collected through heart punctuation and was centrifuged at 1000 rpm for 15 min to collect serum for ELISAs. The centrifugation step was repeated until at least 300 µl of serum was collected. Serum samples were frozen at -80°C.

ELISAs for mouse IL-6 and CXCL1 were performed according to manufacturer's protocol using a tecan plate washer for automated washing. Serum samples were diluted 5-fold and absorbance was measured as described in **chapter 3.4.2**. The average absorbance of the blanks was subtracted from all experimental wells. In addition, the values measured with the reference wavelength were subtracted from the corresponding values at 450 nm. The Gen5 software on SynergyNeo was used to determine a standard curve (4 parameter logarithmic) per plate with the pipetted standard values. IL-6 and CXCL1 concentrations were calculated according to the standard curve.

3.8. Analysis of cinnamon extract

Ethanolic *C. verum* bark extract was fractionated using HPLC-diode array detector (DAD) and compounds were identified by high-resolution mass spectrometry (HRMS) and gas chromatography-mass spectrometry (GC-MS).

3.8.1. Fractionation using HPLC-DAD

For separation of compounds present in *C. verum* bark extract, fractionation was performed using a preparative HPLC-DAD system. An HPLC-UV method was developed on a Zorbax Eclipse XDB C18 column connected to a security guard C18 cartridge. Gradient elution (**Table 15**) with a mobile phase consisting of water with 0.1% formic acid (solvent A) and acetonitrile (solvent B) was conducted with a flow rate of 1 ml/min at a column temperature of 25°C.

Table 15: HPLC gradient used for *C. verum* fractionation

Time (min)	Solvent A (%)	Solvent B (%)
0	70	30
20	70	30
25	0	100
45	0	100
47	70	30
60	70	30

Before the injection, cinnamon extract was diluted with high-purity water in a ratio of 1:3 (*v/v*) and was centrifuged for 1 min at 16.000 *g* using a 0.22 µm Spin-X polypropylene centrifuge tube filter. 400 µl of the diluted *C. verum* bark extract was injected into the HPLC-UV and chromatograms were acquired at 210 nm, 250 nm, 280 nm and 300 nm. A fraction collector was used to collect select fractions. Afterwards, all collected fractions were tested on THP-1 monocytes (**chapter 3.2.2**) to identify their TLR4-dependent anti-inflammatory potential. Compounds in the anti-inflammatory fractions were identified using HRMS and GC-MS (**chapter 3.8.2**).

3.8.2. Identification of compounds using HRMS and GC-MS

Anti-inflammatory *C. verum* fractions were further analyzed using HRMS and GC-MS. Before the injection into the HRMS system, 1 ml of the active fractions were dried under nitrogen flow until dryness. Afterwards, the solid residues were reconstituted in 40 µl absolute ethanol.

10 µl of the concentrated fractions were directly injected into the HRMS system without using a column. For analyzing cinnamon fractions, a mobile phase consisting of acetonitrile and water with 0.1% formic acid in a ratio of 7:3 (*v/v*) was conducted with a flow rate of 0.2 ml/min. Compounds in the anti-inflammatory fractions were ionized using electrospray ionization (ESI) in both positive (+) and negative (–) mode (**Table 16**).

Table 16: HRMS settings

Setting type	Adjustment ESI (–)	Adjustment ESI (+)
Gas temperature	325°C	325°C
Sheath gas temperature	295°C	295°C
Drying gas flow rate	5 l/min	5 l/min
Sheath gas flow rate	12 l/min	12 l/min
Nebulizer gas	20 psig	20 psig
Capillary voltage	3500 V	4000 V
Nozzle voltage	2000 V	2000 V
Fragmentor	176 V	176 V
Skimmer	46 V	46.5 V
OCT 1 RF Vpp	750 V	750 V
Range (MS and MS^2 spectra)	20-800 m/z	20-800 m/z
Collision energy	30%	30%

In GC-MS, compounds were separated and analyzed in non-derivatized and derivatized form, for the latter they were silylated with trimethylsilyl methallylsulfinate (SILMAS). Before the injection of the non-derivatized fractions in GC-MS, 1 ml of the active HPLC fractions were dried under nitrogen flow until dryness and the solid residues were reconstituted in 40 µl absolute ethanol. To derivatize the polar compounds in the cinnamon fractions, 1 ml of the HPLC fractions were dried under nitrogen flow until dryness. Afterwards, the solid residues were reconstituted in 200 µl dichloromethane and subsequent addition of 200 µl SILMAS reagent. After 10 min, the derivatized HPLC fractions were finally dried under nitrogen flow until dryness and were redissolved in 500 µl dichloromethane. To separate non-polar and volatile compounds, 1 µl of the concentrated non-derivatized and derivatized fractions were injected into the GC-MS system equipped with a single quadrupole analyzer using a DB-5MS+DG column with the settings displayed in **Table 17**. The recorded chromatograms were processed using NIST 2005 mass spectral library.

Table 17: GC-MS settings

Setting type	Adjustment
Split injection ratio	1:1
Injector temperature	260°C
GC oven program:	
hold	50°C for 1 min
heating	4°C/min up to 300°C
hold	300°C for 15 min
Carrier gas	Helium
Carrier gas flow	1.2 ml/min
Temperature of GC-MS transfer line	290°C
Electron impact (EI) ionization energy	70 eV
Range for MS spectra	35–600 *m/z*
Type of ionization	EI(+)
Ion source temperature	200°C

3.9. Statistical analyses

For statistical analyses of the data obtained by Alamar Blue assay, LightSwitch Luciferase assay, ELISA or Western Blot analysis, an analysis of variance (ANOVA) was accomplished using GraphPad Prism. Unpaired t-test was conducted to test the statistical significance of the results. Values of $p < 0.05$ were considered significant. One-way ANOVA followed by Dunnett's post hoc test was accomplished in GraphPad Prism for statistical analysis of NF-κB translocation. Values of $p < 0.05$ were considered as significant. In mouse experiments, error bars depict standard error of the mean (SEM). In all other graphs, error bars show standard deviation (SD).

4. Results and discussion

4.1. Identification of optimal experimental conditions

Before starting large screening experiments with multiple herbal extracts and their compounds, different assays, incubation times and concentrations were tested to identify the optimal experimental conditions.

4.1.1. Optimizing LPS treatment for HeLa-TLR4 reporter cell line

Different LPS-EB concentrations and incubation times were tested in HeLa-TLR4 reporter cells to select the optimal conditions for further experiments. Incubation with LPS-EB for 1h did not show any difference compared to untreated cells (**Figure 2**). After incubation for at least 4h, treatment with all tested LPS-EB concentrations resulted in a significant increase of promoter activity for the pro-inflammatory cytokine IL-8. The strongest increase was observed after 8h LPS-EB treatment. Therefore, this incubation time was selected as standard for subsequent experiments with the tested cell line. To have a robust assay not affected by potential small batch-dependent differences in LPS-EB activity or cell-dependent differences in LPS-EB sensitivity, 25 ng/ml LPS-EB was chosen as standard concentration to stimulate HeLa-TLR4 reporter cells in further experiments.

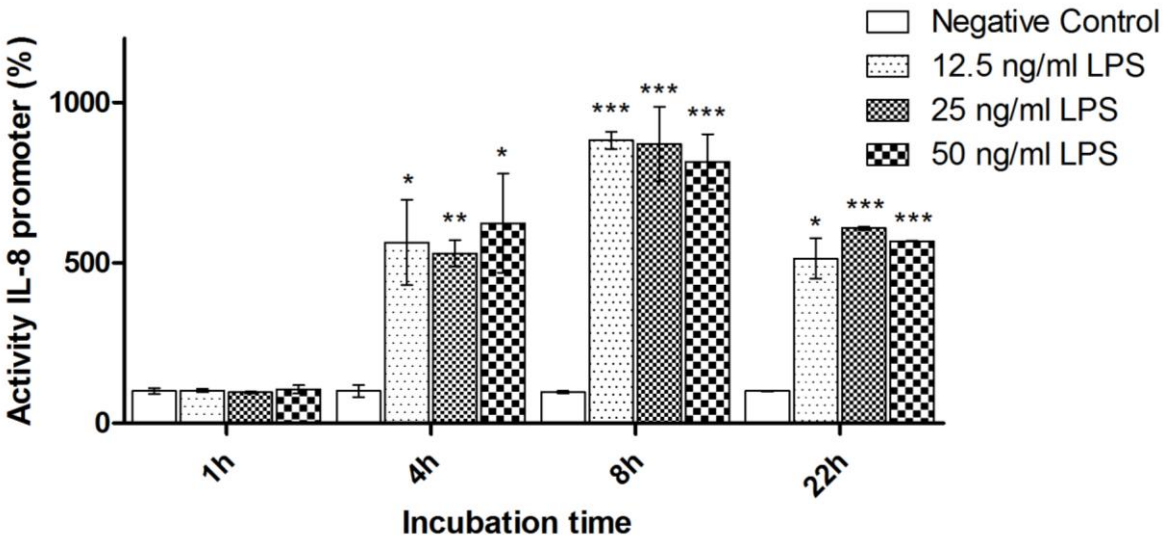

Figure 2: Optimizing LPS treatment for HeLa-TLR4 reporter cell line
HeLa-TLR4 reporter cells were incubated with different concentrations of LPS-EB and different incubation times. Activity of IL-8 promoter was measured using LightSwitch Luciferase assay and was normalized to respective negative control (untreated cells). Data represent mean ± SD ($n \geq 2$). Unpaired t-test: ***p < 0.0001, **p < 0.01, *p < 0.05 compared to negative control.

4.1.2. Comparison of different cell viability assays

MTT assay, WST-8 assay and Alamar Blue assay were tested regarding their suitability to be the standard viability assay for subsequent experiments. Where feasible, the cell viability assays were combined with a measurement of IL-8 promoter activity (Luciferase assay), with or without prior washing steps. Cell viability measured with WST-8 and Alamar Blue assay were comparable for HeLa-TLR4 reporter cells stimulated with LPS-EB (**Figure 3A**). A slightly higher cell viability was measured with the MTT assay after the same LPS-EB treatment. IL-8 promoter activity was decreased after prior incubation with WST-8 assay, especially when a washing step with PBS was added between WST-8 assay and Luciferase measurements, compared to direct Luciferase measurement (**Figure 3B**). A measurement of cell viability with Alamar Blue assay prior to Luciferase assay did not decrease the measured Luciferase activity, even after adding a washing step with PBS.

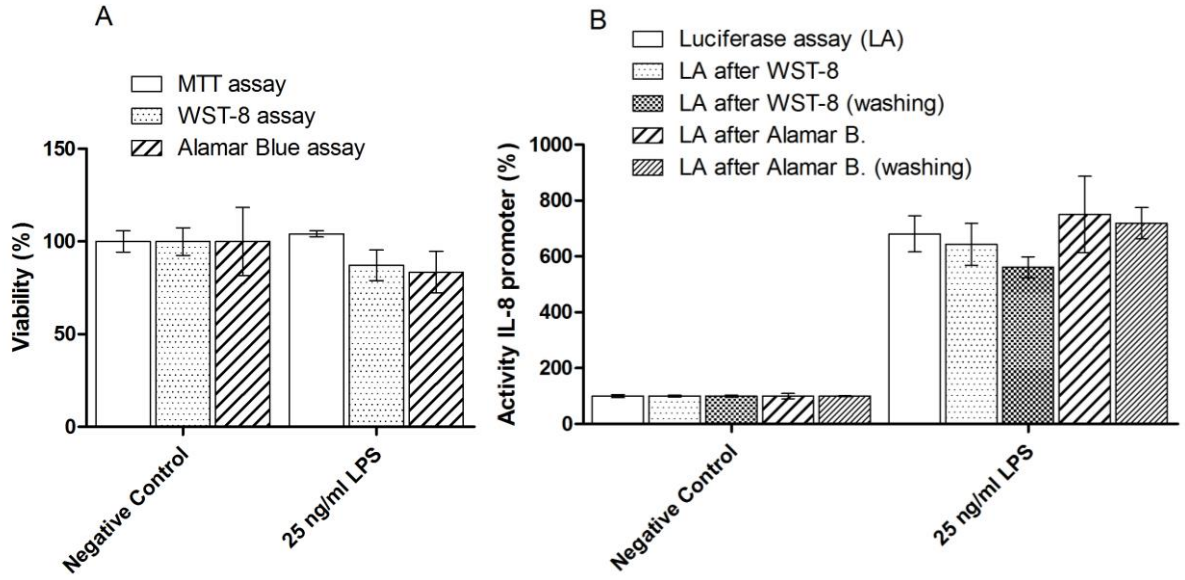

Figure 3: Comparison of different cell viability assays
HeLa-TLR4 reporter cells were incubated with LPS-EB (25 ng/ml) or medium (negative control). Viability (**A**) was measured using MTT assay, WST-8 assay or Alamar Blue assay (Alamar B.) and was normalized to negative control. Activity of IL-8 promoter (**B**) was measured using LightSwitch Luciferase assay (LA), either directly or after different cell viability assays (with or without washing steps between viability assays and Luciferase assay). Data were normalized to negative control and represent mean ± SD ($n \geq 2$).

Since WST-8 and Alamar Blue assay are both based on coloured substrates with measurement of their absorption, a washing step between viability assay and Luciferase assay might reduce the influences on the luminescence-based Luciferase assay. MTT assay is known to cause cell damage and should therefore be considered as end-point assay (Lü et al., 2012). In contrast, the toxicity of WST-8 assay is considered very low (Merck, 2018b) and Alamar Blue assay is even stated to be performed with non-toxic substances (Thermo Fisher Scientific, 2016), which enables after both viability assays further analyses with the same cells, e.g. Luciferase assay. In addition to time and cost saving, cell viability and data for TLR4 activity can be received from the same cells, which enormously increases the

comparability. Considering all these points, Alamar Blue assay was chosen as standard viability assay for all subsequent measurements.

4.1.3. Investigation of nickel solutions as substitution for LPS

Nickel solutions were tested on HeLa-TLR4 reporter cells whether their TLR4 stimulatory activity might be favorable compared to stimulation with LPS. During incubation with up to 100 ng/ml LPS-EB, a viability of 90-95% was observed, compared to the viability of untreated cells (**Figure 4A**). These values were slightly lower when incubated with LPS-EB ultrapure (80-90%). After incubation with $NiCl_2$ and $NiSO_4$ with concentrations up to 250 µg/ml, the same viability ranges were observed. In higher concentrations, both solutions resulted in dose-dependent toxic effects. An increase of TLR4 stimulation was observed after incubation with different concentrations of both LPS types, which was slightly higher after incubation with LPS-EB ultrapure (**Figure 4B**). To receive a comparable TLR4 stimulation, $NiCl_2$ and $NiSO_4$ had to be added in much higher concentrations (µg/ml-range instead of ng/ml-range). Furthermore, both nickel solutions showed a maximum of TLR4 stimulation at a concentration of 250 µg/ml. A further increase of the concentration was observed to possess less stimulatory effects.

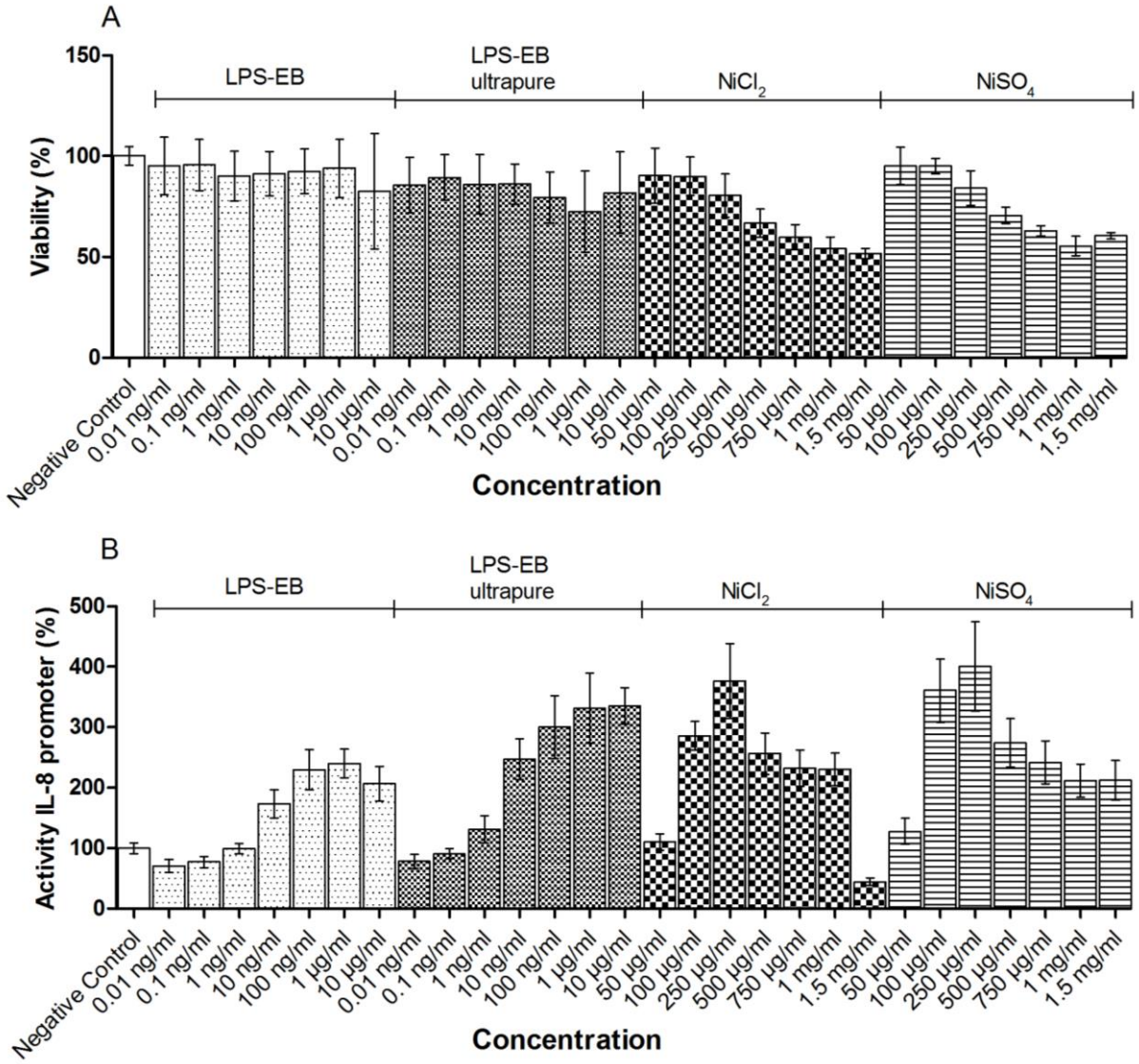

Figure 4: Comparison of different TLR4 agonists
HeLa-TLR4 reporter cells were incubated with LPS-EB, LPS-EB ultrapure, $NiCl_2$ and $NiSO_4$ in different concentrations. Viability (**A**) was measured using Alamar Blue assay and was normalized to negative control (untreated cells). Activity of IL-8 promoter (**B**) was measured using LightSwitch Luciferase assay and was normalized to negative control. Data represent mean ± SD ($n \geq 9$). Unpaired t-test (**B**): ***$p < 0.0001$ after incubation with LPS-EB ≥ 10 ng/ml, LPS-EB ultrapure ≥ 1 ng/ml, $NiCl_2$ ≥ 100 µg/ml and all tested $NiSO_4$ concentrations compared to negative control.

Combining viability and TLR4 activity data, LPS-EB and LPS-EB ultrapure are suitable TLR4 agonists for HeLa-TLR4 reporter cells, especially in concentrations up to 100 ng/ml. Furthermore, $NiCl_2$ and $NiSO_4$ comprise an alternative with good TLR4 agonistic activity, but higher toxicity than stimulation with LPS. Since treatment with $NiSO_4$ leads to a slightly higher TLR4 stimulation and cell viability in comparison to the treatment with the same concentrations of $NiCl_2$, $NiSO_4$ should be the preferred nickel solution to induce TLR4 stimulation. Due to less toxic effects combined with higher TLR4 stimulatory activity, LPS-EB and, to a smaller extend, LPS-EB ultrapure were used for further experiments. Nevertheless, $NiCl_2$ and $NiSO_4$ remain a cheaper alternative to the classical LPS-treatment with a recommended concentration based on our experiments of 100-250 µg/ml (approximately

0.4-1 mM) for 8h to stimulate HeLa-TLR4 reporter cells. This is in line with findings from literature, where treatment with at least 0.5 mM nickel has been observed to significantly induce TLR4 stimulation in cell culture (Schmidt et al., 2010; Oblak et al., 2015). Furthermore, nickel was demonstrated to directly activate human TLR4, whereas stimulation of mouse TLR4 has not been observed (Schmidt et al., 2010). Although nickel seems to depend on other human TLR4 sequences for receptor stimulation than LPS, it requires, analog to LPS treatment, MD-2 for triggering both MyD88-dependent and MyD88-independent signaling pathways (Schmidt et al., 2010; Oblak et al., 2015).

4.1.4. Optimizing LPS treatment for THP-1 monocytes

THP-1 monocytes were tested with different LPS-EB concentrations and incubation times to select the optimal conditions for further experiments. Cell viability (**Figure 5A**) was more consistent after 4h and 16h incubation with LPS-EB (2h incubation with Alamar Blue solution) compared to measurement after 8h LPS-EB incubation (1h incubation with Alamar Blue solution). Therefore, Alamar Blue incubation should be performed for at least 2h. ELISA was established as new method in our group for analyzing changes in cytokine release. A dose-dependent increase in IL-8 secretion was measured after incubation with LPS-EB, reaching the detection limit at 250 ng/ml LPS-EB (**Figure 5B**). Due to the good viability and sufficient stimulation of IL-8 secretion, 50 ng/ml LPS-EB for 4h was chosen as standard incubation for THP-1 monocytes. In literature, THP-1 monocytes have been reported to be stimulated by LPS using various incubation times and concentrations. Often even concentrations in µg/ml- or mg/ml-range were used, which seemed to be not necessary for our experiments (Baqui et al., 1999; Chanput et al., 2010; Trotter et al., 2017).

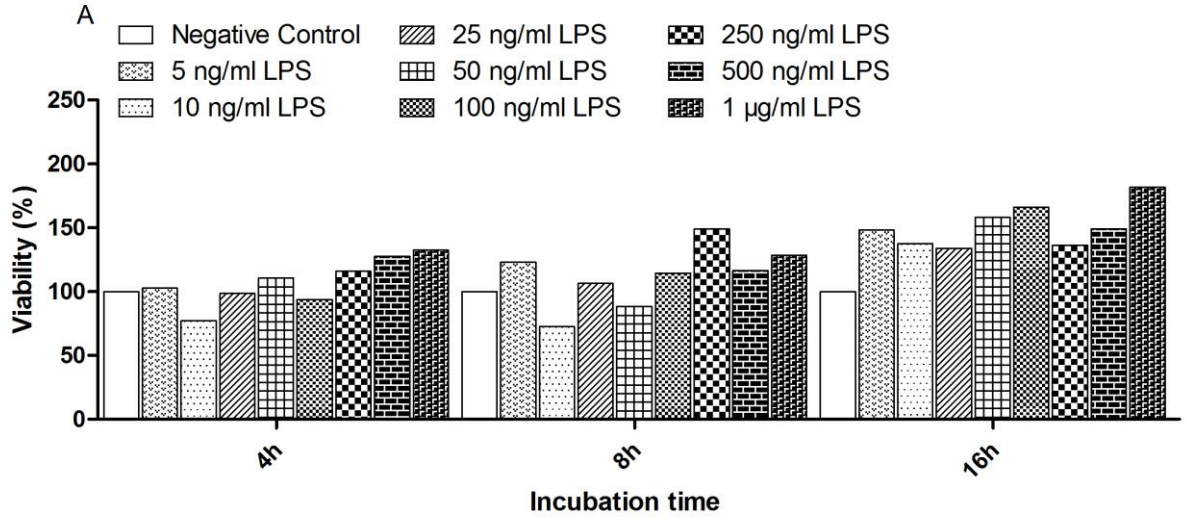

Figure continues on next page

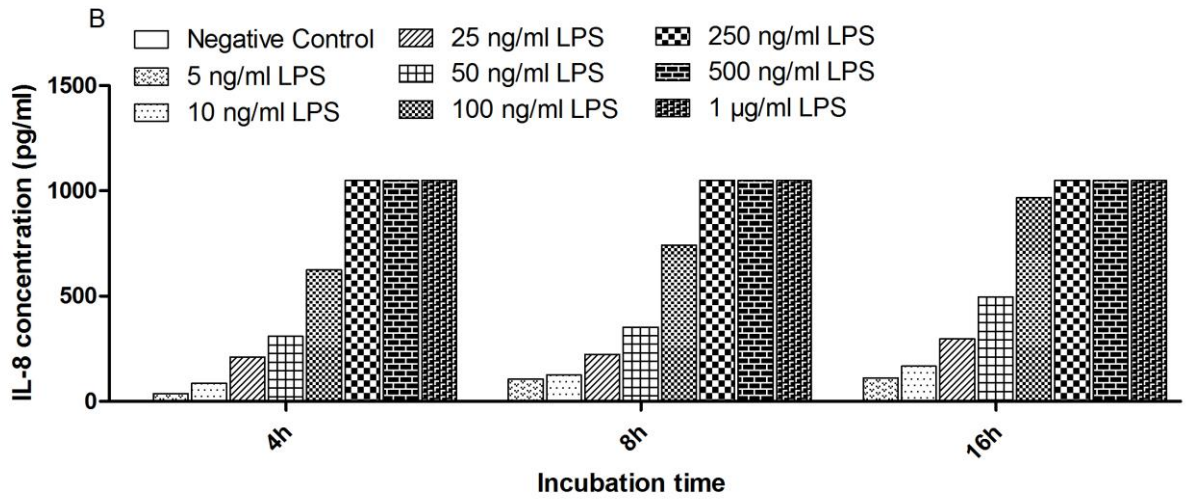

Figure 5: Optimizing LPS treatment for THP-1 monocytes
THP-1 monocytes were incubated with different concentrations of LPS-EB and different incubation times. Viability (**A**) was measured using Alamar Blue assay and was normalized to negative control (untreated cells). IL-8 concentration (**B**) was measured using ELISA. Data represent mean ± SD (*n*=2).

4.2. Screening of different extracts for their anti-inflammatory effects

Different, mainly herbal, extracts were screened in several cell culture-based assays on their anti-inflammatory effects, in particular on their influences on stimulated TLR2- and TLR4-dependent signaling pathways.

4.2.1. Screening for TLR-dependent anti-inflammatory effects

99 ethanolic extracts consisting of 96 herbal, one cyanobacterial, one green algal and one lichen extracts were tested in a first screening for their anti-inflammatory effects in stimulated HeLa-TLR4 reporter cells and THP-1 monocytes. Especially the ten extracts *Castanea sativa* (sweet chestnut), *Cinchona pubescens* (cinchona), *C. verum* (cinnamon), *Salix alba* (white willow), *Rheum palmatum* (rhubarb), *Alchemilla vulgaris* (common lady's mantle), *Humulus lupulus* (hops), *Vaccinium myrtillus* (bilberries), *Curcuma longa* (turmeric) and *Arctostaphylos uva-ursi* (bearberry) displayed major anti-inflammatory effects combined with high cell viabilities (**Figure 6**). All other extracts are graphically displayed in the appendix (**Figure 31**). In a general comparison of both cell lines, HeLa-TLR4 reporter cells were more sensitive to toxic effects in most of the treatments. Viability above 85% could be observed in THP-1 monocytes after treatment with the ten most promising extracts in concentrations up to 1%, with exception of *Humulus lupulus* cones and *Arctostaphylos uva-ursi* leaves. For some

extracts, e.g. those of *Castanea sativa* leaves, *C. verum* bark, *Humulus lupulus* cones and *Curcuma longa* root, comparable anti-inflammatory effects were observed in both cell lines, whereas other extracts like *Cinchona pubescens* bark and *Rheum palmatum* root were revealed to have a higher anti-inflammatory potential in THP-1 monocytes than in HeLa-TLR4 reporter cells. Most of the extracts were shown to possess a threshold for TLR4 mitigation (e.g. between 0.3% and 0.6% for *C. verum* extract), in contrast to *Castanea sativa* extract, which showed anti-inflammatory effects already at low concentrations.

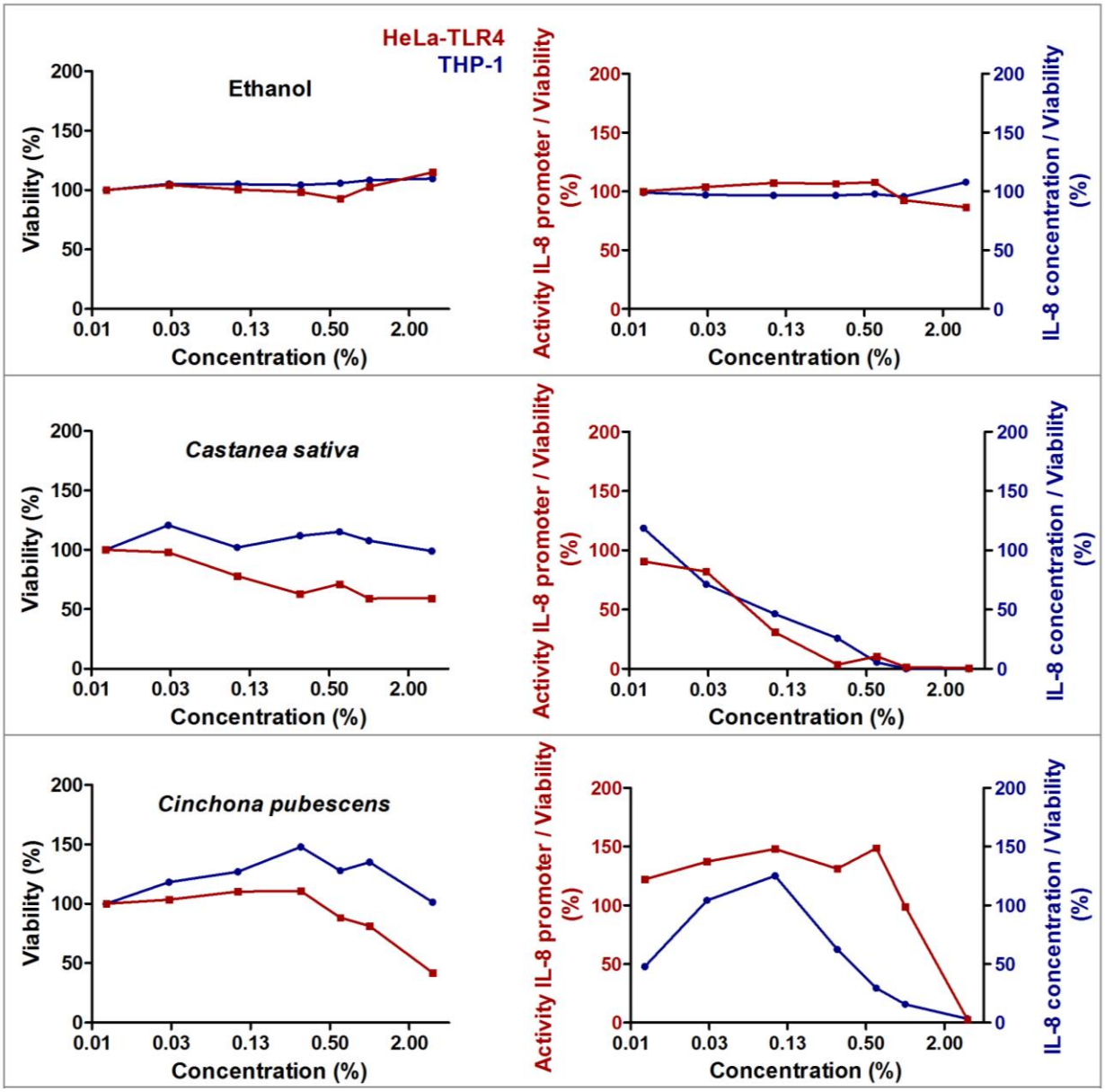

Figure continues on next page

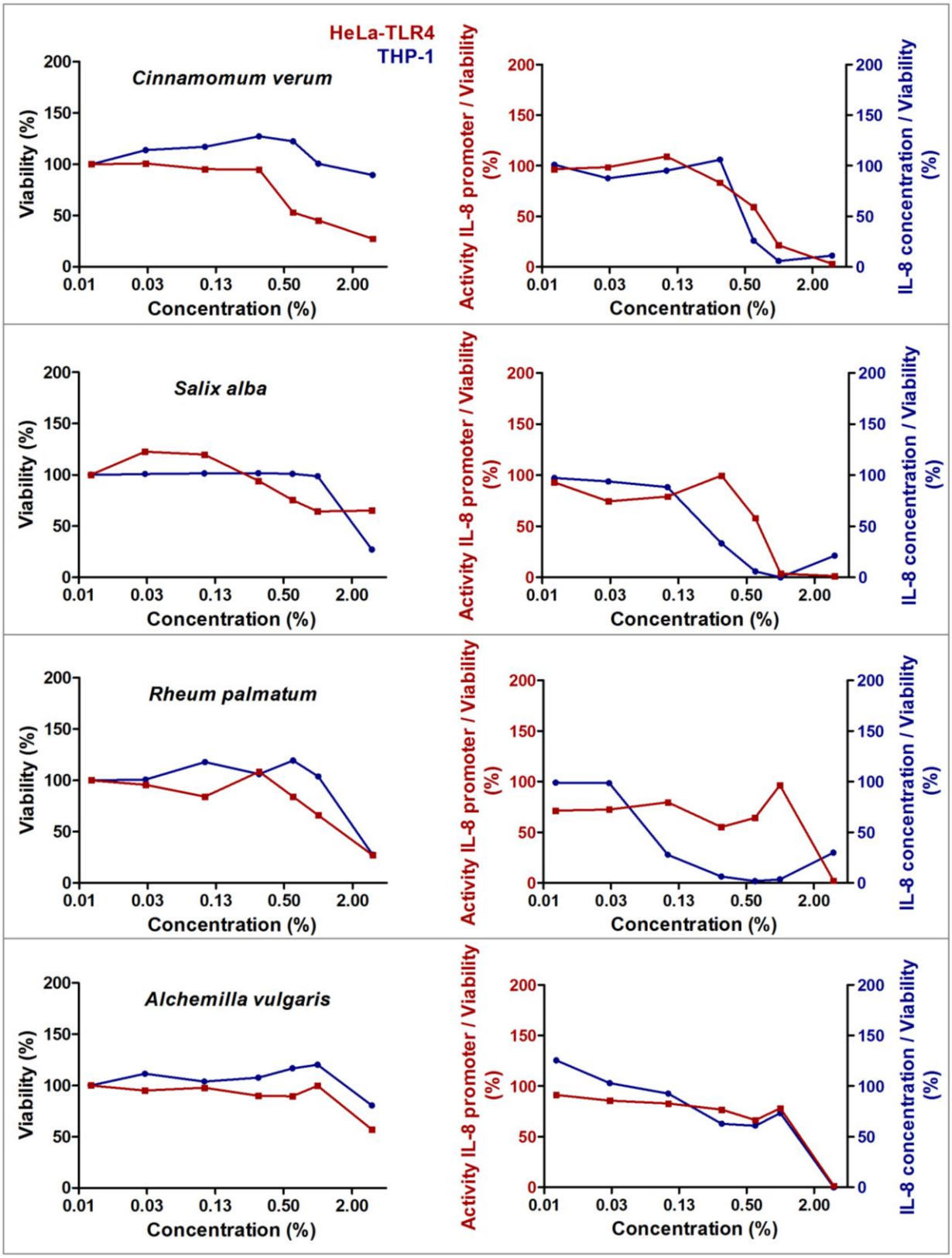

Figure continues on next page

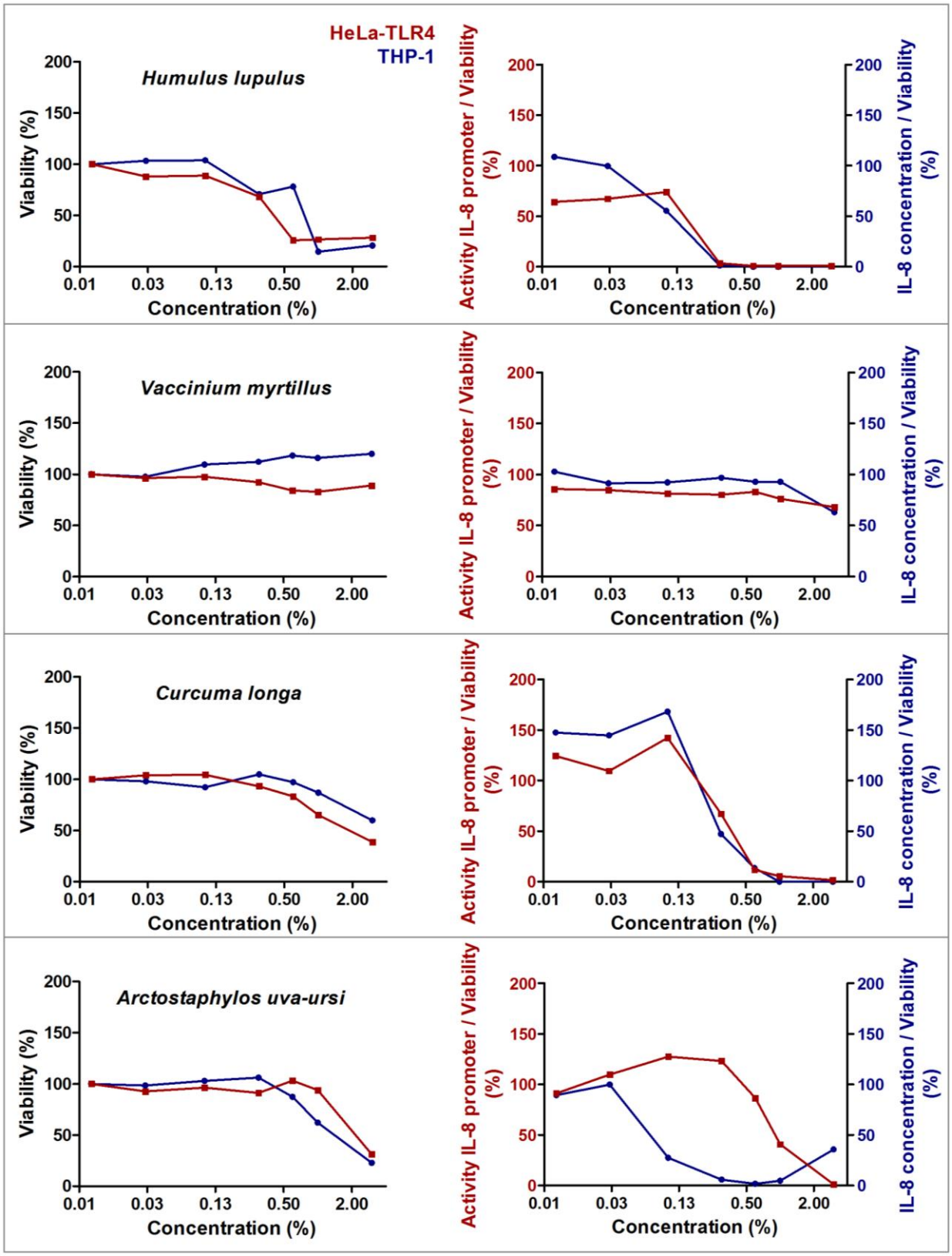

Figure 6: Cell viability and anti-inflammatory effects of ten most promising extracts
HeLa-TLR4 reporter cells (red) and THP-1 monocytes (blue) were incubated with extracts in different concentrations or vehicle 70% ethanol, followed by stimulation with LPS-EB. Viability (Alamar Blue assay) was normalized to negative control. TLR4 receptor activity (Renilla luciferase expression for HeLa-TLR4 reporter cell line and IL-8 ELISA for THP-1 monocytes) was normalized to vehicle-treated cells. Data are displayed as viability (%) in upper graphs and TLR4 activity divided by normalized viability in lower graphs. Data represent mean ($n \geq 2$). Further extracts are graphically displayed in appendix **Figure 31**.

A ranking of the extracts according to their anti-inflammatory potential is displayed in **Table 18** for the 25 most promising extracts and in appendix **Table 22** for all extracts. In both tables, heat maps display TLR4 stimulation normalized to viability with anti-inflammatory effects shown in green and pro-inflammatory effects shown in red.

Table 18: Anti-inflammatory activity of 25 most promising ethanolic extracts
HeLa-TLR4 reporter cells and THP-1 monocytes were incubated with extracts in different concentrations or vehicle 70% ethanol, followed by stimulation with LPS-EB. Viability (Alamar Blue assay) was normalized to negative control (*Viability (%)*). TLR4 receptor activity (Renilla luciferase expression for HeLa-TLR4 reporter cell line and IL-8 ELISA for THP-1 monocytes) was normalized to vehicle-treated cells (*TLR4-Activity*). Data are displayed as TLR4 stimulation divided by viability and ranked ascending by the following formula: (150 - *Viability (%)*)*(2**TLR4-Activity* + 100) weighted in a ratio of 2:1 for THP-1 monocytes vs. HeLa-TLR4 reporter cells. The 25 extracts with the highest mitigation of LPS-induced inflammatory signal are displayed in this table. Further extracts are shown in appendix **Table 22**. Data represent mean ($n \geq 2$).

Inflammatory scale **Toxicity**

anti-inflammatory pro-inflammatory viability < 75%

			HeLa-TLR4 reporter cell line							THP-1 monocytes						
Latin name	**Common English name**	**Used part**	**0.01%**	**0.03%**	**0.1%**	**0.3%**	**0.6%**	**1%**	**3%**	**0.01%**	**0.03%**	**0.1%**	**0.3%**	**0.6%**	**1%**	**3%**
Ethanol control			100,00	101,30	103,67	102,01	93,23	85,77	90,26	98,88	97,04	96,54	96,59	97,67	95,66	107,91
Castanea sativa	Sweet chestnut	Leaf	90,53	82,03	30,91	3,53	10,59	1,34	0,79	118,69	71,34	46,42	25,73	5,65	0,00	0,00
Cinchona pubescens	Cinchona	Bark	122,15	137,25	148,02	131,28	148,76	98,71	2,77	47,68	104,26	125,10	62,37	29,49	15,68	3,49
Cinnamomum verum	Cinnamon	Bark	96,77	98,57	109,17	83,50	59,41	21,59	3,24	101,16	87,70	95,31	106,02	26,08	6,08	11,36
Salix alba	White willow	Bark	93,03	74,48	79,05	99,83	58,02	3,79	1,45	97,50	93,93	88,45	33,44	5,95	0,00	21,34
Rheum palmatum	Rhubarb	Root	71,38	72,58	79,60	55,28	64,48	96,37	2,34	99,17	98,60	27,86	6,42	1,94	3,57	29,89
Alchemilla vulgaris	Common lady's mantle	Whole plant	91,35	85,79	82,86	76,83	66,53	78,18	1,63	125,37	102,96	92,63	62,93	60,89	73,46	0,00
Humulus lupulus	Hops	Flower	64,31	67,38	74,08	3,57	1,10	0,92	0,96	108,76	99,78	55,66	1,46	0,00	0,00	0,73
Vaccinium myrtillus	Bilberries	Fruit/berry/ seed	86,00	84,71	81,50	80,48	83,01	76,30	68,10	102,84	91,37	92,22	96,85	92,91	92,95	63,02
Curcuma longa	Turmeric	Root	124,40	109,62	142,43	67,28	11,92	5,54	1,83	127,14	110,90	115,73	45,39	8,99	0,00	15,80
Arctostaphylos uva-ursi	Bearberry	Leaf	91,28	109,88	127,59	123,26	86,52	40,81	1,18	89,45	99,97	27,43	5,97	1,72	4,71	35,80
Allium ursinum	Wild garlic	Leaf	115,74	118,86	97,71	91,94	81,27	78,25	42,93	105,80	109,20	77,64	38,94	24,16	5,90	11,21
Hypericum perforatum	St John's wort	Whole plant	120,77	104,44	85,91	83,69	71,41	53,35	14,06	91,44	85,40	90,32	71,54	51,19	32,03	1,14
Arnicae montana	Arnica	Flower	114,17	96,34	2,78	2,14	2,61	2,55	1,28	144,96	146,96	11,90	0,70	0,69	1,67	0,53
Aloe ferox	Aloe	Whole plant	105,30	105,90	82,53	58,19	27,69	5,15	1,30	123,82	117,87	88,51	38,22	9,71	7,37	0,13
Cynara scolymus	Artichoke	Leaf	109,98	112,42	117,52	100,14	90,16	31,21	1,99	47,40	53,68	127,22	228,92	16,56	6,13	2,86
Salvia officinalis	Salvia	Leaf	94,88	96,95	107,50	89,57	73,14	17,55	2,65	94,87	87,05	79,10	72,53	97,48	42,03	0,00
Ginkgo biloba	Ginkgo	Leaf	107,04	120,25	119,37	90,15	44,17	4,77	2,22	124,31	101,09	22,26	7,98	16,68	9,27	0,00
Tanacetum parthenium	Feverfew	Whole plant	127,34	111,53	120,04	114,28	99,98	68,82	2,22	129,88	139,58	123,43	124,51	72,56	21,24	6,12
Vigna radiata	Mung bean (dried)	Fruit/berry/ seed	83,31	85,02	87,84	85,99	69,53	52,04	25,33	121,14	141,32	120,83	62,61	38,87	23,18	11,00
Betula verrucosa	Weeping birch	Juice/resin	144,10	148,90	136,35	139,46	143,77	154,99	88,24	120,90	131,27	106,29	88,92	93,49	94,35	93,18
Filipendula ulmaria	Meadowsweet	Flower	120,04	113,11	130,06	117,06	106,72	131,55	52,01	132,40	135,84	124,42	75,12	23,05	8,87	1,88
Matricaria chamomilla	Chamomile	Whole plant	100,35	104,50	90,84	78,36	84,92	5,43	1,26	107,39	110,30	81,01	78,37	109,61	0,00	0,00
Spirulina	Spirulina	Whole cyanobacteria	93,17	100,77	107,05	92,24	76,80	50,64	3,57	142,68	138,71	169,61	74,85	20,59	2,70	36,20
Gentiana lutea	Gentian	Root	120,08	105,07	118,69	89,81	89,96	82,85	39,06	80,63	60,91	89,51	140,23	62,51	43,53	2,92
Quercus robur	English oak	Bark	143,68	142,56	127,88	124,88	134,53	106,17	8,76	106,31	116,82	88,62	57,00	35,67	16,07	16,81

Since HeLa-TLR4 reporter cells were co-transfected with human TLR4, MD-2 and CD14, they may not exhibit all cross-links to other TLR4 related pathways. In contrast, THP-1 monocytes naturally express several innate immune receptors, so the results revealed with THP-1 monocytes may rather display the physiological situation in the body. For ranking of the extracts, effects on THP-1 monocytes and HeLa-TLR4 reporter cells were therefore weighted in a ratio of 2:1. Furthermore, TLR4 inhibition was calculated with a higher impact than effects on cell viability. In general, extract concentrations resulting in viabilities below 75% (marked in the heat maps in grey) should be considered cautiously. Here, the influences on TLR4-dependent cytokine production might be dominated by toxic effects. Interestingly, three bark extracts were within the top five anti-inflammatory extracts in this study (number 2: *Cinchona pubescens*, number 3: *C. verum* and number 4: *Salix alba*). Since various extracts demonstrated potent anti-inflammatory activities, the most promising candidates were additionally tested in a comparative assay for the potential ability to specific antagonize TLR4 (**chapter 4.2.2**).

Incubation with the extract of *Juniperus communis* (common juniper) showed by far the highest pro-inflammatory potential (appendix **Figure 31** and **Table 22**), so a LAL assay was performed to analyze if this effect might be due to endotoxin contamination. With an endotoxin level below detection range, a potential LPS contamination of the sample was excluded. The TLR4 stimulatory effects of *Juniperus communis* without toxicity in low doses might also be an interesting starting point for further research. Depending on the conditions in different phases of cancer development and metastasis, TLR4 stimulation might possess not only procancer, but also anticancer effects. Hereby, TLR4 stimulation induces the cytotoxic T-cell immune response, leading to the apoptosis of cancer cells (Awasthi, 2014).

Besides the testing of 99 ethanolic extracts for their anti-inflammatory effects in different cell culture-based assay systems, further interesting extracts comprising cyanobacteria and plant samples in different solvents were applied to the THP-1 anti-inflammatory assay system.

LPS-stimulated THP-1 monocytes preincubated with eight cyanobacteria species domiciled in different habitats and ecological niches (*Microcystis aeruginosa* (*Mic*), *Cylindrospermum siamensis* (*Cyl*), *Anabaena ambigua* (*Ana*), *Lyngbya lagerheimii* (*Lyn*) and *Planktothrix agardhii* (*Pla*) originated in fresh water environment, *Synechocystis* sp. (*Syn*) and *Phormidium* sp. (*Pho*) in marine environment and *Nostoc* sp. (*Nos*) in soil environment) resulted for all treatments in a viability above 90% compared to solvent (PBS) treated cells (**Figure 7A**). In comparison of all treatments, *Nos* was the only cyanobacteria, which significantly mitigated LPS-induced TLR4 stimulation divided by normalized viability (**Figure**

7B). Using 1 µg/ml *Nos*, the LPS-induced TLR4 stimulation in THP-1 monocytes was reduced by 60.3% and 10 µg/ml *Nos* resulted even in 87.6% reduction compared to solvent treatment.

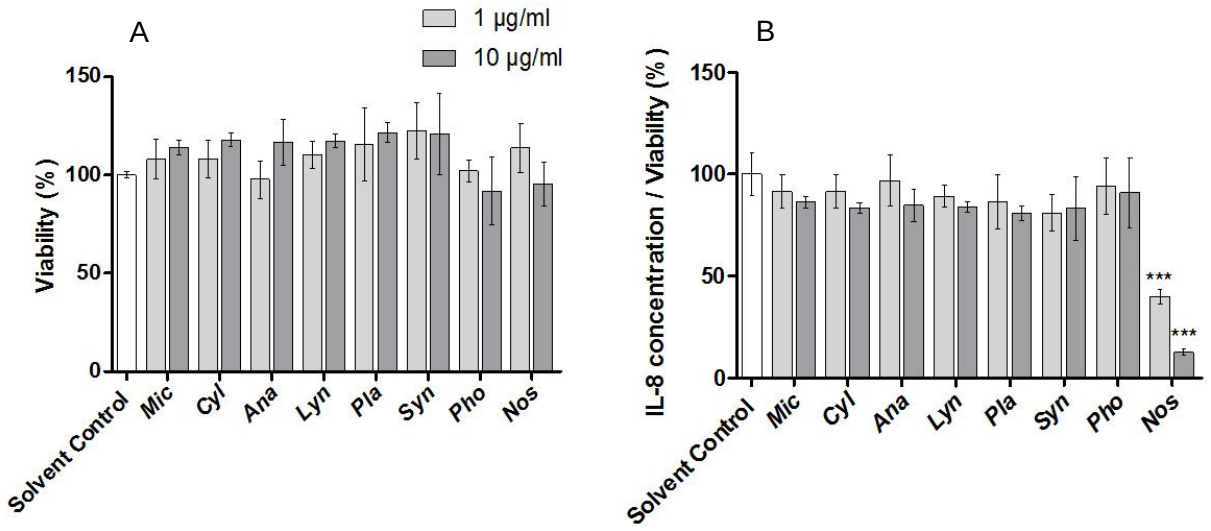

Figure 7: Cell viability and anti-inflammatory effects of different cyanobacteria species
THP-1 monocytes were incubated with different cyanobacteria species or PBS control, followed by stimulation with LPS-EB. **A:** Viability (Alamar Blue assay) was normalized to solvent-treated cells. **B:** IL-8 concentration (ELISA) was divided by normalized viability and was normalized to solvent-treated cells. Data represent mean ± SD (*n*=3); unpaired t-test: ***p < 0.0005 compared to solvent control. *Mic*: *Microcystis aeruginosa*, *Cyl*: *Cylindrospermum siamensis*, *Ana*: *Anabaena ambigua*, *Lyn*: *Lyngbya lagerheimii*, *Pla*: *Planktothrix agardhii*, *Syn*: *Synechocystis* sp., *Pho*: *Phormidium* sp., *Nos*: *Nostoc* sp.

In literature, some cyanobacterial LPS, e.g. from *Oscillatoria planktothrix*, have been reported to inhibit TLR4 stimulation. The TLR4 antagonistic cyanobacterial LPS have been described to compete with bacterial LPS for TLR4 binding sides and therefore to reduce pro-inflammatory cytokine release and toxin shock (Macagno et al., 2006; Durai et al., 2015). In addition to our observed anti-inflammatory effects of *Nos* (SAG 70.79), further *Nostoc* spp. have been described to possess anti-inflammatory potentials (Kapuścik et al., 2013; Itoh et al., 2014). However, to the best of our knowledge, the anti-inflammatory effect of the *Nos* tested in this study, has been first described by our findings (Lang-Yona et al., 2018).

Another investigated plant extract was *Fallopia japonica* Houtt. (Japanese knotweed). Viability of LPS-stimulated THP-1 monocytes preincubated with *Fallopia japonica* leaves redissolved in 70% acetonitrile, 70% acetone or 70% ethanol was for all samples above 95% compared to LPS-stimulated cells pretreated with solvent control (**Figure 8A**). Viability of LPS-stimulated THP-1 monocytes preincubated with the corresponding root samples was above 84%. No anti-inflammatory activity was observed after *Fallopia japonica* treatment in the same experiment (**Figure 8B**). Although *Fallopia japonica* samples redissolved in acetone generally resulted in lower inflammatory responses, no significant anti-inflammatory effects were observed compared to solvent control. The highest pro-inflammatory effects

were identified for treatment with 100 µg/ml *Fallopia japonica* extracts, especially for root samples redissolved in acetonitrile or ethanol.

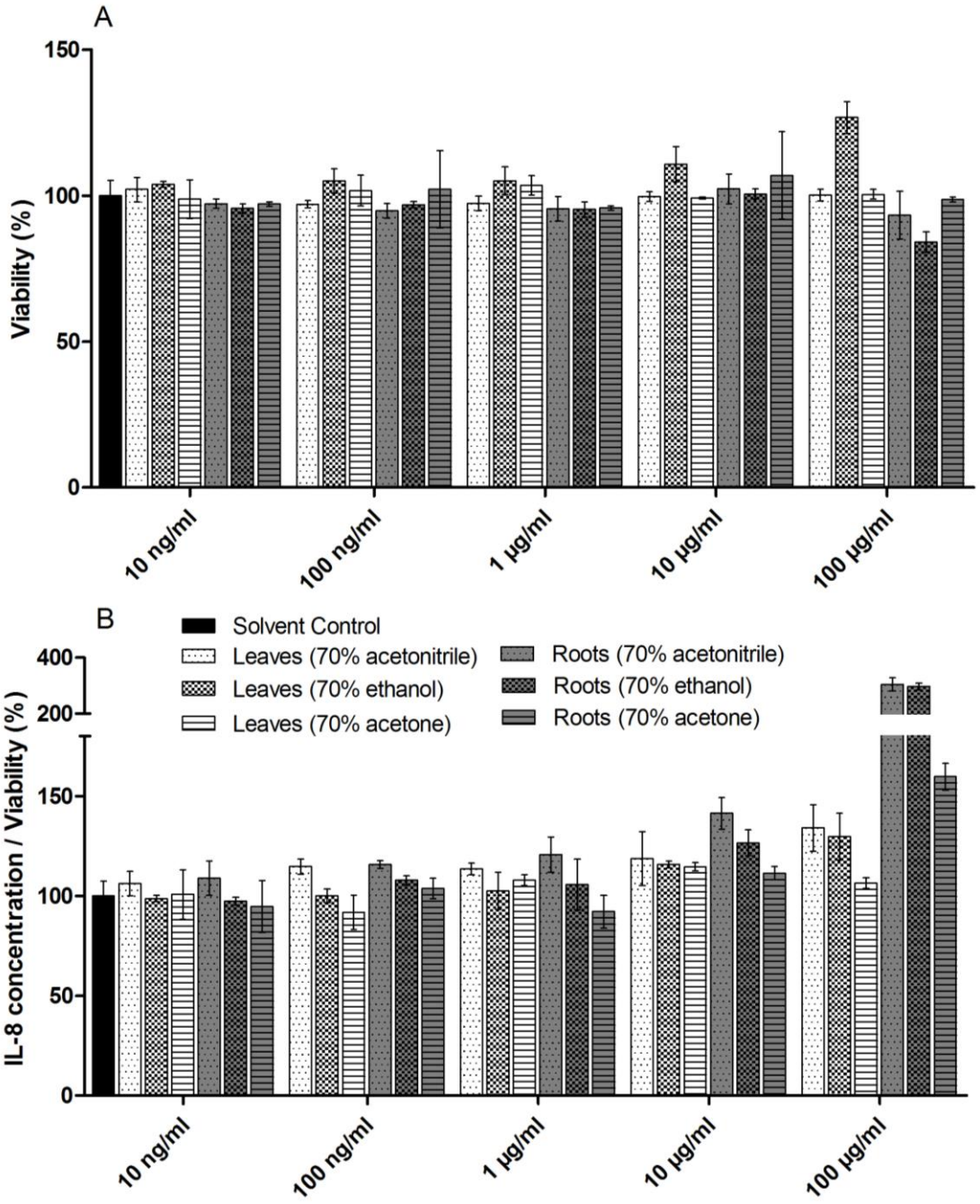

Figure 8: Cell viability and anti-inflammatory effects of *Fallopia japonica* samples
THP-1 monocytes were incubated with *Fallopia japonica* samples or solvent control, followed by stimulation with LPS-EB. **A**: Viability (Alamar Blue assay) normalized to solvent-treated cells. **B**: IL-8 concentration (ELISA) divided by normalized viability. Data represent mean ± SD ($n \geq 2$); unpaired t-test: no significance (*$p < 0.05$) compared to solvent control.

Fallopia japonica is one of the world's most common invasive species and used in traditional Chinese medicine for centuries due to its beneficial health effects (Sohn et al., 2016). Several compounds within *Fallopia japonica*, e.g. resveratrol, emodin and anthraquinone glycosides, have been shown in literature to reduce inflammatory effects (Han et al., 2015;

Uddin et al., 2016). In addition, an ethanolic root extract of *Fallopia japonica* has been reported to inhibit the activation of high-mobility group box-1 (HMGB1)/receptor for advanced glycation end products (RAGE)/NF-κB pathways in diabetic retinas, leading to a preventive effect against diabetes-induced damages (Sohn et al., 2016). Furthermore, *Fallopia japonica* and its active compounds, resveratrol and emodin, have been observed to possess TLR9-induced antiviral activities (Lin et al., 2015). Nevertheless, to the best of our knowledge, influences of *Fallopia japonica* on TLR4-induced inflammatory processes are not reported so far.

4.2.2. Screening for exclusive TLR4 antagonistic effects

In addition to the identification of anti-inflammatory herbal extracts in HeLa-TLR4 reporter cells and THP-1 monocytes, 28 ethanolic extracts with strong anti-inflammatory activities were tested for the potential ability to specific antagonize TLR4. A comparative assay with stimulated HEK-TLR2 and HEK-TLR4 reporter cells was performed to discriminate between direct TLR4 antagonistic effects and interference with the downstream signaling pathway shared by TLR2 and TLR4 signaling. A main outcome of the experiments was that all extracts mitigated the stimulated TLR2- and TLR4-dependent response (**Figure 9** with the five most promising extracts and appendix **Figure 32** with all other tested extracts). This leads in general to the assumption that all tested extracts interfere with the NF-κB/AP-1 signaling pathways of both TLR2 and TLR4. So, no exclusive TLR4 antagonist was found among the tested extracts.

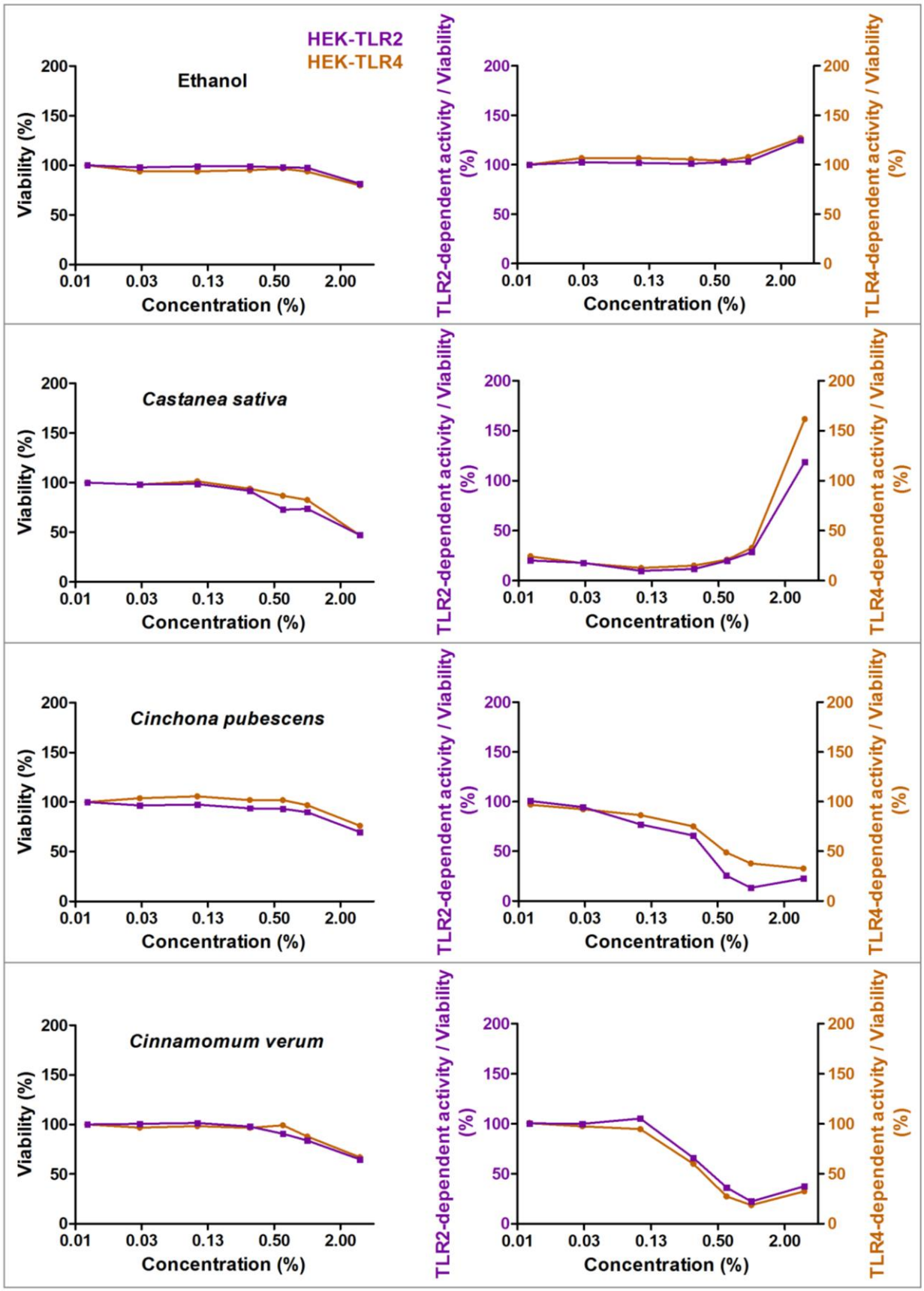

Figure continues on next page

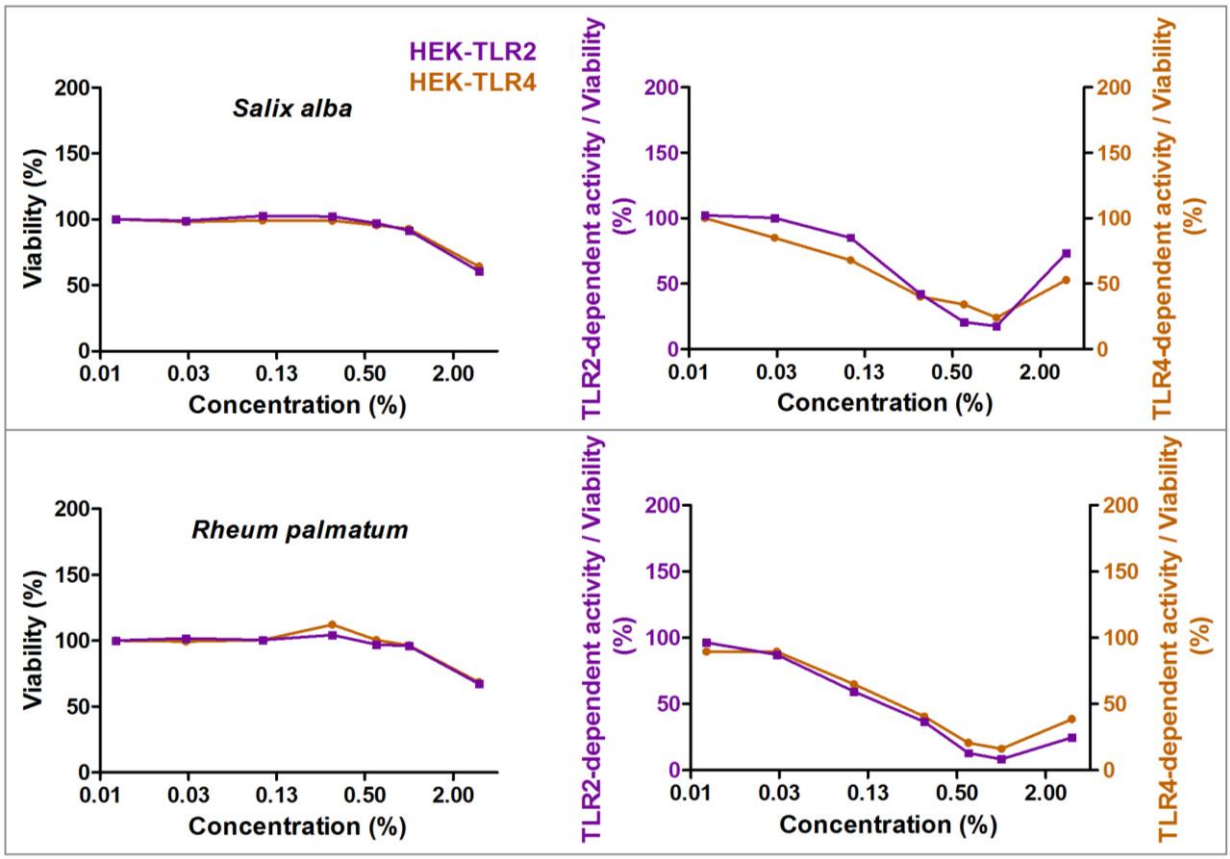

Figure 9: Cell viability and anti-inflammatory effects of five most promising extracts tested for exclusive TLR4 antagonistic activity
HEK-TLR2 (purple) and HEK-TLR4 reporter cells (orange) were incubated with extracts in different concentrations or vehicle 70% ethanol, followed by stimulation with Pam2CSK4 (HEK-TLR2 reporter cells) or LPS-EB ultrapure (HEK-TLR4 reporter cells). Viability (Alamar Blue assay) was normalized to negative control. TLR2 and TLR4 receptor activity (SEAP production) were normalized to vehicle-treated cells. Data are displayed as viability (%) in upper graphs and receptor activity divided by viability in lower graphs. Data represent mean ($n \geq 4$). Further extracts are graphically displayed in appendix **Figure 32**.

A comparable dose-dependent anti-inflammatory effect in HEK-TLR2 and HEK-TLR4 reporter cells was shown for most of the extracts, especially the ten most promising candidates. Interestingly, *Castanea sativa* leaves mitigated the TLR2- and TLR4-dependent inflammatory response already at 0.01% extract in cell culture medium, accompanied with a cell viability around 100%. An increase of the inflammatory activity was observed for most of the extracts at concentrations between 1% and 3% in cell culture medium, which is most probably induced by toxic effects at these concentrations. Heat maps of the five most promising extracts (**Table 19**) and of all tested 28 extracts (appendix **Table 23**) display the TLR2- and TLR4-dependent stimulation with anti-inflammatory activity shown in green to pro-inflammatory activity shown in red. Ranking of the extracts was adopted from **Table 18** and appendix **Table 22** (HeLa-TLR4 and THP-1 screening).

Table 19: TLR2 and TLR4 specific antagonistic activity of five most promising ethanolic extracts
HEK-TLR2 and HEK-TLR4 reporter cells were incubated with extracts in different concentrations or vehicle 70% ethanol, followed by stimulation with Pam2CSK4 (HEK-TLR2 reporter cells) or LPS-EB ultrapure (HEK-TLR4 reporter cells). Viability (Alamar Blue assay) was normalized to negative control. TLR2 and TLR4 receptor activity (SEAP production) were normalized to vehicle-treated cells. Data are displayed as receptor stimulation divided by normalized viability. The five extracts with the highest mitigation of LPS-induced inflammatory signal from **Table 18** are displayed in this table. Further extracts are shown in appendix **Table 23**. Data represent mean ($n \geq 4$).

Inflammatory scale **Toxicity**

anti-inflammatory pro-inflammatory viability < 75%

			HEK-TLR2 reporter cell line							HEK-TLR4 reporter cell line						
Latin name	Common English name	Used part	0.01%	0.03%	0.1%	0.3%	0.6%	1%	3%	0.01%	0.03%	0.1%	0.3%	0.6%	1%	3%
Ethanol control			100,00	102,45	101,84	101,03	102,55	103,43	124,76	100,00	106,70	106,82	105,37	103,93	107,97	127,11
Castanea sativa	Sweet chestnut	Leaf	20,06	17,83	9,78	11,82	19,94	28,56	118,82	24,28	17,36	12,78	15,09	20,87	32,77	161,75
Cinchona pubescens	Cinchona	Bark	100,53	94,50	77,03	65,89	25,61	13,17	22,78	96,97	92,46	86,34	75,11	48,95	37,82	32,81
Cinnamomum verum	Cinnamon	Bark	100,40	100,11	105,47	65,88	36,23	22,34	37,65	100,75	97,62	94,69	59,98	27,50	18,82	32,43
Salix alba	White willow	Bark	102,12	100,18	85,03	42,14	20,67	17,65	73,17	100,01	85,03	67,85	40,08	34,16	24,12	52,75
Rheum palmatum	Rhubarb	Root	96,48	87,24	59,40	36,53	13,11	8,17	24,68	89,65	89,52	64,85	40,62	20,74	16,27	38,65

As 99 ethanolic extracts were tested in the screening for TLR-dependent anti-inflammatory effects, not all of them will be discussed in detail. The focus will be set on the ten most promising candidates identified with the presented *in vitro* assays, including *Castanea sativa* leaves, *Cinchona pubescens* bark, *C. verum* bark, *Salix alba* bark, *Rheum palmatum* root, *Alchemilla vulgaris* plant, *Humulus lupulus* cones, *Vaccinium myrtillus* berries, *Curcuma longa* root and *Arctostaphylos uva-ursi* leaves. Especially *Castanea sativa* leaves and *Alchemilla vulgaris* plant extracts represent promising candidates for further investigations, since their influences on TLR2 and TLR4 signaling pathways were, to the best of our knowledge, observed in this study for the first time.

Castanea sativa (sweet chestnut) – leaves

In our assays, strong dose-dependent anti-inflammatory effects, represented by decreased IL-8 concentrations, were observed after incubation with sweet chestnut leaf extract. In addition, high anti-inflammatory activity in the comparative HEK-TLR2/HEK-TLR4 assay system, even at low extract concentrations, were shown for the same extract. Sweet chestnut, which was utilized in traditional medicine to treat skin and soft tissue infections, is extensively used in chestnuts production (Quave et al., 2015). In current studies, several beneficial health effects have been revealed for its fruit, e.g. antioxidant and antimicrobial effects (de Vasconcelos et al., 2010; Quave et al., 2015; Pinto et al., 2017). Direct antioxidant effects and influences on vitamin A and redox-sensitive signaling pathways have been postulated for the carotenoid content in fruits and leaves (de Vasconcelos et al., 2010). However, concerning the anti-inflammatory effects of sweet chestnut leaves, only limited

information have been reported so far and to the best of our knowledge, its properties to mitigate TLR2 or TLR4 stimulation have not yet been described.

Alchemilla vulgaris (common lady's mantle) – whole plant

In our experiments, common lady's mantle plant extract led to a decrease of LPS-induced cytokine production and showed inhibitory effects on stimulated signaling pathways of both TLR2 and TLR4. Thus, these results offer a promising starting point for further investigations. In Europe, common lady's mantle has been traditionally used for the treatment of diverse disorders, e.g. urogenital diseases, eczema, inflammation, diarrhea and sepsis (Kiselova et al., 2006; Takır et al., 2015). But also in current studies, several beneficial health effects have been revealed, e.g. antiviral, antioxidant and wound healing properties (Kiselova et al., 2006; Shrivastava et al., 2007; Takır et al., 2015; Filippova, 2017). However, to the best of our knowledge, our observed inhibition of LPS-induced cytokine production and the mitigation of both TLR2 and TLR4 signaling pathways have not been reported yet.

In addition to *Castanea sativa* and *Alchemilla vulgaris*, which are newly described to have TLR2- and TLR4-dependent anti-inflammatory activities, anti-inflammatory effects of the eight remaining promising extracts were supported by existing descriptions in the literature. However, general anti-inflammatory effects or specific mitigation of TLR2 and TLR4 signaling pathways have often been solely observed for single compounds within the extracts but not for the complex whole extracts themselves. Consequently, further compounds within these extracts might contribute to the observed beneficial health effects.

Arctostaphylos uva-ursi (bearberry) – leaves

In our assays, bearberry leaves showed strong dose-dependent anti-inflammatory activities in several cell lines. In traditional medicine, bearberry leaves have been used as treatment for infections of the lower urinary tract. But also in modern medicine, they have been proven to possess antiseptic and anti-adhesion properties (Yarnell, 2002). The phenolic glycoside arbutin, an active compound in bearberry, has been revealed to possess antioxidant and anti-inflammatory effects, e.g. reduction of pro-inflammatory cytokine production and inflammation-related genes including IL-1β, TNF-α, monocyte chemoattractant protein-1 (MCP-1) and IL-6, as well as inhibition of NF-κB translocation into the cell nucleus (Lee and Kim, 2012). While arbutin was observed to be the major active compound in bearberry extract, the whole extract is required for the complete pharmaceutical activity (de Arriba et al., 2013). The observed anti-inflammatory effects for arbutin are supported by our experiments with whole bearberry extract, which has, based on our present knowledge, not yet been reported to influence TLR2 or TLR4 signaling pathways.

Cinchona pubescens (cinchona) – bark

In our experiments, we could show that whole cinchona bark extract diminished LPS-induced inflammatory signals, especially in THP-1 monocytes and the comparative HEK-TLR2/HEK-TLR4 assay system. Cinchonine from cinchona bark have been observed to inhibit both TLR2 and TLR4 signaling pathways *in vivo* (Jung et al., 2012), which is consistent with our *in vitro* data of cinchona bark extract. However, to the best of our knowledge, our observed mitigation of TLR2 and TLR4 signaling pathways by whole cinchona bark extract has not been described previously. Other compounds besides cinchonine might contribute to its potent anti-inflammatory effects.

Humulus lupulus (hops) – cones

A strong decrease of pro-inflammatory cytokine production was observed after hops treatment in different cell culture-based assays. Female hops cones, which are extensively used in the brewing industry, have been reported to contain several active compounds, especially flavonoids. Different biological activities have been described for hop flavonoids, among others, anticarcinogenic, antioxidant, antimicrobial, anti-inflammatory and estrogenic properties (Karabin et al., 2015). Particularly, xanthohumol has been observed to effectively inhibit the metabolism of arachidonic acid through inhibition of COX-1 and COX-2 (Gerhäuser, 2005). Moreover, xanthohumol has been shown to inhibit the LPS-dependent production of NO, IL-1β and TNF-α, as well as to mitigate the activation of NF-κB signaling (Lee et al., 2011). The mitigation of the TLR4-dependent signaling has been attributed to the binding of xanthohumol to MD-2 (Fu et al., 2016). However, further compounds in hops extract might contribute to our observed strong anti-inflammatory effects, since also the MD-2-independent TLR2 signaling pathway was mitigated by *Humulus lupulus* extract.

Salix alba (white willow) – bark

In our assays, strong dose-dependent anti-inflammatory effects, represented by decreased pro-inflammatory cytokine production, were observed after white willow incubation in TLR2- and TLR4-stimulated cell lines. White willow is one of the herbal extracts commonly known for its potent beneficial health effects (**chapter 1.1**). Various *in vitro* and *in vivo* studies demonstrate its anti-inflammatory effects such as the inhibition of the production of several pro-inflammatory cytokines, e.g. TNF-α and inhibition of NF-κB translocation (Bonaterra et al., 2010; Shara and Stohs, 2015), which is supported by the data obtained by us. Although the beneficial health effects have mainly been credited to salicin, this compound cannot completely explain the anti-inflammatory effects. Further compounds of white willow, especially polyphenols such as flavonoids and proanthocyanidins, have therefore been suggested to contribute to its overall activity, which might also broaden the underlying

mechanisms of action (Nahrstedt et al., 2007; Bonaterra et al., 2010; Vlachojannis et al., 2011).

Curcuma longa (turmeric) – root

Our results demonstrate that the TLR2/TLR4 signaling pathways are molecular targets of turmeric extract. This was also confirmed by literature, where curcuma and some of its compounds, especially curcumin and aromatic-turmerone, have been observed to influence several TLR2 and TLR4 signaling pathway molecules. LPS-induced NF-κB activation and expression of TLR4, IRAK1 and TRAF6 have been mitigated after turmeric extract treatment (Angel-Morales et al., 2012). Furthermore, curcumin, one of the main compounds in turmeric extract, has been demonstrated to mitigate both LPS-induced MyD88-dependent and MyD88-independent TLR4 signaling pathways, leading, among others, to an attenuation of TNF-α, IL-6 and ROS production as well as inhibition of NF-κB, IRF3 and MyD88 (Youn et al., 2006b; Zhu et al., 2014; Yu et al., 2016). Furthermore, another compound of turmeric, aromatic-turmerone, has been described to decrease the release of pro-inflammatory mediators via TLR4 signaling pathway (Chen et al., 2018).

Rheum palmatum (rhubarb) – root

In our experiments, rhubarb root extract led to a decrease of LPS-induced cytokine production in cell cultures and showed inhibitory effects on stimulated signaling pathways of both TLR2 and TLR4. In line with our data, rhubarb root has been described in literature to significantly mitigate TLR2 and TLR4 protein and mRNA expression *in vivo* (Liu et al., 2008; Yao et al., 2015). Emodin, which can be isolated from *Rheum palmatum* rhizomes, has been reported to influence several inflammation and cancer related target molecules, e.g. it decreases the activity of the important molecules NF-κB and AKT in TLR2 and TLR4 signaling pathways (Shrimali et al., 2013; Janeczko et al., 2017). For complete TLR4 stimulation, the TLR4/MD-2 complex has to translocate into lipid rafts, where clustering takes place (Pike, 2003; Szabo et al., 2007). Emodin has been observed to suppress LPS-dependent cytokine and chemokine production, as well as IκBα degradation and NF-κB activation by disruption of the lipid rafts (Meng et al., 2010). Nevertheless, further compounds within the complex mixture of rhubarb extract might contribute to its inhibitory effects on TLR2- and TLR4-mediated signaling.

Vaccinium myrtillus (bilberries) – berries

In our experiments, we could show that bilberry extract mitigated LPS-induced inflammatory signals. Bilberry extract has been reported to possess *in vivo* anti-inflammatory effects, e.g. by inhibition of LPS-induced liver mRNA levels of iNOS, TNF-α, IL-1β and IL-6 as well as

protein levels of iNOS, TNF-α and NF-κB (Luo et al., 2014). These anti-inflammatory effects are supported by our data, which show a decrease of LPS-induced cytokine production after treatment with bilberry extract. People suffering from metabolic syndrome showed in a randomized, controlled dietary intervention with bilberry supplementation a reduction of serum high-sensitivity C-reactive protein (CRP), IL-6, IL-12 and LPS concentrations. In the same study, a downregulation of genes associated with TLR4 signaling pathway has been observed. Generally, a regular bilberry intake was stated to potentially decrease low-grade inflammation, which in long-term might result in a reduction of cardiometabolic risk (Kolehmainen et al., 2012). In a second study, these anti-inflammatory effects have been confirmed. Here, consumption of bilberry juice led to decreased plasma concentrations of CRP, IL-6 and IL-15 in patients with increased risk factor for cardiovascular disease (Karlsen et al., 2010). Both human studies showed not only the anti-inflammatory effects of bilberries but also demonstrated their oral effectiveness. Furthermore, polyphenols present in bilberry e.g. quercetin, resveratrol and epicatechin, have been shown *in vitro* to inhibit LPS-induced NF-κB activation in the same publication (Karlsen et al., 2010).

C. verum (cinnamon) – bark

Cinnamon bark extract strongly mitigated pro-inflammatory cytokine production in stimulated signaling pathways of both TLR2 and TLR4 in our performed experiments. Several beneficial health effects have been reported in literature for cinnamon, e.g. anti-inflammatory effects on alcohol-induced steatosis and colitis in mice (Kanuri et al., 2009; Hagenlocher et al., 2016; Hagenlocher et al., 2017). Furthermore, ethanolic extracts revealed anti-inflammatory activities by inhibition of TNF-α, IL-1β and IL-6 production as well as NF-κB activation (Ho et al., 2013; Gunawardena et al., 2014), which is supported by our data. The main compound of cinnamon bark, *trans*-cinnamaldehyde, has been shown to suppress pro-inflammatory cytokine secretion and TLR4 receptor oligomerization (Chao et al., 2008; Youn et al., 2008; Gunawardena et al., 2015; Hagenlocher et al., 2015). Our observed inhibition of TLR2 and TLR4 signaling pathways indicates that cinnamon extract should act on further mechanisms than pure inhibition of receptor oligomerization. Further investigations of cinnamon extract and its active compounds are reported in **chapter 4.3**.

Summarizing the screening results, various ethanolic herbal extracts, especially bark extracts, were shown to mitigate stimulated TLR2 and TLR4 signaling pathways. The underlying mechanisms are often still unknown. Since TLR pathways are relevant for diverse inflammatory diseases, the identification of TLR-modulating extracts might contribute to possible new treatment strategies.

4.2.3. Inhibition of NF-κB p65 translocation

To investigate the potential to inhibit NF-κB p65 translocation, ten extracts with the highest anti-inflammatory effects identified in HeLa-TLR4 and THP-1 screening (**chapter 4.2.1** and **4.2.2**) were selected to be further analyzed using fluorescence microscopy. Compared to vehicle control, incubation with *Castanea sativa* leaves, *C. verum* bark, *Salix alba* bark, *Rheum palmatum* root, *Humulus lupulus* cones, *Curcuma longa* root as well as *Arctostaphylos uva-ursi* leaves inhibited LPS-induced NF-κB translocation in HeLa-TLR4 dual reporter cells (**Figure 10** and **Figure 11**). This is in line with the observed anti-inflammatory effects in cell culture screening. Interestingly, *Cinchona pubescens* bark, *Alchemilla vulgaris* plant and *Vaccinium myrtillus* berries, which showed strong anti-inflammatory effects in the cell culture-based assays (**chapter 4.2.1** and **4.2.2**), did not significantly mitigate the LPS-induced NF-κB translocation into the cell nucleus.

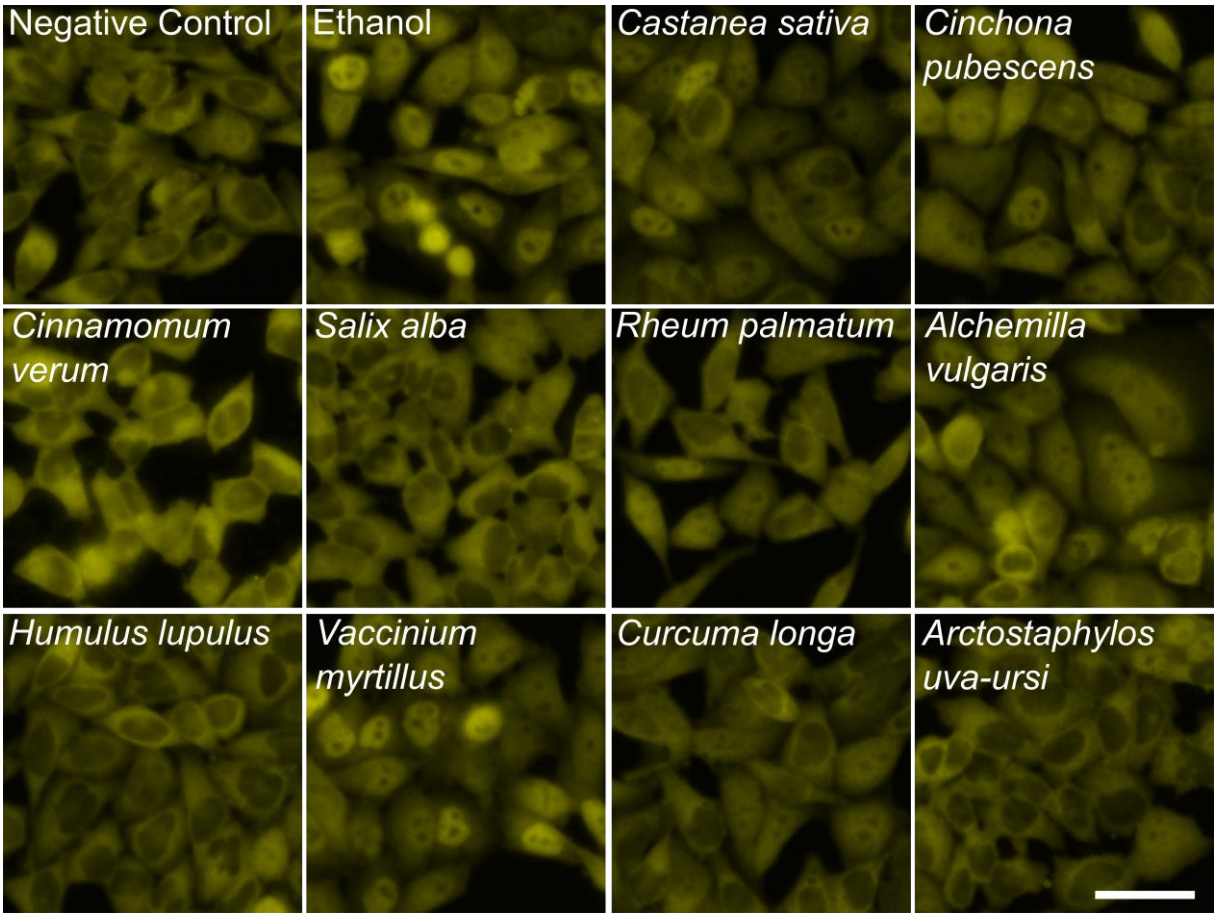

Figure 10: Influence of ten most promising extracts on NF-κB p65 translocation
Fluorescence images of HeLa-TLR4 dual reporter cells incubated with extracts or vehicle 70% ethanol, followed by stimulation with LPS-EB. Negative control: untreated cells. Cells were stained for NF-κB p65. Fluorescence microscopy images were cropped and adjusted in brightness and contrast. Scale bar = 50 µm.

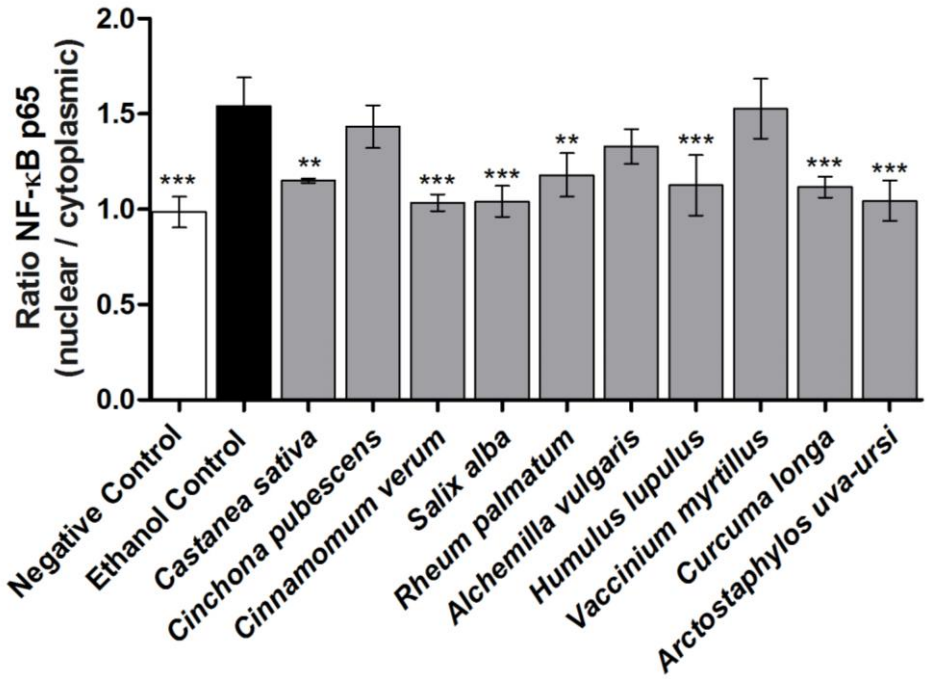

Figure 11: Quantitative influence on NF-κB p65 translocation of ten most promising extracts
HeLa-TLR4 dual reporter cells were incubated with extracts or vehicle 70% ethanol, followed by stimulation with LPS-EB. Negative control: untreated cells. Cells were stained for NF-κB p65. Data are displayed as mean fluorescence ratios of nuclear to cytoplasmic NF-κB p65. Data represent mean ± SD (*n*=3, 72 images (fields) per experiment and per treatment condition); Dunnett's post hoc test: ***p < 0.001, **p < 0.01 compared to ethanol control.

Summarizing, seven extracts mitigated NF-κB p65 translocation, whereas three further extracts showed no influence on NF-κB p65 translocation. Since all ten tested extracts were observed to possess anti-inflammatory effects in HeLa-TLR4 and THP-1 screening as well as in the comparative HEK-TLR2/HEK-TLR4 assay, other signaling pathways, such as activation of TNF or IL-1 receptor might lead to the observed translocation of NF-κB in LPS-stimulated cells treated with *Cinchona pubescens* bark, *Alchemilla vulgaris* plant and *Vaccinium myrtillus* berries. Alternatively, these extracts might also influence the signaling cascade downstream of NF-κB translocation, e.g. the expression of pro-inflammatory cytokine genes. Furthermore, in the NF-κB translocation experiments the incubation time differed from those used in HeLa TLR4 and THP-1 screening (1h vs. 4h/8h LPS incubation). This might also explain the controversy results between both assay systems. Different LPS incubation times were chosen for the experiments since HeLa-TLR4 reporter cells and THP-1 monocytes showed the best LPS-induced receptor stimulation after 4h and 8h (**chapter 4.1.1** and **4.1.4**), whereas NF-κB showed the highest translocation into the cell nucleus after 1-2h incubation with LPS (data not shown). For most of the extracts, the observed mitigation of NF-κB activation is in line with finding in literature, e.g. *Salix alba* (Bonaterra et al., 2010; Shara and Stohs, 2015), *Curcuma longa* (Angel-Morales et al., 2012), *Rheum palmatum* (Lui et al., 2008; Yao et al., 2015) and *C. verum* (Ho et al., 2013; Gunawardena et al., 2014). Arbutin present in *Arctostaphylos uva-ursi* (Lee and Kim, 2012)

and xanthohumol present in *Humulus lupulus* (Albini et al., 2006; Lee et al., 2011) have additionally been reported to inhibit NF-κB activation. Nevertheless, inhibition of NF-κB translocation by the whole extracts of *Arctostaphylos uva-ursi* leaves and *Humulus lupulus* cones were first reported by our findings. In both extracts, other compounds besides arbutin and xanthohumol might contribute to these effects. *Castanea sativa* leaves were, to the best of our knowledge, newly described to influence NF-κB translocation.

4.2.4. Repolarization of macrophages

Ten extracts with the highest anti-inflammatory effects identified in HeLa-TLR4 and THP-1 screening (**chapter 4.2.1**) were selected to be tested for their potential to repolarize pro-inflammatory M1 macrophages to anti-inflammatory M2 macrophages. The viability of stimulated THP-1 macrophages after treatment with different extracts was above 85% compared to untreated cells, with the exception of the treatment with *Humulus lupulus* extract (64% viability) (**Figure 12A**). All select extracts, except *Salix alba* and *Vaccinium myrtillus*, significantly mitigated the LPS-induced TNF secretion (**Figure 12B**). Several extracts, especially *Rheum palmatum* root and *Arctostaphylos uva-ursi* leaves furthermore significantly increased the production of IL-10 (**Figure 12C**).

M1 macrophages are involved in inflammatory responses and inhibition of tumor cells, whereas M2 macrophages contribute to tissue repair and angiogenesis (Fraternale et al., 2015). Mitigation of the pro-inflammatory marker TNF accompanied with increased secretion of the anti-inflammatory IL-10 indicates a polarization from M1 macrophages to M2 macrophages, which was especially shown after treatment with *Rheum palmatum* root and *Arctostaphylos uva-ursi* leaves. Both extracts were also observed to possess strong anti-inflammatory effects in different cell culture-based assays (**chapter 4.2.1** and **4.2.2**) as well as to significantly inhibit LPS-induced NF-κB translocation (**chapter 4.2.3**). To the best of our knowledge, repolarization from M1 macrophages to M2 macrophages after incubation with our select extracts has only been described for *Curcuma longa*. In murine RAW macrophages, *Curcuma longa* induced a shift from M1 macrophages with a decrease of pro-inflammatory cytokines to M2 macrophages and an increase of anti-inflammatory cytokines (Li et al., 2017). The decreased TNF secretion could also be observed in the experiments presented in **Figure 12**, whereas an increase of anti-inflammatory IL-10 was not detected here. A longer incubation of THP-1 M1 macrophages in our assay system with *Curcuma longa* might lead to the reported increase of IL-10.

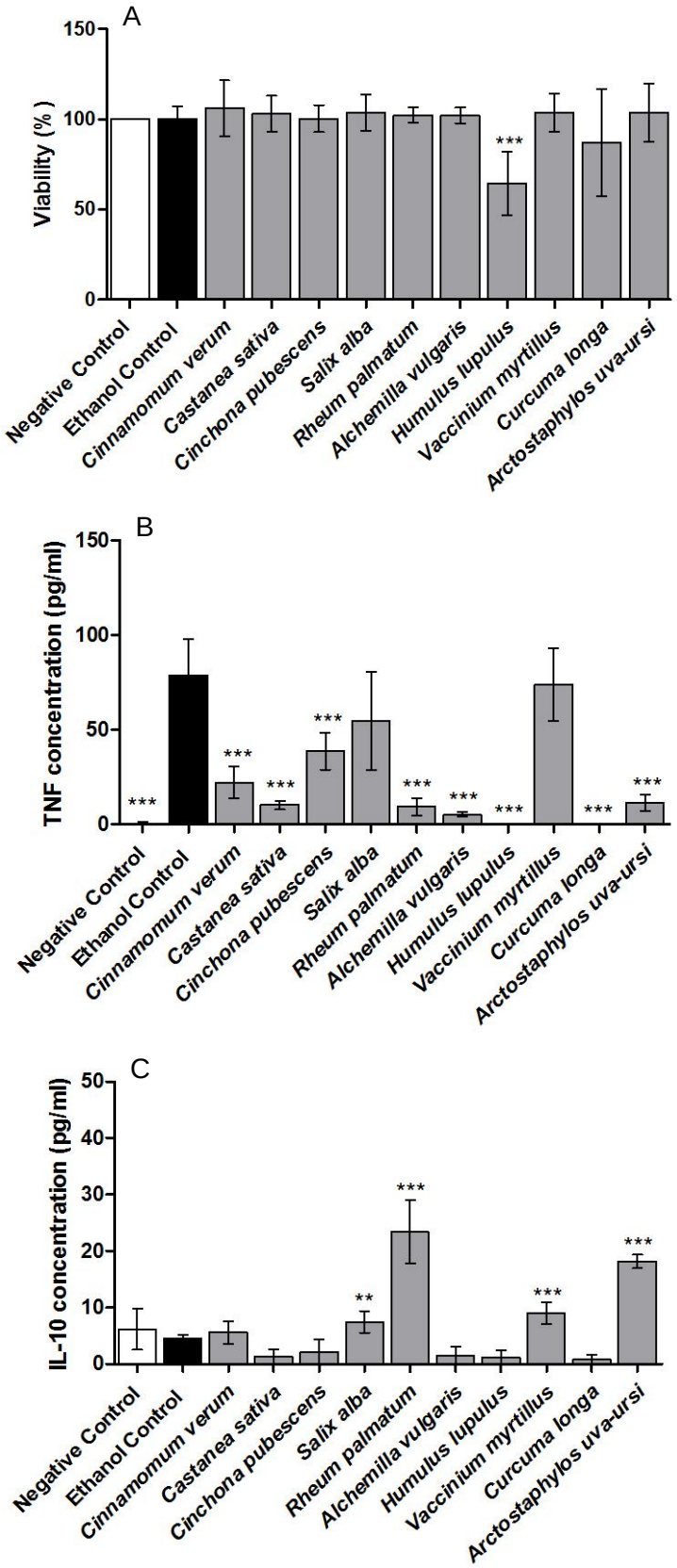

Figure 12: Effects of ten most promising extracts on macrophage polarization
THP-1 M1 macrophages were incubated with extracts or vehicle 70% ethanol, followed by stimulation with LPS-EB. Negative control: untreated M1 macrophages. **A**: Viability (Alamar Blue assay) normalized to viability of untreated cells. **B**: TNF concentration (ELISA) in pg/ml. **C**: IL-10 concentration (ELISA) in pg/ml. Data represent mean ± SD of 2 independent experiments (each with *n*=3); unpaired t-test: ***p < 0.001, **p < 0.005 compared to ethanol control.

4.3. Analysis of *C. verum* bark extract and its active compounds

In previous screening experiments (**chapter 4.2**), *C. verum* bark extract was observed to be one of the extracts with the highest anti-inflammatory potential. Its investigated effects are displayed more detailed in **Figure 13**, **Figure 14** and **Figure 15**.

Viability of unstimulated THP-1 monocytes treated with *C. verum* extract or vehicle ethanol was above 88% for all tested concentrations compared to untreated cells (**Figure 13A**). Possible toxic effects of *C. verum* extract (or vehicle) affecting the IL-8 secretion could therefore largely be excluded. Treatment with *C. verum* extract in different concentrations, especially up to 1% extract in cell culture medium, resulted in unstimulated THP-1 monocytes in no noteworthy IL-8 secretion normalized to viability (**Figure 13B**). This leads to the assumption that *C. verum* extract and the used vehicle do not stimulate TLR4 activity by themselves in concentrations up to 1% in cell culture medium, combined with no toxic effects. In higher concentrations, toxic effects might result in the production of DAMPs, which further stimulate TLR4 and lead to a secretion of pro-inflammatory cytokines, like IL-8 (Lucas and Maes, 2013).

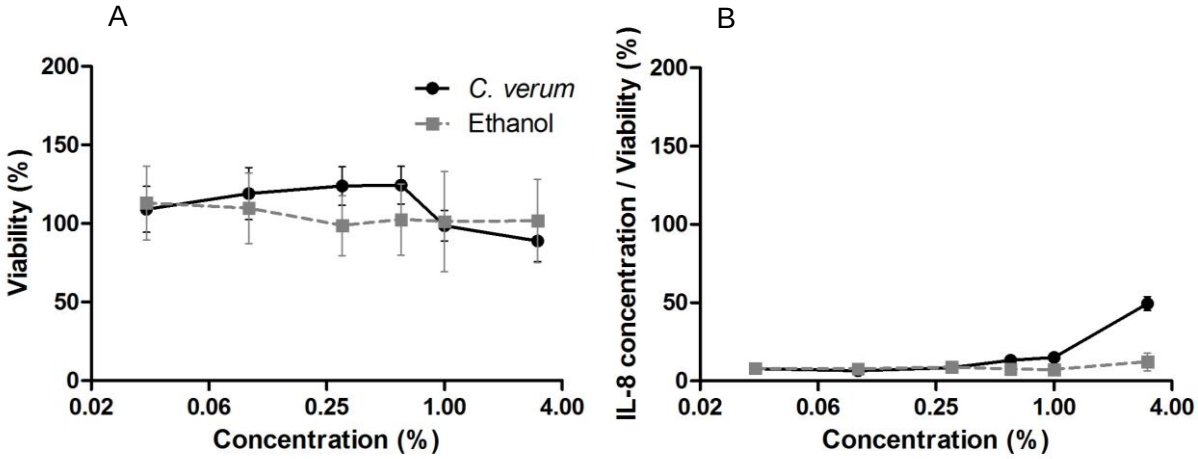

Figure 13: Cell viability and anti-inflammatory effects of *C. verum* bark extract in unstimulated THP-1 monocytes
THP-1 monocytes were incubated with *C. verum* bark extract in different concentrations or vehicle 70% ethanol, without further stimulation. **A**: Viability (Alamar Blue assay) normalized to viability of untreated cells. **B**: IL-8 concentration (ELISA) divided by normalized viability. Data represent mean ± SD (*n*=6).

In line with the viability observed in unstimulated THP-1 monocytes treated with cinnamon extract, LPS-stimulated THP-1 monocytes pretreated with cinnamon extract showed for all tested *C. verum* concentrations and the vehicle ethanol a viability above 92% compared to untreated cells (**Figure 14A**). Small amounts of ethanol have been reported to mitigate the LPS-stimulated TLR4 response (Szabo et al., 2007). To only show effects based on cinnamon treatment, IL-8 secretion of ethanol-treated THP-1 monocytes was set to 100%.

LPS-induced IL-8 secretion normalized to viability was significantly reduced in cells treated with *C. verum* extract in concentrations of 0.6%, 1% and 3% (**Figure 14B**).

These results are in line with literature, where comparable amounts of *C. verum* extract have been reported to possess anti-inflammatory effects in murine RAW macrophages (Kanuri et al., 2009) and in a mouse model of colitis (Hagenlocher et al., 2016).

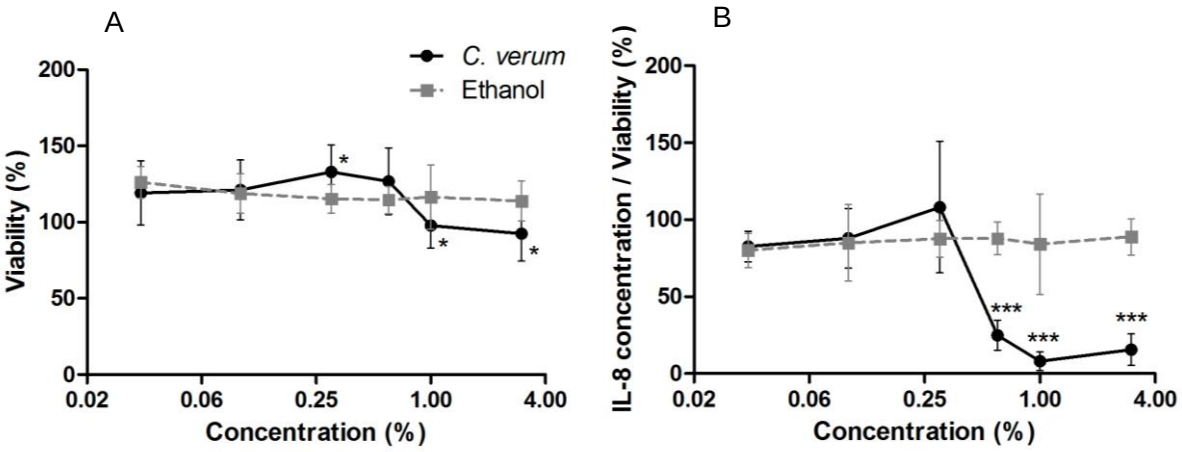

Figure 14: Cell viability and anti-inflammatory effects of *C. verum* bark extract on stimulated THP-1 monocytes

THP-1 monocytes were incubated with *C. verum* bark extract in different concentrations or vehicle 70% ethanol, followed by stimulation with LPS-EB. **A**: Viability (Alamar Blue assay) normalized to viability of untreated cells. **B**: IL-8 concentration (ELISA) divided by normalized viability. Data represent mean ± SD (*n*=9); unpaired t-test: ***p < 0.0001, *p < 0.05 compared to respective ethanol control.

C. verum extract was tested in the stimulated HEK-TLR2/HEK-TLR4 comparative assay to identify possible direct interferences with TLR4. Treatment with 0.01% to 3% *C. verum* extract resulted in a viability above 80% compared to the respective ethanol-treated cells (**Figure 15A**). For the same concentrations, a dose-dependent decrease of TLR2 and TLR4 activity was observed, which was comparable for both cell lines (**Figure 15B**). This indicates an influence of *C. verum* extract on downstream signaling pathways common for both TLR2 and TLR4, such as the central NF-κB/AP-1 signaling.

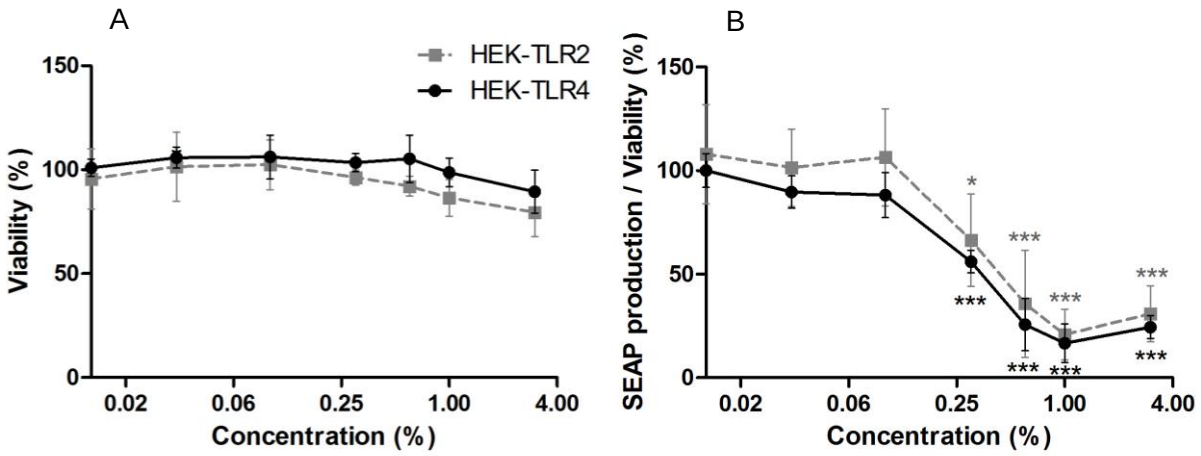

Figure 15: *C. verum* bark extract tested for exclusive TLR4 antagonistic activity
HEK-TLR2 (grey, dashed line) and HEK-TLR4 reporter cells (black, full line) were incubated with *C. verum* bark extract in different concentrations or vehicle 70% ethanol, followed by stimulation with Pam2CSK4 (HEK-TLR2 reporter cells) or LPS-EB ultrapure (HEK-TLR4 reporter cells). **A:** Viability (Alamar Blue assay) normalized to ethanol-treated cells. **B:** TLR2 or TLR4 receptor response (SEAP production) normalized to ethanol control and divided by normalized viability. Data represent mean ± SD (*n*=5); unpaired t-test: ***p < 0.001, *p < 0.05 compared to respective ethanol control, no significance (*p < 0.05) between cell lines.

Based on the strong anti-inflammatory effects, *C. verum* extract was selected to be further analyzed in an inflammatory mouse model to confirm its advantageous effects *in vivo*. Furthermore, *C. verum* extract was analyzed to identify its active compounds and the mechanisms responsible for its beneficial health effects.

4.3.1. Effects in inflammatory mouse model

Due to the highly promising anti-inflammatory effects of *C. verum* extract in cell culture-based assays, it was additionally tested in a mouse model on ATI-induced gastrointestinal inflammation. Oral gavage application of 50 µl *C. verum* extract diluted in 150 µl PBS resulted in C57BL/6 wild type mice in mitigated ATI-induced CXCL1 and IL-6 serum concentrations, when compared with ethanol pretreatment (**Figure 16**). This tendency was not significant in the conducted short-term mouse experiment with five animals per group, but comprises a good starting point for further experiments using an increased number of animals and/or a longer treatment period.

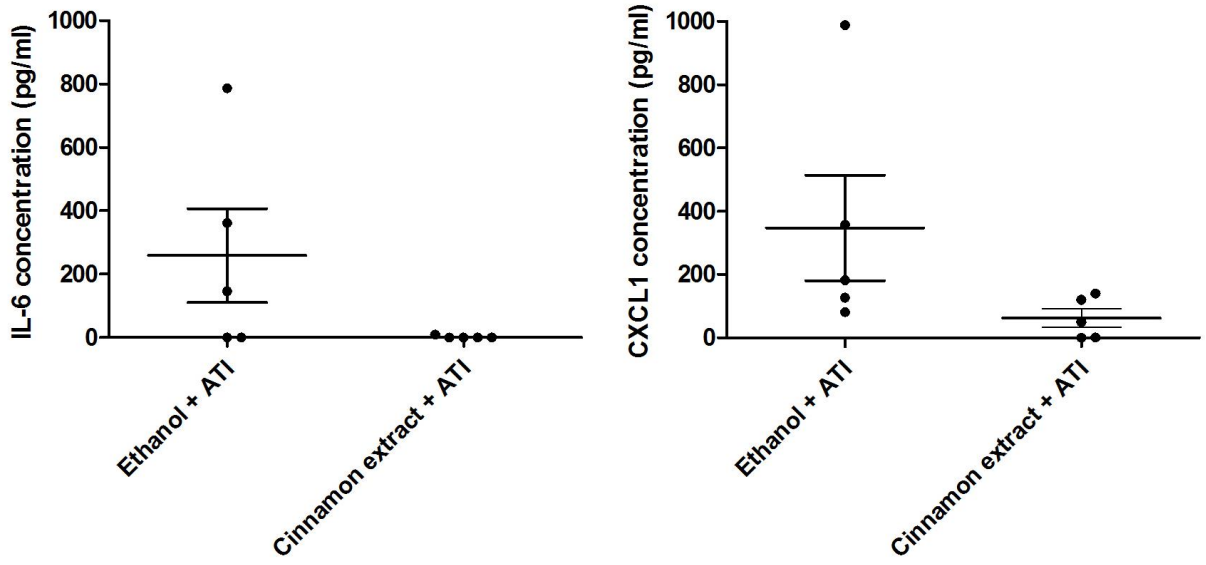

Figure 16: *C. verum* bark extract tested in inflammatory mouse model
Male C57BL/6 wild type mice were pretreated with *C. verum* bark extract or ethanol by oral gavage, followed by induction of gastrointestinal inflammation by ATIs. CXCL1 and IL-6 serum concentrations were measured using ELISAs. Data represent mean ± SEM (*n*=5). No significance (*p < 0.05) between both treatment groups.

In literature, oral administration of cinnamon extract has been observed to suppress clinical symptoms in mouse models of multiple sclerosis (Mondal and Pahan, 2015). Furthermore, cinnamon extract in drinking water has been shown to possess anti-inflammatory effects in a mouse model of alcohol-induced fatty liver (Kanuri et al., 2009) and on colitis in IL-10 knockout mice (Hagenlocher et al., 2016; Hagenlocher et al., 2017).

4.3.2. Fractionation and identification of compounds

HPLC fractionation of *C. verum* bark extract was performed to identify the main compounds responsible for its strong anti-inflammatory effects. On a peak-based selection, 15 fractions (fraction A to fraction O, **Table 20**) were collected and tested for their anti-inflammatory activities in LPS-stimulated THP-1 monocytes.

Table 20: Retention times of select HPLC *C. verum* fractions

Fraction name	Retention time (min)
Fraction A	3.20 – 4.00
Fraction B	4.60 – 6.20
Fraction C	6.21 – 7.30
Fraction D	7.31 – 7.99
Fraction E	8.00 – 10.00
Fraction F	10.10 – 10.60
Fraction G	10.80 – 11.80
Fraction H	13.40 – 13.90
Fraction I	15.60 – 17.10
Fraction J	18.20 – 20.00

Fraction name	Retention time (min)
Fraction K	21.60 – 22.60
Fraction L	23.60 – 24.50
Fraction M	25.40 – 27.40
Fraction N	27.45 – 30.10
Fraction O	50.00 – 52.50

A significant decrease of IL-8 secretion normalized to viability was observed in LPS-stimulated THP-1 monocytes treated with seven of the collected fractions, when compared to treatment with the solvent control (**Figure 17** and **Figure 18**). Incubation with the rest of the collected fractions resulted in no effects on the LPS-induced IL-8 production or in an increase.

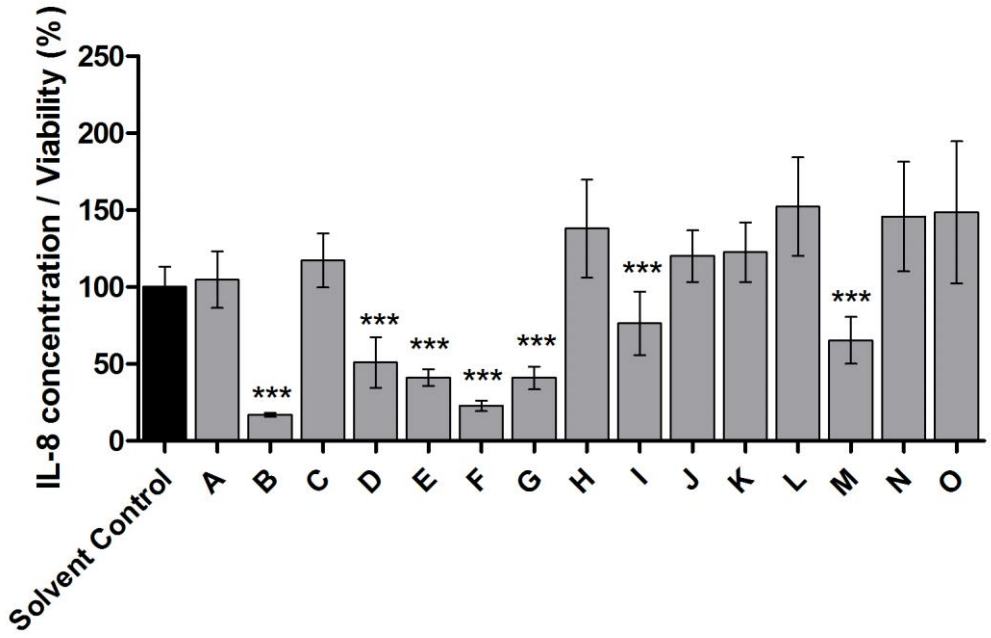

Figure 17: HPLC *C. verum* fractions tested for anti-inflammatory effects in THP-1 monocytes
THP-1 monocytes were incubated with HPLC *C. verum* fractions or solvent control, followed by stimulation with LPS-EB. IL-8 concentration (ELISA) and cell viability (Alamar Blue assay) normalized to viability of untreated cells were measured. Data display IL-8 concentration divided by normalized viability and normalized to solvent-treated cells. Data represent mean ± SD of 3 independent experiments (each with *n*=3); unpaired t-test (only anti-inflammatory effects marked): ***p < 0.0001 compared to solvent control.

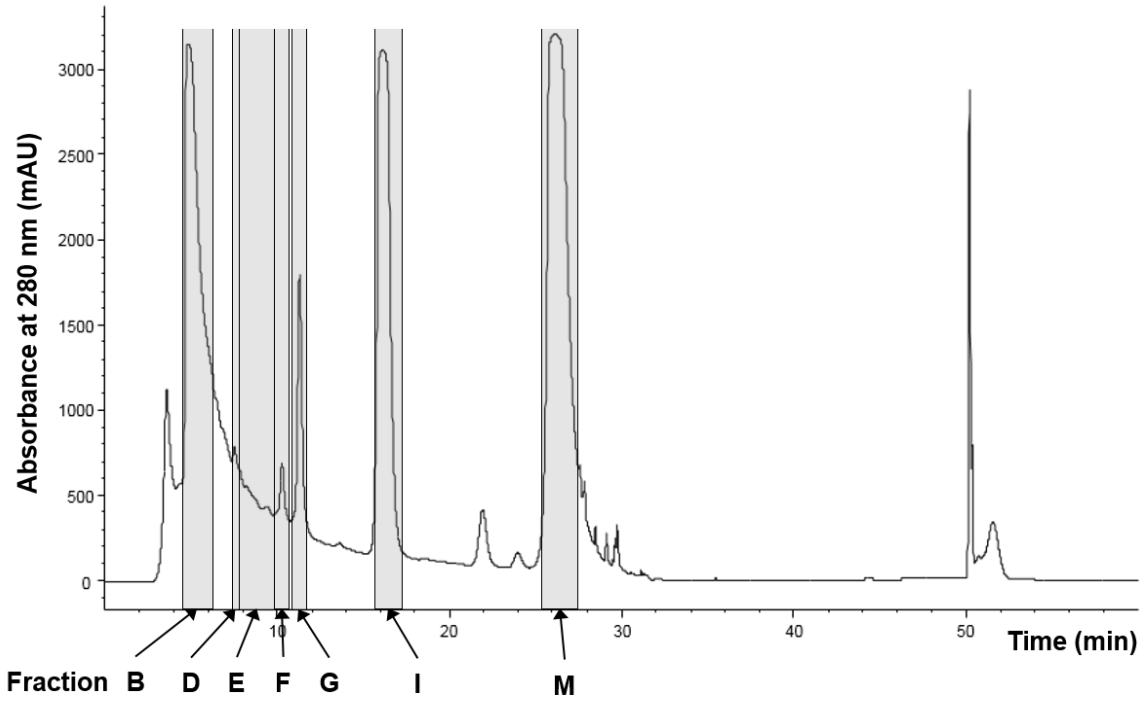

Figure 18: Chromatogram of HPLC *C. verum* extract fractionation
Cinnamon fractions inducing significant anti-inflammatory effects in THP-1 monocytes (**Figure 17**) are shown in grey.

Anti-inflammatory fractions showing a TLR4 response in LPS-stimulated THP-1 monocytes below 77% of the response after incubation with solvent control (fraction B: 16.9% of solvent control, fraction D: 50.9%, fraction E: 41.1%, fraction F: 22.8%, fraction G: 40.9%, fraction I: 76.4% and fraction M: 65.4%) were further analyzed using HRMS and GC-MS to identify the compounds present in these fractions.

HRMS spectra of the select fractions were acquired using ESI in positive (+) and negative (–) mode. The mass peaks obtained in (–)ESI-MS spectrum from fraction M (*m/z* 255.23, 283.26, 311.17, 329.23 and 529.46), the only coloured fraction, are displayed in **Figure 19**.

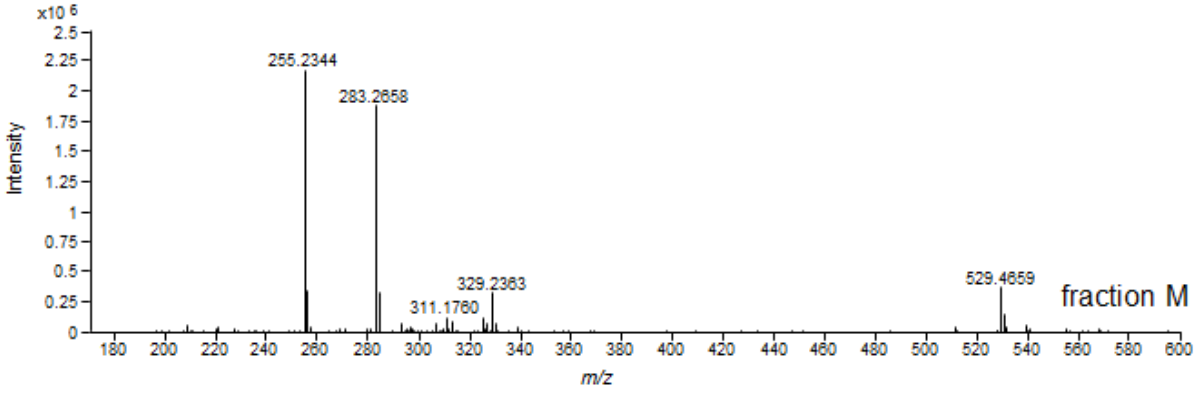

Figure 19: (–)ESI-MS spectrum of *C. verum* fraction M

The ion with *m/z* 311.17 and its product ion in the MS^2 (*m/z* 183.01) were additionally observed in the blank and therefore not further analyzed. In contrast, mass peaks at *m/z* 255.23 and *m/z* 283.26 indicate the presence of palmitic acid and stearic acid in the investigated fraction (Murphy, 2015). This was also in line with Mass Hunter formula calculator hits ($C_{18}H_{36}O_2$ and $C_{16}H_3O_2$, respectively) and mass peaks observed after the injection of standards for palmitic and stearic acid. The ion with *m/z* 329.23 and its product ion in the MS^2 with *m/z* 171.1 could be assigned to 9,10,13-trihydroxy-11-octadecenoic acid (9,10,13-TriHOME(11)), which was also in agreement with Mass Hunter software hits ($C_{18}H_{34}O_5$) (Hurtado Fernández, 2014; Strassburg et al., 2015). The ion peak at *m/z* 529.46 was preliminary identified as octadecyl 3,5-di-tert-butyl-4-hydroxyhydrocinnamate ($C_{35}H_{62}O_3$), also referred to as Irganox 1076 (Duderstadt and Fischer, 2008).

In addition to HRMS, compounds were analyzed using a GC-MS method. This method enabled the identification of *p*-cymene, methyl salicylate, 1-tetradecanol (myristyl alcohol), cinnamyl alcohol and cinnamaldehyde in the non-derivatized fractions, whereas trimethyl silyl esters of cinnamyl methyl ether, cinnamic acid and benzoic acid were identified in the derivatized fractions (**Figure 20** and **Table 21**).

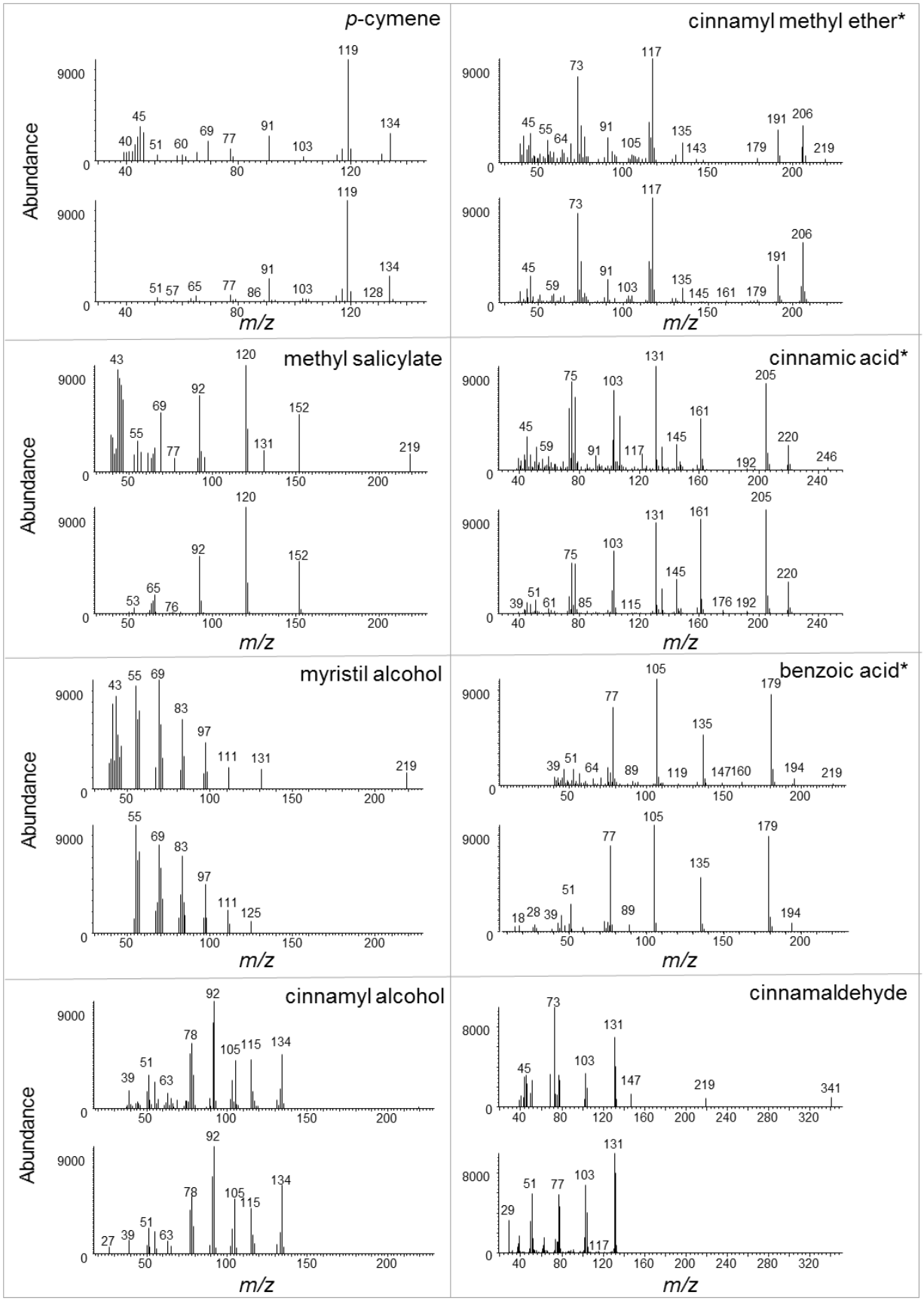

Figure 20: GC-MS spectra of compounds identified in HPLC fractions of *C. verum*
Compounds identified in the anti-inflammatory HPLC *C. verum* fractions (**Figure 17** and **Figure 18**). Asterisks (*) indicate the identification of the respective trimethyl silyl esters in the derivatized fractions. The upper spectra belong to the compounds observed in the anti-inflammatory fractions, while the lower spectra correspond to the compounds included in NIST mass spectral library.

Table 21: Compounds identified in anti-inflammatory HPLC *C. verum* fractions
12 compounds were identified in anti-inflammatory HPLC *C. verum* fractions (**Figure 17** and **Figure 18**) using GC-MS[1] and HRMS[2]

Fraction name	Identified compound
Fraction B	*p*-Cymene[1]
	Methyl salicylate[1]
Fraction D	1-Tetradecanol (myristyl alcohol)[1]
Fraction F	Cinnamyl alcohol[1]
	Cinnamyl methyl ether[1]
	Cinnamic acid[1]
	Benzoic acid[1]
Fraction M	Cinnamaldehyde[1]
	Stearic acid[2]
	Palmitic acid[2]
	9,10,13,TriHOME(11)[2]
	Octadecyl 3,5-di-*tert*-butyl-4-hydroxyhydrocinnamate[2]

In literature, *p*-cymene, cinnamyl alcohol, cinnamic acid and cinnamaldehyde have been shown to be present in *C. verum* extract, with cinnamaldehyde as major compound in this extract (Jayaprakasha and Rao, 2011; Khuwijitjaru et al., 2012; Gunawardena et al., 2015; Swider et al., 2016). To the best of our knowledge, other compounds from **Table 21** were not reported to be present in cinnamon bark extract so far.

4.3.3. TLR-dependent anti-inflammatory effects

Compounds, which were identified in the analyzed *C. verum* extract using HRMS and GC-MS, were purchased as standard compounds and tested on LPS-stimulated THP-1 monocytes for their anti-inflammatory effects (**Figure 21**).

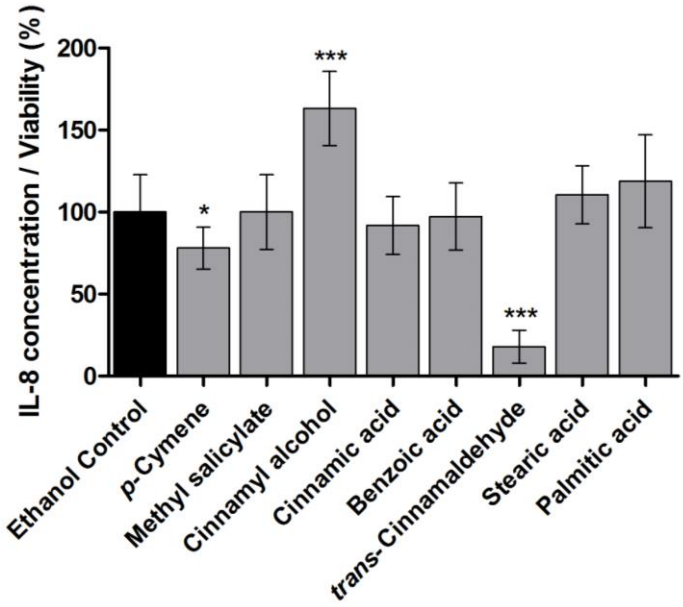

Figure 21: Anti-inflammatory effects of select *C. verum* compounds
THP-1 monocytes were incubated with compounds present in *C. verum* bark extract (each with 25 µg/ml) or vehicle 70% ethanol, followed by stimulation with LPS-EB. IL-8 concentration (ELISA) and viability (Alamar Blue assay) normalized to viability of untreated cells were measured. Data display IL-8 concentration divided by normalized viability and normalized to ethanol-treated cells. Data represent mean ± SD of 3 independent experiments (each with *n*=3); unpaired t-test: ***p < 0.0001, *p < 0.05 compared to solvent control.

Treatment of THP-1 monocytes with 25 µg/ml *trans*-cinnamaldehyde or *p*-cymene significantly mitigated the LPS-induced TLR4 stimulation. These findings are in line with reported *in vivo* effects in literature, where *p*-cymene has been shown to possess anti-inflammatory effects e.g. in LPS-induced acute lung injury and mouse models for elastase-induced emphysema (Xie et al., 2012; Games et al., 2016). That applies also for cinnamaldehyde, where various anti-inflammatory effects in literature support our data (de Cássia da Silveira et al., 2014; Gunawardena et al., 2015; Zhu et al., 2017). Interestingly, cinnamyl alcohol was the only significant pro-inflammatory compound in our performed assay system. In literature, this compound was shown to possess anti-inflammatory effects by slightly inhibiting NO, TNF-α and IL-6 production in LPS-activated BV2 microglia (Ho et al., 2013; Gunawardena et al., 2015). Other studies revealed that cinnamyl alcohol has only little or no anti-inflammatory effects in LPS-stimulated cell culture assays (Liao et al., 2012).

Cinnamaldehyde has been shown in literature to mitigate TLR4 receptor oligomerization resulting in an inhibition of TLR4 stimulation (Youn et al., 2008). When testing whole cinnamon extract in the HEK-TLR2/HEK-TLR4 comparative assay system on TLR4 specific antagonism, the direct TLR4 antagonistic activity of cinnamaldehyde could not be confirmed (**chapter 4.2.2**). Therefore, *trans*-cinnamaldehyde was tested in the same assay system to verify the direct TLR4 inhibitory effects shown by Youn et al., 2008. Compared to treatment with vehicle control, *trans*-cinnamaldehyde concentrations from 10 µg/ml to 50 µg/ml led to a significant mitigation of Pam2CSK4- or LPS-induced stimulation in HEK-TLR2 and HEK-TLR4 reporter cells (**Figure 22**). The comparable anti-inflammatory effects observed in both cell lines indicate an involvement of *trans*-cinnamaldehyde in both TLR2 and TLR4 signaling pathways and therefore a mechanism beyond sole TLR4 antagonism and the inhibition of TLR4 receptor oligomerization (Youn et al., 2008).

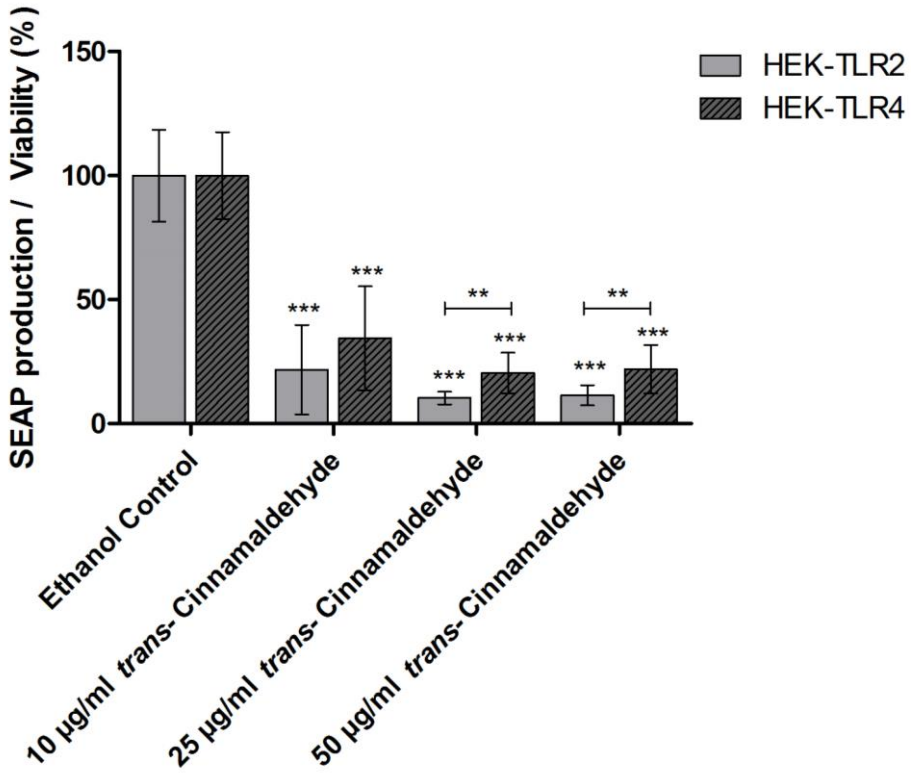

Figure 22: *trans*-Cinnamaldehyde tested for exclusive TLR4 antagonistic effects
HEK-TLR2 and HEK-TLR4 reporter cells were incubated with *trans*-cinnamaldehyde or vehicle 70% ethanol, followed by stimulation with Pam2CSK4 (HEK-TLR2 reporter cells) or LPS-EB ultrapure (HEK-TLR4 reporter cells). TLR2 or TLR4 receptor response (SEAP production) and viability (Alamar Blue assay) normalized to viability of untreated cells were measured. Data are displayed as receptor stimulation divided by normalized viability. Data represent mean ± SD (*n*=5); unpaired t-test: **p < 0.01 comparison of both cell lines; ***p < 0.0001 compared to ethanol.

In contrast to the anti-inflammatory effects shown for *trans*-cinnamaldehyde in the comparative HEK-TLR2/HEK-TLR4 assay system, *p*-cymene did not mitigate Pam2CSK4- or LPS-EB ultrapure-induced stimulation (**Figure 23**). Both reporter cell lines, HEK-TLR2 and HEK-TLR4, do not naturally contain but were stably co-transfected with human TLR2 and CD14 or human TLR4, MD-2 and CD14 co-receptor genes. Since they may not exhibit all co-factors of other TLR2- and TLR4-related pathways, *p*-cymene may still be active by influencing signaling pathways absent in these two reporter cell lines.

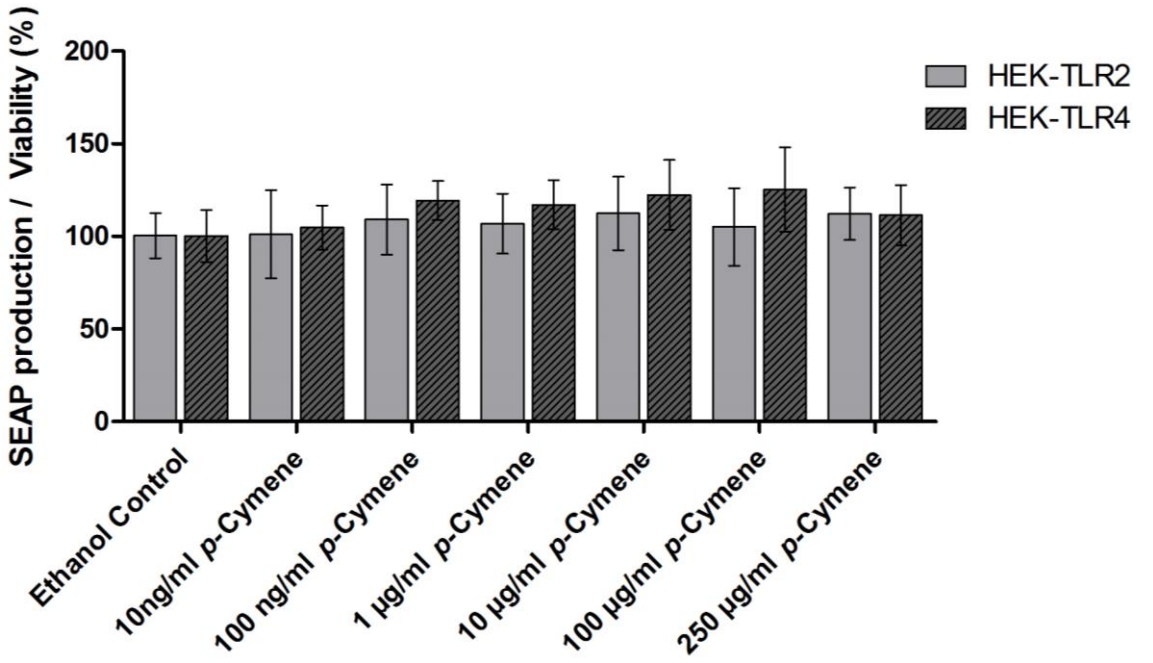

Figure 23: *p*-Cymene tested for exclusive TLR4 antagonistic effects
HEK-TLR2 and HEK-TLR4 reporter cells were incubated with different concentrations of *p*-cymene or vehicle 70% ethanol, followed by stimulation with Pam2CSK4 (HEK-TLR2 reporter cells) or LPS-EB ultrapure (HEK-TLR4 reporter cells). TLR2 or TLR4 receptor response (SEAP production) and viability (Alamar Blue assay) normalized to viability of untreated cells were measured. Data are displayed as receptor stimulation divided by normalized viability. Data represent mean ± SD (*n*=5); unpaired t-test: no significance in comparison of both cell lines or compared to ethanol.

Since herbal extracts are complex mixtures containing multiple compounds, their beneficial health effects are often not solely due to single compound activities. The efficacy in these matrices is often even based on synergistic effects instead of pure additive effects (Stickel and Schuppan, 2007; Wink, 2008; Wink, 2015). Therefore, compounds identified in cinnamon extract were pooled according to their specific fractions and were tested for synergistic effects in LPS-stimulated THP-1 monocytes (**Figure 24**).

Incubation of LPS-stimulated THP-1 monocytes with a combination of methyl salicylate and *p*-cymene, which were identified in fraction B, was not observed to possess synergistic effects compared to incubation with the respective compounds combined with vehicle ethanol (**Figure 24A**). The same results were shown for a combination of cinnamyl alcohol, cinnamic acid and benzoic acid, which were all present in fraction F (**Figure 24B**). The only synergistic effect in the fraction-dependent pooling was shown for palmitic acid and stearic acid from fraction M (**Figure 24C**). After incubation of LPS-stimulated THP-1 monocytes with a combination of both acids, a significant decrease of TLR4 stimulation was observed compared to incubation with the respective compounds combined with ethanol. Nevertheless, the TLR4 stimulation normalized to viability of THP-1 monocytes was still above those when treated with the vehicle alone. Therefore, no anti-inflammatory effect was observed, but the pro-inflammatory effects of palmitic acid and stearic acid when given alone were significantly reduced.

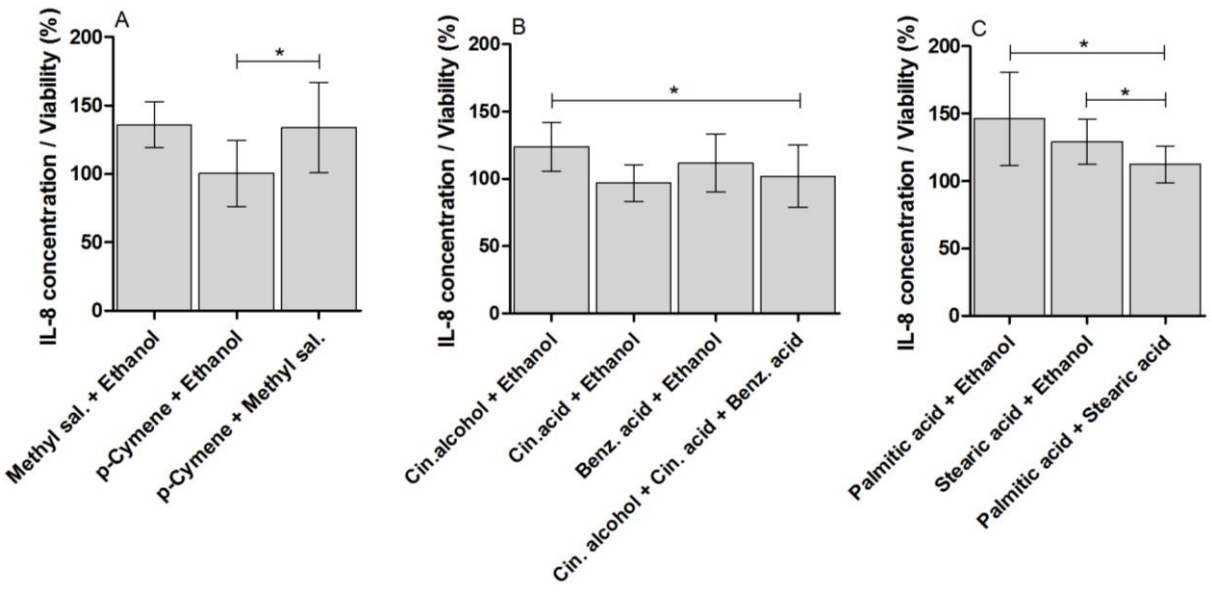

Figure 24: Fraction-dependent synergistic effects
THP-1 monocytes were incubated with combinations of different compounds from *C. verum* extract (each with 25 µg/ml) or vehicle 70% ethanol, followed by stimulation with LPS-EB. **A**: Compounds in cinnamon fraction B, **B**: Compounds in fraction F, **C**: Compounds in fraction M. IL-8 concentration (ELISA) and viability (Alamar Blue assay) normalized to viability of untreated cells were measured. Data are displayed as IL-8 concentration divided by normalized viability and normalized to vehicle-treated cells. Data represent mean ± SD of 3 independent experiments (each with *n*=3); unpaired t-test: *p < 0.05. Methyl sal.: Methyl salicylate; Cin. alcohol: Cinnamyl alcohol; Cin. acid: Cinnamic acid; Benz. acid: Benzoic acid.

When testing the identified *C. verum* compounds in LPS-stimulated THP-1 monocytes, *trans*-cinnamaldehyde was identified to possess the highest anti-inflammatory effects (**Figure 21**). Consequently, all compounds were additionally pooled with *trans*-cinnamaldehyde to identify possible synergistic effects within *C. verum* extract (**Figure 25**).

The combination of *trans*-cinnamaldehyde with *p*-cymene, cinnamyl alcohol or cinnamic acid showed strong synergistic effects on the LPS-induced inflammatory activity in THP-1 monocytes. The anti-inflammatory effects were significant not only when compared to pure solvent control (70% ethanol), but also when compared to a combination of *trans*-cinnamaldehyde and solvent control, which itself led to a reduction of IL-8 secretion to a level of 30.7% compared to ethanol treatment. Combined treatment of *trans*-cinnamaldehyde with cinnamic acid or *p*-cymene led to a further IL-8 reduction to 13.4% and 11.2%, respectively. A combination of *trans*-cinnamaldehyde and cinnamyl alcohol resulted in the lowest IL-8 secretion with 3.2% of normalized IL-8 secretion after ethanol treatment in LPS-stimulated THP-1 monocytes.

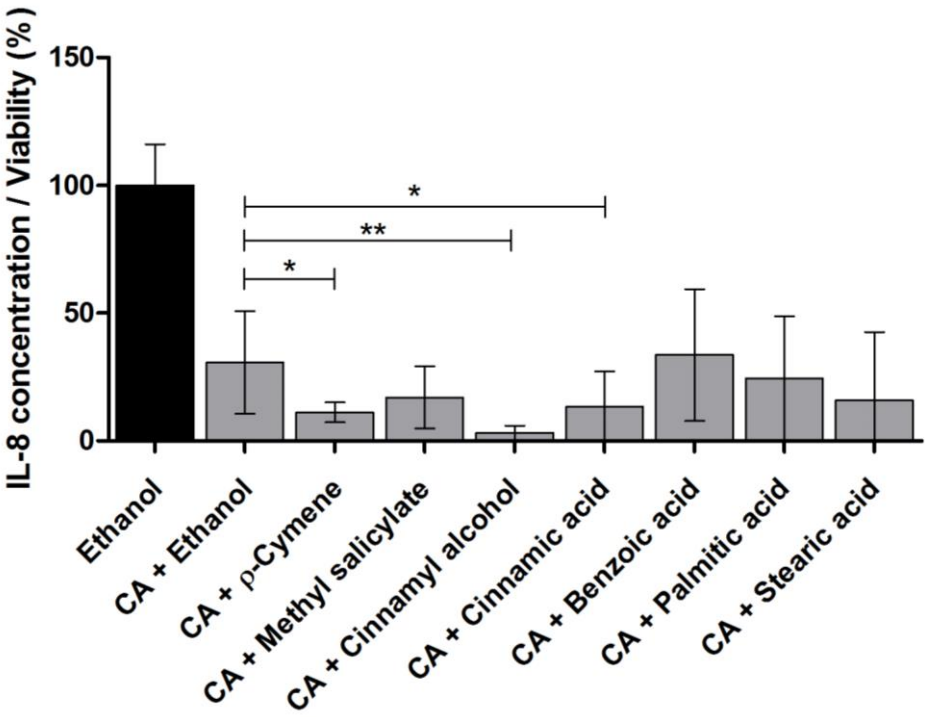

Figure 25: Synergistic effects of *C. verum* extract compounds
THP-1 monocytes were incubated with a combination of *trans*-cinnamaldehyde (CA) and other compounds in *C. verum* extract (each with 25 µg/ml) or vehicle 70% ethanol, followed by stimulation with LPS-EB. IL-8 concentration (ELISA) and viability (Alamar Blue assay) normalized to viability of untreated cells were measured. Data are displayed as IL-8 concentration divided by normalized viability and normalized to vehicle-treated cells. Data represent mean ± SD ($n \geq 6$); unpaired t-test: ***p < 0.0001 all treatments compared to ethanol control (not marked); **p < 0.005, *p < 0.05 compared to incubation with CA + Ethanol.

Controlled by redox conditions, cinnamaldehyde and cinnamyl alcohol are known for *in vivo* transformation into another, combined with the possibility of cinnamaldehyde to be oxidized to cinnamic acid (**Figure 26**) (Zhu et al., 2017).

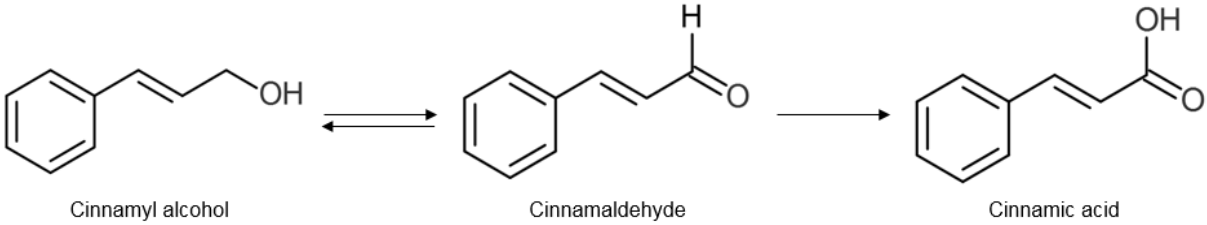

Figure 26: Transformation of cinnamaldehyde
In vivo transformation of cinnamaldehyde and cinnamyl alcohol into another. Cinnamaldehyde can also be oxidized to cinnamic acid.

A (partial) transformation might therefore explain the synergistic effects of cinnamaldehyde with cinnamic acid and cinnamyl alcohol identified in the performed THP-1 assay. This hypothesis is very unlikely due to the observed pro-inflammatory effects of cinnamyl alcohol in the same assay system when added alone (**Figure 21**). An involvement of the pH of the system in the synergistic effects is also doubtful. Benzoic acid, which did not shown any synergistic effects when combined with *trans*-cinnamaldehyde (**Figure 25**), has a pKa value comparable to cinnamic acid (pKa benzoic acid: 4.204; pKa *cis*-cinnamic acid: 3.88;

pKa *trans*-cinnamic acid: 4.44) (Vanýsek, 2014). Possible stabilizing effects of *p*-cymene, cinnamyl alcohol and/or cinnamic acid on the aldehyde functional group of *trans*-cinnamaldehyde might be another hypothesis to explain the strong synergistic effects when combined with *trans*-cinnamaldehyde. With the shown results, a first mechanistic basis is provided for the empirical observation that the efficacy of complex herbal extracts is often not completely displayed by their isolated active compounds (Wink, 2008; Wink, 2015). Nevertheless, the underlying mechanisms of the significant synergistic effects for combinations of *trans*-cinnamaldehyde with *p*-cymene, cinnamyl alcohol and cinnamic acid are not yet fully resolved.

4.3.4. Influence on repolarization of macrophages

Cytokine assays were used to identify the potential of different *C. verum* compounds to repolarize pro-inflammatory M1 macrophages to anti-inflammatory M2 macrophages. The viability of LPS-stimulated THP-1 macrophages after treatment with *C. verum* compounds was for all treatments above 80% (**Figure 27A**). TNF, as marker for pro-inflammatory M1 macrophages, was especially mitigated after treatment with *trans*-cinnamaldehyde but a significant decrease was also observed after cinnamyl alcohol treatment (**Figure 27B**). However, no significant increase of IL-10, a marker for the anti-inflammatory M2 macrophages, was observed in LPS-stimulated THP-1 macrophages after different treatments compared to ethanol control, with the exception of unstimulated cells (**Figure 27C**).

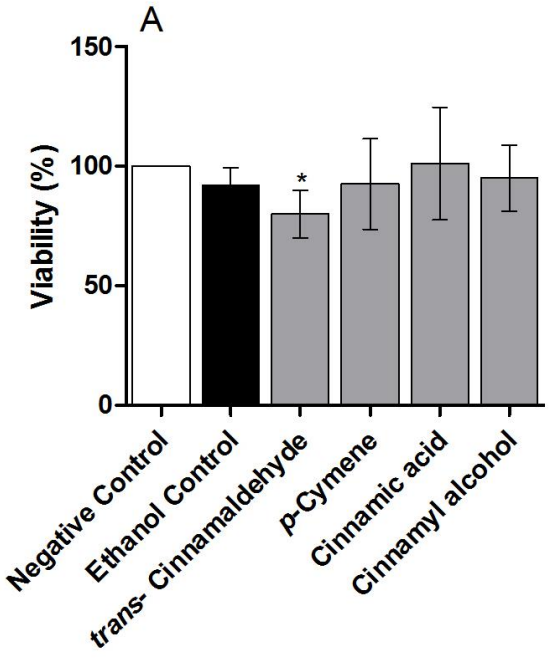

Figure continues on next page

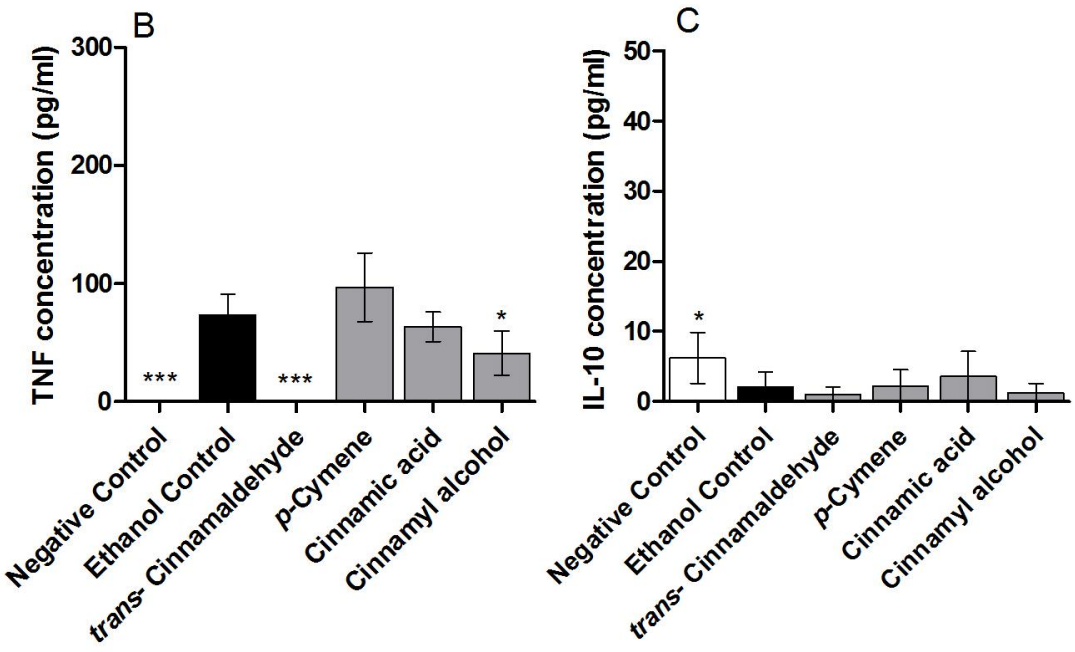

Figure 27: Effects of *C. verum* compounds on macrophage polarization
THP-1 M1 macrophages were incubated with different compounds (25 µg/ml) present in cinnamon extract or vehicle 70% ethanol, followed by stimulation with LPS-EB. Negative control: untreated M1 macrophages. **A**: Viability (Alamar Blue assay) normalized to viability of untreated cells. **B**: TNF secretion (ELISA) in pg/ml. **C**: IL-10 secretion (ELISA) in pg/ml. Data represent mean ± SD of 2 independent experiments (each with *n*=3); unpaired t-test (only anti-inflammatory effects marked): ***p < 0.001, *p < 0.05 compared to ethanol control.

Since after the treatment with different *C. verum* compounds only the secretion of the LPS-induced pro-inflammatory marker TNF was mitigated without an increase of the M2 specific anti-inflammatory marker IL-10, no full switch from pro-inflammatory M1 macrophages to anti-inflammatory M2 macrophages was observed. Nevertheless, *trans*-cinnamaldehyde strongly inhibited the TNF production. A longer incubation of THP-1 M1 macrophages with this compound might lead to a switch to M2 macrophages. To the best of our knowledge, a repolarization from M1 macrophages to M2 macrophages for the tested *C. verum* compounds has also not been reported so far.

4.3.5. Influence on phosphorylation of TLR signaling pathway molecules

To investigate possible mechanisms by which *C. verum* extract, *trans*-cinnamaldehyde and *p*-cymene inhibit the LPS-induced production of pro-inflammatory cytokines in THP-1 monocytes, phosphorylation ratio of the molecules AKT, IκBα and p38 were determined.

As shown in **Figure 28A**, only slight changes in protein level of AKT were observed in THP-1 monocytes after different treatments. In contrast, treatment of LPS-stimulated THP-1 monocytes with *C. verum* extract, *trans*-cinnamaldehyde and *p*-cymene resulted in a strong

mitigation of AKT phosphorylation (**Figure 28B**). The same effects were observed for the relative ratio of P-AKT to AKT protein level (**Figure 28C**).

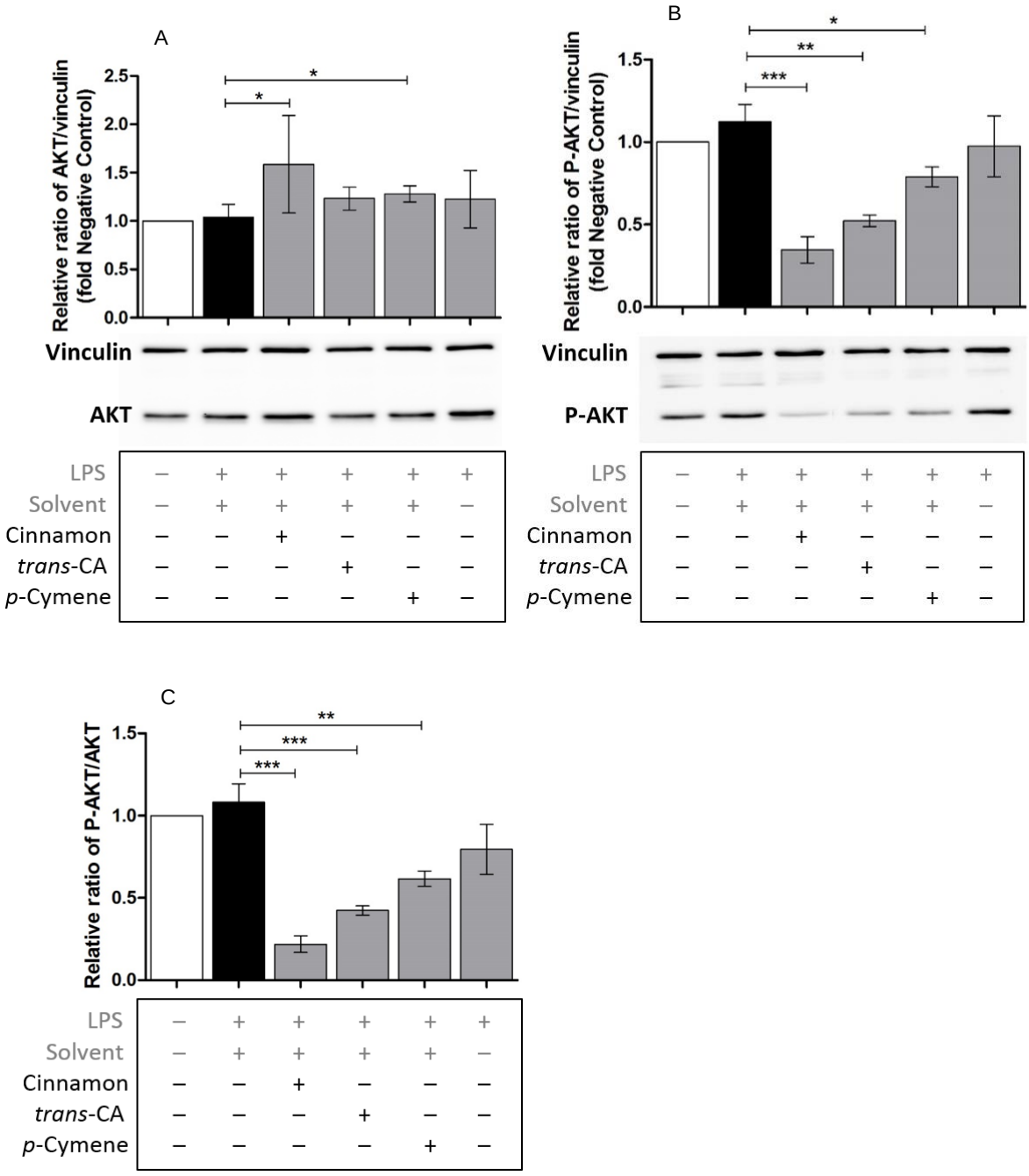

Figure 28: Effects of *C. verum* extract, *trans*-cinnamaldehyde and *p*-cymene on AKT phosphorylation
THP-1 monocytes were incubated with *C. verum* extract (0.6%), its active compounds (25 µg/ml) or vehicle ethanol, followed by stimulation with LPS-EB. AKT and P-AKT protein level were measured using Western Blot analysis. Data display relative protein expression normalized to vinculin loading control and normalized to negative control (untreated cells). **A**: AKT protein level normalized to vinculin, **B**: P-AKT protein level normalized to vinculin, **C**: P-AKT protein level normalized to AKT protein level. Data represent mean ± SD (*n*=3); unpaired t-test: ***p < 0.001, **p < 0.005, *p < 0.05 compared to solvent control. *trans*-CA: *trans*-cinnamaldehyde.

IκBα protein level in THP-1 monocytes was reduced after LPS treatment compared to negative control (**Figure 29A**). This reduction was mitigated after treatment with *C. verum*

extract, *trans*-cinnamaldehyde and *p*-cymene, which was significant for *trans*-cinnamaldehyde treatment. As shown in **Figure 29B**, LPS-stimulated THP-1 monocytes treated with *C. verum* extract, *trans*-cinnamaldehyde and *p*-cymene resulted in a mitigation of IκBα phosphorylation, which was significant for treatment with *C. verum* extract and *trans*-cinnamaldehyde compared to solvent control. The same mitigations but significant for all three treatments were observed for the relative ratio of P-IκBα to IκBα protein level (**Figure 29C**).

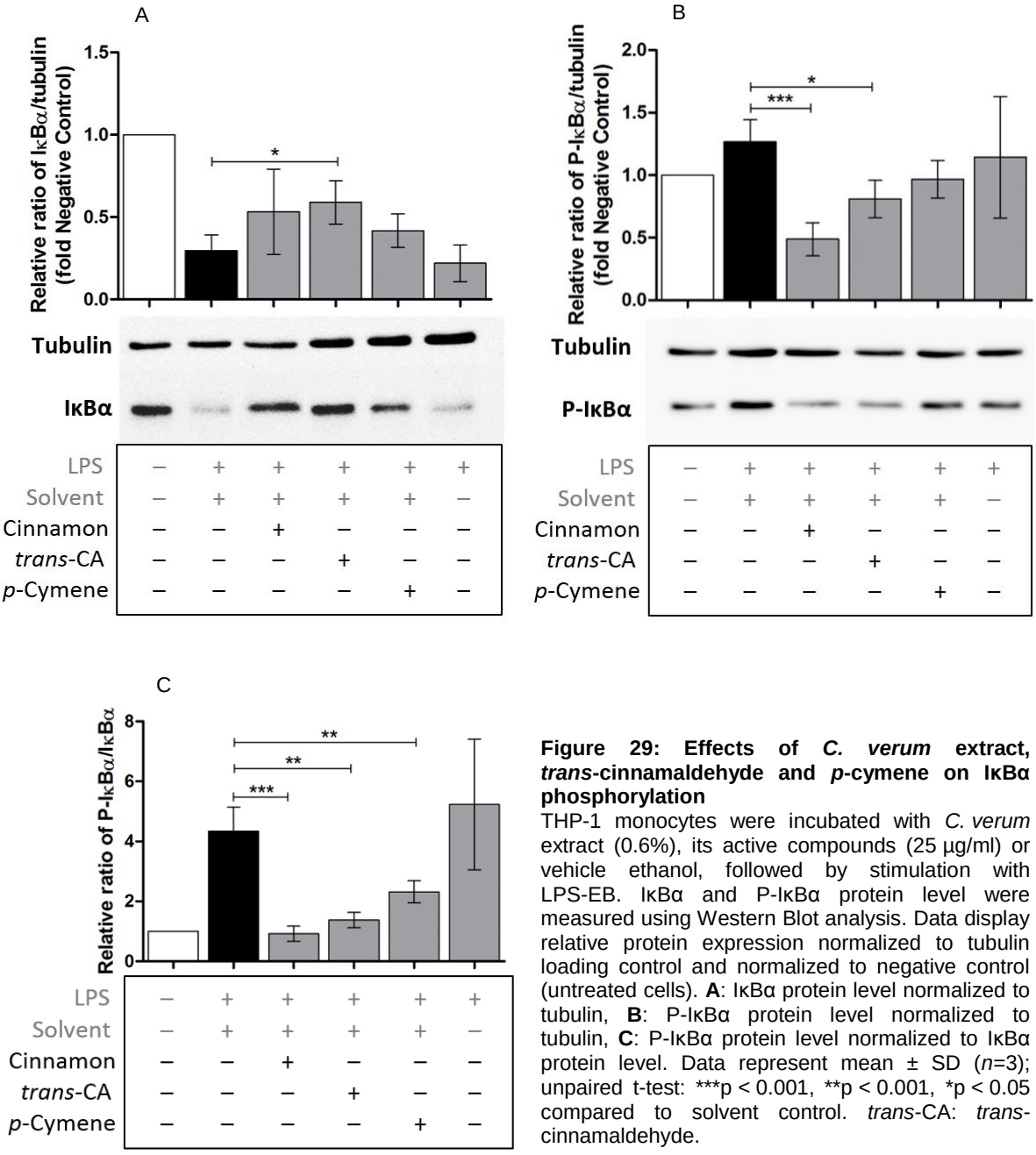

Figure 29: Effects of *C. verum* extract, *trans*-cinnamaldehyde and *p*-cymene on IκBα phosphorylation
THP-1 monocytes were incubated with *C. verum* extract (0.6%), its active compounds (25 µg/ml) or vehicle ethanol, followed by stimulation with LPS-EB. IκBα and P-IκBα protein level were measured using Western Blot analysis. Data display relative protein expression normalized to tubulin loading control and normalized to negative control (untreated cells). **A**: IκBα protein level normalized to tubulin, **B**: P-IκBα protein level normalized to tubulin, **C**: P-IκBα protein level normalized to IκBα protein level. Data represent mean ± SD (*n*=3); unpaired t-test: ***p < 0.001, **p < 0.001, *p < 0.05 compared to solvent control. *trans*-CA: *trans*-cinnamaldehyde.

Only slight changes in protein level of p38 were observed in THP-1 monocytes after different treatments (**Figure 30A**). Treatment of LPS-stimulated THP-1 monocytes with *C. verum* extract and *p*-cymene resulted in a small but significant increase of p38 phosphorylation compared to solvent control treatment (**Figure 30B**). After *p*-cymene treatment, an increase was also observed for the relative ratio of P-p38 to p38 protein level (**Figure 30C**).

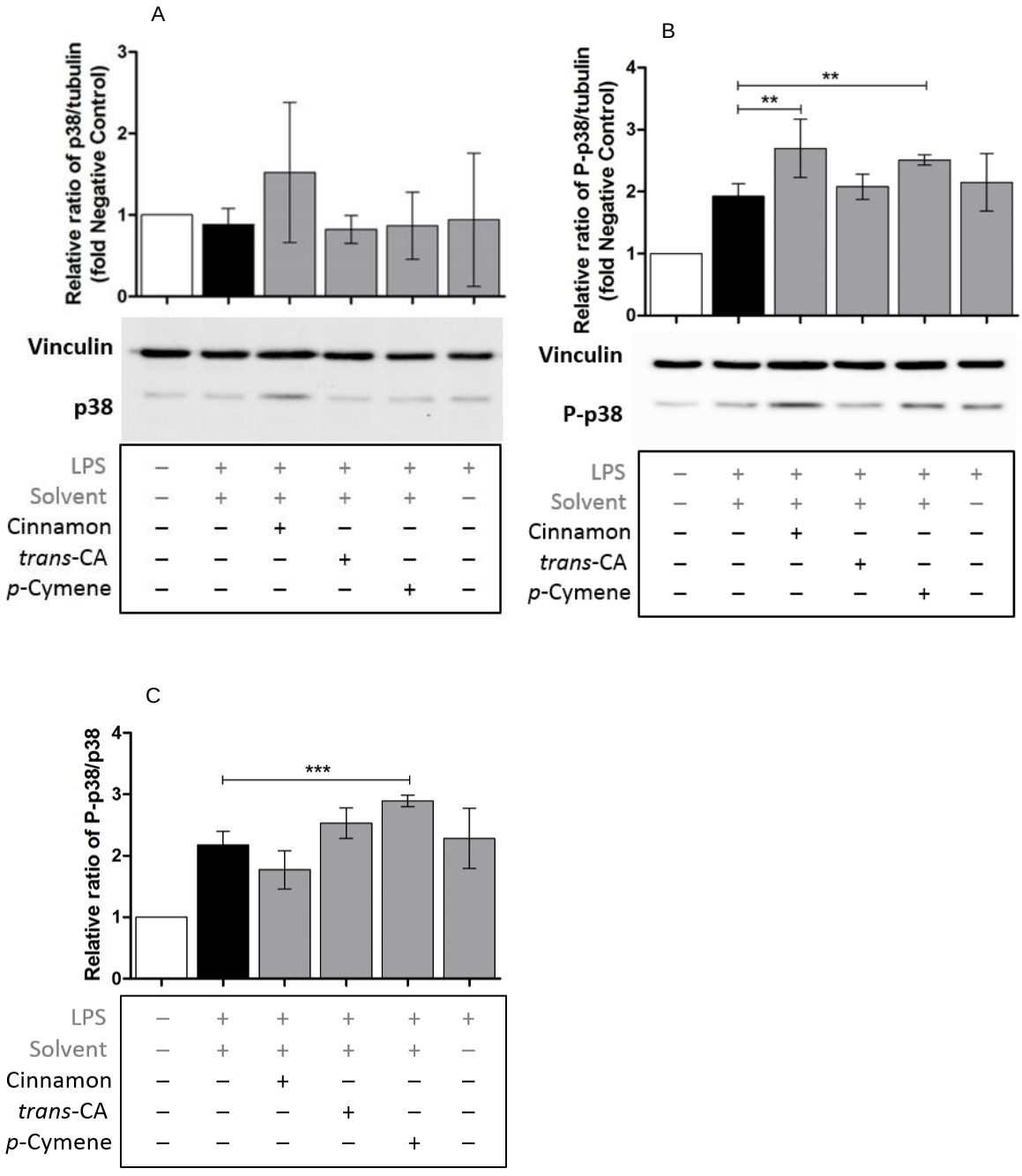

Figure 30: Effects of *C. verum* extract, *trans*-cinnamaldehyde and *p*-cymene on p38 phosphorylation
THP-1 monocytes were incubated with *C. verum* extract (0.6%), its active compounds (25 µg/ml) or vehicle ethanol, followed by stimulation with LPS-EB. p38 and P-p38 protein level were measured using Western Blot analysis. Data display relative protein expression normalized to tubulin loading control and normalized to negative control (untreated cells). **A**: p38 protein level normalized to vinculin, **B**: P-p38 protein level normalized to vinculin, **C**: P-p38 protein level normalized to p38 protein level. Data represent mean ± SD (*n*=3); unpaired t-test: ***p < 0.005, **p < 0.001, compared to solvent control. *trans*-CA: *trans*-cinnamaldehyde.

Based on the findings described above, it can be concluded that *C. verum* bark extract, *trans*-cinnamaldehyde and *p*-cymene inhibit the pro-inflammatory signal transduction of early TLR2 and TLR4 signaling pathway molecules.

AKT is a protein phosphorylated after TLR4 stimulation via the PI3K pathway and is known to regulate the transcriptional activity of NF-κB via the induction of IκBα phosphorylation and subsequent degradation (Bai et al., 2009; Yang et al., 2016). In line with our findings, cinnamon extract has been reported to inhibit phosphorylation of AKT in U251 human glioma cells in the presence of hypoxia conditions (Zhang et al., 2017) as well as in tetradecanoylphorbol-13-acetate (TPA)-induced human umbilical vein endothelial cells (HUVEC) (Bansode et al., 2013). Furthermore, the AKT phosphorylation level was reduced in activated macrophages after treatment with the cinnamaldehyde derivative 4-hydroxycinnamaldehyde-galactosamine (Ka et al., 2016). In contrast, treatment of mice with cinnamaldehyde without further stimulation resulted in a significant increase of AKT phosphorylation (Li et al., 2012). If the lack of stimulation might be responsible for this controversy effect, would be an interesting point for further investigations. In contrast to cinnamon extract and *trans*-cinnamaldehyde, whose observed influences on AKT phosphorylation ratio were supported by literature data, to the best of our knowledge, our observed inhibitory effects of *p*-cymene on AKT phosphorylation have not yet been reported elsewhere.

AKT is known from literature to induce the phosphorylation of IκBα. The subsequent degradation of IκBα, an inhibitor of NF-κB, leads to the activation of NF-κB and its translocation into the cell nucleus (Bai et al., 2009; Yang et al., 2016). Since a significant decrease of AKT phosphorylation was observed after treatment with *C. verum* extract, *trans*-cinnamaldehyde and *p*-cymene, the same tendency was expected for IκBα phosphorylation. This assumption could be confirmed with the performed experiments. In accordance with our reveled decrease of IκBα phosphorylation after incubation with *C. verum* extract, the same extract has also been reported to significantly reduce IκBα phosphorylation in mice with IL-10 knockout (Hagenlocher et al., 2016). The same tendency has also been shown in LPS-stimulated murine macrophages (Kanuri et al., 2009). Furthermore, its active compound cinnamaldehyde has been reported to significantly suppress IκBα phosphorylation and degradation in a mouse model for myocarditis (Zhang et al., 2012). In addition, our observed significant *p*-cymene-dependent decrease of P-IκBα/IκBα protein level, is in line with *in vivo* findings in the literature using an LPS-induced mouse model (Xie et al., 2012).

Another important protein in the LPS-stimulated TLR signaling pathway is p38, a MAPK, which leads primarily to the activation of AP-1, but also of NF-κB. Both transcription factors contribute to the expression of several pro-inflammatory cytokines, e.g. IL-1, IL-6, IL-8 and TNF-α (Cuadrado and Nebreda, 2010; Yang et al., 2016; Lee and Kim, 2017). Contrarious to

our data, IgE-stimulated human intestinal mast cells showed an attenuation of p38 phosphorylation after incubation with *C. verum* extract for 18h (Hagenlocher et al., 2013). Since we have chosen rather short incubation times (2h *C. verum* extract treatment, followed by 1h LPS stimulation), not all changes in the MAPK phosphorylation might already be visible at this time point, which would possibly explain the discrepancies between both measurements. Cinnamaldehyde has been revealed in literature to induce the phosphorylation of p38 in murine inguinal adipocytes (Jiang et al., 2017a). In contrast, inhibition of p38 MAPK signaling pathway has been observed in rats fed with cinnamaldehyde without prior stimuli (Kim et al., 2007). Our results showed no significant influence of *trans*-cinnamaldehyde on p38 phosphorylation level. Contrarious to our observed significant increase of p38 phosphorylation after *p*-cymene treatment in LPS-stimulated THP-1 monocytes, *p*-cymene treatment in a LPS-induced acute lung injury mouse model revealed a dose-dependent significant mitigation of p38 phosphorylation (Xie et al., 2012). Interestingly, the observed mitigation of P-IκBα/IκBα protein ratio after *p*-cymene treatment in the same study has been in line with our data. Whether the disagreement on the influences on p38 phosphorylation might be due to the different interactions of the MAPK in diverse cell types, a lack of transferability between the performed cell culture-based assays and mouse models, or if different incubation times and concentrations might reveal a contrary result would be interesting for further analysis.

Taken together, *C. verum* extract, *trans*-cinnamaldehyde and *p*-cymene were generally shown to attenuate the LPS-induced stimulation of early TLR2 and TLR4 signaling pathway molecules. The anti-inflammatory potential was especially demonstrated by mitigating the LPS-induced AKT and IκBα phosphorylation, both important molecules in the inflammatory cascade. Since AKT and IκBα are involved in the regulation of several pro-inflammatory cytokines (Ghosh and Dass, 2016), these finding could explain the observed reduced secretion of IL-8 in different stimulated cell lines in response to treatment with *C. verum* extract, *trans*-cinnamaldehyde and *p*-cymene. Nevertheless, the direct target(s) of *C. verum* extract, *trans*-cinnamaldehyde and *p*-cymene within the signaling cascade have to be elucidated.

5. Conclusions

Taken together, this research provides novel information on anti-inflammatory herbal extracts and their active compounds. Furthermore, it revealed a great potential still hidden in this field of research. With the performed broad screening experiments, extracts with previously unknown anti-inflammatory effects on multiple TLR signaling pathways were identified. In particular, the strongly anti-inflammatory extracts from *Castanea sativa* leaves and *Alchemilla vulgaris* plant provide a great basis for further investigations since only limited information are reported concerning their TLR-dependent beneficial health effects. This research gives also an important new insight into possible mechanisms of action. Besides the exclusion of direct TLR4 antagonistic activities for all tested extracts, mitigation of NF-κB translocation and/or the potential to repolarize pro-inflammatory M1 macrophages to anti-inflammatory M2 macrophages were described for several extracts. This work supports therefore the view that the different compounds within the complex herbal mixtures might target various molecules involved in inflammatory processes.

C. verum showed not only promising anti-inflammatory properties in the performed screening experiments *in vitro* but is also reported in literature to exhibit strong anti-inflammatory effects *in vitro* and *in vivo*. Therefore, we focused in the second part of our research on *C. verum* bark extract. With its fractionation, we revealed several compounds previously not known to be present in *C. verum* bark extract, e.g. methyl salicylate, stearic acid and palmitic acid. Importantly, we could also show formerly unknown synergistic effects between active compounds in *C. verum* bark extract and other compounds, which do not exhibit anti-inflammatory activities by themselves. This demonstrates that even the well-studied cinnamon is far from being completely explored. Especially the target molecules of *C. verum* bark extract and its active compounds still need to be investigated. With our findings, we could demonstrate an influence on early TLR2 and TLR4 signaling pathway molecules and therefore pave the way for systematic and targeted analyses. Nevertheless, it should be taken into account that besides the applied compounds themselves, also their metabolization products might interact with the TLR signaling pathways, which further complicates the identification of the responsible molecules and mechanism(s). Taken together, this work provides important new insight into the pharmacological possibilities of herbal extracts and especially those of *C. verum* bark extract. Given that therapeutic doses of *C. verum* bark extract and/or its active compounds exert no toxic effects, our results may contribute to the development of new oral treatment strategies for different inflammatory diseases.

6. Lists

6.1. List of abbreviations

Abbreviation	Full name
AChE	Acetylcholinesterase
ADI	Acceptable daily intake
Alamar B.	Alamar Blue assay
ALP	Alkaline phosphatase
ALT	Alanine transaminase
Ana	*Anabaena ambigua*
ANOVA	Analysis of variance
AP-1	Activator protein 1
APS	Ammonium persulfate
AST	Aspartate transaminase
ATI	Amylase trypsin inhibitor
BCA	Bicinchoninic acid
Benz. acid	Benzoic acid
BSA	Bovine serum albumin
C.	*Cinnamomum*
CA	*trans*-Cinnamaldehyde
CCK-8	Cell Counting Kit-8
CCL	Chemokine (C-C motif) ligand
CD	Cluster of differentiation
Cin. acid	Cinnamic acid
Cin. alcohol	Cinnamyl alcohol
CNS	Central nervous system
COPD	Chronic obstructive pulmonary disease
COX	Cyclooxygenase
CRP	C-reactive protein
CXCL	Chemokine (C-X-C motif) ligand
Cyl	*Cylindrospermum siamensis*
DAAD	Deutscher Akademischer Austauschdienst
DAD	Diode array detector
DAMP	Damage associated molecular pattern
DAPI	4',6-Diamidino-2-phenylindole
DMEM	Dulbecco's Modified Eagle Medium
DMSO	Dimethylsulfoxid
DTT	Dithiothreitol
ECL	Enhanced chemiluminescence
EFSA	European food safety authority
EGCG	Epigallocatechin-3-gallate
EI	Electron impact
ELISA	Enzyme-linked immunosorbent assay
ERK	Extracellular signal-regulated kinase
ESI	Electrospray ionization
EU/ml	Endotoxin unit/ml
FCS	Fetal calf serum

Abbreviation	Full name
FDA	Food and drug administration
Fg	Fibrinogen
GC	Gas chromatography
GP	Glucan phosphate
GSH	Glutathione
HCl	Hydrogen chloride
HEK	Human embryonic kidney
HeLa	Henrietta Lacks
HMGB1	High-mobility group box-1
Hmox1	Heme oxygenase (decycling) 1
HPLC	High-performance liquid chromatography
HRMS	High-resolution mass spectrometry
HRP	Horseradish peroxidase
HUVEC	Human umbilical vein endothelial cells
IBD	Inflammatory bowel disease
IFN	Interferon
IKK	IκB kinase
IL	Interleukin
iNOS	Inducible nitric oxide synthase
IRAK	IL-1 receptor-associated kinase
IRF	Interferon regulatory factor
IκB	NF-κB inhibitor
JNK	c-Jun N-terminal kinase
LA	Luciferase assay
LAL	*Limulus* Amebocyte Lysate
LBP	Lipid binding protein
LDH	Lactate dehydrogenase
LOX	Lipoxygenase
LPS	Lipopolysaccharide
Lyn	*Lyngbya lagerheimii*
M1	Classical activated type 1
M2	Alternatively activated type 2
MAL	MyD88 adapter-like
MAPK	Mitogen-activated protein kinase
MCP-1	Monocyte chemoattractant protein-1
MD-2	Myeloid differentiation factor 2
MDA	Malondialdehyde
Methyl sal.	Methyl salicylate
Mic	*Microcystis aeruginosa*
MPCA	Mainz Program for Chemical Allergology
MPGC	Max Planck Graduate Center
MPO	Myeloperoxidase
MS	Mass spectrometry
MSRV-Env	Multiple sclerosis associated retrovirus envelope protein
MTT	3-(4,5-Dimethylthiazol-2-yl)-2,5-diphenyltetrazolium bromide
MyD88	Myeloid differentiation primary response 88
NaCl	Sodium chloride
NADH	Nicotinamide adenine dinucleotide

Abbreviation	Full name
NADPH	Nicotinamide adenine dinucleotide phosphate
NF-κB	Nuclear factor-κB
NLRP3	NOD-like receptor family pyrin domain-containing 3
NO	Nitric oxide
Nos	*Nostoc* sp.
Nrf2	Nuclear factor erythroid 2-related factor 2
PAGE	Polyacrylamide gel electrophoresis
PAMP	Pathogen-associated molecular pattern
PBMC	Peripheral blood mononuclear cell
PBS	Phosphate-buffered saline
PGE_2	Prostaglandin E_2
Pho	*Phormidium* sp.
PI3K	Phosphatidylinositol 3-kinase
PKB	Protein kinase B
Pla	*Planktothrix agardhii*
PMA	Phorbol 12-myristate 13-acetate
PPARγ	Peroxisome proliferator-activated receptor gamma
Q-TOF	Quadrupole-time-of-flight
RAGE	Receptor for advanced glycation end products
RANKL	Receptor activator of nuclear factor kappa-B ligand
RNS	Reactive nitrogen species
ROS	Reactive oxygen species
RPMI	Roswell Park Memorial Institute
RT	Room temperature
SD	Standard deviation
SDS	Sodium dodecyl sulfate
SEAP	Secreted embryonic alkaline phosphatase
SEM	Standard error of the mean
SILMAS	Trimethylsilyl methallylsulfinate
SOD	Superoxide dismutase
Syn	*Synechocystis* sp.
TAK1	Transforming growth factor β-activated kinase 1
TBK1	TANK-binding kinase 1
TBS	Tris-buffered saline
TBS-T	Tris-buffered saline with Tween-20
TDI	Tolerable daily intake
TEMED	Tetramethylethylenediamine
TGFβ1	Transforming growth factor beta 1
TIM	Institute of Translational Immunology
TIRAP	TIR domain containing adaptor protein
TLR	Toll-like receptor
TMB	Tetramethylbenzidine
TNF	Tumor necrosis factor
TPA	Tetradecanoylphorbol-13-acetate
TRAF6	Tumor necrosis factor receptor-associated factor 6
TRAM	TRIF-related adaptor molecule
trans-CA	*trans*-Cinnamaldehyde
TRIF	TIR-domain-containing adapter-inducing interferon-β

Abbreviation	Full name
WST-8	2-(2-Methoxy-4-nitrophenyl)-3-(4-nitrophenyl)-5-(2,4-disulfophenyl)-2H-tetrazolium,monosodium salt

6.2. List of figures

Figure 1: Simplified TLR4 signaling pathway 16
Figure 2: Optimizing LPS treatment for HeLa-TLR4 reporter cell line 53
Figure 3: Comparison of different cell viability assays....54
Figure 4: Comparison of different TLR4 agonists....56
Figure 5: Optimizing LPS treatment for THP-1 monocytes 58
Figure 6: Cell viability and anti-inflammatory effects of ten most promising extracts 61
Figure 7: Cell viability and anti-inflammatory effects of different cyanobacteria species....64
Figure 8: Cell viability and anti-inflammatory effects of *Fallopia japonica* samples....65
Figure 9: Cell viability and anti-inflammatory effects of five most promising extracts tested for exclusive TLR4 antagonistic activity 68
Figure 10: Influence of ten most promising extracts on NF-κB p65 translocation 74
Figure 11: Quantitative influence on NF-κB p65 translocation of ten most promising extracts 75
Figure 12: Effects of ten most promising extracts on macrophage polarization....77
Figure 13: Cell viability and anti-inflammatory effects of *C. verum* bark extract in unstimulated THP-1 monocytes....78
Figure 14: Cell viability and anti-inflammatory effects of *C. verum* bark extract on stimulated THP-1 monocytes....79
Figure 15: *C. verum* bark extract tested for exclusive TLR4 antagonistic activity 80
Figure 16: *C. verum* bark extract tested in inflammatory mouse model....81
Figure 17: HPLC *C. verum* fractions tested for anti-inflammatory effects in THP-1 monocytes 82
Figure 18: Chromatogram of HPLC *C. verum* extract fractionation 83
Figure 19: (–)ESI-MS spectrum of *C. verum* fraction M 83
Figure 20: GC-MS spectra of compounds identified in HPLC fractions of *C. verum*....85
Figure 21: Anti-inflammatory effects of select *C. verum* compounds....86
Figure 22: *trans*-Cinnamaldehyde tested for exclusive TLR4 antagonistic effects....88
Figure 23: *p*-Cymene tested for exclusive TLR4 antagonistic effects....89
Figure 24: Fraction-dependent synergistic effects 90
Figure 25: Synergistic effects of *C. verum* extract compounds 91
Figure 26: Transformation of cinnamaldehyde....91
Figure 27: Effects of *C. verum* compounds on macrophage polarization 93
Figure 28: Effects of *C. verum* extract, *trans*-cinnamaldehyde and *p*-cymene on AKT phosphorylation....94
Figure 29: Effects of *C. verum* extract, *trans*-cinnamaldehyde and *p*-cymene on IκBα phosphorylation....95

Figure 30: Effects of *C. verum* extract, *trans*-cinnamaldehyde and *p*-cymene on p38 phosphorylation 96
Figure 31: Cell viability and anti-inflammatory effects of ethanolic extracts XXXII
Figure 32: Cell viability and anti-inflammatory effects of extracts tested for exclusive TLR4 antagonistic activity XLI

6.3. List of tables

Table 1: Overview of plants and their active compounds comprising beneficial effects 3
Table 2: Cinnamon species 18
Table 3: Main compounds of *C. verum* 19
Table 4: Used equipment 23
Table 5: Used consumables 24
Table 6: Used chemicals 25
Table 7: Ethanolic extracts tested for anti-inflammatory properties 28
Table 8: Cyanobacteria extracts tested for anti-inflammatory properties 31
Table 9: Antibodies for detection of NF-κB translocation 34
Table 10: Primary antibodies for Western Blot analysis 35
Table 11: Secondary antibodies for Western Blot analysis 35
Table 12: Alamar Blue fluorescence measurement settings 44
Table 13: LightSwitch Luciferase luminescence measurement settings 45
Table 14: Human ELISA absorbance measurement settings 46
Table 15: HPLC gradient used for *C. verum* fractionation 50
Table 16: HRMS settings 51
Table 17: GC-MS settings 52
Table 18: Anti-inflammatory activity of 25 most promising ethanolic extracts 62
Table 19: TLR2 and TLR4 specific antagonistic activity of five most promising ethanolic extracts 69
Table 20: Retention times of select HPLC *C. verum* fractions 81
Table 21: Compounds identified in anti-inflammatory HPLC *C. verum* fractions 86
Table 22: Anti-inflammatory activity of ethanolic extracts XXXIII
Table 23: TLR2 and TLR4 specific antagonistic activity of select ethanolic extracts XLII

7. References

Abraham K, Wöhrlin F, Lindtner O, Heinemeyer G, Lampen A (2010) Toxicology and risk assessment of coumarin: focus on human data. Mol Nutr Food Res. 54(2):228-39. doi: 10.1002/mnfr.200900281.

Abraham K, Pfister M, Wöhrlin F, Lampen A (2011) Relative bioavailability of coumarin from cinnamon and cinnamon-containing foods compared to isolated coumarin: a four-way crossover study in human volunteers. Mol Nutr Food Res. 55(4):644-53. doi: 10.1002/mnfr.201000394.

Achan J, Talisuna AO, Erhart A, Yeka A, Tibenderana JK, Baliraine FN, Rosenthal PJ, D'Alessandro U (2011) Quinine, an old anti-malarial drug in a modern world: role in the treatment of malaria. Malar J. 10:144. doi: 10.1186/1475-2875-10-144.

Albini A, Dell'Eva R, Vené R, Ferrari N, Buhler DR, Noonan DM, Fassina G (2006) Mechanisms of the antiangiogenic activity by the hop flavonoid xanthohumol: NF-kappaB and Akt as targets. FASEB J. 20(3):527-9.

Alexandre JTM, Sousa LHT, Lisboa MRP, Furlaneto FAC, do Val DR, Marques M, Vasconcelos HC, de Melo IM, Leitão R, Castro Brito GA, Goes P (2017) Anti-inflammatory and antiresorptive effects of *Calendula officinalis* on inflammatory bone loss in rats. Clin Oral Investig. [Epub ahead of print]. doi: 10.1007/s00784-017-2308-7.

Allen-Hall L, Arnason JT, Cano P, Lafrenie RM (2010) *Uncaria tomentosa* acts as a potent TNF-alpha inhibitor through NF-kappaB. J Ethnopharmacol. 127(3):685-93. doi: 10.1016/j.jep.2009.12.004.

Amirghofran Z, Hashemzadeh R, Javidnia K, Golmoghaddam H, Esmaeilbeig A (2011) *In vitro* immunomodulatory effects of extracts from three plants of the *Labiatae* family and isolation of the active compound(s). J Immunotoxicol. 8(4):265-73. doi: 10.3109/1547691X.2011.590828.

An J, Minie M, Sasaki T, Woodward JJ, Elkon KB (2017) Antimalarial Drugs as Immune Modulators: New Mechanisms for Old Drugs. Annu Rev Med. 68:317-330.

Angel-Morales G, Noratto G, Mertens-Talcott SU (2012) Standardized curcuminoid extract (*Curcuma longa* l.) decreases gene expression related to inflammation and interacts with associated microRNAs in human umbilical vein endothelial cells (HUVEC). Food Funct. 3(12):1286-93. doi: 10.1039/c2fo30023k.

Aprotosoaie AC, Costache II, Miron A (2016) Anethole and Its Role in Chronic Diseases. Adv Exp Med Biol. 929:247-267.

Arab L, Liu W, Elashoff D (2009) Green and black tea consumption and risk of stroke: a meta-analysis. Stroke. 40(5):1786-92. doi: 10.1161/STROKEAHA.108.538470.

Arçari DP, Bartchewsky W Jr, dos Santos TW, Oliveira KA, DeOliveira CC, Gotardo ÉM, Pedrazzoli J Jr, Gambero A, Ferraz LF, Carvalho Pde O, Ribeiro ML (2011) Anti-inflammatory effects of yerba maté extract (*Ilex paraguariensis*) ameliorate insulin resistance in mice with high fat diet-induced obesity. Mol Cell Endocrinol. 335(2):110-5. doi: 10.1016/j.mce.2011.01.003.

Aviram A, Tsoukias NM, Melnick SJ, Resek AP, Ramachandran C (2012) Inhibition of nitric oxide synthesis in mouse macrophage cells by feverfew supercritical extract. Phytother Res. 26(4):541-5. doi: 10.1002/ptr.3594.

Awasthi S (2014) Toll-like receptor-4 modulation for cancer immunotherapy. Front Immunol. 5:328. doi: 10.3389/fimmu.2014.00328.

Ayoobi F, Shamsizadeh A, Fatemi I, Vakilian A, Allahtavakoli M, Hassanshahi G, Moghadam-Ahmadi A (2017) Bio-effectiveness of the main flavonoids of *Achillea millefolium* in the pathophysiology of neurodegenerative disorders- a review. Iran J Basic Med Sci. 20(6):604-612. doi: 10.22038/IJBMS.2017.8827.

Badescu M, Badulescu O, Badescu L, Ciocoiu M (2015) Effects of *Sambucus nigra* and *Aronia melanocarpa* extracts on immune system disorders within diabetes mellitus. Pharm Biol. 53(4):533-9. doi: 10.3109/13880209.2014.931441.

Bai D, Ueno L, Vogt PK (2009) Akt-mediated regulation of NFkappaB and the essentialness of NFkappaB for the oncogenicity of PI3K and Akt. Int J Cancer. 125(12):2863-70. doi: 10.1002/ijc.24748.

Bais S, Abrol N, Prashar Y, Kumari R (2017) Modulatory effect of standardised amentoflavone isolated from *Juniperus communis* L. agianst Freund's adjuvant induced arthritis in rats (histopathological and X Ray anaysis). Biomed Pharmacother. 86:381-392. doi: 10.1016/j.biopha.2016.12.027.

Baliga MS, Joseph N, Venkataranganna MV, Saxena A, Ponemone V, Fayad R (2012) Curcumin, an active component of turmeric in the prevention and treatment of ulcerative colitis: preclinical and clinical observations. Food Funct. 3(11):1109-17. doi: 10.1039/c2fo30097d.

Bansode RR, Leung T, Randolph P, Williams LL, Ahmedna M (2013) Cinnamon extract inhibits angiogenesis in zebrafish and human endothelial cells by suppressing VEGFR1, VEGFR2, and PKC-mediated MAP kinase. Food Sci Nutr. 1(1):74-82. doi: 10.1002/fsn3.13.

Baqui AA, Meiller TF, Falkler WA (1999) Enhanced interleukin-8 production in THP-1 human monocytic cells by lipopolysaccharide from oral microorganisms and granulocyte-macrophage colony-stimulating factor. Oral Microbiol Immunol. 14(5):275-80.

Bazazzadegan N, Dehghan Shasaltaneh M, Saliminejad K, Kamali K, Banan M, Khorram Khorshid HR (2017) The Effects of *Melilotus officinalis* Extract on Expression of Daxx, Nfkb and Vegf Genes in the Streptozotocin-Induced Rat Model of Sporadic Alzheimer's Disease. Avicenna J Med Biotechnol. 9(3):133-137.

Bellinghausen I, Weigmann B, Zevallos V, Maxeiner J, Reißig S, Waisman A, Schuppan D, Saloga J (2018) Wheat amylase-trypsin inhibitors exacerbate intestinal and airway allergic immune responses in humanized mice. J Allergy Clin Immunol. pii: S0091-6749(18)30444-5. doi: 10.1016/j.jaci.2018.02.041. [Epub ahead of print]

Ben Salem M, Affes H, Athmouni K, Ksouda K, Dhouibi R, Sahnoun Z, Hammami S, Zeghal KM (2017) Chemicals Compositions, Antioxidant and Anti-Inflammatory Activity of *Cynara scolymus* Leaves Extracts, and Analysis of Major Bioactive Polyphenols by HPLC. Evid Based Complement Alternat Med. 2017:4951937. doi: 10.1155/2017/4951937.

Bonaterra GA, Heinrich EU, Kelber O, Weiser D, Metz J, Kinscherf R (2010) Anti-inflammatory effects of the willow bark extract STW 33-I (Proaktiv(®)) in LPS-activated human monocytes and differentiated macrophages. Phytomedicine. 17(14):1106-13. doi: 10.1016/j.phymed.2010.03.022.

Bonaterra GA, Schwendler A, Hüther J, Schwarzbach H, Schwarz A, Kolb C, Abdel-Aziz H, Kinscherf R (2018) Neurotrophic, Cytoprotective, and Anti-inflammatory Effects of St. John's

Wort Extract on Differentiated Mouse Hippocampal HT-22 Neurons. Front Pharmacol. 8:955. doi: 10.3389/fphar.2017.00955.

Bortolotti M, Porta S (2011) Effect of red pepper on symptoms of irritable bowel syndrome: preliminary study. Dig Dis Sci. 56(11):3288-95. doi: 10.1007/s10620-011-1740-9.

Bracesco N, Sanchez AG, Contreras V, Menini T, Gugliucci A (2011) Recent advances on *Ilex paraguariensis* research: minireview. J Ethnopharmacol. 136(3):378-84. doi: 10.1016/j.jep.2010.06.032.

Budai MM, Varga A, Milesz S, Tőzsér J, Benkő S (2013) *Aloe vera* downregulates LPS-induced inflammatory cytokine production and expression of NLRP3 inflammasome in human macrophages. Mol Immunol. 56(4):471-9. doi: 10.1016/j.molimm.2013.05.005.

Bundy R, Walker AF, Middleton RW, Wallis C, Simpson HC (2008) Artichoke leaf extract (*Cynara scolymus*) reduces plasma cholesterol in otherwise healthy hypercholesterolemic adults: a randomized, double blind placebo controlled trial. Phytomedicine. 15(9):668-75. doi: 10.1016/j.phymed.2008.03.001.

Büssing A, Raak C, Ostermann T (2012) Quality of life and related dimensions in cancer patients treated with mistletoe extract (iscador): a meta-analysis. Evid Based Complement Alternat Med. 2012:219402. doi: 10.1155/2012/219402.

Calliste CA, Trouillas P, Allais DP, Duroux JL (2005) *Castanea sativa* Mill. leaves as new sources of natural antioxidant: an electronic spin resonance study. J Agric Food Chem. 53(2):282-8.

Carvalho AR, Costa G, Figueirinha A, Liberal J, Prior JAV, Lopes MC, Cruz MT, Batista MT (2017) *Urtica* spp.: Phenolic composition, safety, antioxidant and anti-inflammatory activities. Food Res Int. 99(Pt 1):485-494. doi: 10.1016/j.foodres.2017.06.008.

Catarino MD, Silva AMS, Cruz MT, Cardoso SM (2017) Antioxidant and anti-inflammatory activities of *Geranium robertianum* L. decoctions. Food Funct. 8(9):3355-3365. doi: 10.1039/c7fo00881c.

Chahal DS, Sivamani RK, Isseroff RR, Dasu MR (2013) Plant-based modulation of Toll-like receptors: an emerging therapeutic model. Phytother Res. 27(10):1423-38. doi: 10.1002/ptr.4886.

Chanput W, Mes J, Vreeburg RA, Savelkoul HF, Wichers HJ (2010) Transcription profiles of LPS-stimulated THP-1 monocytes and macrophages: a tool to study inflammation modulating effects of food-derived compounds. Food Funct. 1(3):254-61. doi: 10.1039/c0fo00113a.

Chao LK, Hua KF, Hsu HY, Cheng SS, Lin IF, Chen CJ, Chen ST, Chang ST (2008) Cinnamaldehyde inhibits pro-inflammatory cytokines secretion from monocytes/macrophages through suppression of intracellular signaling. Food Chem Toxicol. 46(1):220-231.

Chen M, Chang YY, Huang S, Xiao LH, Zhou W, Zhang LY, Li C, Zhou RP, Tang J, Lin L, Du ZY, Zhang K (2018) Aromatic-turmerone Attenuates LPS-Induced Neuroinflammation and Consequent Memory Impairment by Targeting TLR4-Dependent Signaling Pathway. Mol Nutr Food Res. 62(2). doi: 10.1002/mnfr.201700281.

Cheong DHJ, Arfuso F, Sethi G, Wang L, Hui KM, Kumar AP, Tran T (2018) Molecular targets and anti-cancer potential of escin. Cancer Lett. 422:1-8. doi: 10.1016/j.canlet.2018.02.027.

Chizzola R, Lohwasser U, Franz C (2018) Biodiversity within Melissa officinalis: Variability of Bioactive Compounds in a Cultivated Collection. Molecules. 23(2). pii: E294. doi: 10.3390/molecules23020294.

Choi KW, Park HJ, Jung DH, Kim TW, Park YM, Kim BO, Sohn EH, Moon EY, Um SH, Rhee DK, Pyo S (2010) Inhibition of TNF-α-induced adhesion molecule expression by diosgenin in mouse vascular smooth muscle cells via downregulation of the MAPK, Akt and NF-κB signaling pathways. Vascul Pharmacol. 53(5-6):273-80. doi: 10.1016/j.vph.2010.09.007.

Choi MJ, Park JS, Park JE, Kim HS, Kim HS (2017) Galangin Suppresses Pro-Inflammatory Gene Expression in Polyinosinic-Polycytidylic Acid-Stimulated Microglial Cells. Biomol Ther (Seoul). 25(6):641-647. doi: 10.4062/biomolther.2017.173.

Clark K, Nanda S, Cohen P (2013) Molecular control of the NEMO family of ubiquitin-binding proteins. Nat Rev Mol Cell Biol. 14(10):673-85. doi: 10.1038/nrm3644.

Cooper R, Morré DJ, Morré DM (2005) Medicinal benefits of green tea: Part I. Review of noncancer health benefits. J Altern Complement Med. 11(3):521-8.

Corren J, Lemay M, Lin Y, Rozga L, Randolph RK (2008) Clinical and biochemical effects of a combination botanical product (ClearGuard) for allergy: a pilot randomized double-blind placebo-controlled trial. Nutr J. 7:20. doi: 10.1186/1475-2891-7-20.

Cravotto G, Boffa L, Genzini L, Garella D (2010) Phytotherapeutics: an evaluation of the potential of 1000 plants. J Clin Pharm Ther. 35(1):11-48. doi: 10.1111/j.1365-2710.2009.01096.x.

Cuadrado A, Nebreda AR (2010) Mechanisms and functions of p38 MAPK signalling. Biochem J. 429(3):403-17. doi: 10.1042/BJ20100323.

Cullen S, Ponnappan S, Ponnappan U (2015) Redox-regulated pathway of tyrosine phosphorylation underlies NF-κB induction by an atypical pathway independent of the 26S proteasome. Biomolecules. 5(1):95-112. doi: 10.3390/biom5010095.

Da-Costa-Rocha I, Bonnlaender B, Sievers H, Pischel I, Heinrich M (2014) *Hibiscus sabdariffa* L. - a phytochemical and pharmacological review. Food Chem. 165:424-43. doi: 10.1016/j.foodchem.2014.05.002.

Dalli E, Colomer E, Tormos MC, Cosín-Sales J, Milara J, Esteban E, Sáez G (2011) *Crataegus laevigata* decreases neutrophil elastase and has hypolipidemic effect: a randomized, double-blind, placebo-controlled trial. Phytomedicine. 18(8-9):769-75. doi: 10.1016/j.phymed.2010.11.011.

de Arriba SG, Naser B, Nolte KU (2013) Risk assessment of free hydroquinone derived from *Arctostaphylos Uva-ursi folium* herbal preparations. Int J Toxicol. 32(6):442-53. doi: 10.1177/1091581813507721.

de Cássia da Silveira E Sá R, Andrade LN, Dos Reis Barreto de Oliveira R, de Sousa DP (2014) A review on anti-inflammatory activity of phenylpropanoids found in essential oils. Molecules. 19(2):1459-80. doi: 10.3390/molecules19021459.

de Vasconcelos MC, Bennett RN, Rosa EA, Ferreira-Cardoso JV (2010) Composition of European chestnut (*Castanea sativa* Mill.) and association with health effects: fresh and processed products. J Sci Food Agric. 90(10):1578-89.

Desborough MJR, Keeling DM (2017) The aspirin story - from willow to wonder drug. Br J Haematol. 177(5):674-683. doi: 10.1111/bjh.

Dodge HH, Zitzelberger T, Oken BS, Howieson D, Kaye J (2008) A randomized placebo-controlled trial of *Ginkgo biloba* for the prevention of cognitive decline. Neurology. 70(19 Pt 2):1809-17. doi: 10.1212/01.wnl.0000303814.13509.db.

Dragos D, Gilca M, Gaman L, Vlad A, Iosif L, Stoian I, Lupescu O (2017) Phytomedicine in Joint Disorders. Nutrients. 9(1). pii: E70. doi: 10.3390/nu9010070.

Drummond EM, Harbourne N, Marete E, Martyn D, Jacquier J, O'Riordan D, Gibney ER (2013) Inhibition of proinflammatory biomarkers in THP1 macrophages by polyphenols derived from chamomile, meadowsweet and willow bark. Phytother Res. 27(4):588-94. doi: 10.1002/ptr.4753.

Duderstadt RE, Fischer SM (2008) Effect of organic mobile phase composition on signal responses for selected polyalkene additive compounds by liquid chromatography-mass spectrometry. J Chromatogr A. 1193:70-78. doi: 10.1016/j.chroma.2008.03.086.

Durai P, Batool M, Choi S (2015) Structure and Effects of Cyanobacterial Lipopolysaccharides. Mar Drugs. 13(7):4217-30. doi: 10.3390/md13074217.

Ebrahimi H, Fallahi M, Khamaneh AM, Ebrahimi Saadatlou MA, Saadat S, Keyhanmanesh R (2016) Effect of α-Hederin on IL-2 and IL-17 mRNA and miRNA-133a Levels in Lungs of Ovalbumin-Sensitized Male Rats. Drug Dev Res. 77(2):87-93. doi: 10.1002/ddr.21292.

Ebrahimpour S, Fazeli M, Mehri S, Taherianfard M, Hosseinzadeh H (2017) Boswellic Acid Improves Cognitive Function in a Rat Model Through Its Antioxidant Activity: Neuroprotective effect of Boswellic acid. J Pharmacopuncture. 20(1):10-17. doi: 10.3831/KPI.2017.20.001.

Eidi A, Eidi M, Esmaeili E (2006) Antidiabetic effect of garlic (*Allium sativum* L.) in normal and streptozotocin-induced diabetic rats. Phytomedicine. 13(9-10):624-9.

El-Gabalawy H, Guenther LC, Bernstein CN (2010) Epidemiology of immune-mediated inflammatory diseases: incidence, prevalence, natural history, and comorbidities. J Rheumatol Suppl. 85:2-10. doi: 10.3899/jrheum.091461.

Elseweidy MM, Askar ME, Elswefy SE, Shawky M (2017) Vanillin as a new modulator candidate for renal injury induced by cisplatin in experimental rats. Cytokine. 99:260-265. doi: 10.1016/j.cyto.2017.07.025.

Engel K, Schmidt U, Reuter J, Weckesser S, Simon-Haarhaus B, Schempp CM (2007) *Usnea barbata* extract prevents ultraviolet-B induced prostaglandin E2 synthesis and COX-2 expression in HaCaT keratinocytes. J Photochem Photobiol B. 89(1):9-14.

Ernst E, Schmidt K (2005) Ukrain - a new cancer cure? A systematic review of randomised clinical trials. BMC Cancer. 5:69.

Esatbeyoglu T, Obermair B, Dorn T, Siems K, Rimbach G, Birringer M (2017) Sesquiterpene Lactone Composition and Cellular Nrf2 Induction of *Taraxacum officinale* Leaves and Roots and Taraxinic Acid β-d-Glucopyranosyl Ester. J Med Food. 20(1):71-78. doi: 10.1089/jmf.2016.0105.

Fakhrudin N, Dwi Astuti E, Sulistyawati R, Santosa D, Susandarini R, Nurrochmad A, Wahyuono S (2017) n-Hexane Insoluble Fraction of *Plantago lanceolata* Exerts Anti-Inflammatory Activity in Mice by Inhibiting Cyclooxygenase-2 and Reducing Chemokines Levels. Sci Pharm. 85(1). pii: E12. doi: 10.3390/scipharm85010012.

Farzaei MH, Abbasabadi Z, Ardekani MR, Rahimi R, Farzaei F (2013) Parsley: a review of ethnopharmacology, phytochemistry and biological activities. J Tradit Chin Med. 33(6):815-26.

Fawole OA, Amoo SO, Ndhlala AR, Light ME, Finnie JF, Van Staden J (2010) Anti-inflammatory, anticholinesterase, antioxidant and phytochemical properties of medicinal plants used for pain-related ailments in South Africa. J Ethnopharmacol. 127(2):235-41. doi: 10.1016/j.jep.2009.11.015.

Filippova EI (2017) Antiviral Activity of Lady's Mantle (Alchemilla vulgaris L.) Extracts against Orthopoxviruses. Bull Exp Biol Med. 163(3):374-377. doi: 10.1007/s10517-017-3807-x.

Fotland TØ, Paulsen JE, Sanner T, Alexander J, Husøy T (2012) Risk assessment of coumarin using the bench mark dose (BMD) approach: children in Norway which regularly eat oatmeal porridge with cinnamon may exceed the TDI for coumarin with several folds. Food Chem Toxicol. 50(3-4):903-12. doi: 10.1016/j.fct.2011.12.005.

Franciškoviċ M, Gonzalez-Pérez R, Orčić D, Sánchez de Medina F, Martínez-Augustin O, Svirčev E, Simin N, Mimica-Dukić N (2017) Chemical Composition and Immuno-Modulatory Effects of *Urtica dioica* L. (Stinging Nettle) Extracts. Phytother Res. 31(8):1183-1191. doi: 10.1002/ptr.5836.

Fraternale A, Brundu S and Magnani M (2015) Polarization and Repolarization of Macrophages. J Clin Cell Immunol. 6: 319. doi: 10.4172/2155-9899.1000319.

Freires IA, Alves LA, Ferreira GL, Jovito Vde C, de Castro RD, Cavalcanti AL (2013) A Randomized Clinical Trial of *Schinus terebinthifolius* Mouthwash to Treat Biofilm-Induced Gingivitis. Evid Based Complement Alternat Med. 2013:873907. doi: 10.1155/2013/873907.

Fu W, Chen L, Wang Z, Zhao C, Chen G, Liu X, Dai Y, Cai Y, Li C, Zhou J, Liang G (2016) Determination of the binding mode for anti-inflammatory natural product xanthohumol with myeloid differentiation protein 2. Drug Des Devel Ther. 10:455-63. doi: 10.2147/DDDT.S98466.

Fujioka S, Niu J, Schmidt C, Sclabas GM, Peng B, Uwagawa T, Li Z, Evans DB, Abbruzzese JL, Chiao PJ (2004) NF-kappaB and AP-1 connection: mechanism of NF-kappaB-dependent regulation of AP-1 activity. Mol Cell Biol. 24(17):7806-19.

Fujisawa S, Murakami Y (2016) Eugenol and Its Role in Chronic Diseases. Adv Exp Med Biol. 929:45-66.

Gagnier JJ, Chrubasik S, Manheimer E (2004) *Harpgophytum procumbens* for osteoarthritis and low back pain: a systematic review. BMC Complement Altern Med. 4:13.

Gagnier JJ, Oltean H, van Tulder MW, Berman BM, Bombardier C, Robbins CB (2016) Herbal Medicine for Low Back Pain: A Cochrane Review. Spine (Phila Pa 1976). 41(2):116-33. doi: 10.1097/BRS.0000000000001310.

Games E, Guerreiro M, Santana FR, Pinheiro NM, de Oliveira EA, Lopes FD, Olivo CR, Tibério IF, Martins MA, Lago JH, Prado CM (2016) Structurally Related Monoterpenes *p*-Cymene, Carvacrol and Thymol Isolated from Essential Oil from Leaves of *Lippia sidoides* Cham. (*Verbenaceae*) Protect Mice against Elastase-Induced Emphysema. Molecules. 21(10).

Gayathri B, Manjula N, Vinaykumar KS, Lakshmi BS, Balakrishnan A (2007) Pure compound from *Boswellia serrata* extract exhibits anti-inflammatory property in human PBMCs and

mouse macrophages through inhibition of TNFalpha, IL-1beta, NO and MAP kinases. Int Immunopharmacol. 7(4):473-82.

Genin M, Clement F, Fattaccioli A, Raes M, Michiels C (2015) M1 and M2 macrophages derived from THP-1 cells differentially modulate the response of cancer cells to etoposide. BMC Cancer. 15:577. doi: 10.1186/s12885-015-1546-9.

Gerhäuser C (2005) Beer constituents as potential cancer chemopreventive agents. Eur J Cancer. 41(13):1941-54.

Ghorbani A, Esmaeilizadeh M (2017) Pharmacological properties of *Salvia officinalis* and its components. J Tradit Complement Med. 7(4):433-440. doi: 10.1016/j.jtcme.2016.12.014.

Ghosh S, Dass JF (2016) Study of pathway cross-talk interactions with NF-κB leading to its activation via ubiquitination or phosphorylation: A brief review. Gene. 584(1):97-109. doi: 10.1016/j.gene.2016.03.008.

Giaginis C, Giagini A, Theocharis S (2009) Peroxisome proliferator-activated receptor-gamma (PPAR-gamma) ligands as potential therapeutic agents to treat arthritis. Pharmacol Res. 60(3):160-9. doi: 10.1016/j.phrs.2009.02.005.

Giannetti BM, Staiger C, Bulitta M, Predel HG (2010) Efficacy and safety of comfrey root extract ointment in the treatment of acute upper or lower back pain: results of a double-blind, randomised, placebo controlled, multicentre trial. Br J Sports Med. 44(9):637-41. doi: 10.1136/bjsm.2009.058677.

Goel A, Kunnumakkara AB, Aggarwal BB (2008) Curcumin as "Curecumin": from kitchen to clinic. Biochem Pharmacol. 75(4):787-809.

Growther JR (2002). In Walker JM (ed) The ELISA Guidebook, 2nd edition. Human Press, New York, pp. 16-21.

Gründemann C, Lengen K, Sauer B, Garcia-Käufer M, Zehl M, Huber R (2014) *Equisetum arvense* (common horsetail) modulates the function of inflammatory immunocompetent cells. BMC Complement Altern Med. 14:283. doi: 10.1186/1472-6882-14-283.

Gunawardena D, Govindaraghavan S, Münch G (2014) Anti-inflammatory properties of cinnamon polyphenols and their monomeric precursors. In: Watson RR, Preedy VR, Zibadi S (ed) Polyphenols in Human Health and Disease, volume 1. Elsevier, Amsterdam, Boston, Heidelberg, London, New York, Oxford, Paris, San Diego, San Francisco, Singapore, Sydney, Tokyo, pp. 30:409-425.

Gunawardena D, Karunaweera N, Lee S, van Der Kooy F, Harman DG, Raju R, Bennett L, Gyengesi E, Sucher NJ, Münch G (2015) Anti-inflammatory activity of cinnamon (*C. zeylanicum* and *C. cassia*) extracts–identification of E-cinnamaldehyde and *o*-methoxy cinnamaldehyde as the most potent bioactive compounds. Food Funct. 6(3):910-9. doi: 10.1039/c4fo00680a.

Habtemariam S (2002) Hamamelitannin from Hamamelis virginiana inhibits the tumour necrosis factor-alpha (TNF)-induced endothelial cell death in vitro. Toxicon. 40(1):83-8.

Hagenlocher Y, Bergheim I, Zacheja S, Schäffer M, Bischoff SC, Lorentz A (2013) Cinnamon extract inhibits degranulation and de novo synthesis of inflammatory mediators in mast cells. Allergy. 68(4):490-7. doi: 10.1111/all.12122.

Hagenlocher Y, Hösel A, Bischoff SC, Lorentz A (2016) Cinnamon extract reduces symptoms, inflammatory mediators and mast cell markers in murine IL-10(-/-) colitis. J Nutr Biochem. 30:85-92. doi: 10.1016/j.jnutbio.2015.11.015.

Hagenlocher Y, Kiessling K, Schäffer M, Bischoff SC, Lorentz A (2015) Cinnamaldehyde is the main mediator of cinnamon extract in mast cell inhibition. Eur J Nutr. 54(8):1297-309. doi: 10.1007/s00394-014-0810-0.

Hagenlocher Y, Satzinger S, Civelek M, Feilhauer K, Köninger J, Bischoff SC, Lorentz A (2017) Cinnamon reduces inflammatory response in intestinal fibroblasts *in vitro* and in colitis *in vivo* leading to decreased fibrosis. Mol Nutr Food Res. 61(9). doi: 10.1002/mnfr.201601085.

Han G, Xia J, Gao J, Inagaki Y, Tang W, Kokudo N (2015) Anti-tumor effects and cellular mechanisms of resveratrol. Drug Discov Ther. 9(1):1-12. doi: 10.5582/ddt.2015.01007.

Han SS, Keum YS, Seo HJ, Chun KS, Lee SS, Surh YJ (2001) Capsaicin suppresses phorbol ester-induced activation of NF-kappaB/Rel and AP-1 transcription factors in mouse epidermis. Cancer Lett. 164(2):119-26.

Hariri M, Ghiasvand R (2016) Cinnamon and Chronic Diseases. Adv Exp Med Biol. 929:1-24.

Hauptman PJ, Kelly RA (1999) Digitalis. Circulation. 99(9):1265-70.

Herranz-López M, Olivares-Vicente M, Encinar JA, Barrajón-Catalán E, Segura-Carretero A, Joven J, Micol V (2017) Multi-Targeted Molecular Effects of *Hibiscus sabdariffa* Polyphenols: An Opportunity for a Global Approach to Obesity. Nutrients. 9(8). pii: E907. doi: 10.3390/nu9080907.

Herz C, Tran HT, Márton MR, Maul R, Baldermann S, Schreiner M, Lamy E (2017) Evaluation of an Aqueous Extract from Horseradish Root (*Armoracia rusticana* Radix) against Lipopolysaccharide-Induced Cellular Inflammation Reaction. Evid Based Complement Alternat Med. 2017:1950692. doi: 10.1155/2017/1950692.

Ho SC, Chang KS, Chang PW (2013) Inhibition of neuroinflammation by cinnamon and its main components. Food Chem. 138(4):2275-82. doi: 10.1016/j.foodchem.2012.12.020.

Hong JW, Yang GE, Kim YB, Eom SH, Lew JH, Kang H (2012) Anti-inflammatory activity of cinnamon water extract *in vivo* and *in vitro* LPS-induced models. BMC Complement Altern Med. 12:237. doi: 10.1186/1472-6882-12-237.

Hosni AA, Abdel-Moneim AA, Abdel-Reheim ES, Mohamed SM, Helmy H (2017) Cinnamaldehyde potentially attenuates gestational hyperglycemia in rats through modulation of PPARγ, proinflammatory cytokines and oxidative stress. Biomed Pharmacother. 88:52-60. doi: 10.1016/j.biopha.2017.01.054.

Huang N, Rizshsky L, Hauck CC, Nikolau BJ, Murphy PA, Birt DF (2012) The inhibition of lipopolysaccharide-induced macrophage inflammation by 4 compounds in *Hypericum perforatum* extract is partially dependent on the activation of SOCS3. Phytochemistry. 76:106-16. doi: 10.1016/j.phytochem.2011.12.001.

Hughes-Formella BJ, Bohnsack K, Rippke F, Benner G, Rudolph M, Tausch I, Gassmueller J (1998) Anti-inflammatory effect of hamamelis lotion in a UVB erythema test. Dermatology. 196(3):316-22.

Hurtado Fernández E (2014) Avocado (Persica Americana): complementarity of different omics technologies for its metabolic characterization. Dissertation, University of Granada.

InvivoGen (2016) Product Datasheet HEK-Blue™ hTLR4 Cells from website http://www.invivogen.com/hek-blue-htlr4 (30.12.2016).

Itoh T, Tsuchida A, Muramatsu Y, Ninomiya M, Ando M, Tsukamasa Y, Koketsu M (2014) Antimicrobial and anti-inflammatory properties of nostocionone isolated from *Nostoc commune* Vauch and its derivatives against *Propionibacterium acnes*. Anaerobe. 27:56-63. doi: 10.1016/j.anaerobe.2014.03.006.

Janeczko M, Masłyk M, Kubiński K, Golczyk H (2017) Emodin, a natural inhibitor of protein kinase CK2, suppresses growth, hyphal development, and biofilm formation of *Candida albicans*. Yeast. 34(6):253-265. doi: 10.1002/yea.3230.

Jayaprakasha GK, Jagan Mohan Rao L, Sakariah KK (2000) Chemical composition of the flower oil of *Cinnamomum zeylanicum* blume. J Agric Food Chem. 48(9):4294-5.

Jayaprakasha GK, Jagan Mohan Rao L, Sakariah KK (2003) Volatile constituents from *Cinnamomum zeylanicum* fruit stalks and their antioxidant activities. J Agric Food Chem. 51(15):4344-8.

Jayaprakasha GK, Rao LJ (2011) Chemistry, biogenesis, and biological activities of *Cinnamomum zeylanicum*. Crit Rev Food Sci Nutr. 51(6):547-62. doi: 10.1080/10408391003699550.

Jiang J, Emont MP, Jun H, Qiao X, Liao J, Kim DI, Wu J (2017a) Cinnamaldehyde induces fat cell-autonomous thermogenesis and metabolic reprogramming. Metabolism. 77:58-64. doi: 10.1016/j.metabol.2017.08.006.

Jiang K, Ma X, Guo S, Zhang T, Zhao G, Wu H, Wang X, Deng G (2017b) Anti-inflammatory Effects of Rosmarinic Acid in Lipopolysaccharide-Induced Mastitis in Mice. Inflammation. 41(2):437-448. doi: 10.1007/s10753-017-0700-8.

Joe B, Vijaykumar M, Lokesh BR (2004) Biological properties of curcumin-cellular and molecular mechanisms of action. Crit Rev Food Sci Nutr. 44(2):97-111.

Jovanović JA, Mihailović M, Uskoković AS, Grdović N, Dinić S, Poznanović G, Mujić I, Vidaković M (2017) Evaluation of the Antioxidant and Antiglycation Effects of *Lactarius deterrimus* and *Castanea sativa* Extracts on Hepatorenal Injury in Streptozotocin-Induced Diabetic Rats. Front Pharmacol. 8:793. doi: 10.3389/fphar.2017.00793.

Jung SA, Choi M, Kim S, Yu R, Park T (2012) Cinchonine Prevents High-Fat-Diet-Induced Obesity through Downregulation of Adipogenesis and Adipose Inflammation. PPAR Res. 2012:541204.

Junker Y, Zeissig S, Kim SJ, Barisani D, Wieser H, Leffler DA, Zevallos V, Libermann TA, Dillon S, Freitag TL, Kelly CP, Schuppan D (2012) Wheat amylase trypsin inhibitors drive intestinal inflammation via activation of toll-like receptor 4. J Exp Med. 209(13):2395-408. doi: 10.1084/jem.20102660.

Ka SM, Kuoping Chao L, Lin JC, Chen ST, Li WT, Lin CN, Cheng JC, Jheng HL, Chen A, Hua KF (2016) A low toxicity synthetic cinnamaldehyde derivative ameliorates renal inflammation in mice by inhibiting NLRP3 inflammasome and its related signaling pathways. Free Radic Biol Med. 2016 91:10-24. doi: 10.1016/j.freeradbiomed.2015.12.003.

Kang S, Min H (2012) Ginseng, the 'Immunity Boost': The Effects of *Panax ginseng* on Immune System. J Ginseng Res. 36(4):354-68. doi: 10.5142/jgr.2012.36.4.354.

Kanuri G, Weber S, Volynets V, Spruss A, Bischoff SC, Bergheim I (2009) Cinnamon extract protects against acute alcohol-induced liver steatosis in mice. J Nutr. 139(3):482-7. doi: 10.3945/jn.108.100495.

Kapuścik A, Hrouzek P, Kuzma M, Bártová S, Novák P, Jokela J, Pflüger M, Eger A, Hundsberger H, Kopecký J (2013) Novel Aeruginosin-865 from *Nostoc* sp. as a potent anti-inflammatory agent. Chembiochem. 14(17):2329-37. doi: 10.1002/cbic.201300246.

Karabin M, Hudcova T, Jelinek L, Dostalek P (2015) Biotransformations and biological activities of hop flavonoids. Biotechnol Adv. 33(6 Pt 2):1063-90. doi: 10.1016/j.biotechadv.2015.02.009.

Karlsen A, Paur I, Bøhn SK, Sakhi AK, Borge GI, Serafini M, Erlund I, Laake P, Tonstad S, Blomhoff R (2010) Bilberry juice modulates plasma concentration of NF-kappaB related inflammatory markers in subjects at increased risk of CVD. Eur J Nutr. 49(6):345-55. doi: 10.1007/s00394-010-0092-0.

Kasper S, Caraci F, Forti B, Drago F, Aguglia E (2010) Efficacy and tolerability of *Hypericum* extract for the treatment of mild to moderate depression. Eur Neuropsychopharmacol. 20(11):747-65. doi: 10.1016/j.euroneuro.2010.07.005.

Katanić J, Boroja T, Mihailović V, Nikles S, Pan SP, Rosić G, Selaković D, Joksimović J, Mitrović S, Bauer R (2016) *In vitro* and *in vivo* assessment of meadowsweet (*Filipendula ulmaria*) as anti-inflammatory agent. J Ethnopharmacol. 193:627-636. doi: 10.1016/j.jep.2016.10.015.

Kazemipoor M, Radzi CW, Hajifaraji M, Haerian BS, Mosaddegh MH, Cordell GA (2013) Antiobesity effect of caraway extract on overweight and obese women: a randomized, triple-blind, placebo-controlled clinical trial. Evid Based Complement Alternat Med. 2013:928582. doi: 10.1155/2013/928582.

Kesavan R, Potunuru UR, Nastasijević B, T A, Joksić G, Dixit M (2013) Inhibition of vascular smooth muscle cell proliferation by *Gentiana lutea* root extracts. PLoS One. 8(4):e61393. doi: 10.1371/journal.pone.0061393.

Khafaga AF, El-Sayed YS (2018) Spirulina ameliorates methotrexate hepatotoxicity via antioxidant, immune stimulation, and proinflammatory cytokines and apoptotic proteins modulation. Life Sci. 196:9-17. doi: 10.1016/j.lfs.2018.01.010.

Khan A, Safdar M, Ali Khan MM, Khattak KN, Anderson RA (2003) Cinnamon improves glucose and lipids of people with type 2 diabetes. Diabetes Care. 26(12):3215-8.

Khuwijitjaru P, Sayputikasikorn N, Samuhasaneetoo S, Penroj P, Siriwongwilaichat P, Adachi S (2012) Subcritical water extraction of flavoring and phenolic compounds from cinnamon bark (*Cinnamomum zeylanicum*). J Oleo Sci. 61(6):349-55.

Kienle GS, Kiene H (2010) Review article: Influence of *Viscum album* L (European mistletoe) extracts on quality of life in cancer patients: a systematic review of controlled clinical studies. Integr Cancer Ther. 9(2):142-57. doi: 10.1177/1534735410369673.

Kim DH, Kim CH, Kim MS, Kim JY, Jung KJ, Chung JH, An WG, Lee JW, Yu BP, Chung HY (2007) Suppression of age-related inflammatory NF-κB activation by cinnamaldehyde. Biogerontology. 8(5):545-54.

Kim KM, Lee JY, Im AR, Chae S (2018) Phycocyanin Protects Against UVB-induced Apoptosis Through the PKC α/βII-Nrf-2/HO-1 Dependent Pathway in Human Primary Skin Cells. Molecules. 23(2). pii: E478. doi: 10.3390/molecules23020478.

Kirichenko TV, Sobenin IA, Nikolic D, Rizzo M, Orekhov AN (2016) Anti-cytokine therapy for prevention of atherosclerosis. Phytomedicine. 23(11):1198-210. doi: 10.1016/j.phymed.2015.12.002.

Kiselova Y, Ivanova D, Chervenkov T, Gerova D, Galunska B, Yankova T (2006) Correlation between the *in vitro* antioxidant activity and polyphenol content of aqueous extracts from Bulgarian herbs. Phytother Res. 20(11):961-5.

Knobloch J, Chikosi SJ, Yanik S, Rupp J, Jungck D, Koch A (2016) A systemic defect in Toll-like receptor 4 signaling increases lipopolysaccharide-induced suppression of IL-2-dependent T-cell proliferation in COPD. Am J Physiol Lung Cell Mol Physiol. 310(1):L24-39. doi: 10.1152/ajplung.00367.2014.

Kolac UK, Ustuner MC, Tekin N, Ustuner D, Colak E, Entok E (2017) The Anti-Inflammatory and Antioxidant Effects of *Salvia officinalis* on Lipopolysaccharide-Induced Inflammation in Rats. J Med Food. 20(12):1193-1200. doi: 10.1089/jmf.2017.0035.

Kolehmainen M, Mykkänen O, Kirjavainen PV, Leppänen T, Moilanen E, Adriaens M, Laaksonen DE, Hallikainen M, Puupponen-Pimiä R, Pulkkinen L, Mykkänen H, Gylling H, Poutanen K, Törrönen R (2012) Bilberries reduce low-grade inflammation in individuals with features of metabolic syndrome. Mol Nutr Food Res. 56(10):1501-10. doi: 10.1002/mnfr.201200195.

Koll R, Buhr M, Dieter R, Pabst H, Predel HG, Petrowicz O, Giannetti B, Klingenburg S, Staiger C (2004) Efficacy and tolerance of a comfrey root extract (Extr. *Rad. Symphyti*) in the treatment of ankle distorsions: results of a multicenter, randomized, placebo-controlled, double-blind study. Phytomedicine. 11(6):470-7.

Krebs S, Omer TN, Omer B (2010) Wormwood (*Artemisia absinthium*) suppresses tumour necrosis factor alpha and accelerates healing in patients with Crohn's disease - A controlled clinical trial. Phytomedicine. 17(5):305-9. doi: 10.1016/j.phymed.2009.10.013.

Ku CS, Pham TX, Park Y, Kim B, Shin MS, Kang I, Lee J (2013) Edible blue-green algae reduce the production of pro-inflammatory cytokines by inhibiting NF-κB pathway in macrophages and splenocytes. Biochim Biophys Acta. 1830(4):2981-8. doi: 10.1016/j.bbagen.2013.01.018.

Kuo CL, Chi CW, Liu TY (2004) The anti-inflammatory potential of berberine *in vitro* and *in vivo*. Cancer Lett. 203(2):127-37.

Lang-Yona N, Kunert AT, Vogel L, Kampf CJ, Bellinghausen I, Saloga J, Schink A, Ziegler K, Lucas K, Schuppan D, Pöschl U, Weber B, Fröhlich-Nowoisky J (2018) Fresh water, marine and terrestrial cyanobacteria display distinct allergen characteristics. Sci Total Environ. 612:767-774. doi: 10.1016/j.scitotenv.2017.08.069.

Lass C, Vocanson M, Wagner S, Schempp CM, Nicolas JF, Merfort I, Martin SF (2008) Anti-inflammatory and immune-regulatory mechanisms prevent contact hypersensitivity to *Arnica montana* L. Exp Dermatol. 17(10):849-57. doi: 10.1111/j.1600-0625.2008.00717.x.

Lee HG, Kim H, Oh WK, Yu KA, Choe YK, Ahn JS, Kim DS, Kim SH, Dinarello CA, Kim K, Yoon DY (2004) Tetramethoxy hydroxyflavone p7F downregulates inflammatory mediators via the inhibition of nuclear factor kappaB. Ann N Y Acad Sci. 1030:555-68.

Lee HJ, Kim KW (2012) Anti-inflammatory effects of arbutin in lipopolysaccharide-stimulated BV2 microglial cells. Inflamm Res. 61(8):817-25. doi: 10.1007/s00011-012-0474-2.

Lee HS, Kang P, Kim KY, Seol GH (2015) *Foeniculum vulgare* Mill. Protects against Lipopolysaccharide-induced Acute Lung Injury in Mice through ERK-dependent NF-κB Activation. Korean J Physiol Pharmacol. 19(2):183-9. doi: 10.4196/kjpp.2015.19.2.183.

Lee IS, Lim J, Gal J, Kang JC, Kim HJ, Kang BY, Choi HJ (2011) Anti-inflammatory activity of xanthohumol involves heme oxygenase-1 induction via NRF2-ARE signaling in microglial BV2 cells. Neurochem Int. 58(2):153-60. doi: 10.1016/j.neuint.2010.11.008.

Lee JK, Kim NJ (2017) Recent Advances in the Inhibition of p38 MAPK as a Potential Strategy for the Treatment of Alzheimer's Disease. Molecules. 22(8). pii: E1287. doi: 10.3390/molecules22081287.

Lemhadri A, Hajji L, Michel JB, Eddouks M (2006) Cholesterol and triglycerides lowering activities of caraway fruits in normal and streptozotocin diabetic rats. J Ethnopharmacol. 106(3):321-6.

LGC Standards (2016) Product Information THP-1 (ATCC TIB-202) from website http://www.lgcstandards-atcc.org/products/all/TIB-202.aspx?geo_country=de#generalinformation (26.01.2018).

Li B, Hu Y, Zhao Y, Cheng M, Qin H, Cheng T, Wang Q, Peng X, Zhang X (2017) Curcumin Attenuates Titanium Particle-Induced Inflammation by Regulating Macrophage Polarization *In Vitro* and *In Vivo*. Front Immunol. 8:55. doi: 10.3389/fimmu.2017.00055.

Li J, Liu T, Wang L, Guo X, Xu T, Wu L, Qin L, Sun W (2012) Antihyperglycemic and antihyperlipidemic action of cinnamaldehyde in C57BLKS/J db/db mice. J Tradit Chin Med. 32(3):446-52.

Liao JC, Deng JS, Chiu CS, Hou WC, Huang SS, Shie PH, Huang GJ (2012) Anti-Inflammatory Activities of *Cinnamomum cassia* Constituents *In Vitro* and *In Vivo*. Evid Based Complement Alternat Med. 2012:429320. doi: 10.1155/2012/429320.

Lim JD, Lee SR, Kim T, Jang SA, Kang SC, Koo HJ, Sohn E, Bak JP, Namkoong S, Kim HK, Song IS, Kim N, Sohn EH, Han J (2015) Fucoidan from *Fucus vesiculosus* protects against alcohol-induced liver damage by modulating inflammatory mediators in mice and HepG2 cells. Mar Drugs. 13(2):1051-67. doi: 10.3390/md13021051.

Lin CJ, Lin HJ, Chen TH, Hsu YA, Liu CS, Hwang GY, Wan L (2015) *Polygonum cuspidatum* and its active components inhibit replication of the influenza virus through toll-like receptor 9-induced interferon beta expression. PLoS One. 10(2):e0117602. doi: 10.1371/journal.pone.0117602.

Liu Q, Manzano D, Tanić N, Pesic M, Bankovic J, Pateraki I, Ricard L, Ferrer A, de Vos R, van de Krol S, Bouwmeester H (2014) Elucidation and in planta reconstitution of the parthenolide biosynthetic pathway. Metab Eng. 23:145-53. doi: 10.1016/j.ymben.2014.03.005.

Liu Y, Yan F, Liu Y, Zhang C, Yu H, Zhang Y, Zhao Y (2008) Aqueous extract of rhubarb stabilizes vulnerable atherosclerotic plaques due to depression of inflammation and lipid accumulation. Phytother Res. 22(7):935-42. doi: 10.1002/ptr.2429.

Liu YT, Gong PH, Xiao FQ, Shao S, Zhao DQ, Yan MM, Yang XW (2018) Chemical Constituents and Antioxidant, Anti-Inflammatory and Anti-Tumor Activities of *Melilotus officinalis* (Linn.) Pall. Molecules. 23(2). pii: E271. doi: 10.3390/molecules23020271.

Lü L, Zhang L, Wai MS, Yew DT, Xu J (2012) Exocytosis of MTT formazan could exacerbate cell injury. Toxicol In Vitro. 26(4):636-44. doi: 10.1016/j.tiv.2012.02.006.

Lucas K, Maes M (2013) Role of the Toll Like receptor (TLR) radical cycle in chronic inflammation: possible treatments targeting the TLR4 pathway. Mol Neurobiol. 48(1):190-204. doi: 10.1007/s12035-013-8425-7.

Luo H, Lv XD, Wang GE, Li YF, Kurihara H, He RR (2014) Anti-inflammatory effects of anthocyanins-rich extract from bilberry (*Vaccinium myrtillus* L.) on croton oil-induced ear edema and *Propionibacterium acnes* plus LPS-induced liver damage in mice. Int J Food Sci Nutr. 65(5):594-601. doi: 10.3109/09637486.2014.886184.

Lupinacci E, Meijerink J, Vincken JP, Gabriele B, Gruppen H, Witkamp RF (2009) Xanthohumol from hop (*Humulus lupulus* L.) is an efficient inhibitor of monocyte chemoattractant protein-1 and tumor necrosis factor-alpha release in LPS-stimulated RAW 264.7 mouse macrophages and U937 human monocytes. J Agric Food Chem. 57(16):7274-81. doi: 10.1021/jf901244k.

Macagno A, Molteni M, Rinaldi A, Bertoni F, Lanzavecchia A, Rossetti C, Sallusto F (2006) A cyanobacterial LPS antagonist prevents endotoxin shock and blocks sustained TLR4 stimulation required for cytokine expression. J Exp Med. 203(6):1481-92.

Madeira A, Burgelin I, Perron H, Curtin F, Lang AB, Faucard R (2016) MSRV envelope protein is a potent, endogenous and pathogenic agonist of human toll-like receptor 4: Relevance of GNbAC1 in multiple sclerosis treatment. J Neuroimmunol. 291:29-38. doi: 10.1016/j.jneuroim.2015.12.006.

Magni P, Ruscica M, Dozio E, Rizzi E, Beretta G, Maffei Facino R (2012) Parthenolide inhibits the LPS-induced secretion of IL-6 and TNF-α and NF-κB nuclear translocation in BV-2 microglia. Phytother Res. 26(9):1405-9. doi: 10.1002/ptr.3732.

Marzocco S, Calabrone L, Adesso S, Larocca M, Franceschelli S, Autore G, Martelli G, Rossano R (2015) Anti-inflammatory activity of horseradish (*Armoracia rusticana*) root extracts in LPS-stimulated macrophages. Food Funct. 6(12):3778-88. doi: 10.1039/c5fo00475f.

Mazor RL, Menendez IY, Ryan MA, Fiedler MA, Wong HR (2000) Sesquiterpene lactones are potent inhibitors of interleukin 8 gene expression in cultured human respiratory epithelium. Cytokine. 12(3):239-45.

McAlees JW, Whitehead GS, Harley IT, Cappelletti M, Rewerts CL, Holdcroft AM, Divanovic S, Wills-Karp M, Finkelman FD, Karp CL, Cook DN (2015) Distinct Tlr4-expressing cell compartments control neutrophilic and eosinophilic airway inflammation. Mucosal Immunol. 8(4):863-73. doi: 10.1038/mi.2014.117.

Meng G, Liu Y, Lou C, Yang H (2010) Emodin suppresses lipopolysaccharide-induced pro-inflammatory responses and NF-κB activation by disrupting lipid rafts in CD14-negative endothelial cells. Br J Pharmacol. 161(7):1628-44. doi: 10.1111/j.1476-5381.2010.00993.x.

Merck (2018a) Product Datasheet Cell Proliferation Kit I (MTT) from website https://www.sigmaaldrich.com/catalog/product/roche/11465007001?lang=de&region=DE (26.01.2018).

Merck (2018b) Product Datasheet Cell Counting Kit – 8 from website https://www.sigmaaldrich.com/catalog/product/sigma/96992?lang=de&region=DE (26.01.2018).

Meyre-Silva C, Yunes RA, Schlemper V, Campos-Buzzi F, Cechinel-Filho V (2005) Analgesic potential of marrubiin derivatives, a bioactive diterpene present in *Marrubium vulgare* (Lamiaceae). Farmaco. 60(4):321-6.

Mix JA, Crews WD Jr (2002) A double-blind, placebo-controlled, randomized trial of *Ginkgo biloba* extract EGb 761 in a sample of cognitively intact older adults: neuropsychological findings. Hum Psychopharmacol. 17(6):267-77.

Mohd Yusof YA (2016) Gingerol and Its Role in Chronic Diseases. Adv Exp Med Biol. 929:177-207.

Momin RA, De Witt DL, Nair MG (2003) Inhibition of cyclooxygenase (COX) enzymes by compounds from *Daucus carota* L. Seeds. Phytother Res. 17(8):976-9.

Mondal S, Pahan K (2015) Cinnamon ameliorates experimental allergic encephalomyelitis in mice via regulatory T cells: implications for multiple sclerosis therapy. PLoS One. 10(1):e0116566. doi: 10.1371/journal.pone.0116566.

Mroueh M, Saab Y, Rizkallah R (2004) Hepatoprotective activity of *Centaurium erythraea* on acetaminophen-induced hepatotoxicity in rats. Phytother Res. 18(5):431-3.

Murai M, Tamayama Y, Nishibe S (1995) Phenylethanoids in the herb of *Plantago lanceolata* and inhibitory effect on arachidonic acid-induced mouse ear edema. Planta Med. 61(5):479-80.

Murphy RC (2015) Fatty acids, Tandem Mass Spectrometry of Lipids: Molecular Analysis of Complex Lipids. In Murphy RC (ed) New Development in Mass Spectrometry. Tandem Mass Spectrometry of Lipids, No. 4. Royal Society of Chemistry, Cambridge pp. 1:1-39.

Nahrstedt A, Schmidt M, Jäggi R, Metz J, Khayyal MT (2007) Willow bark extract: the contribution of polyphenols to the overall effect. Wien Med Wochenschr. 157(13-14):348-51.

Najafi S, Koujan SE, Manifar S, Kharazifard MJ, Kidi S, Hajheidary S (2017) Preventive Effect of *Glycyrrhiza Glabra* Extract on Oral Mucositis in Patients Under Head and Neck Radiotherapy: A Randomized Clinical Trial. J Dent (Tehran). 14(5):267-274.

Nakano S, Takekoshi H, Nakano M (2007) Chlorella (*Chlorella pyrenoidosa*) supplementation decreases dioxin and increases immunoglobulin a concentrations in breast milk. J Med Food. 10(1):134-42.

Nakano S, Takekoshi H, Nakano M (2010) *Chlorella pyrenoidosa* supplementation reduces the risk of anemia, proteinuria and edema in pregnant women. Plant Foods Hum Nutr. 65(1):25-30. doi: 10.1007/s11130-009-0145-9.

Nam SM, Choi JH, Yoo DY, Kim W, Jung HY, Kim JW, Kang SY, Park J, Kim DW, Kim WJ, Yoon YS, Hwang IK (2013) *Valeriana officinalis* extract and its main component, valerenic acid, ameliorate D-galactose-induced reductions in memory, cell proliferation, and neuroblast differentiation by reducing corticosterone levels and lipid peroxidation. Exp Gerontol. 48(11):1369-77. doi: 10.1016/j.exger.2013.09.002.

Nastasijević B, Lazarević-Pašti T, Dimitrijević-Branković S, Pašti I, Vujačić A, Joksić G, Vasić V (2012) Inhibition of myeloperoxidase and antioxidative activity of *Gentiana lutea* extracts. J Pharm Biomed Anal. 66:191-6. doi: 10.1016/j.jpba.2012.03.052.

Ng SC, Shi HY, Hamidi N, Underwood FE, Tang W, Benchimol EI, Panaccione R, Ghosh S, Wu JCY, Chan FKL, Sung JJY, Kaplan GG (2018) Worldwide incidence and prevalence of inflammatory bowel disease in the 21st century: a systematic review of population-based studies. Lancet. 390(10114):2769-2778. doi: 10.1016/S0140-6736(17)32448-0.

Nhiem NX, Kiem PV, Minh CV, Kim N, Park S, Lee HY, Kim ES, Kim YH, Kim S, Koh YS, Kim SH (2013) Diarylheptanoids and flavonoids from *viscum album* inhibit LPS-stimulated

production of pro-inflammatory cytokines in bone marrow-derived dendritic cells. J Nat Prod. 76(4):495-502. doi: 10.1021/np300490v.

Nielsen SE, Young JF, Daneshvar B, Lauridsen ST, Knuthsen P, Sandström B, Dragsted LO (1999) Effect of parsley (*Petroselinum crispum*) intake on urinary apigenin excretion, blood antioxidant enzymes and biomarkers for oxidative stress in human subjects. Br J Nutr. 81(6):447-55.

Novus Biologicals (2018) Product Datasheet TLR4 Reporter Cell Line NBP2-26263 from website http://www.novusbio.com/TLR4-Reporter-Cell-Line_NBP2-26263.html (26.01.2018).

Oblak A, Pohar J, Jerala R (2015) MD-2 determinants of nickel and cobalt-mediated activation of human TLR4. PLoS One. 10(3):e0120583. doi: 10.1371/journal.pone.0120583.

Okombo J, Ohuma E, Picot S, Nzila A (2011) Update on genetic markers of quinine resistance in *Plasmodium falciparum*. Mol Biochem Parasitol. 177(2):77-82. doi: 10.1016/j.molbiopara.2011.01.012.

Oliveira JR, de Jesus Viegas D, Martins APR, Carvalho CAT, Soares CP, Camargo SEA, Jorge AOC, de Oliveira LD (2017) *Thymus vulgaris* L. extract has antimicrobial and anti-inflammatory effects in the absence of cytotoxicity and genotoxicity. Arch Oral Biol. 82:271-279. doi: 10.1016/j.archoralbio.2017.06.031.

Omer B, Krebs S, Omer H, Noor TO (2007) Steroid-sparing effect of wormwood (*Artemisia absinthium*) in Crohn's disease: a double-blind placebo-controlled study. Phytomedicine. 14(2-3):87-95.

Paduch R, Woźniak A, Niedziela P, Rejdak R (2014) Assessment of eyebright (*euphrasia officinalis* L.) extract activity in relation to human corneal cells using *in vitro* tests. Balkan Med J. 31(1):29-36. doi: 10.5152/balkanmedj.2014.8377.

Pari L, Tewas D, Eckel J (2008) Role of curcumin in health and disease. Arch Physiol Biochem. 114(2):127-49. doi: 10.1080/13813450802033958.

Park JE, Cuong TD, Hung TM, Lee I, Na M, Kim JC, Ryoo S, Lee JH, Choi JS, Woo MH, Min BS (2011) Alkaloids from *Chelidonium majus* and their inhibitory effects on LPS-induced NO production in RAW264.7 cells. Bioorg Med Chem Lett. 21(23):6960-3. doi: 10.1016/j.bmcl.2011.09.128.

Park SJ, Lee MY, Son BS, Youn HS (2009) TBK1-targeted suppression of TRIF-dependent signaling pathway of Toll-like receptors by 6-shogaol, an active component of ginger. Biosci Biotechnol Biochem. 73(7):1474-1478.

Park SJ, Youn HS (2010) Suppression of homodimerization of toll-like receptor 4 by isoliquiritigenin. Phytochemistry. 71(14-15):1736-40. doi: 10.1016/j.phytochem.2010.07.008.

Pergola C, Rossi A, Dugo P, Cuzzocrea S, Sautebin L (2006) Inhibition of nitric oxide biosynthesis by anthocyanin fraction of blackberry extract. Nitric Oxide. 15(1):30-9.

Peri F, Calabrese V (2014) Toll-like receptor 4 (TLR4) modulation by synthetic and natural compounds: an update. J Med Chem. 57(9):3612-3622. doi: 10.1021/jm401006s.

Pike LJ (2003) Lipid rafts: bringing order to chaos. J Lipid Res. 44(4):655-67.

Pimentel GD, Lira FS, Rosa JC, Caris AV, Pinheiro F, Ribeiro EB, Oller do Nascimento CM, Oyama LM (2013) Yerba mate extract (*Ilex paraguariensis*) attenuates both central and

peripheral inflammatory effects of diet-induced obesity in rats. J Nutr Biochem. 24(5):809-18. doi: 10.1016/j.jnutbio.2012.04.016.

Pinto D, Rodrigues F, Braga N, Santos J, Pimentel FB, Palmeira-de-Oliveira A, Oliveira MB (2017) The *Castanea sativa* bur as a new potential ingredient for nutraceutical and cosmetic outcomes: preliminary studies. Food Funct. 8(1):201-208.

Pittler MH, Schmidt K, Ernst E (2003) Hawthorn extract for treating chronic heart failure: meta-analysis of randomized trials. Am J Med. 114(8):665-74.

Ponder A, Long MD (2013) A clinical review of recent findings in the epidemiology of inflammatory bowel disease. Clin Epidemiol. 5:237-47. doi: 10.2147/CLEP.S33961.

Potrich FB, Allemand A, da Silva LM, Dos Santos AC, Baggio CH, Freitas CS, Mendes DA, Andre E, Werner MF, Marques MC (2010) Antiulcerogenic activity of hydroalcoholic extract of *Achillea millefolium* L.: involvement of the antioxidant system. J Ethnopharmacol. 130(1):85-92. doi: 10.1016/j.jep.2010.04.014.

Prasad S, Aggarwal BB (2014) Chronic Diseases Caused by Chronic Inflammation Require Chronic Treatment: Anti-inflammatory Role of Dietary Spices. J Clin Cell Immunol. 5:238. doi:10.4172/2155-9899.1000238.

Quave CL, Lyles JT, Kavanaugh JS, Nelson K, Parlet CP, Crosby HA, Heilmann KP, Horswill AR (2015) *Castanea sativa* (European Chestnut) Leaf Extracts Rich in Ursene and Oleanene Derivatives Block *Staphylococcus aureus* Virulence and Pathogenesis without Detectable Resistance. PLoS One. 10(8):e0136486.

Radha MH, Laxmipriya NP (2014) Evaluation of biological properties and clinical effectiveness of *Aloe vera*: A systematic review. J Tradit Complement Med. 5(1):21-6. doi: 10.1016/j.jtcme.2014.10.006.

Ranasinghe P, Jayawardena R, Pigera S, Wathurapatha WS, Weeratunga HD, Premakumara GAS, Katulanda P, Constantine GR, Galappaththy P (2017) Evaluation of pharmacodynamic properties and safety of *Cinnamomum zeylanicum* (Ceylon cinnamon) in healthy adults: a phase I clinical trial. BMC Complement Altern Med. 17(1):550. doi: 10.1186/s12906-017-2067-7.

Ranković B, Kosanić M, Stanojković T, Vasiljević P, Manojlović N (2012) Biological activities of *Toninia candida* and *Usnea barbata* together with their norstictic acid and usnic acid constituents. Int J Mol Sci. 13(11):14707-22. doi: 10.3390/ijms131114707.

Rao PV, Gan SH (2014) Cinnamon: a multifaceted medicinal plant. Evid Based Complement Alternat Med. 2014:642942. doi: 10.1155/2014/642942.

Reuter J, Huyke C, Casetti F, Theek C, Frank U, Augustin M, Schempp C (2008) Anti-inflammatory potential of a lipolotion containing coriander oil in the ultraviolet erythema test. J Dtsch Dermatol Ges. 6(10):847-51. doi: 10.1111/j.1610-0387.2008.06704.x.

Rocha J, Eduardo-Figueira M, Barateiro A, Fernandes A, Brites D, Bronze R, Duarte CM, Serra AT, Pinto R, Freitas M, Fernandes E, Silva-Lima B, Mota-Filipe H, Sepodes B (2015) Anti-inflammatory effect of rosmarinic acid and an extract of *Rosmarinus officinalis* in rat models of local and systemic inflammation. Basic Clin Pharmacol Toxicol. 116(5):398-413. doi: 10.1111/bcpt.12335.

Rodriguez Villanueva J, Martín Esteban J, Rodríguez Villanueva L (2016) Solving the puzzle: What is behind our forefathers' anti-inflammatory remedies? J Intercult Ethnopharmacol. 6(1):128-143. doi: 10.5455/jice.20161204021732.

Rojas-Duran R, González-Aspajo G, Ruiz-Martel C, Bourdy G, Doroteo-Ortega VH, Alban-Castillo J, Robert G, Auberger P, Deharo E (2012) Anti-inflammatory activity of Mitraphylline isolated from *Uncaria tomentosa* bark. J Ethnopharmacol. 143(3):801-4. doi: 10.1016/j.jep.2012.07.015.

Rosa SI, Rios-Santos F, Balogun SO, Martins DT (2016) Vitexin reduces neutrophil migration to inflammatory focus by down-regulating pro-inflammatory mediators via inhibition of p38, ERK1/2 and JNK pathway. Phytomedicine. 23(1):9-17. doi: 10.1016/j.phymed.2015.11.003.

Rosas EC, Correa LB, Pádua Tde A, Costa TE, Mazzei JL, Heringer AP, Bizarro CA, Kaplan MA, Figueiredo MR, Henriques MG (2015) Anti-inflammatory effect of Schinus terebinthifolius Raddi hydroalcoholic extract on neutrophil migration in zymosan-induced arthritis. J Ethnopharmacol. 175:490-8. doi: 10.1016/j.jep.2015.10.014.

Safayhi H, Boden SE, Schweizer S, Ammon HP (2000) Concentration-dependent potentiating and inhibitory effects of *Boswellia* extracts on 5-lipoxygenase product formation in stimulated PMNL. Planta Med. 66(2):110-3.

Sahpaz S, Garbacki N, Tits M, Bailleul F (2002) Isolation and pharmacological activity of phenylpropanoid esters from *Marrubium vulgare*. J Ethnopharmacol. 79(3):389-92.

Said O, Saad B, Fulder S, Khalil K, Kassis E (2011) Weight loss in animals and humans treated with "weighlevel", a combination of four medicinal plants used in traditional arabic and islamic medicine. Evid Based Complement Alternat Med. 2011:874538. doi: 10.1093/ecam/nen067.

Sandoval M, Charbonnet RM, Okuhama NN, Roberts J, Krenova Z, Trentacosti AM, Miller MJ (2000) Cat's claw inhibits TNFalpha production and scavenges free radicals: role in cytoprotection. Free Radic Biol Med. 29(1):71-8.

Santos Araújo M do C, Farias IL, Gutierres J, Dalmora SL, Flores N, Farias J, de Cruz I, Chiesa J, Morsch VM, Chitolina Schetinger MR (2012) *Uncaria tomentosa*-Adjuvant Treatment for Breast Cancer: Clinical Trial. Evid Based Complement Alternat Med. 2012:676984. doi: 10.1155/2012/676984.

Sarma A, Scott NS (2016) Aspirin Use in Women: Current Perspectives and Future Directions. Curr Atheroscler Rep. 18(12):74.

Sautebin L, Rossi A, Serraino I, Dugo P, Di Paola R, Mondello L, Genovese T, Britti D, Peli A, Dugo G, Caputi AP, Cuzzocrea S (2004) Effect of anthocyanins contained in a blackberry extract on the circulatory failure and multiple organ dysfunction caused by endotoxin in the rat. Planta Med. 70(8):745-52.

Schmidt M, Raghavan B, Müller V, Vogl T, Fejer G, Tchaptchet S, Keck S, Kalis C, Nielsen PJ, Galanos C, Roth J, Skerra A, Martin SF, Freudenberg MA, Goebeler M (2010) Crucial role for human Toll-like receptor 4 in the development of contact allergy to nickel. Nat Immunol. 11(9):814-9. doi: 10.1038/ni.1919.

Schuppan D, Gisbert-Schuppan K (2018). In Tägliches Brot: Krank durch Weizen, Gluten und ATI, 1st edition. Springer-Verlag GmbH, Berlin, pp. 63ff.

Schuppan D, Pickert G, Ashfaq-Khan M, Zevallos V (2015) Non-celiac wheat sensitivity: differential diagnosis, triggers and implications. Best Pract Res Clin Gastroenterol. 29(3):469-76. doi: 10.1016/j.bpg.2015.04.002.

Schulz V (2006) Safety of St. John's Wort extract compared to synthetic antidepressants. Phytomedicine. 13(3):199-204.

Senchina DS, Flagel LE, Wendel JF, Kohut ML (2006) Phenetic comparison of seven *Echinacea* species based on immunomodulatory characteristics. Econ Bot. 60(3):205-211.

Shanks GD (2016) Historical Review: Problematic Malaria Prophylaxis with Quinine. Am J Trop Med Hyg. 95(2):269-72. doi: 10.4269/ajtmh.16-0138.

Shara M, Stohs SJ (2015) Efficacy and Safety of White Willow Bark (*Salix alba*) Extracts. Phytother Res. 29(8):1112-6. doi: 10.1002/ptr.5377.

Sharma M, Anderson SA, Schoop R, Hudson JB (2009) Induction of multiple pro-inflammatory cytokines by respiratory viruses and reversal by standardized *Echinacea*, a potent antiviral herbal extract. Antiviral Res. 83(2):165-70. doi: 10.1016/j.antiviral.2009.04.009.

Sheng X, Zhang Y, Gong Z, Huang C, Zang YQ (2008) Improved Insulin Resistance and Lipid Metabolism by Cinnamon Extract through Activation of Peroxisome Proliferator-Activated Receptors. PPAR Res. 2008:581348. doi: 10.1155/2008/581348.

Shergis JL, Zhang AL, Zhou W, Xue CC (2013) *Panax ginseng* in randomised controlled trials: a systematic review. Phytother Res. 27(7):949-65. doi: 10.1002/ptr.4832.

Shirakami Y, Sakai H, Kochi T, Seishima M, Shimizu M (2016) Catechins and Its Role in Chronic Diseases. Adv Exp Med Biol. 929:67-90.

Shrimali D, Shanmugam MK, Kumar AP, Zhang J, Tan BK, Ahn KS, Sethi G (2013) Targeted abrogation of diverse signal transduction cascades by emodin for the treatment of inflammatory disorders and cancer. Cancer Lett. 341(2):139-49. doi: 10.1016/j.canlet.2013.08.023.

Shrivastava R, Cucuat N, John GW (2007) Effects of *Alchemilla vulgaris* and glycerine on epithelial and myofibroblast cell growth and cutaneous lesion healing in rats. Phytother Res. 21(4):369-73.

Singh R, De S, Belkheir A (2013) *Avena sativa* (Oat), a potential neutraceutical and therapeutic agent: an overview. Crit Rev Food Sci Nutr. 53(2):126-44. doi: 10.1080/10408398.2010.526725.

Slavich GM, Irwin MR (2014) From stress to inflammation and major depressive disorder: a social signal transduction theory of depression. Psychol Bull. 140(3):774-815. doi: 10.1037/a0035302.

Smigiel KS, Parks WC (2018) Macrophages, Wound Healing, and Fibrosis: Recent Insights. Curr Rheumatol Rep. 20(4):17. doi: 10.1007/s11926-018-0725-5.

Sohn E, Kim J, Kim CS, Lee YM, Kim JS (2016) Extract of *Polygonum cuspidatum* Attenuates Diabetic Retinopathy by Inhibiting the High-Mobility Group Box-1 (HMGB1) Signaling Pathway in Streptozotocin-Induced Diabetic Rats. Nutrients. 8(3):140. doi: 10.3390/nu8030140.

Soleimani D, Paknahad Z, Askari G, Iraj B, Feizi A (2016) Effect of garlic powder consumption on body composition in patients with nonalcoholic fatty liver disease: A randomized, double-blind, placebo-controlled trial. Adv Biomed Res. 5:2. doi: 10.4103/2277-9175.174962.

Speranza G, Morelli CF, Tubaro A, Altinier G, Durì L, Manitto P (2005) Aloeresin I, an anti-inflammatory 5-methylchromone from cape aloe. Planta Med. 71(1):79-81.

Staiger C (2013) Comfrey root: from tradition to modern clinical trials. Wien Med Wochenschr. 163(3-4):58-64. doi: 10.1007/s10354-012-0162-4.

Stickel F, Schuppan D (2007) Herbal medicine in the treatment of liver diseases. Dig Liver Dis. 39:293–304.

Strassburg K, Molly BJ, Mallet C, Duesterloh A, Bendik I, Hankemeier T, Langridge J, Vreeken RJ, Astarita G (2015) Targeted lipidomics of oxylipins (oxygenated fatty acids). In Waters Application Note, Waters Corporation, Milford, pp. 1-11.

Suman S, Shukla Y (2016) Diallyl Sulfide and Its Role in Chronic Diseases Prevention. Adv Exp Med Biol. 929:127-144.

Sun Z, Wang H, Wang J, Zhou L, Yang P (2014) Chemical Composition and Anti-Inflammatory, Cytotoxic and Antioxidant Activities of Essential Oil from Leaves of *Mentha piperita* Grown in China. PLoS One. 9(12):e114767. doi: 10.1371/journal.pone.0114767.

Swider JR, Jankowski JA, Sobevski A (2016) Direct, real-time mass spectrometry analysis of cinnamon. Am Lab. 36-39.

Szabo G, Dolganiuc A, Dai Q, Pruett SB (2007) TLR4, ethanol, and lipid rafts: a new mechanism of ethanol action with implications for other receptor-mediated effects. J Immunol. 178(3):1243-9.

Tak PP, Firestein GS (2001) NF-kappaB: a key role in inflammatory diseases. J Clin Invest. 107(1):7-11.

Takeuchi O, Akira S (2001) Toll-like receptors; their physiological role and signal transduction system. Int Immunopharmacol. 1(4):625-35.

Takır S, Altun IH, Sezgi B, Süzgeç-Selçuk S, Mat A, Uydeş-Doğan BS (2015) Vasorelaxant and blood pressure lowering effects of *alchemilla vulgaris*: A comparative study of methanol and aqueous extracts. Pharmacogn Mag. 11(41):163-9. doi: 10.4103/0973-1296.149733.

Tang D, Dong Y, Ren H, Li L, He C (2014) A review of phytochemistry, metabolite changes, and medicinal uses of the common food mung bean and its sprouts (*Vigna radiata*). Chem Cent J. 8(1):4. doi: 10.1186/1752-153X-8-4.

Thermo Fisher Scientific (2016). Product Datasheet AlamarBlue – Rapid & Accurate Cell Health Indicator from website https://www.thermofisher.com/de/de/home/brands/molecular-probes/key-molecular-probes-products/alamarblue-rapid-and-accurate-cell-health-indicator.html (26.01.2018).

Tidswell M, Tillis W, Larosa SP, Lynn M, Wittek AE, Kao R, Wheeler J, Gogate J, Opal SM; Eritoran Sepsis Study Group (2010) Phase 2 trial of eritoran tetrasodium (E5564), a toll-like receptor 4 antagonist, in patients with severe sepsis. Crit Care Med. 38(1):72-83. doi: 10.1097/CCM.0b013e3181b07b78.

Trifan A, Opitz SEW, Josuran R, Grubelnik A, Esslinger N, Peter S, Bräm S, Meier N, Wolfram E (2018) Is comfrey root more than toxic pyrrolizidine alkaloids? Salvianolic acids among antioxidant polyphenols in comfrey (*Symphytum officinale* L.) roots. Food Chem Toxicol. 112:178-187. doi: 10.1016/j.fct.2017.12.051.

Trotter LA, Patel D, Dubin S, Guerra C, McCloud V, Lockwood P, Messer R, Wataha JC, Lewis JB (2017) Violet/blue light activates Nrf2 signaling and modulates the inflammatory response of THP-1 monocytes. Photochem Photobiol Sci. 16(6):883-889. doi: 10.1039/c6pp00299d.

Uddin Z, Song YH, Curtis-Long MJ, Kim JY, Yuk HJ, Park KH (2016) Potent bacterial neuraminidase inhibitors, anthraquinone glucosides from *Polygonum cuspidatum* and their inhibitory mechanism. J Ethnopharmacol. 193:283-292. doi: 10.1016/j.jep.2016.08.026.

Ukiya M, Akihisa T, Yasukawa K, Tokuda H, Suzuki T, Kimura Y (2006) Anti-inflammatory, anti-tumor-promoting, and cytotoxic activities of constituents of marigold (*Calendula officinalis*) flowers. J Nat Prod. 69(12):1692-6.

Vanýsek P (2014). In Haynes WM, Lide DR, Bruno TJ (ed) CRC Handbook of Chemistry and Physics, 95th edition. CRC Press, Boca Raton, London, New York, pp. 5:94-104.

Vigo E, Cepeda A, Gualillo O, Perez-Fernandez R (2005) In-vitro anti-inflammatory activity of *Pinus sylvestris* and *Plantago lanceolata* extracts: effect on inducible NOS, COX-1, COX-2 and their products in J774A.1 murine macrophages. J Pharm Pharmacol. 57(3):383-91.

Villalva M, Jaime L, Aguado E, Nieto JA, Reglero G, Santoyo S (2018) Anti-Inflammatory and Antioxidant Activities from the Basolateral Fraction of Caco-2 Cells Exposed to a Rosmarinic Acid Enriched Extract. J Agric Food Chem. 66(5):1167-1174. doi: 10.1021/acs.jafc.7b06008.

Vlachojannis J, Magora F, Chrubasik S (2011) Willow species and aspirin: different mechanism of actions. Phytother Res. 25(7):1102-4. doi: 10.1002/ptr.3386.

Walker AF, Marakis G, Simpson E, Hope JL, Robinson PA, Hassanein M, Simpson HC (2006) Hypotensive effects of hawthorn for patients with diabetes taking prescription drugs: a randomised controlled trial. Br J Gen Pract. 56(527):437-43.

Walsh D, McCarthy J, O'Driscoll C, Melgar S (2013) Pattern recognition receptors--molecular orchestrators of inflammation in inflammatory bowel disease. Cytokine Growth Factor Rev. 24(2):91-104. doi: 10.1016/j.cytogfr.2012.09.003.

Weinmann S, Roll S, Schwarzbach C, Vauth C, Willich SN (2010) Effects of *Ginkgo biloba* in dementia: systematic review and meta-analysis. BMC Geriatr. 10:14. doi: 10.1186/1471-2318-10-14.

Williams CA, Hoult JR, Harborne JB, Greenham J, Eagles J (1995) A biologically active lipophilic flavonol from *Tanacetum parthenium*. Phytochemistry. 38(1):267-70.

Wink M (2008) Evolutionary advantage and molecular modes of action of multi-component mixtures used in phytomedicine. Curr. Drug Metab. 9(10):996–1009.

Wink M (2015) Modes of Action of Herbal Medicines and Plant Secondary Metabolites. Medicines. 2(3):251–286. doi: 10.3390/medicines2030251.

Woehrlin F, Fry H, Abraham K, Preiss-Weigert A (2010) Quantification of flavoring constituents in cinnamon: high variation of coumarin in cassia bark from the German retail market and in authentic samples from indonesia. J Agric Food Chem. 58(19):10568-75. doi: 10.1021/jf102112p.

Woelkart K, Bauer R (2007) The role of alkamides as an active principle of *echinacea*. Planta Med. 73(7):615-23.

Wu TT, Tsai CW, Yao HT, Lii CK, Chen HW, Wu YL, Chen PY, Liu KL (2010) Suppressive effects of extracts from the aerial part of *Coriandrum sativum* L. on LPS-induced inflammatory responses in murine RAW 264.7 macrophages. J Sci Food Agric. 90(11):1846-54. doi: 10.1002/jsfa.4023.

Xie G, Chen N, Soromou LW, Liu F, Xiong Y, Wu Q, Li H, Feng H, Liu G (2012) *p*-Cymene protects mice against lipopolysaccharide-induced acute lung injury by inhibiting inflammatory cell activation. Molecules. 17(7):8159-73. doi: 10.3390/molecules17078159.

Yaeesh S, Jamal Q, Khan AU, Gilani AH (2006) Studies on hepatoprotective, antispasmodic and calcium antagonist activities of the aqueous-methanol extract of *Achillea millefolium*. Phytother Res. 20(7):546-51.

Yamada M, Ichikawa T, Ii M, Sunamoto M, Itoh K, Tamura N, Kitazaki (2005) Discovery of novel and potent small-molecule inhibitors of NO and cytokine production as antisepsis agents: synthesis and biological activity of alkyl 6-(N-substituted sulfamoyl)cyclohex-1-ene-1-carboxylate. J Med Chem. 48(23):7457-67.

Yang Y, Lv J, Jiang S, Ma Z, Wang D, Hu W, Deng C, Fan C, Di S, Sun Y, Yi W (2016) The emerging role of Toll-like receptor 4 in myocardial inflammation. Cell Death Dis. 7:e2234. doi: 10.1038/cddis.2016.140.

Yao P, Cui M, Li Y, Deng Y, Wu H (2015) Effects of rhubarb on intestinal flora and toll-like receptors of intestinal mucosa in rats with severe acute pancreatitis. Pancreas. 44(5):799-804. doi: 10.1097/MPA.0000000000000339.

Yarnell E (2002) Botanical medicines for the urinary tract. World J Urol. 20(5):285-93.

Youn HS, Lee JK, Choi YJ, Saitoh SI, Miyake K, Hwang DH, Lee JY (2008) Cinnamaldehyde suppresses toll-like receptor 4 activation mediated through the inhibition of receptor oligomerization. Biochem Pharmacol. 75(2):494-502.

Youn HS, Lee JY, Saitoh SI, Miyake K, Kang KW, Choi YJ, Hwang DH (2006a) Suppression of MyD88- and TRIF-dependent signaling pathways of Toll-like receptor by (-)-epigallocatechin-3-gallate, a polyphenol component of green tea. Biochem Pharmacol. 72(7):850-9.

Youn HS, Saitoh SI, Miyake K, Hwang DH (2006b). Inhibition of homodimerization of Toll-like receptor 4 by curcumin. Biochem Pharmacol. 72(1):62-9.

Yu S, Wang X, He X, Wang Y, Gao S, Ren L, Shi Y (2016) Curcumin exerts anti-inflammatory and antioxidative properties in 1-methyl-4-phenylpyridinium ion (MPP(+))-stimulated mesencephalic astrocytes by interference with TLR4 and downstream signaling pathway. Cell Stress Chaperones. 21(4):697-705. doi: 10.1007/s12192-016-0695-3.

Zarember KA, Godowski PJ (2002) Tissue expression of human Toll-like receptors and differential regulation of Toll-like receptor mRNAs in leukocytes in response to microbes, their products, and cytokines. J Immunol. 168(2):554-61.

Zarubin T, Han J (2005) Activation and signaling of the p38 MAP kinase pathway. Cell Res. 15(1):11-8.

Zevallos VF, Raker VK, Maxeiner J, Scholtes P, Steinbrink K, Schuppan D (2018) Dietary wheat amylase trypsin inhibitors exacerbate murine allergic airway inflammation. Eur J Nutr. doi: 10.1007/s00394-018-1681-6. [Epub ahead of print]

Zevallos VF, Raker V, Tenzer S, Jimenez-Calvente C, Ashfaq-Khan M, Rüssel N, Pickert G, Schild H, Steinbrink K, Schuppan D (2017) Nutritional Wheat Amylase-Trypsin Inhibitors Promote Intestinal Inflammation via Activation of Myeloid Cells. Gastroenterology. 152(5):1100-1113.e12. doi: 10.1053/j.gastro.2016.12.006.

Zhang K, Han ES, Dellinger TH, Lu J, Nam S, Anderson RA, Yim JH, Wen W (2017) Cinnamon extract reduces VEGF expression via suppressing HIF-1α gene expression and inhibits tumor growth in mice. Mol Carcinog. 56(2):436-446. doi: 10.1002/mc.22506.

Zhang Y, Cao W, Xie YH, Yang Q, Li XQ, Liu XX, Wang SW (2012) The comparison of α-bromo-4-chlorocinnamaldehyde and cinnamaldehyde on coxsackie virus B3-induced myocarditis and their mechanisms. Int Immunopharmacol. 14(1):107-13. doi: 10.1016/j.intimp.2012.06.007.

Zhong W, Chi G, Jiang L, Soromou LW, Chen N, Huo M, Guo W, Deng X, Feng H (2013) *p*-Cymene modulates *in vitro* and *in vivo* cytokine production by inhibiting MAPK and NF-κB activation. Inflammation. 36(3):529-37. doi: 10.1007/s10753-012-9574-y.

Zhu HT, Bian C, Yuan JC, Chu WH, Xiang X, Chen F, Wang CS, Feng H, Lin JK (2014) Curcumin attenuates acute inflammatory injury by inhibiting the TLR4/MyD88/NF-κB signaling pathway in experimental traumatic brain injury. J Neuroinflammation. 11:59. doi: 10.1186/1742-2094-11-59.

Zhu R, Liu H, Liu C, Wang L, Ma R, Chen B, Li L, Niu J, Fu M, Zhang D, Gao S (2017) Cinnamaldehyde in diabetes: A review of pharmacology, pharmacokinetics and safety. Pharmacol Res. 122:78-89. doi: 10.1016/j.phrs.2017.05.019.

Zia-Ul-Haq M, Riaz M, De Feo V, Jaafar HZ, Moga M (2014) *Rubus fruticosus* L.: constituents, biological activities and health related uses. Molecules. 19(8):10998-1029. doi: 10.3390/molecules190810998.

8. Acknowledgement

9. Appendix

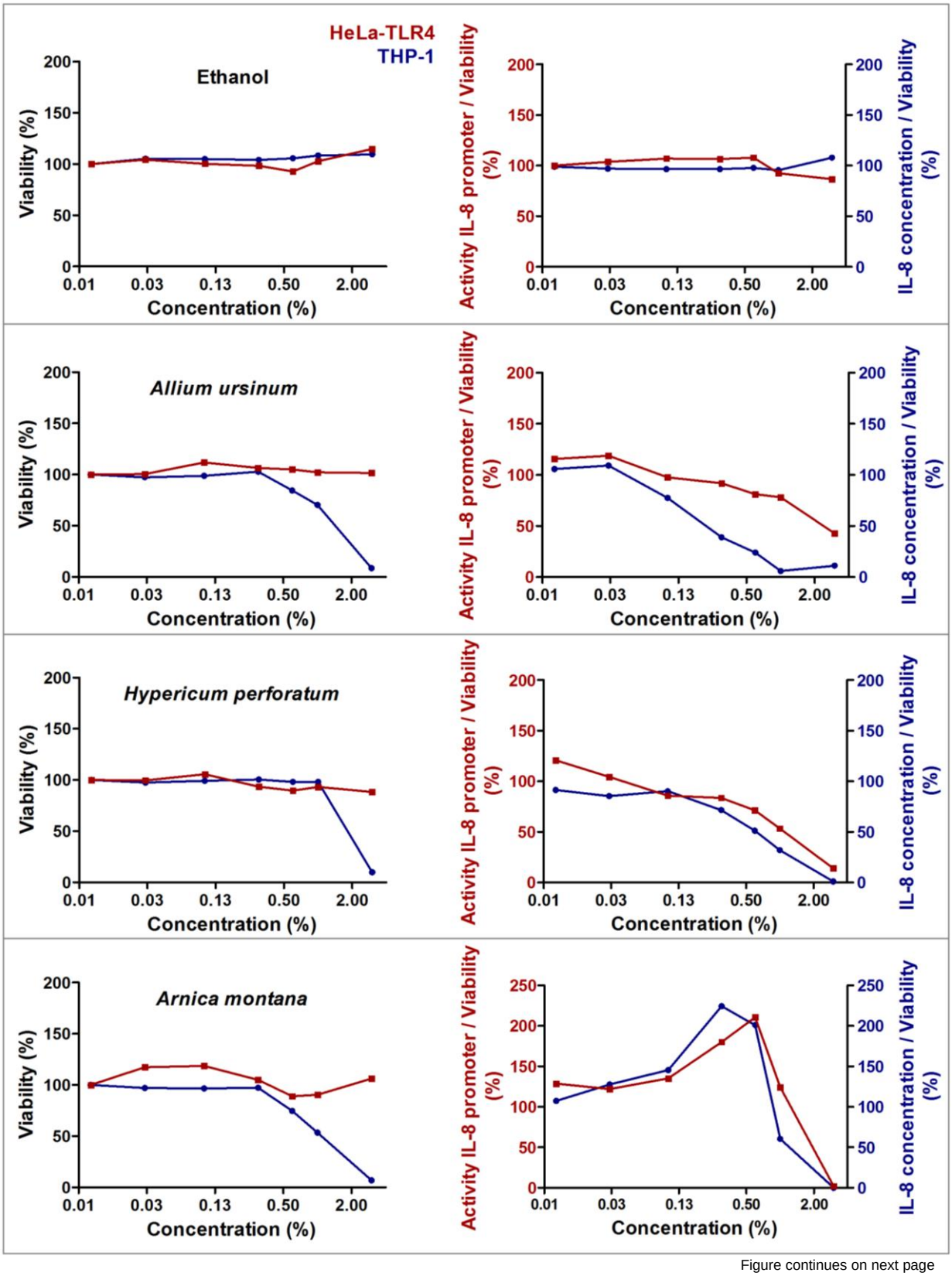

Figure continues on next page

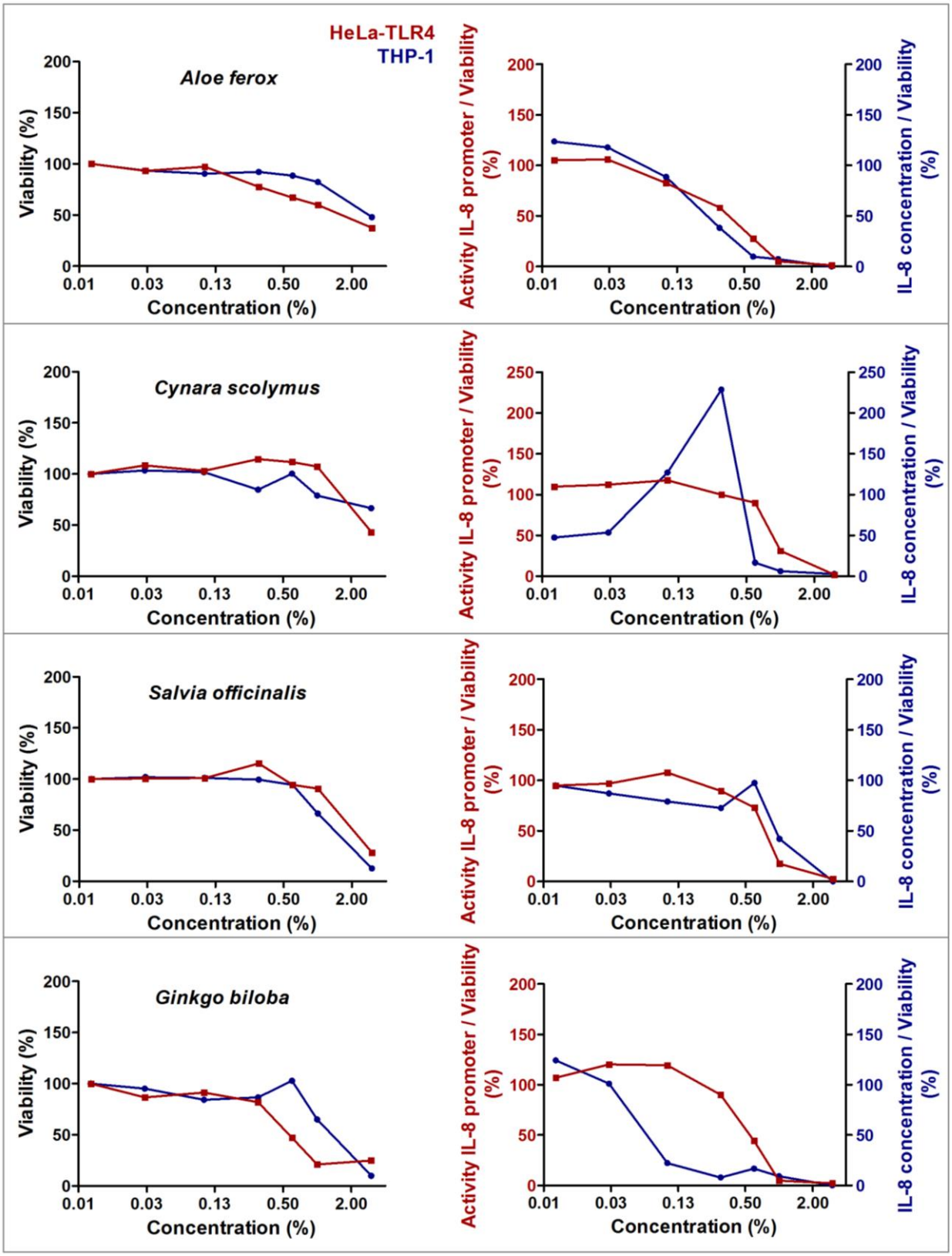

Figure continues on next page

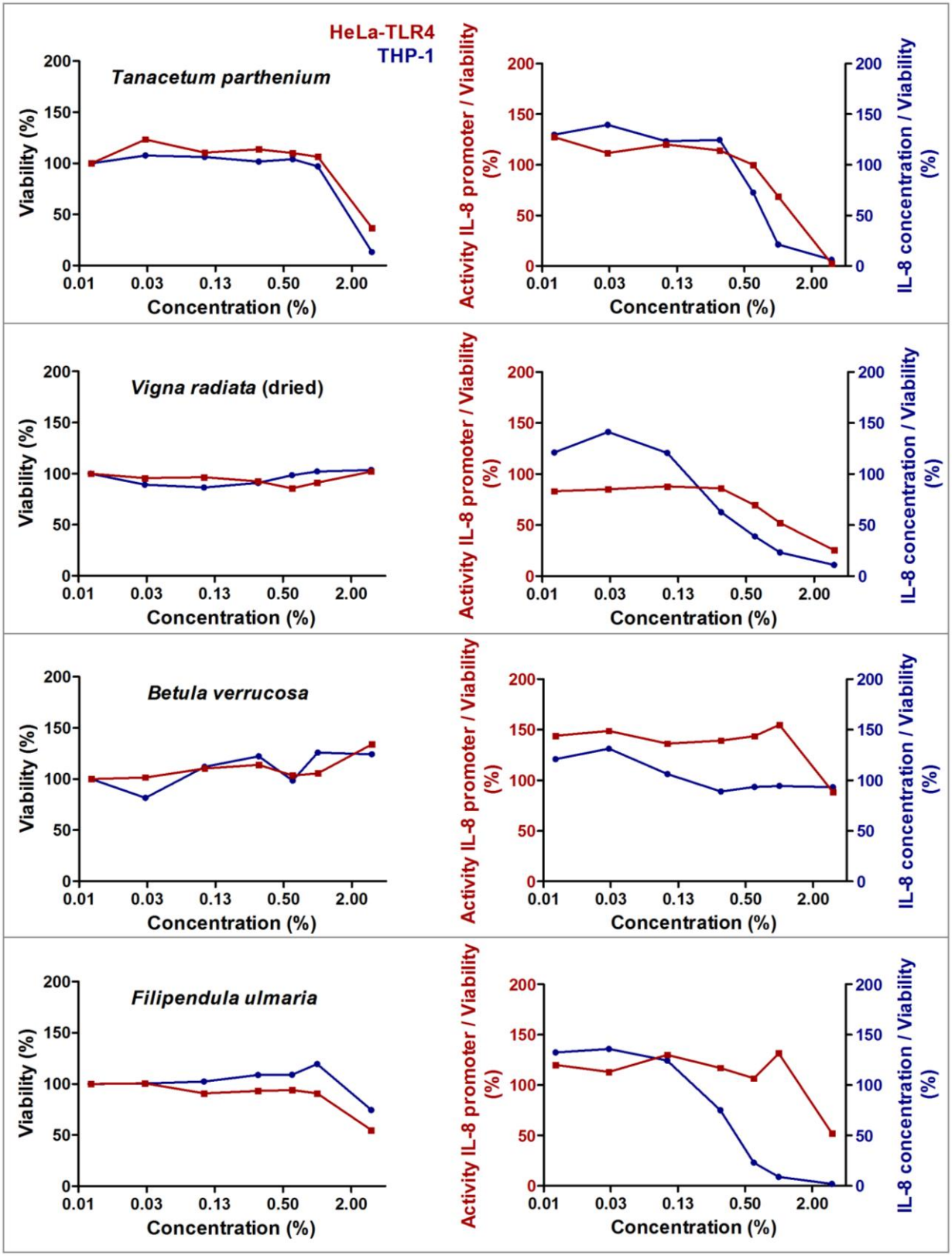

Figure continues on next page

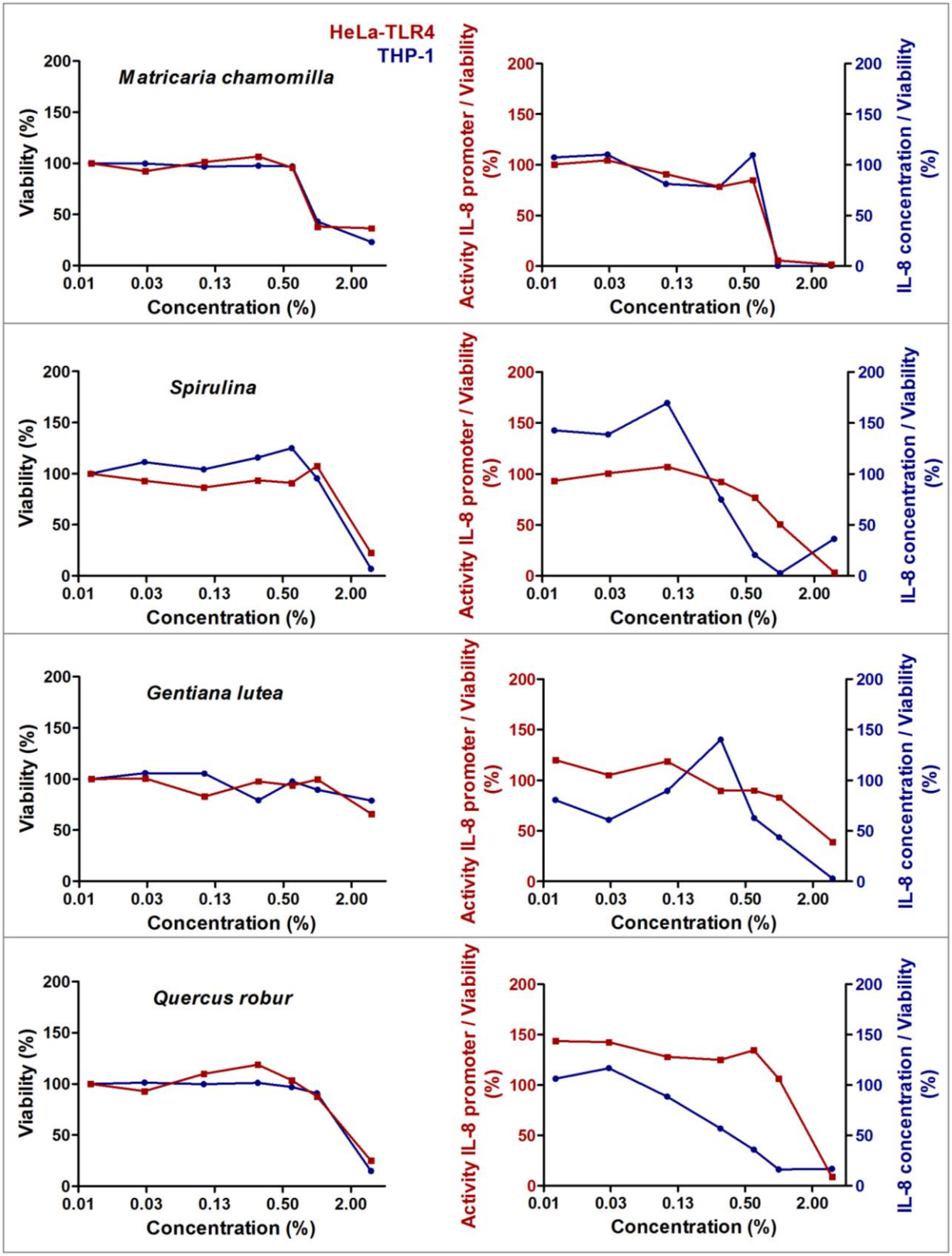

Figure continues on next page

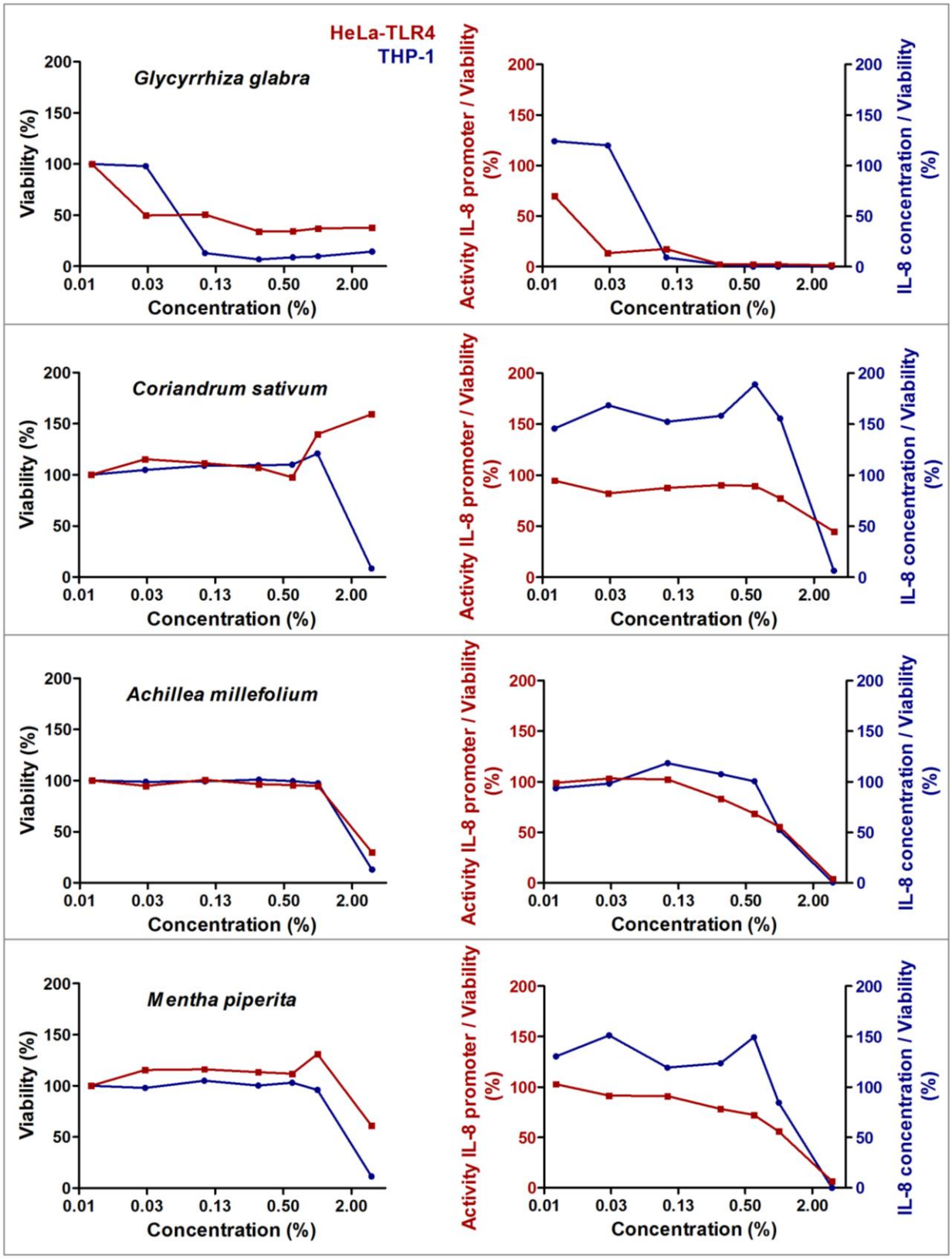

Figure continues on next page

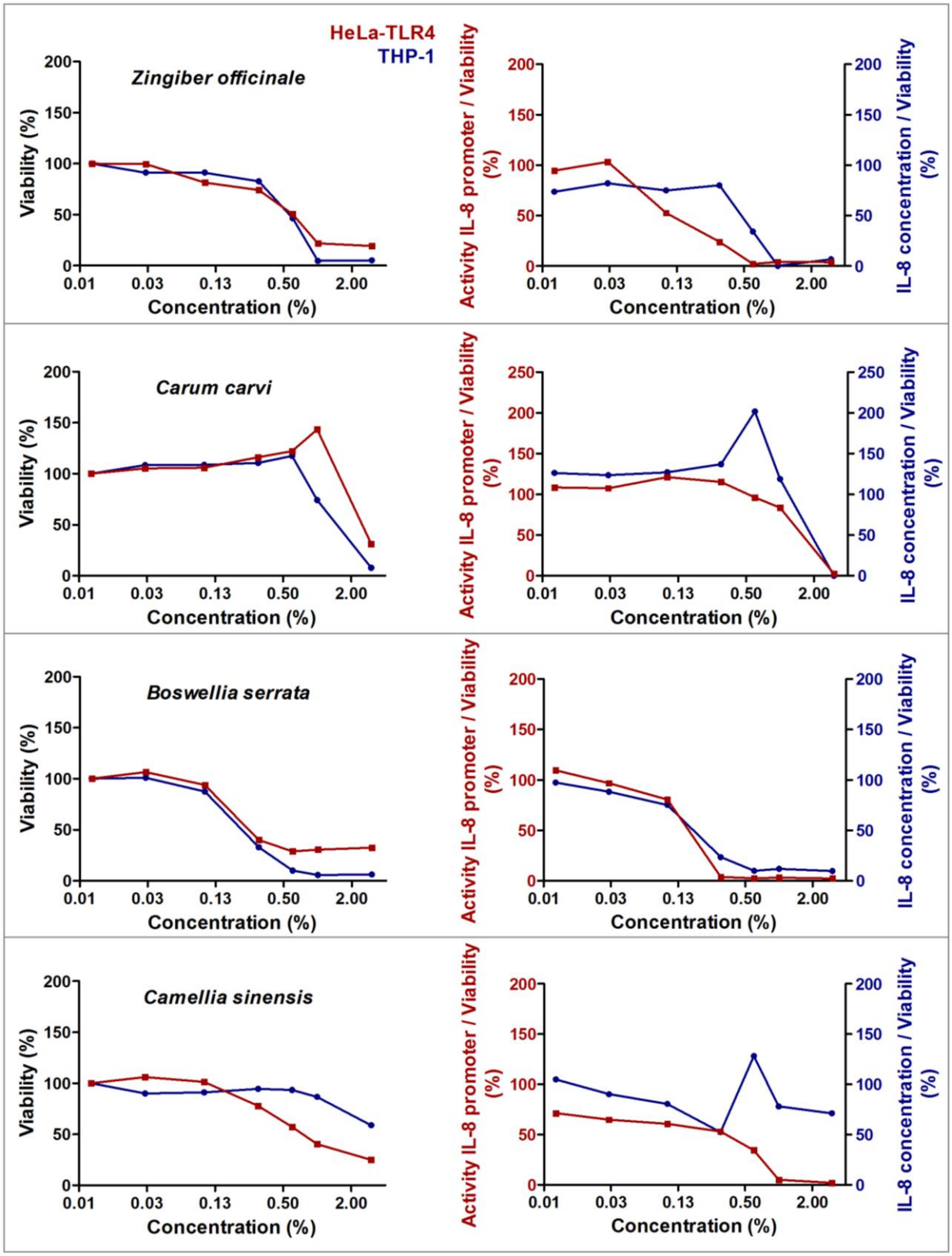

Figure continues on next page

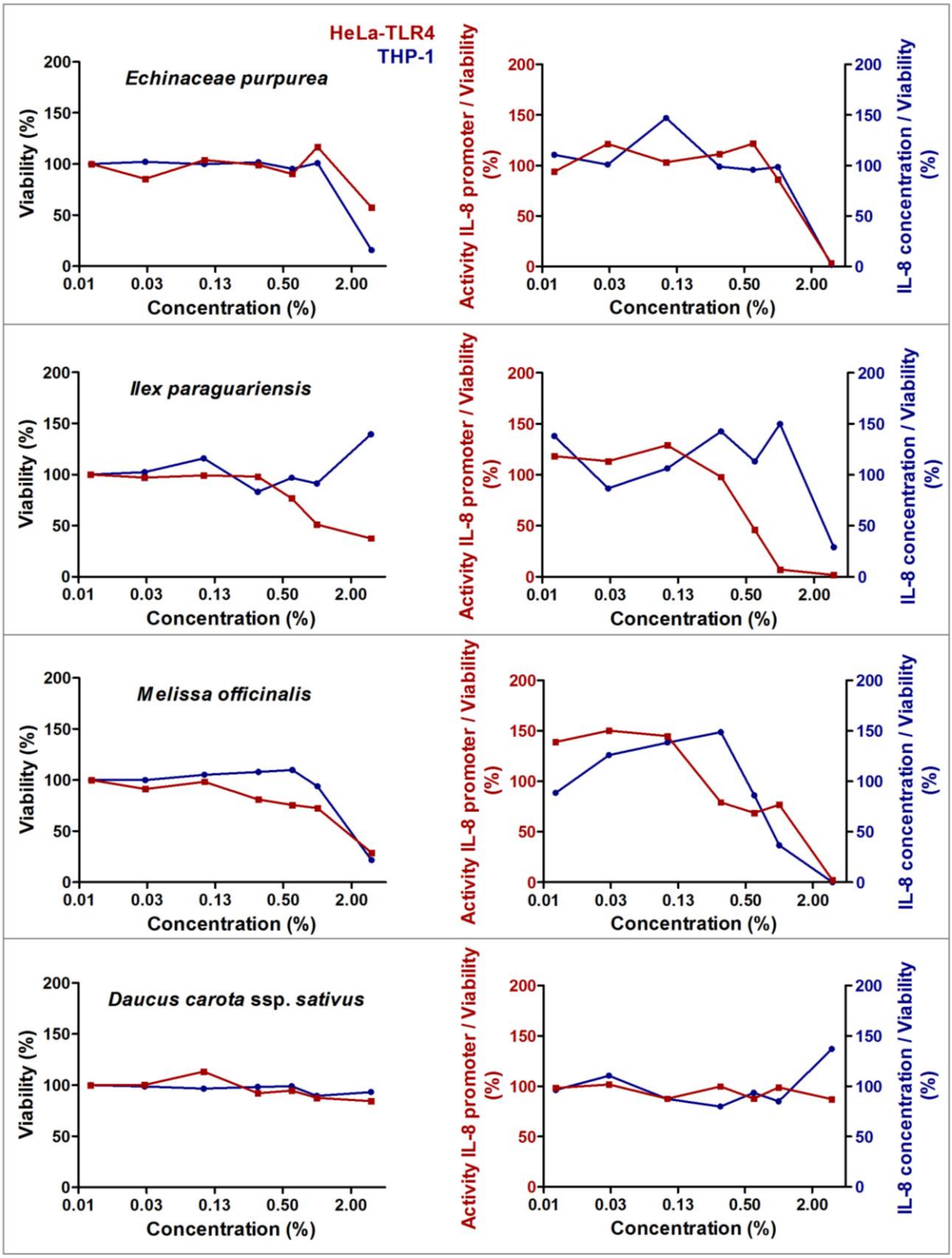

Figure continues on next page

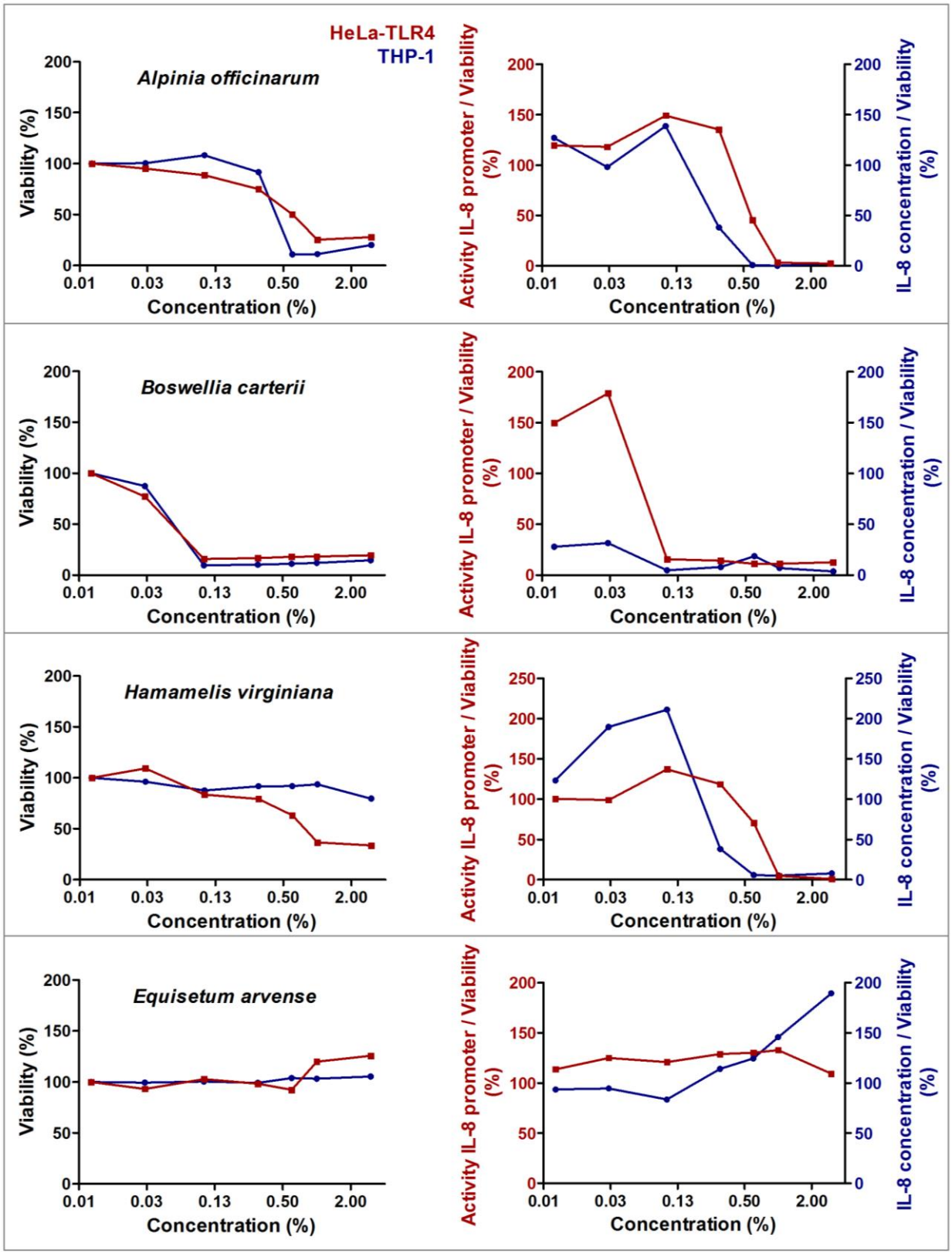

Figure continues on next page

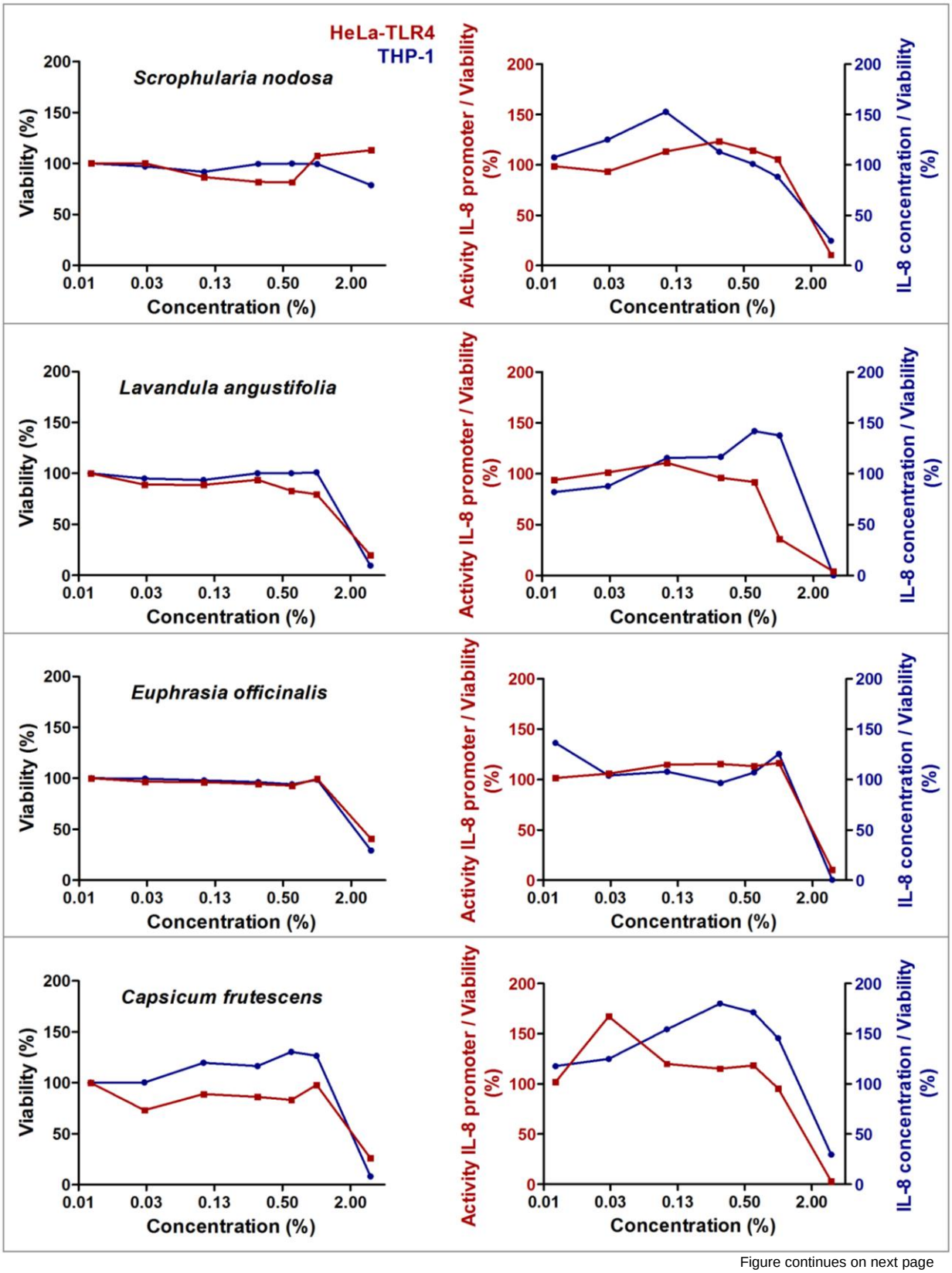

Figure continues on next page

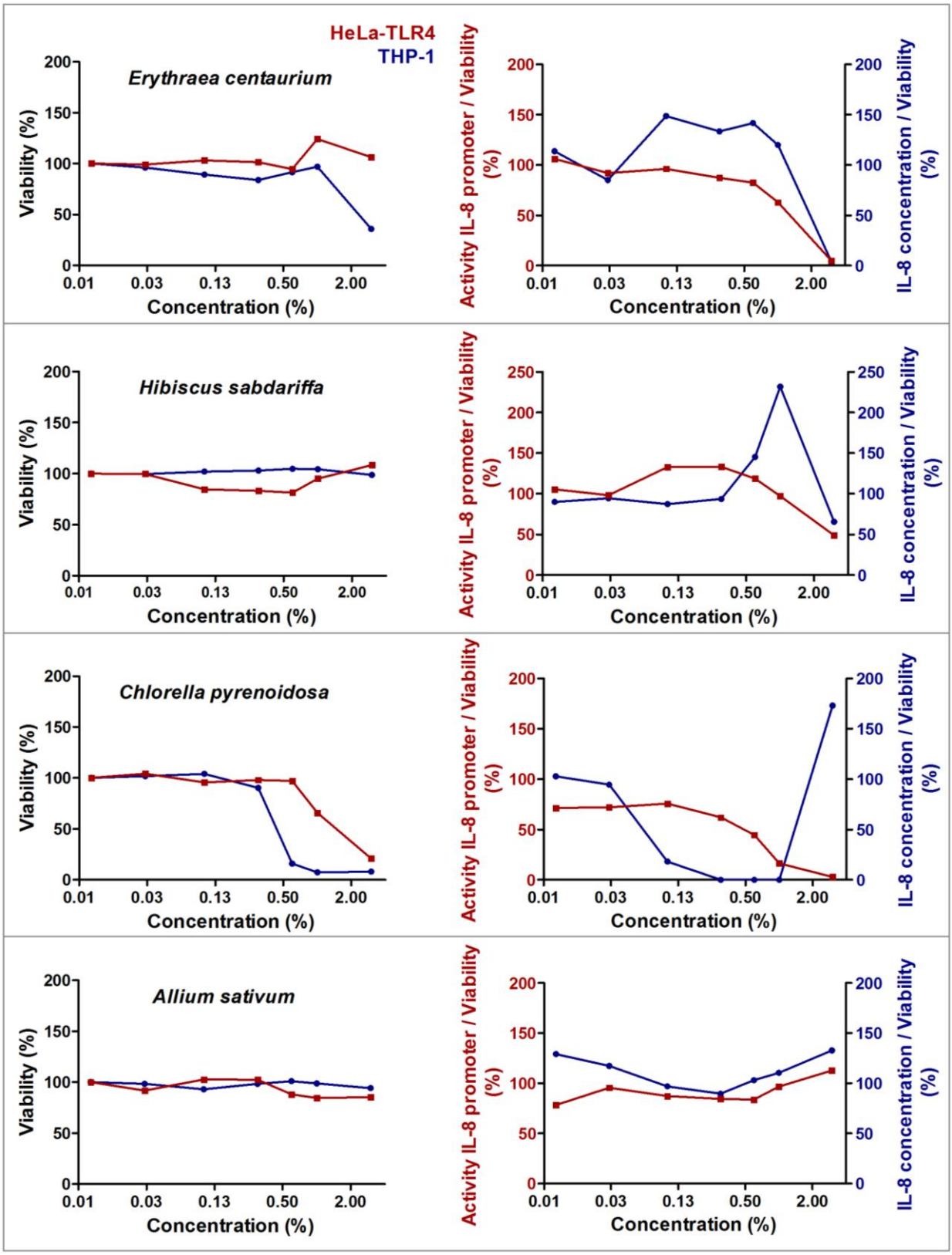

Figure continues on next page

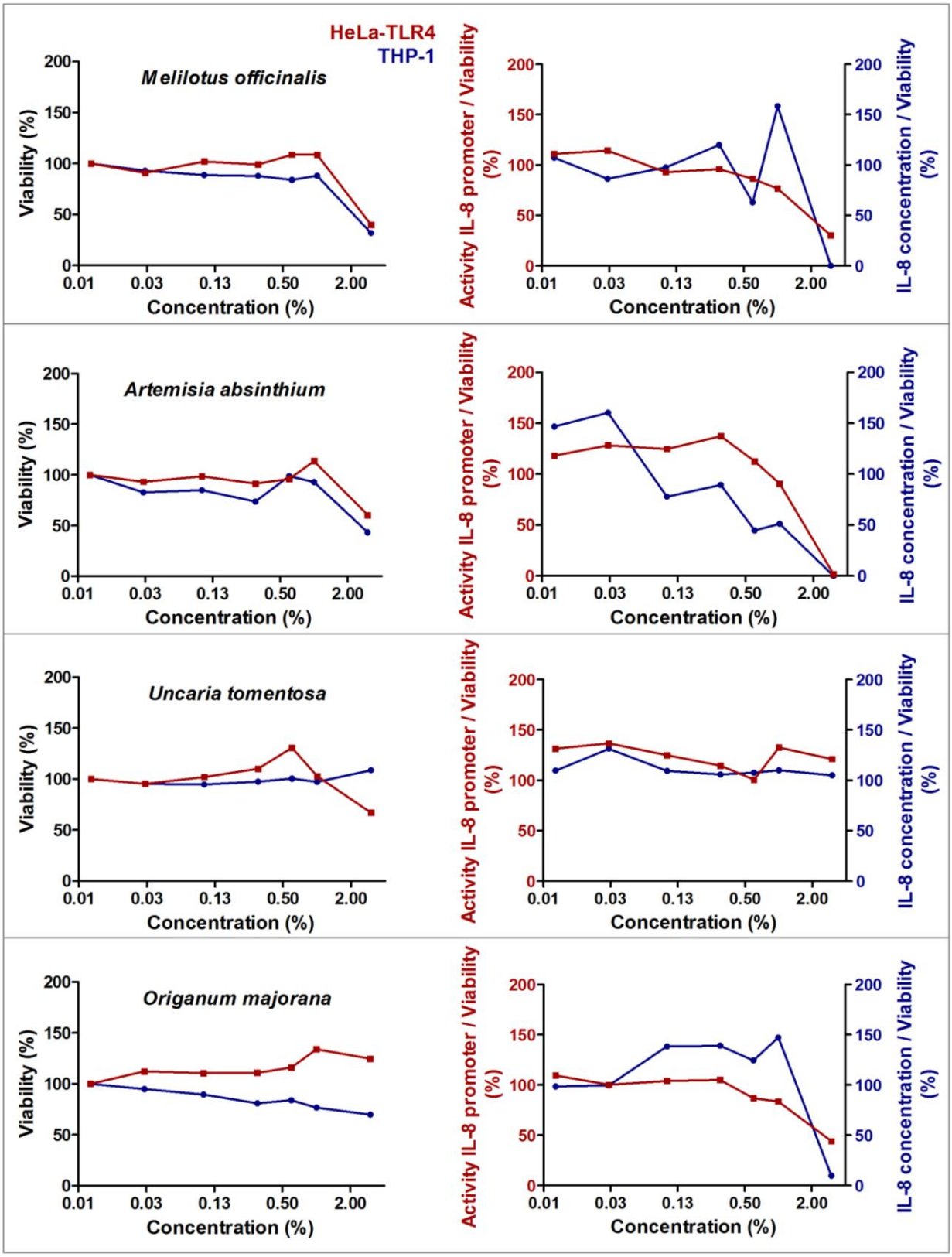

Figure continues on next page

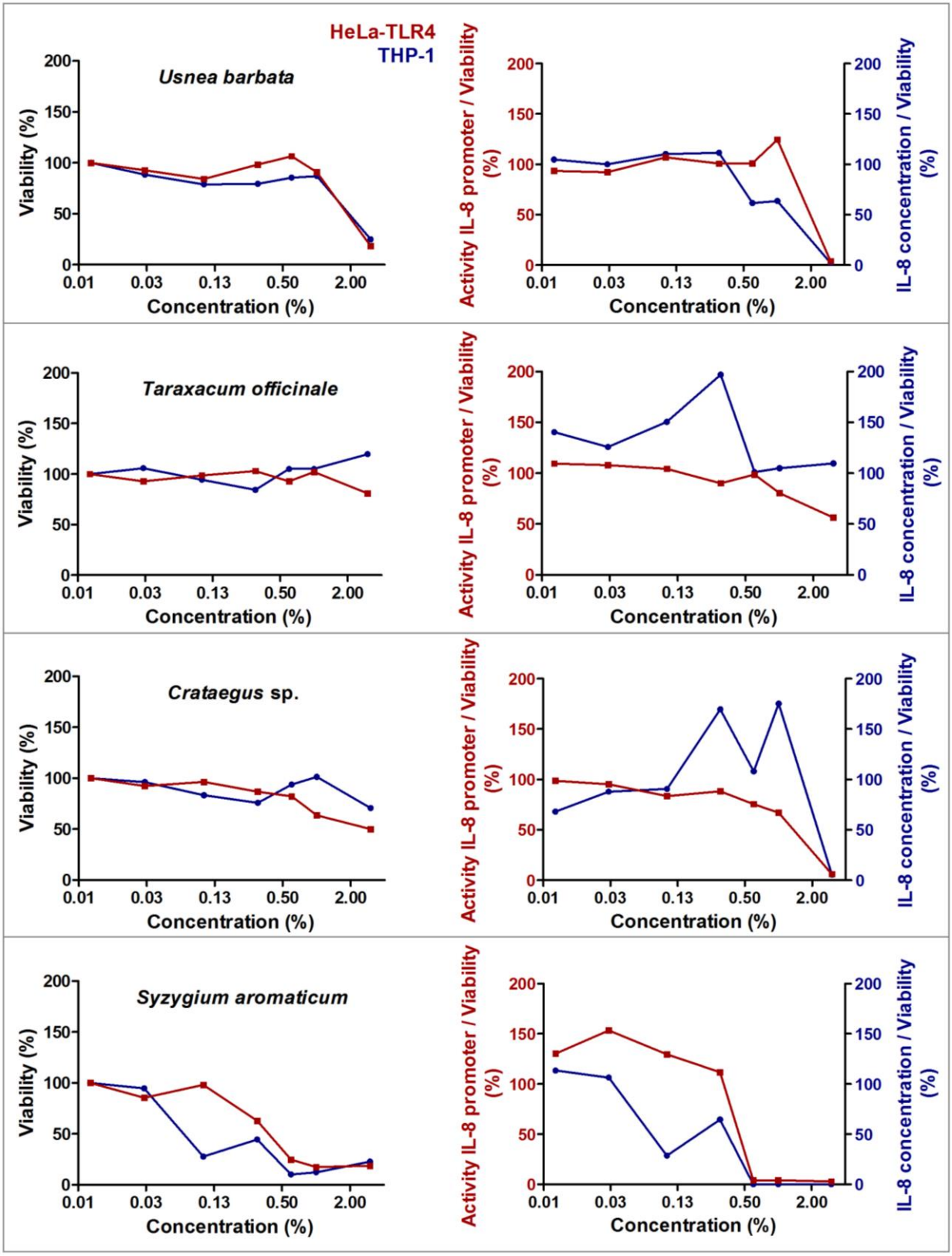

Figure continues on next page

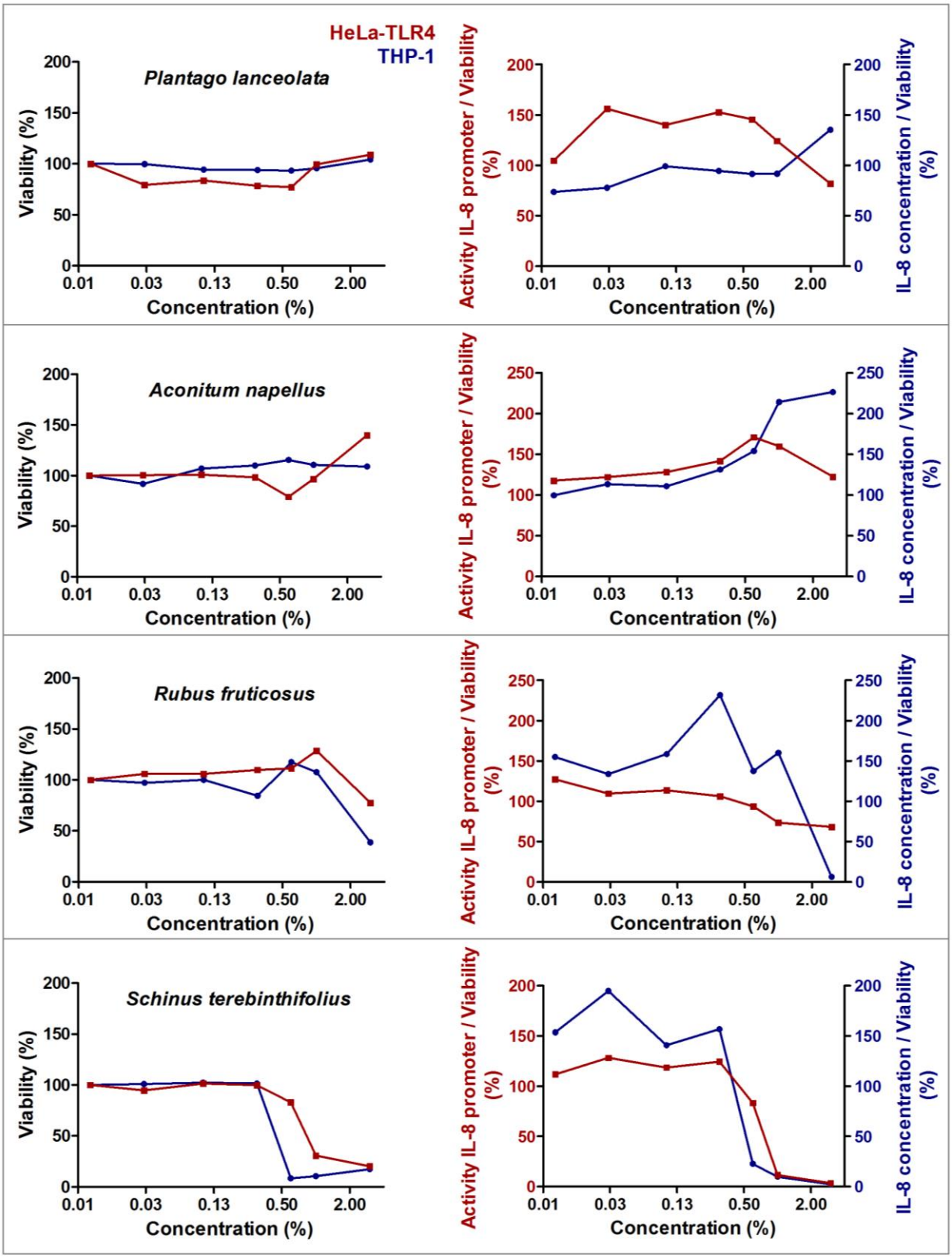

Figure continues on next page

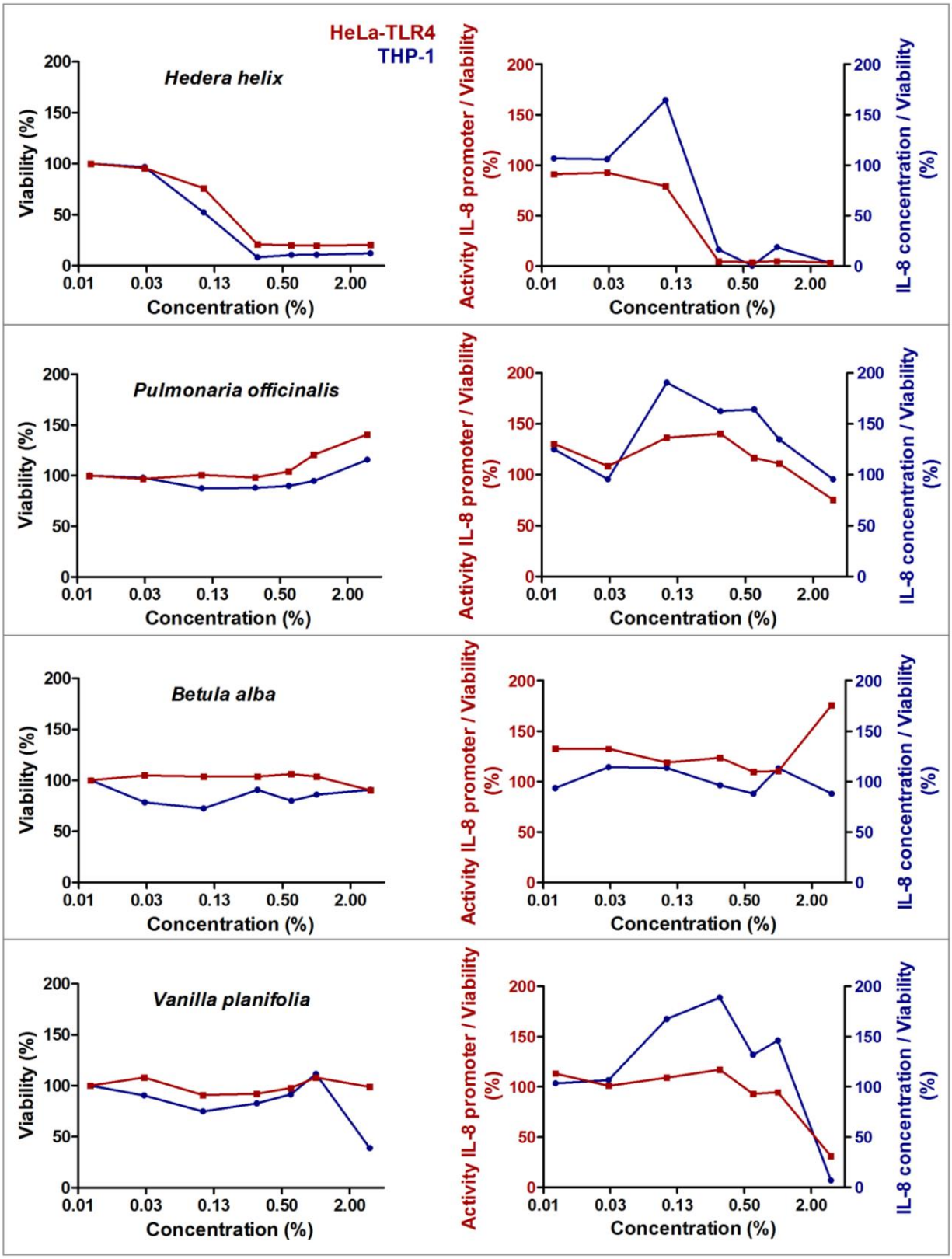

Figure continues on next page

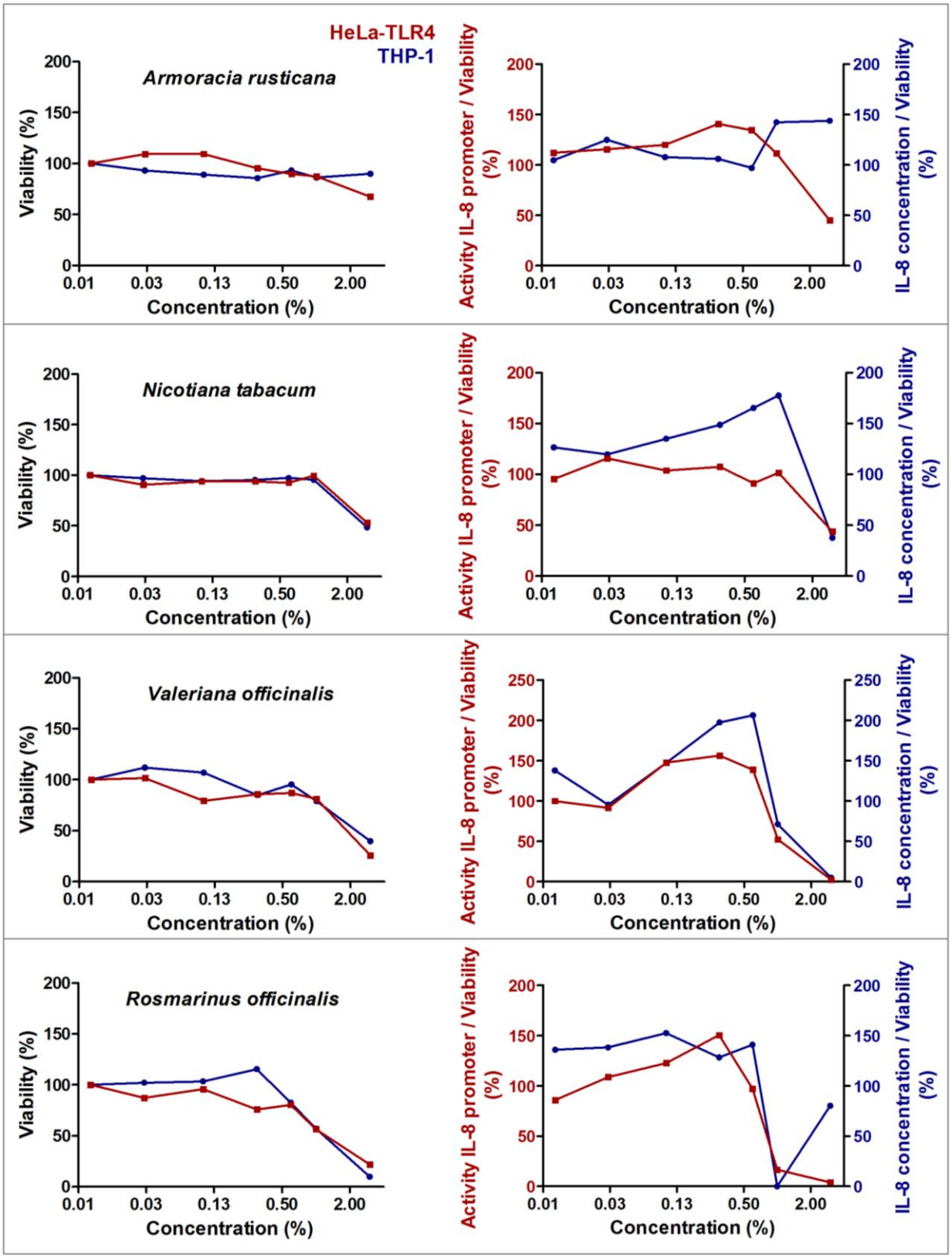

Figure continues on next page

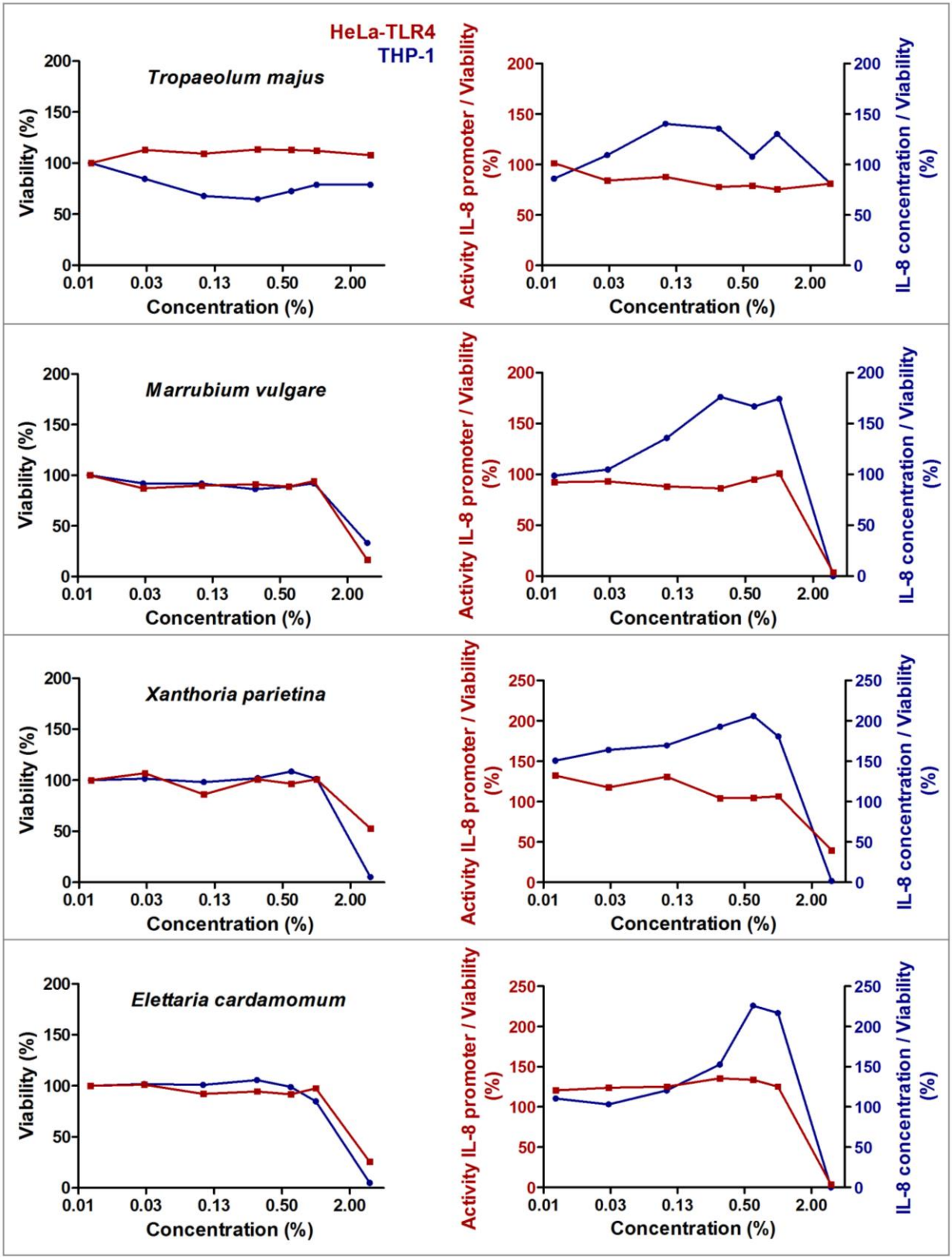

Figure continues on next page

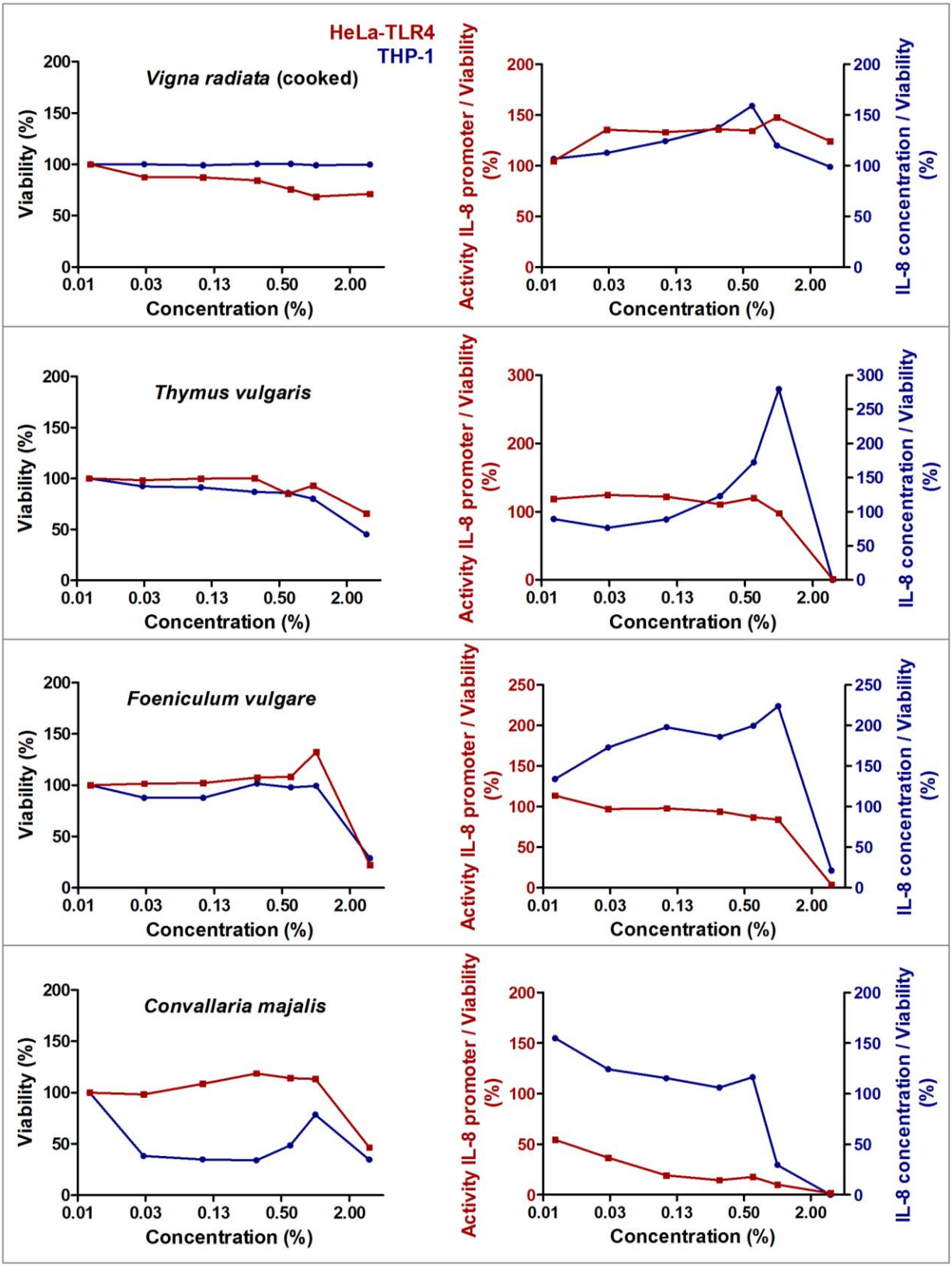

Figure continues on next page

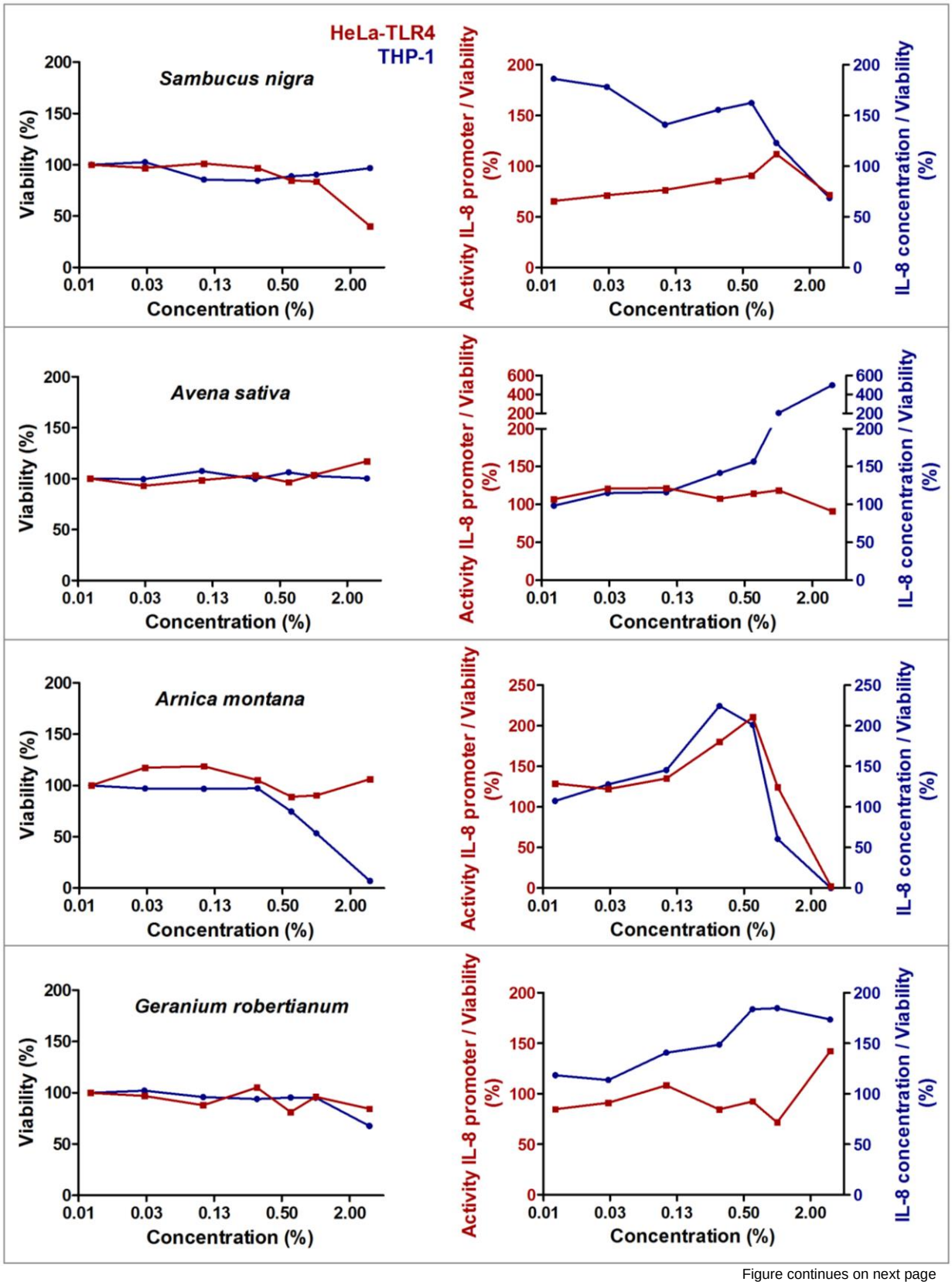

Figure continues on next page

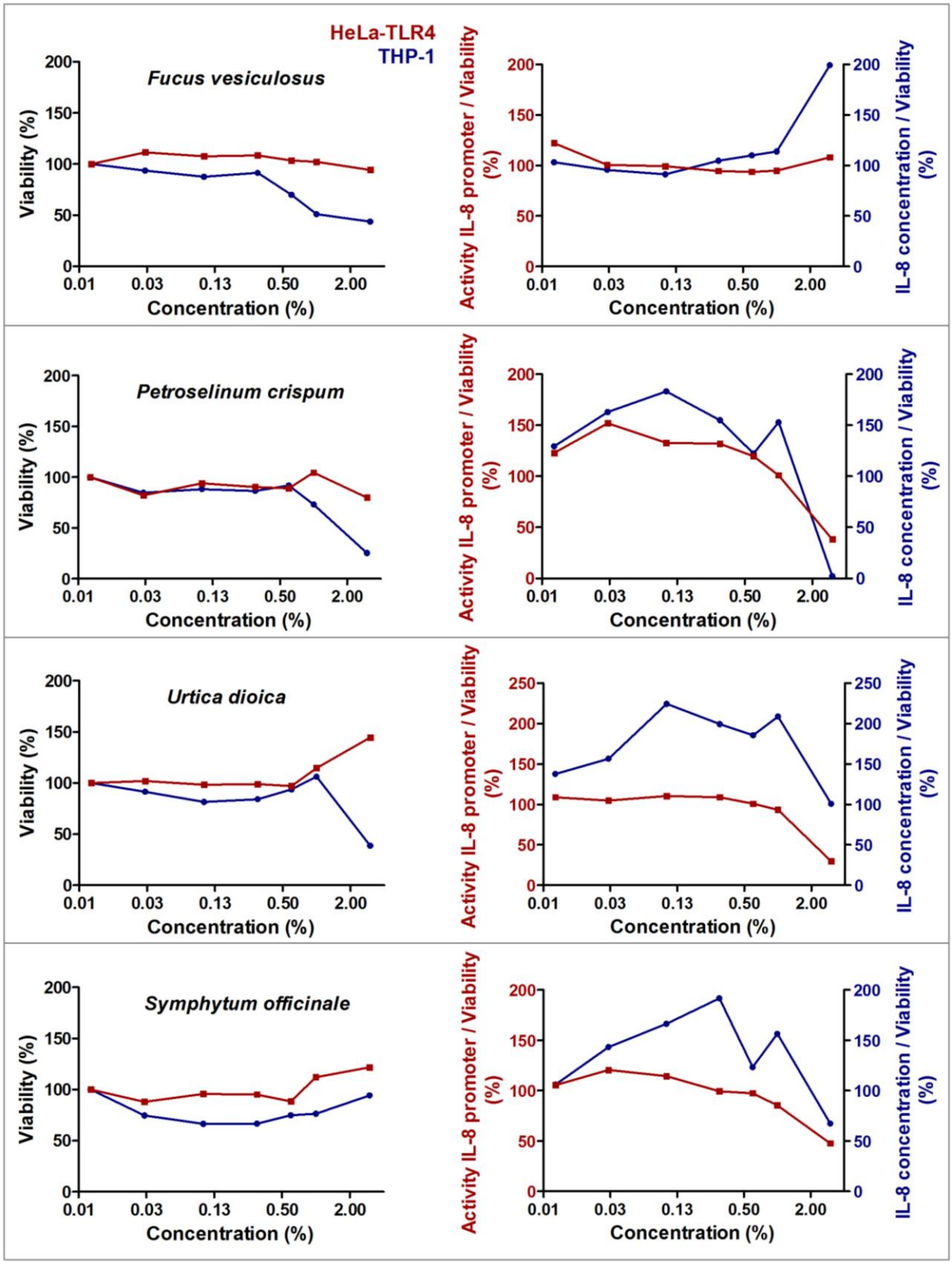

Figure continues on next page

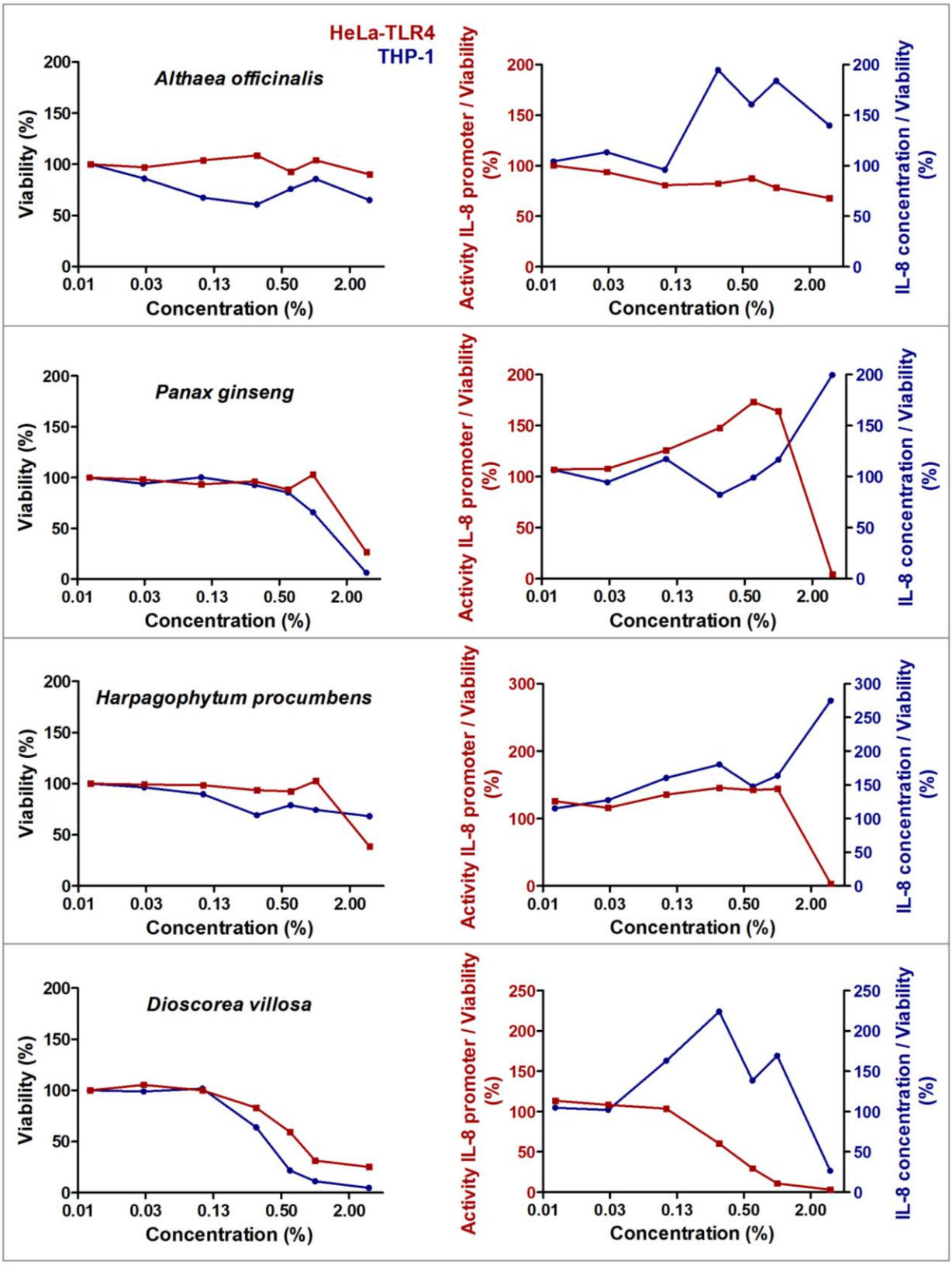

Figure continues on next page

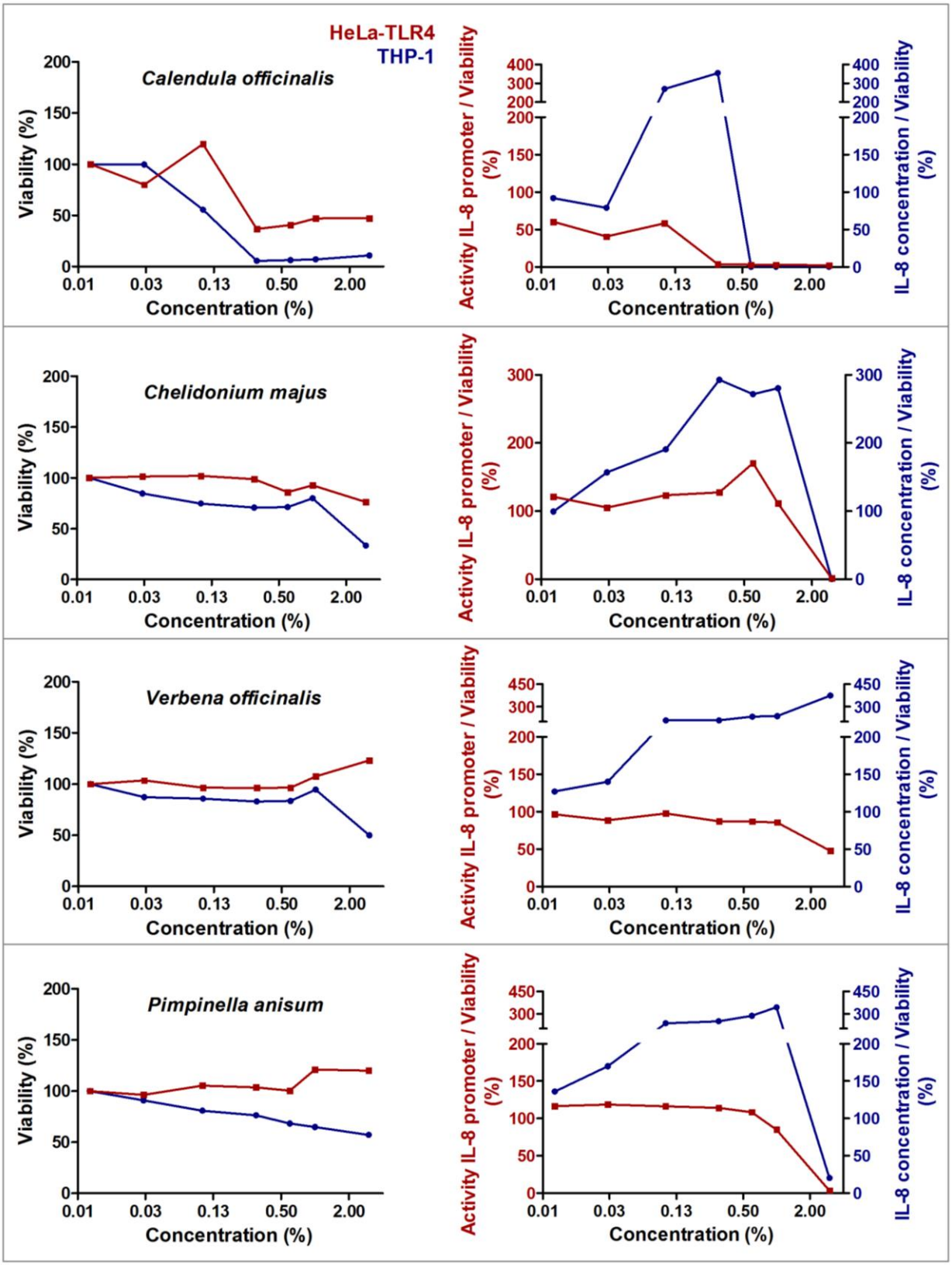

Figure continues on next page

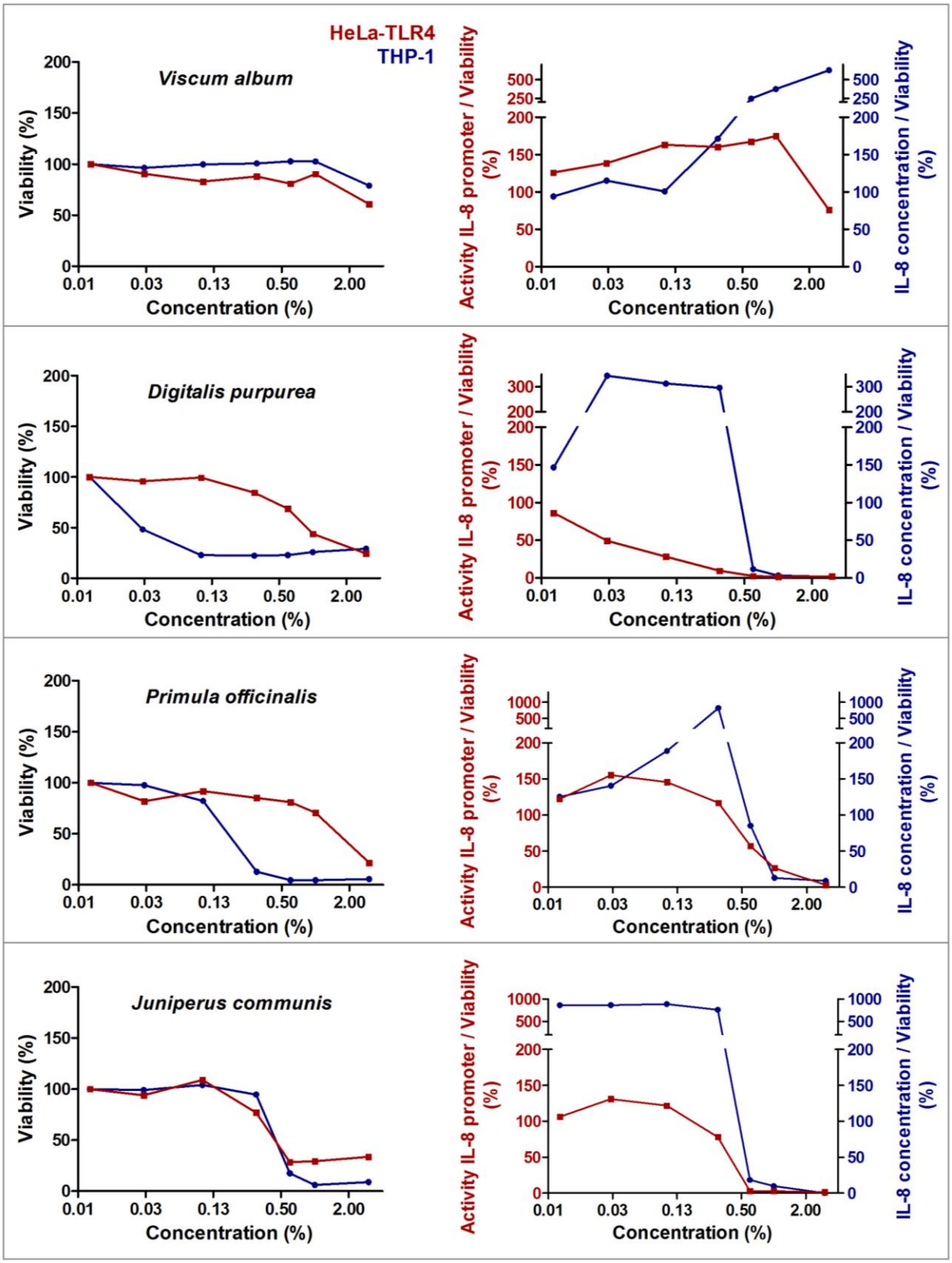

Figure continues on next page

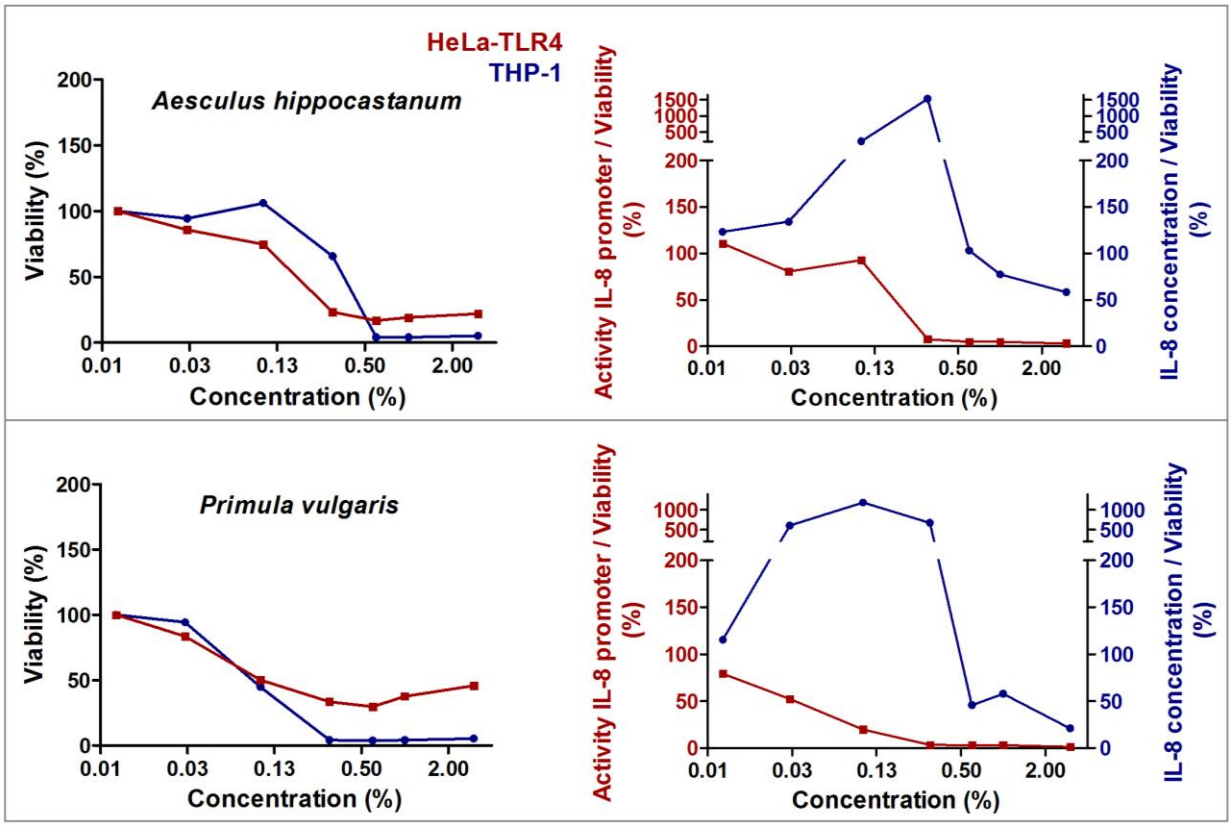

Figure 31: Cell viability and anti-inflammatory effects of ethanolic extracts
HeLa-TLR4 reporter cells (red) and THP-1 monocytes (blue) were incubated with extracts in different concentrations or vehicle 70% ethanol, followed by stimulation with LPS-EB. Viability (Alamar Blue assay) was normalized to negative control. TLR4 receptor activity (Renilla luciferase expression for HeLa-TLR4 reporter cell line and IL-8 ELISA for THP-1 monocytes) was normalized to vehicle-treated cells. Data are displayed as viability (%) in upper graphs and TLR4 activity divided by normalized viability in lower graphs. Data represent mean ($n \geq 2$). The ten extracts with highest anti-inflammatory potential are graphically displayed in **Figure 6**.

Table 22: Anti-inflammatory activity of ethanolic extracts

HeLa-TLR4 reporter cells and THP-1 monocytes were incubated with extracts in different concentrations or vehicle 70% ethanol, followed by stimulation with LPS-EB. Viability (Alamar Blue assay) was normalized to negative control (*Viability (%)*). TLR4 receptor activity (Renilla luciferase expression for HeLa-TLR4 reporter cell line and IL-8 ELISA for THP-1 monocytes) was normalized to vehicle-treated cells (*TLR4-Activity*). Data are displayed as TLR4 stimulation divided by viability and ranked ascending by the following formula: (150 - *Viability (%)*)*(2**TLR4-Activity* + 100) weighted in a ratio of 2:1 for THP-1 monocytes vs. HeLa-TLR4 reporter cells. Data represent mean (*n*≥2).

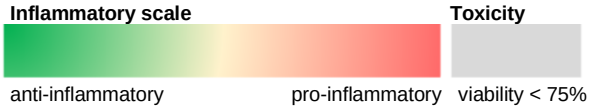

			HeLa-TLR4 reporter cell line							THP-1 monocytes						
Latin name	**Common English name**	**Used part**	**0.01%**	**0.03%**	**0.1%**	**0.3%**	**0.6%**	**1%**	**3%**	**0.01%**	**0.03%**	**0.1%**	**0.3%**	**0.6%**	**1%**	**3%**
Ethanol control			100,00	101,30	103,67	102,01	93,23	85,77	90,26	98,88	97,04	96,54	96,59	97,67	95,66	107,91
Castanea sativa	Sweet chestnut	Leaf	90,53	82,03	30,91	3,53	10,59	1,34	0,79	118,69	71,34	46,42	25,73	5,65	0,00	0,00
Cinchona pubescens	Cinchona	Bark	122,15	137,25	148,02	131,28	148,76	98,71	2,77	47,68	104,26	125,10	62,37	29,49	15,68	3,49
Cinnamomum verum	Cinnamon	Bark	96,77	98,57	109,17	83,50	59,41	21,59	3,24	101,16	87,70	95,31	106,02	26,08	6,08	11,36
Salix alba	White willow	Bark	93,03	74,48	79,05	99,83	58,02	3,79	1,45	97,50	93,93	88,45	33,44	5,95	0,00	21,34
Rheum palmatum	Rhubarb	Root	71,38	72,58	79,60	55,28	64,48	96,37	2,34	99,17	98,60	27,86	6,42	1,94	3,57	29,89
Alchemilla vulgaris	Common lady's mantle	Whole plant	91,35	85,79	82,86	76,83	66,53	78,18	1,63	125,37	102,96	92,63	62,93	60,89	73,46	0,00
Humulus lupulus	Hops	Flower	64,31	67,38	74,08	3,57	1,10	0,92	0,96	108,76	99,78	55,66	1,46	0,00	0,00	0,73
Vaccinium myrtillus	Bilberries	Fruit/berry/ seed	86,00	84,71	81,50	80,48	83,01	76,30	68,10	102,84	91,37	92,22	96,85	92,91	92,95	63,02
Curcuma longa	Turmeric	Root	124,40	109,62	142,43	67,28	11,92	5,54	1,83	127,14	110,90	115,73	45,39	8,99	0,00	15,80
Arctostaphylos uva-ursi	Bearberry	Leaf	91,28	109,88	127,59	123,26	86,52	40,81	1,18	89,45	99,97	27,43	5,97	1,72	4,71	35,80
Allium ursinum	Wild garlic	Leaf	115,74	118,86	97,71	91,94	81,27	78,25	42,93	105,80	109,20	77,64	38,94	24,16	5,90	11,21
Hypericum perforatum	St John's wort	Whole plant	120,77	104,44	85,91	83,69	71,41	53,35	14,06	91,44	85,40	90,32	71,54	51,19	32,03	1,14
Arnicae montana	Arnica	Flower	114,17	96,34	2,78	2,14	2,61	2,55	1,28	144,96	146,96	11,90	0,70	0,69	1,67	0,53
Aloe ferox	Aloe	Whole plant	105,30	105,90	82,53	58,19	27,69	5,15	1,30	123,82	117,87	88,51	38,22	9,71	7,37	0,13
Cynara scolymus	Artichoke	Leaf	109,98	112,42	117,52	100,14	90,16	31,21	1,99	47,40	53,68	127,22	228,92	16,56	6,13	2,86
Salvia officinalis	Salvia	Leaf	94,88	96,95	107,50	89,57	73,14	17,55	2,65	94,87	87,05	79,10	72,53	97,48	42,03	0,00
Ginkgo biloba	Ginkgo	Leaf	107,04	120,25	119,37	90,15	44,17	4,77	2,22	124,31	101,09	22,26	7,98	16,68	9,27	0,00
Tanacetum parthenium	Feverfew	Whole plant	127,34	111,53	120,04	114,28	99,98	68,82	2,22	129,88	139,58	123,43	124,51	72,56	21,24	6,12
Vigna radiata	Mung bean (dried)	Fruit/berry/ seed	83,31	85,02	87,84	85,99	69,53	52,04	25,33	121,14	141,32	120,83	62,61	38,87	23,18	11,00
Betula verrucosa	Weeping birch	Juice/resin	144,10	148,90	136,35	139,46	143,77	154,99	88,24	120,90	131,27	106,29	88,92	93,49	94,35	93,18
Filipendula ulmaria	Meadowsweet	Flower	120,04	113,11	130,06	117,06	106,72	131,55	52,01	132,40	135,84	124,42	75,12	23,05	8,87	1,88
Matricaria chamomilla	Chamomile	Whole plant	100,35	104,50	90,84	78,36	84,92	5,43	1,26	107,39	110,30	81,01	78,37	109,61	0,00	0,00
Spirulina	Spirulina	Whole cyanobacteria	93,17	100,77	107,05	92,24	76,80	50,64	3,57	142,68	138,71	169,61	74,85	20,59	2,70	36,20
Gentiana lutea	Gentian	Root	120,08	105,07	118,69	89,81	89,96	82,85	39,06	80,63	60,91	89,51	140,23	62,51	43,53	2,92
Quercus robur	English oak	Bark	143,68	142,56	127,88	124,88	134,53	106,17	8,76	106,31	116,82	88,62	57,00	35,67	16,07	16,81
Glycyrrhiza glabra	Liquorice	Root	69,76	13,55	17,52	2,60	2,55	2,39	1,41	124,15	119,86	9,19	2,26	0,00	0,00	0,00
Coriandrum sativum	Coriander	Fruit/berry/ seed	94,70	82,24	87,66	90,37	89,65	77,49	44,98	145,74	168,38	152,38	158,20	188,96	155,51	6,45
Achillea millefolium	Common yarrow	Whole plant	99,04	103,48	102,37	83,36	68,35	55,50	4,09	93,70	98,28	118,44	107,59	100,57	52,47	0,54
Mentha piperita	Peppermint	Whole plant	102,97	91,41	91,14	78,20	72,36	55,95	6,57	130,45	151,24	119,30	123,66	149,47	84,49	0,00
Zingiber officinale	Ginger	Root	94,65	103,21	52,82	24,16	2,18	4,32	3,92	73,81	82,12	75,13	80,11	34,29	0,19	6,73

Table continues on next page

Appendix

			HeLa-TLR4 reporter cell line							THP-1 monocytes						
Latin name	**Common English name**	**Used part**	**0.01%**	**0.03%**	**0.1%**	**0.3%**	**0.6%**	**1%**	**3%**	**0.01%**	**0.03%**	**0.1%**	**0.3%**	**0.6%**	**1%**	**3%**
Ethanol control			100,00	101,30	103,67	102,01	93,23	85,77	90,26	98,88	97,04	96,54	96,59	97,67	95,66	107,91
Carum carvi	Caraway	Fruit/berry/ seed	108,52	107,56	121,15	115,23	96,15	83,63	2,63	126,27	123,61	127,15	136,91	201,67	118,87	0,00
Boswellia serrata	Frankincense	Juice/resin	109,56	96,96	80,61	3,87	2,80	3,49	2,35	97,42	88,36	75,32	23,64	10,16	11,86	9,76
Camellia sinensis (L.)	Green tea	Leaf	71,42	64,90	60,73	53,03	34,40	5,10	2,05	104,85	90,19	80,66	52,63	128,30	78,12	71,24
Echinacea purpurea	Purple coneflower	Whole plant	93,87	121,50	103,17	111,27	121,75	86,28	3,42	110,63	100,92	147,05	98,88	95,70	98,35	1,71
Ilex paraguariensis	Yerba mate	Leaf	118,38	113,40	129,00	98,03	46,11	7,19	1,87	138,05	86,82	106,45	142,70	113,19	149,98	29,15
Melissa officinalis	Lemon balm	Leaf	139,03	150,28	144,79	79,25	68,78	76,74	2,31	88,63	126,13	138,48	148,82	86,05	36,73	0,00
Daucus carota ssp. sativus	Carrot	Root	98,38	101,96	87,71	99,88	87,68	98,85	87,26	96,35	110,50	87,33	79,92	93,51	85,16	137,06
Alpinia officinarum	Galangal	Root	119,58	118,04	149,25	135,19	45,52	3,29	2,27	127,08	98,10	138,77	38,12	0,70	0,00	2,44
Boswellia carterii	Frankincense	Whole plant	149,54	178,92	15,63	14,15	11,16	11,09	12,66	27,95	31,63	4,81	7,98	18,51	6,92	3,63
Hamamelis virginiana	Witch hazel	Leaf	100,46	99,15	137,19	118,74	70,76	4,96	1,01	123,19	189,63	211,05	38,28	5,85	5,40	7,92
Equisetum arvense	Field horsetail	Whole plant	113,79	125,14	120,99	128,87	130,20	133,00	109,17	93,55	94,65	83,58	114,07	124,64	145,69	189,41
Scrophularia nodosa	Common figwort	Whole plant	98,78	93,42	113,41	123,22	114,38	105,67	10,92	107,47	125,14	152,78	113,07	101,17	88,26	24,69
Lavandula angustifolia	Lavender	Flower	93,68	101,24	110,76	95,94	91,92	36,15	3,80	81,97	87,67	115,57	116,55	141,91	137,61	0,00
Euphrasia officinalis	Eyebright	Whole plant	101,53	105,92	114,90	115,55	113,31	116,53	10,37	136,41	103,87	107,91	96,64	107,09	125,33	0,38
Capsicum frutescens	Chili	Fruit/berry/ seed	101,94	167,29	120,07	115,20	118,62	95,65	3,07	117,80	124,86	154,50	180,15	171,38	145,55	29,51
Erythraea centaurium	Common centaury	Whole plant	106,04	92,14	96,31	87,33	82,62	62,99	5,13	113,71	85,01	148,74	133,41	141,78	119,84	4,22
Hibiscus sabdariffa	Roselle	Leaf	105,58	98,26	132,94	133,23	118,60	97,39	48,78	90,10	94,55	87,49	93,64	145,26	231,97	65,51
Chlorella pyrenoidosa	Chlorella	Whole green algae	71,44	72,14	75,70	62,00	44,51	16,46	2,86	102,98	94,60	18,27	0,00	0,00	0,00	173,01
Allium sativum	Garlic	Root	78,39	95,63	87,21	84,35	83,82	96,56	112,72	129,06	117,29	96,92	89,62	103,10	110,42	132,77
Melilotus officinalis	Sweet clover	Whole plant	111,02	114,31	92,87	95,90	86,37	76,52	30,05	107,23	86,20	97,54	119,85	62,88	158,37	0,00
Artemisia absinthium	Wormwood	Whole plant	118,20	128,44	124,74	137,46	112,64	90,75	1,69	146,74	160,40	77,99	89,46	44,77	51,21	0,00
Uncaria tomenosa	Cat's claw	Whole plant	131,44	136,66	124,86	114,39	100,57	132,50	121,12	109,66	131,32	109,33	105,76	107,51	109,99	104,97
Origanum majorana	Marjoram	Whole plant	109,40	100,22	104,08	105,12	87,00	83,56	44,13	98,64	99,81	138,44	139,16	124,52	147,26	9,77
Usnea barbata	Barber's itch	Whole plant	93,46	92,28	106,88	100,70	101,15	124,63	3,85	104,78	100,16	110,27	111,35	61,61	63,62	2,27
Taraxacum officinale	Dandelion	Whole plant	109,52	108,09	104,38	90,20	98,79	80,62	56,45	140,46	125,98	150,64	197,11	101,07	104,89	109,75
Crataegus sp.	Hawthorn	Fruit/berry/ seed	98,69	95,22	83,59	88,20	75,56	67,10	6,03	68,02	87,86	90,53	169,63	108,10	175,25	5,53
Syzygium aromaticum	Clove	Flower	130,27	153,49	129,52	111,74	3,84	4,04	2,97	113,40	106,43	28,55	64,60	0,00	0,00	0,00
Plantago lanceolata	Ribwort	Whole plant	104,81	156,04	140,16	152,61	145,60	124,31	81,91	73,59	77,75	99,03	94,45	91,42	91,59	135,20
Aconitum napellus	Monkshood	Whole plant	117,73	122,26	128,16	141,94	171,12	159,82	122,60	99,75	113,53	110,99	131,43	154,05	214,24	226,55
Rubus fruticosus	Blackberry	Leaf	127,50	109,58	113,80	106,40	93,56	73,60	68,53	155,10	133,75	158,55	231,87	137,62	160,15	6,26
Schinus terebinthifolius	Brazilian peppertree	Fruit/berry/ seed	111,76	128,25	118,65	124,42	83,27	11,51	3,58	153,65	194,72	140,78	156,82	22,67	9,93	2,35
Hedera helix	Common ivy	Leaf	91,23	92,82	79,19	4,54	3,93	4,92	3,35	106,81	105,99	164,47	16,45	0,48	18,81	3,05
Pulmonaria officinalis	Common lungwort	Flower	130,49	108,61	136,54	140,36	116,71	111,27	75,45	125,06	95,78	190,61	162,64	164,20	134,71	95,52
Betula alba	Birch	Juice/resin	132,70	132,59	119,10	123,74	109,52	110,59	175,69	93,66	114,38	113,57	96,37	88,04	113,21	88,16
Vanilla planifolia	Vanilla	Fruit/berry/ seed	113,32	101,03	109,01	117,05	92,96	94,61	31,02	103,36	106,83	167,48	188,94	131,81	146,05	6,91
Armoracia rusticana	Horseradish	Root	112,02	115,66	120,07	140,73	134,50	111,66	45,08	104,74	124,98	107,81	106,12	97,03	142,36	143,87
Nicotiana tabacum	Tobacco	Leaf	95,45	115,94	103,93	107,47	91,20	101,64	43,82	126,54	119,78	135,07	148,77	165,43	177,65	37,75
Valeriana officinalis (L.)	Common valerian	Root	100,20	91,61	147,82	156,35	138,95	52,36	2,58	138,12	95,56	147,35	197,61	206,61	71,26	5,16
Rosmarinus officinalis	Rosemary	Leaf	85,92	108,99	122,78	150,67	97,28	16,54	4,02	136,08	138,36	152,73	128,42	141,11	0,15	80,17
Tropaeolum majus	Nasturtium	Whole plant	101,46	84,01	87,90	77,92	79,16	75,39	81,14	86,16	109,46	140,46	135,69	107,73	130,22	81,44
Marrubium vulgare	Common horehound	Whole plant	92,34	93,29	88,32	86,32	95,10	100,87	3,75	98,80	104,74	135,83	176,09	166,83	174,18	0,00

Table continues on next page

Appendix

			HeLa-TLR4 reporter cell line							THP-1 monocytes						
Latin name	**Common English name**	**Used part**	**0.01%**	**0.03%**	**0.1%**	**0.3%**	**0.6%**	**1%**	**3%**	**0.01%**	**0.03%**	**0.1%**	**0.3%**	**0.6%**	**1%**	**3%**
Ethanol control			100,00	101,30	103,67	102,01	93,23	85,77	90,26	98,88	97,04	96,54	96,59	97,67	95,66	107,91
Xanthoria parietina	Common orange lichen	Whole lichen	132,43	117,59	130,84	104,27	104,89	106,46	39,67	150,70	163,97	169,59	192,87	206,05	180,74	1,76
Elettaria cardamomum	Cardamom	Fruit/berry/ seed	120,81	123,83	125,38	135,62	133,76	125,41	3,62	110,45	103,25	120,45	152,87	225,96	216,74	0,00
Vigna radiata	Mung bean (cooked)	Fruit/berry/ seed	104,69	135,60	133,28	135,94	134,61	147,80	124,20	106,85	112,74	124,20	137,77	159,06	119,88	98,96
Thymus vulgaris	Common thyme	Whole plant	118,89	124,53	122,18	110,86	120,29	97,87	1,59	89,27	76,48	88,74	122,81	172,45	279,61	0,00
Foeniculum vulgare	Fennel	Fruit/berry/ seed	113,92	97,22	97,97	94,07	87,06	84,14	3,97	134,14	173,01	197,93	186,12	199,79	223,76	21,35
Convallaria majalis	Lily of the valley	Whole plant	54,48	36,78	19,24	14,57	17,70	10,11	1,72	154,97	124,30	115,50	106,13	116,39	29,53	0,00
Sambucus nigra (L.)	Elderflower	Flower	65,76	71,40	76,66	85,55	90,78	112,07	71,97	186,27	178,06	140,90	155,66	162,33	122,89	68,63
Avena sativa	Oat	Whole plant	106,83	121,15	121,84	107,76	114,50	118,79	91,19	98,22	114,88	116,09	141,54	156,55	204,12	498,22
Arnica montana	Arnica	Whole plant	128,77	122,08	135,39	180,41	210,78	124,21	2,17	107,35	127,87	145,42	224,38	201,18	60,44	0,00
Geranium robertianum	Herb Robert	Whole plant	84,73	91,07	108,37	84,64	92,55	71,75	142,28	118,42	113,83	140,82	148,56	183,75	184,72	173,60
Fucus vesiculosus	Bladderwrack	Whole plant	122,31	100,62	99,24	94,51	93,75	94,92	108,01	103,21	95,74	91,21	104,75	110,16	113,90	199,19
Petroselinum crispum	Parsley	Whole plant	122,97	152,03	133,00	132,12	119,74	101,03	38,49	129,60	163,16	183,36	155,06	122,44	153,04	2,18
Urtica dioica	Stinging nettle	Root	109,01	104,90	110,43	109,07	100,86	93,37	29,81	137,84	156,50	224,44	199,41	185,63	208,82	100,88
Symphytum officinale	Comfrey	Root	105,62	120,61	114,45	99,46	97,54	85,58	47,79	106,24	143,47	166,37	191,76	123,39	156,54	67,34
Althaea officinalis	Marshmallow	Root	100,22	93,79	80,71	82,49	87,56	78,29	67,86	104,25	113,39	96,02	194,59	160,52	183,97	139,71
Panax ginseng	Ginseng	Root	107,05	107,98	125,88	147,96	173,19	164,01	4,13	106,76	94,66	117,42	82,44	99,07	116,80	199,71
Harpagophytum procumbens	Devil's claw	Root	125,75	116,09	135,75	145,66	142,70	144,23	3,68	115,10	127,64	160,49	180,30	147,55	163,53	275,03
Dioscorea villosa	Yam	Root	113,51	108,51	103,64	60,24	29,52	11,04	3,27	104,81	102,20	163,08	224,08	138,65	169,18	26,64
Calendula officinalis	Marigold	Flower	60,30	40,34	58,30	3,49	2,91	2,77	2,19	91,73	78,85	269,59	354,55	0,00	0,00	0,00
Chelidonium majus	Celandine	Root	120,88	105,15	123,10	127,73	170,41	111,32	1,42	99,40	157,00	190,57	292,73	271,52	280,41	0,00
Verbena officinalis	Common vervain	Whole plant	96,47	88,48	97,54	86,98	86,77	85,59	47,65	127,02	140,00	208,28	208,79	233,55	236,51	374,51
Pimpinella anisum	Anise	Fruit/berry/ seed	116,49	118,67	116,39	114,10	108,54	84,98	3,36	136,25	169,95	236,67	250,31	286,11	344,07	20,08
Viscum album	European mistletoe	Whole plant	125,75	138,13	162,97	160,01	166,89	174,64	76,09	93,86	114,91	100,53	170,99	242,81	373,37	625,53
Digitalis purpurea	Common foxglove	Leaf	86,35	49,52	28,50	9,67	2,50	1,49	2,18	146,70	344,09	313,09	296,48	11,91	3,20	1,60
Primula officinalis	Common cowslip	Root	122,30	155,54	145,79	116,90	57,14	26,43	3,07	125,37	140,65	188,90	819,19	85,17	12,98	8,91
Juniperus communis	Common juniper	Fruit/berry/ seed	106,49	131,13	121,88	77,99	3,10	2,84	1,55	859,81	863,37	888,08	759,89	18,31	9,85	0,00
Aesculus hippocastanum	Horse-chestnut	Fruit/berry/ seed	110,81	80,80	92,60	7,84	5,11	5,00	3,20	123,23	134,19	212,88	1537,04	102,98	77,65	58,38
Primula vulgaris	Common primrose	Root	48,96	26,97	24,47	13,49	12,19	8,12	1,52	115,35	604,33	1193,00	674,91	45,73	58,06	21,03

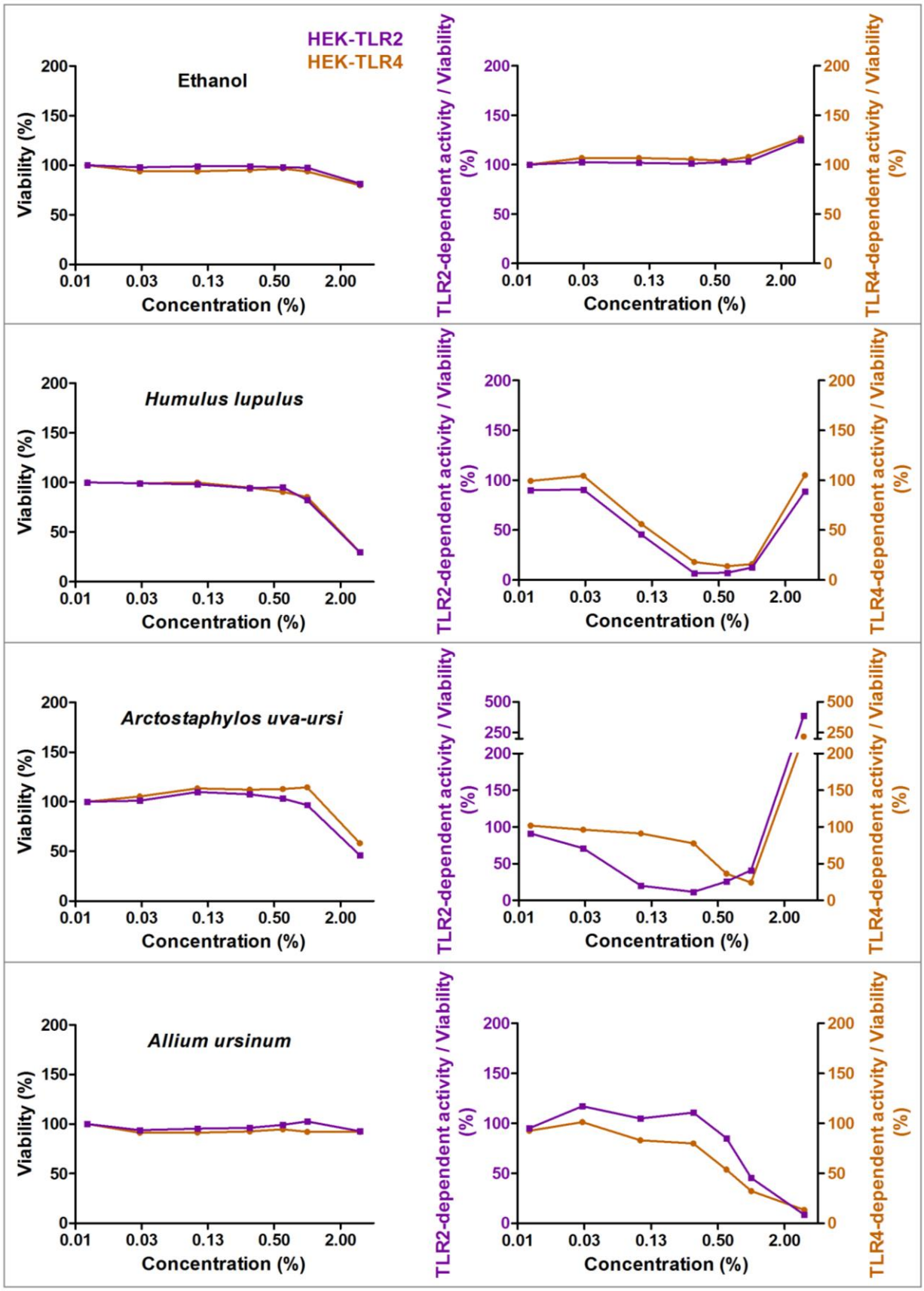

Figure continues on next page

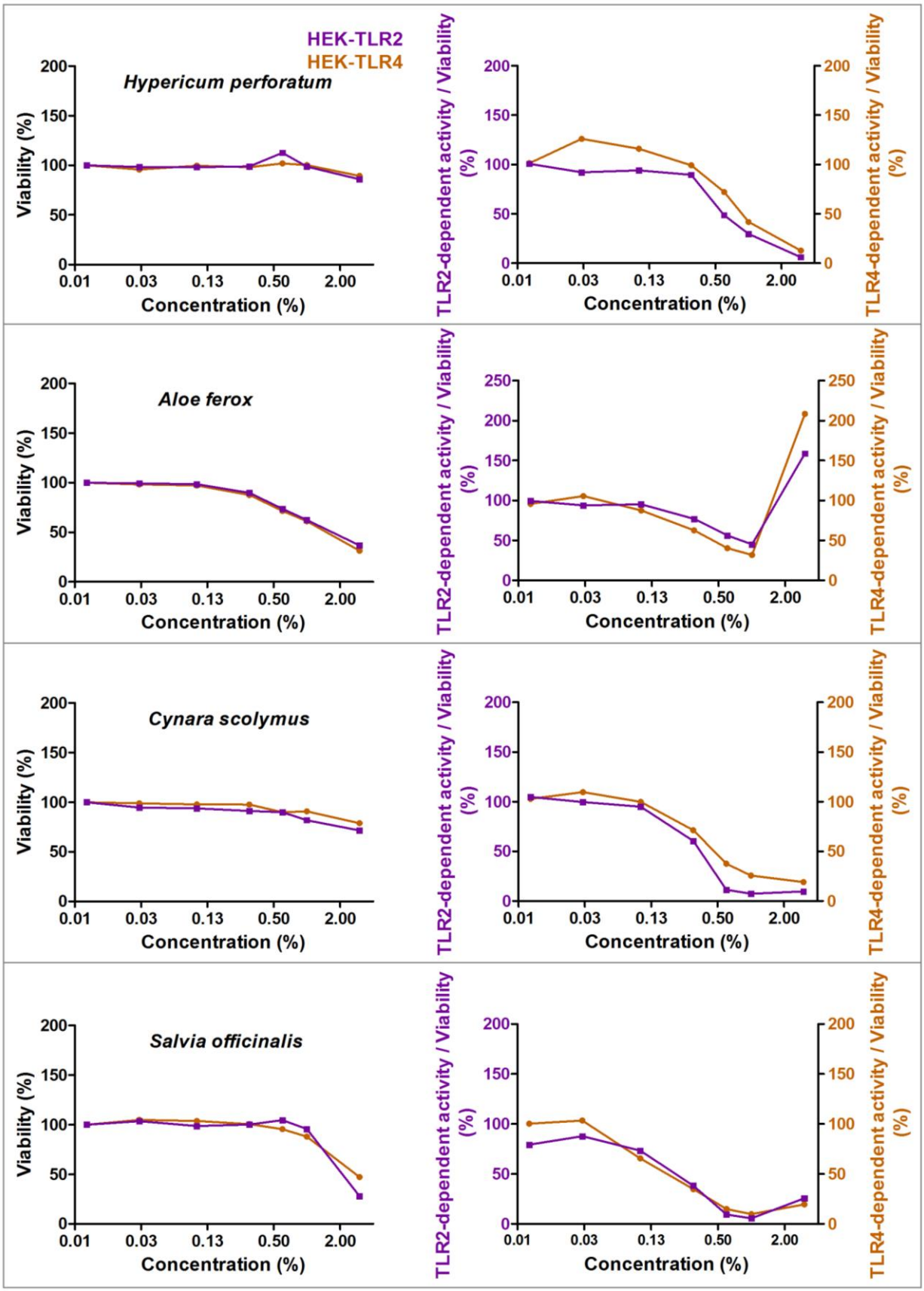

Figure continues on next page

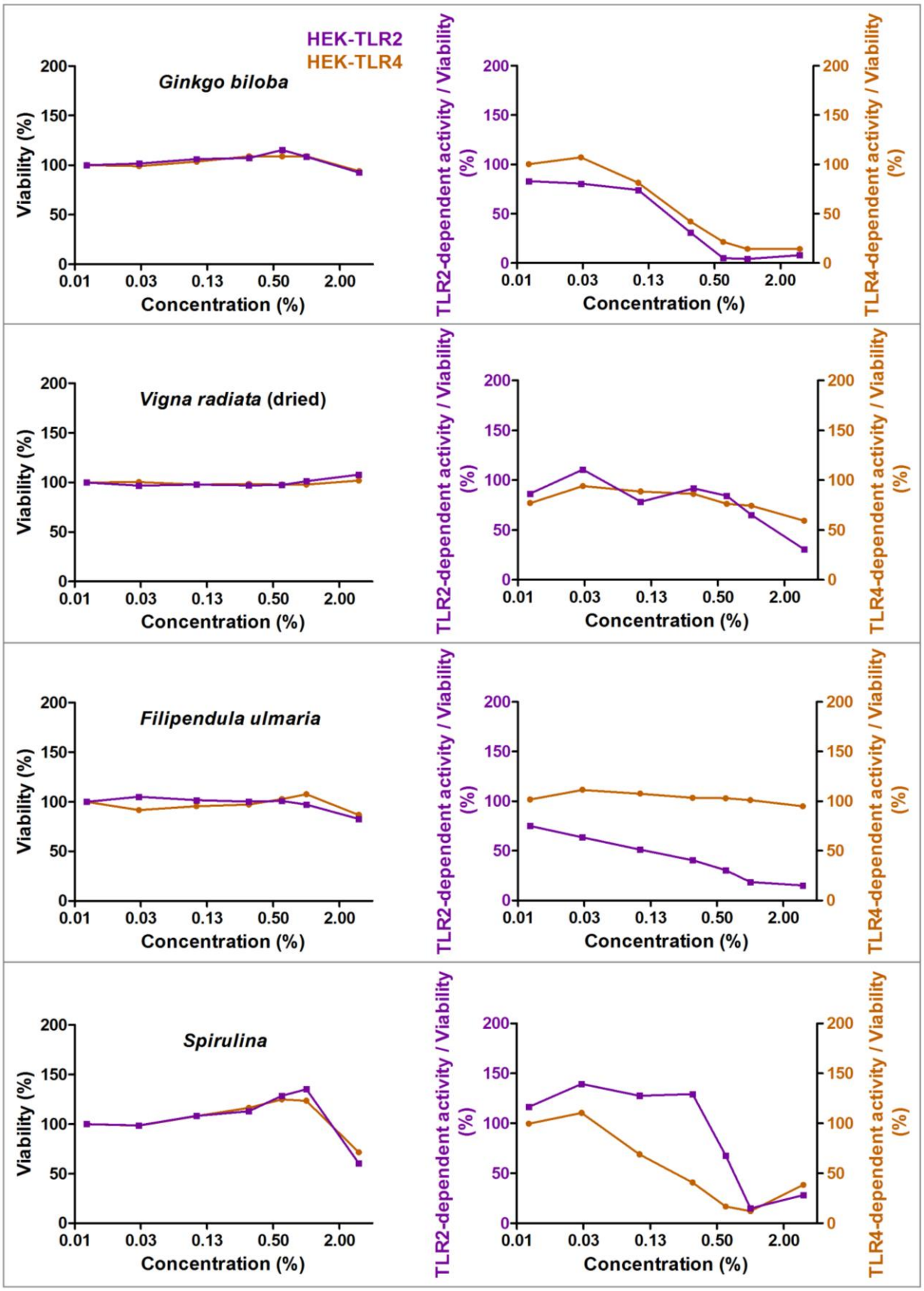

Figure continues on next page

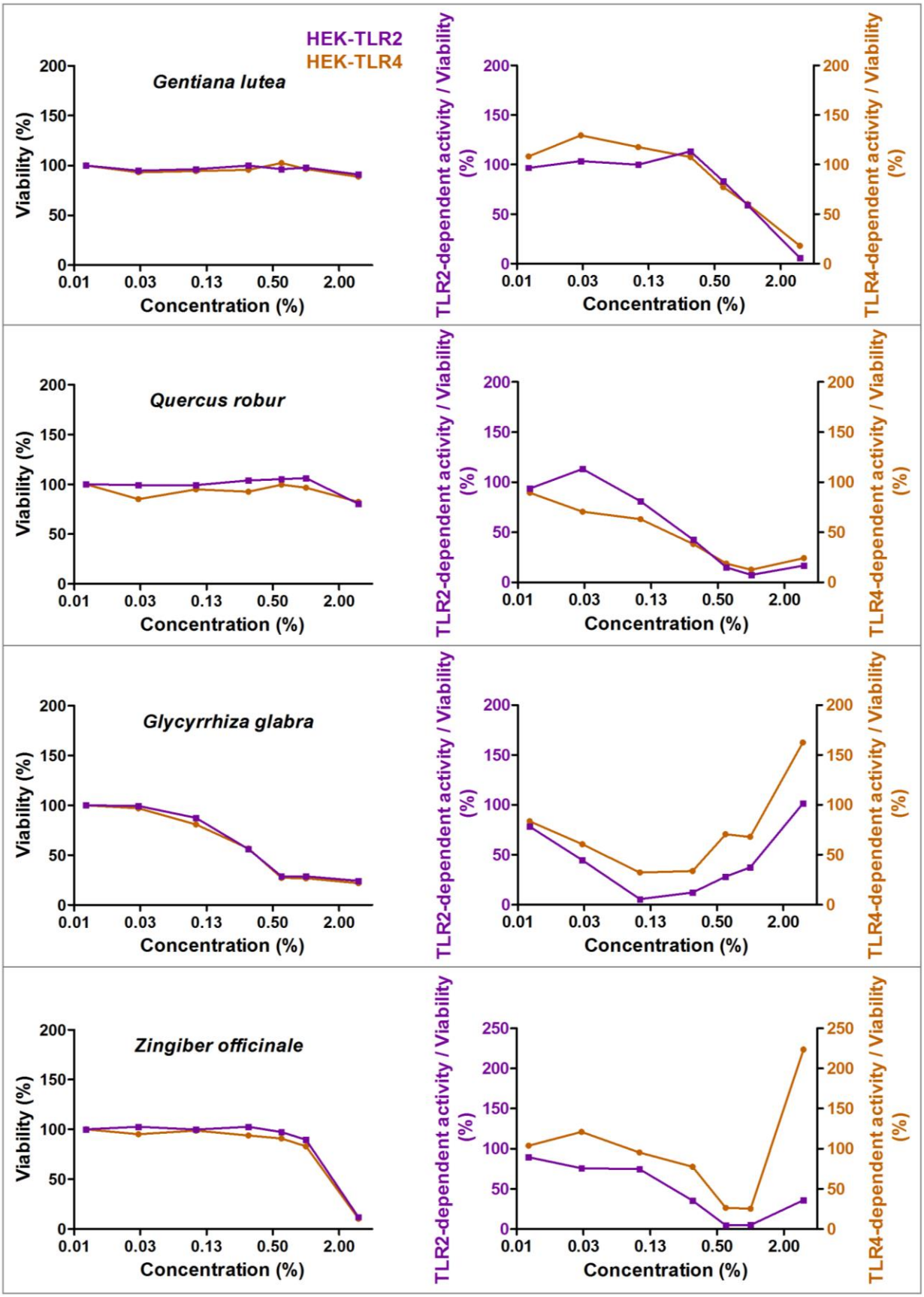

Figure continues on next page

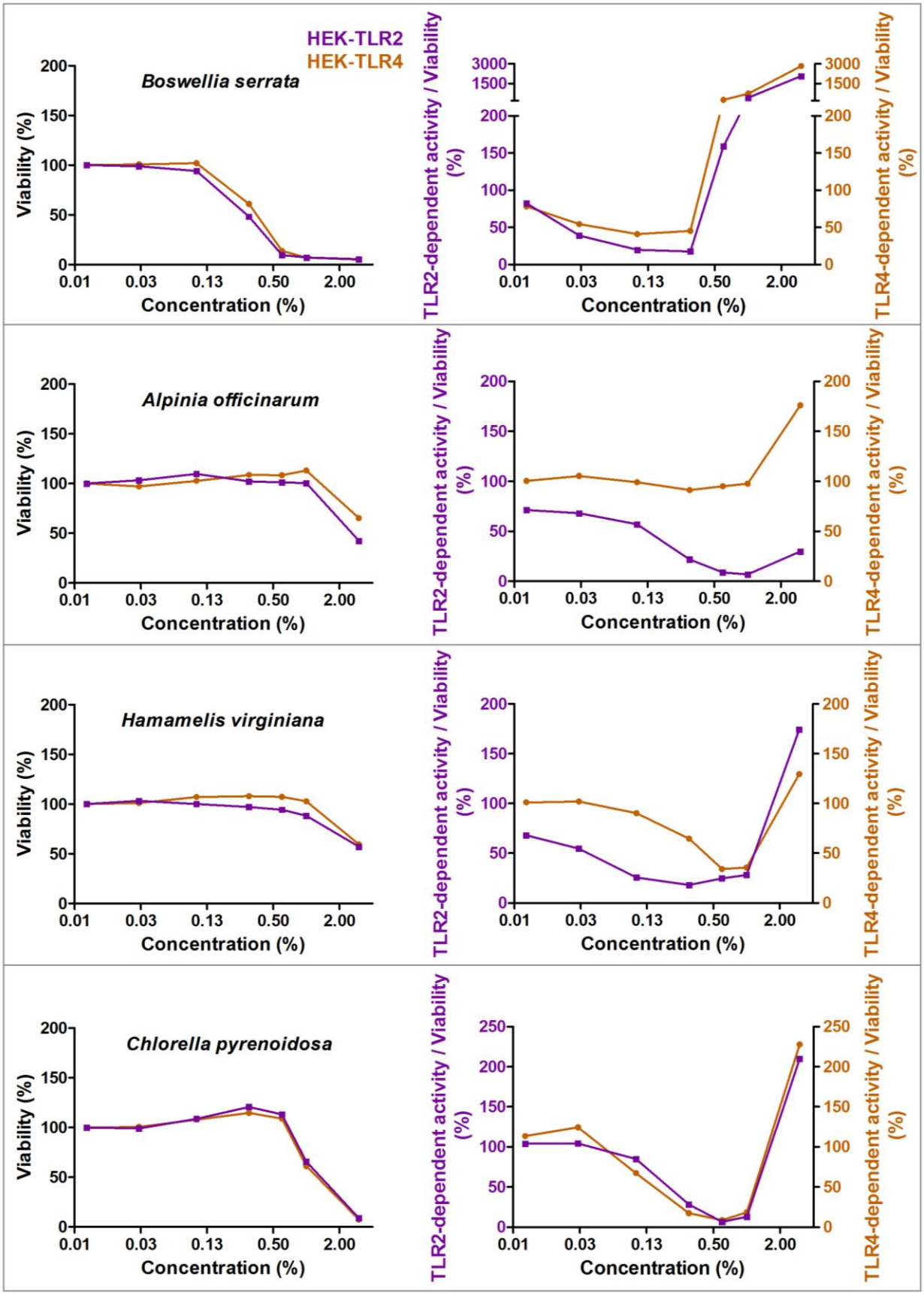

Figure continues on next page

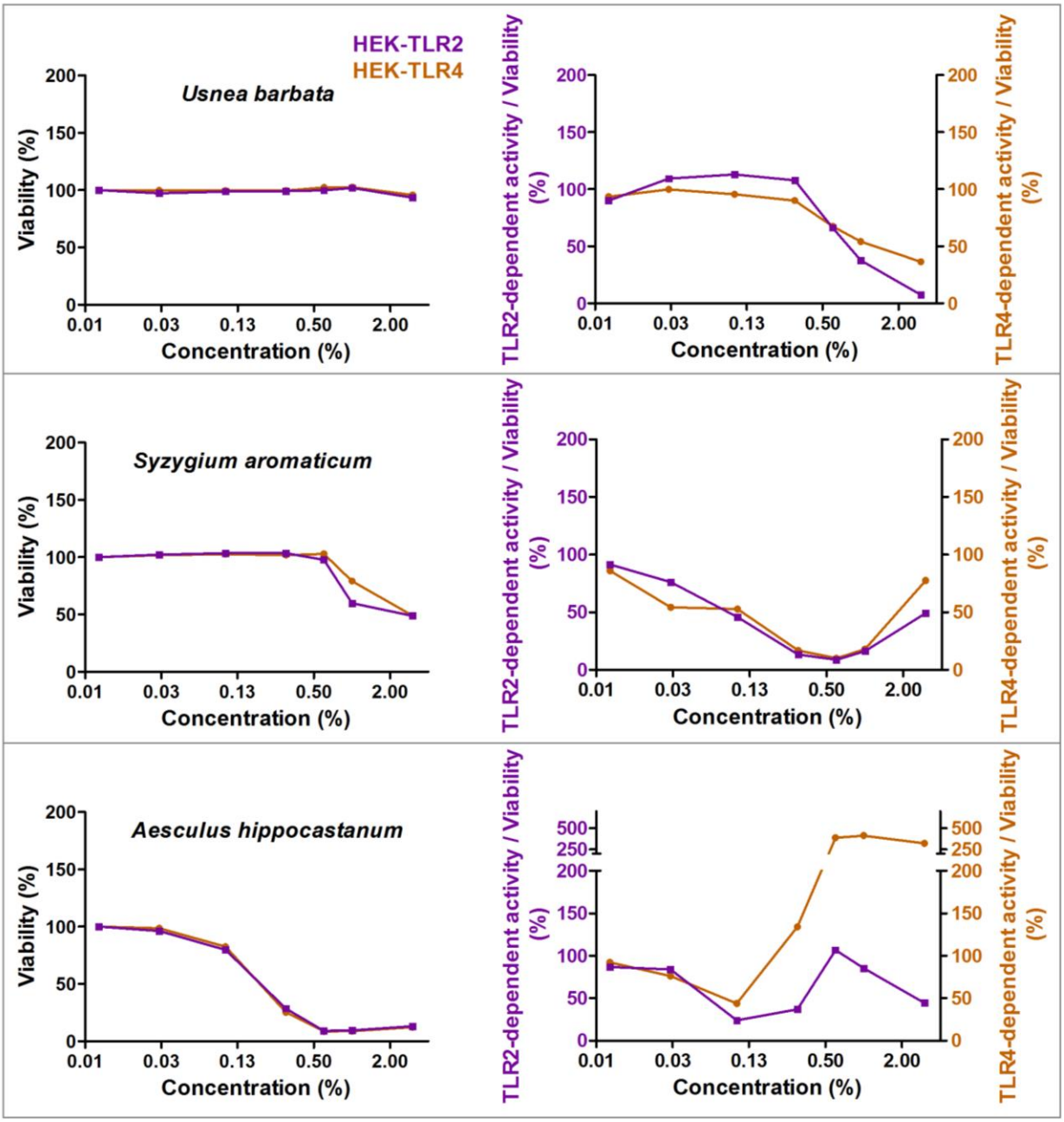

Figure 32: Cell viability and anti-inflammatory effects of extracts tested for exclusive TLR4 antagonistic activity

HEK-TLR2 (purple) and HEK-TLR4 reporter cells (orange) were incubated with extracts in different concentrations or vehicle 70% ethanol, followed by stimulation with Pam2CSK4 (HEK-TLR2 reporter cells) or LPS-EB ultrapure (HEK-TLR4 reporter cells). Viability (Alamar Blue assay) was normalized to negative control. TLR2 and TLR4 receptor activity (SEAP production) were normalized to vehicle-treated cells. Data are displayed as viability (%) in upper graphs and receptor activity divided by viability in lower graphs. Data represent mean ($n \geq 4$). The five extracts with highest anti-inflammatory potential are graphically displayed in **Figure 9**.

Table 23: TLR2 and TLR4 specific antagonistic activity of select ethanolic extracts

HEK-TLR2 and HEK-TLR4 reporter cells were incubated with extracts in different concentrations or vehicle 70% ethanol, followed by stimulation with Pam2CSK4 (HEK-TLR2 reporter cells) or LPS-EB ultrapure (HEK-TLR4 reporter cells). Viability (Alamar Blue assay) was normalized to negative control. TLR2 and TLR4 receptor activity (SEAP production) were normalized to vehicle-treated cells. Data are displayed as receptor stimulation divided by normalized viability. Data represent mean ($n \geq 2$).

Inflammatory scale **Toxicity**

anti-inflammatory pro-inflammatory viability < 75%

			HEK-TLR2 reporter cell line							HEK-TLR4 reporter cell line						
Latin name	**Common English name**	**Used part**	**0.01%**	**0.03%**	**0.1%**	**0.3%**	**0.6%**	**1%**	**3%**	**0.01%**	**0.03%**	**0.1%**	**0.3%**	**0.6%**	**1%**	**3%**
Ethanol control			100,00	102,45	101,84	101,03	102,55	103,43	124,76	100,00	106,70	106,82	105,37	103,93	107,97	127,11
Castanea sativa	Sweet chestnut	Leaf	20,06	17,83	9,78	11,82	19,94	28,56	118,82	24,28	17,36	12,78	15,09	20,87	32,77	161,75
Cinchona pubescens	Cinchona	Bark	100,53	94,50	77,03	65,89	25,61	13,17	22,78	96,97	92,46	86,34	75,11	48,95	37,82	32,81
Cinnamomum verum	Cinnamon	Bark	100,40	100,11	105,47	65,88	36,23	22,34	37,65	100,75	97,62	94,69	59,98	27,50	18,82	32,43
Salix alba	White willow	Bark	102,12	100,18	85,03	42,14	20,67	17,65	73,17	100,01	85,03	67,85	40,08	34,16	24,12	52,75
Rheum palmatum	Rhubarb	Root	96,48	87,24	59,40	36,53	13,11	8,17	24,68	89,65	89,52	64,85	40,62	20,74	16,27	38,65
Humulus lupulus	Hops	Flower	90,21	90,80	45,52	6,84	7,25	12,55	88,75	99,42	104,49	56,15	18,10	13,97	15,99	105,06
Arctostaphylos uva-ursi	Bearberry	Leaf	91,42	71,09	20,16	11,86	25,75	41,19	385,83	101,93	96,18	91,06	77,63	36,71	24,40	217,02
Allium ursinum	Wild garlic	Leaf	95,05	117,18	104,97	110,95	85,31	45,41	8,55	92,64	101,32	83,11	79,90	53,77	32,22	13,36
Hypericum perforatum	St John's wort	Whole plant	100,82	92,09	94,08	89,60	48,53	29,53	6,00	101,20	125,93	115,86	99,00	72,14	41,77	12,66
Aloe ferox	Aloe	Whole plant	99,50	94,02	95,36	76,96	56,33	45,12	158,90	95,70	105,77	87,57	62,60	40,30	32,00	208,70
Cynara scolymus	Artichoke	Leaf	104,96	99,81	95,14	60,38	11,43	7,45	9,75	102,92	109,70	99,86	71,37	37,63	25,76	19,01
Salvia officinalis	Salvia	Leaf	79,45	87,83	73,41	38,26	9,48	5,77	25,80	100,28	103,61	65,58	34,90	14,99	9,98	19,63
Ginkgo biloba	Ginkgo	Leaf	83,06	80,39	74,11	30,88	4,92	4,06	7,87	100,24	107,01	81,26	42,13	21,39	14,24	14,18
Vigna radiata	Mung bean (dried)	Fruit/berry/ seed	86,58	110,71	78,43	91,74	84,41	65,29	30,75	77,04	94,29	88,78	86,30	76,44	74,46	59,49
Filipendula ulmaria	Meadowsweet	Flower	75,12	63,58	51,28	40,60	30,35	18,59	15,08	101,71	111,43	107,58	103,43	102,99	101,11	94,91
Spirulina	Spirulina	Whole cyanobacteria	116,49	139,54	127,71	129,36	67,85	15,01	28,28	99,69	110,62	69,12	40,91	16,95	12,20	38,50
Gentiana lutea	Gentian	Root	96,77	103,65	99,90	113,40	83,38	59,14	5,82	108,21	129,60	117,81	107,54	77,28	60,19	18,10
Quercus robur	English oak	Bark	93,72	113,22	81,11	42,60	15,04	7,52	16,84	89,53	70,65	63,23	38,30	18,82	12,82	24,23
Glycyrrhiza glabra	Liquorice	Root	78,30	44,63	5,56	12,09	28,06	37,27	101,27	83,64	60,59	32,18	33,77	70,66	67,87	162,46
Zingiber officinale	Ginger	Root	89,51	75,69	74,77	35,53	4,69	5,18	35,84	103,89	120,85	95,36	77,68	26,45	25,34	223,46
Boswellia serrata	Frankincense	Juice/resin	82,46	38,96	19,81	17,73	159,07	432,24	2076,63	78,29	54,43	40,86	45,48	288,07	744,11	2813,02
Alpinia officinarum	Galangal	Root	71,36	68,16	57,03	21,85	8,95	6,85	29,83	100,45	105,34	99,27	91,33	95,04	97,57	176,07
Hamamelis virginiana	Witch hazel	Leaf	68,01	54,73	25,63	18,14	24,82	28,25	174,32	101,02	102,08	90,19	64,82	34,21	35,64	129,53
Chlorella pyrenoidosa	Chlorella	Whole algae	103,97	104,34	84,84	28,14	6,63	12,96	209,74	113,66	124,42	67,31	17,39	8,74	18,75	227,74
Usnea barbata	Barber's itch	Whole plant	90,08	109,48	113,03	107,82	66,29	37,56	7,49	93,50	99,92	95,64	90,15	67,63	54,02	36,36
Syzygium aromaticum	Clove	Flower	91,40	76,21	45,89	13,37	8,91	16,47	49,18	86,11	54,39	52,82	16,99	10,06	18,12	77,65
Aesculus hippocastanum	Horse-chestnut	Fruit/berry/ seed	86,76	83,98	24,02	36,87	106,93	85,46	44,41	92,43	76,26	43,91	134,14	388,13	413,57	323,76